



2808986586

REFERENCE ONLY

UNIVERSITY OF LONDON THESIS

Degree PhD Year 2006 Name of Author WONGJoan Bosco Chuen-Chung

COPYRIGHT

This is a thesis accepted for a Higher Degree of the University of London. It is an unpublished typescript and the copyright is held by the author. All persons consulting the thesis must read and abide by the Copyright Declaration below.

COPYRIGHT DECLARATION

I recognise that the copyright of the above-described thesis rests with the author and that no quotation from it or information derived from it may be published without the prior written consent of the author.

LOAN

Theses may not be lent to individuals, but the University Library may lend a copy to approved libraries within the United Kingdom, for consultation solely on the premises of those libraries. Application should be made to: The Theses Section, University of London Library, Senate House, Malet Street, London WC1E 7HU.

REPRODUCTION

University of London theses may not be reproduced without explicit written permission from the University of London Library. Enquiries should be addressed to the Theses Section of the Library. Regulations concerning reproduction vary according to the date of acceptance of the thesis and are listed below as guidelines.

- A. Before 1962. Permission granted only upon the prior written consent of the author. (The University Library will provide addresses where possible).
- B. 1962 - 1974. In many cases the author has agreed to permit copying upon completion of a Copyright Declaration.
- C. 1975 - 1988. Most theses may be copied upon completion of a Copyright Declaration.
- D. 1989 onwards. Most theses may be copied.

This thesis comes within category D.

☐

This copy has been deposited in the Library of

UCL☐

This copy has been deposited in the University of London Library, Senate House, Malet Street, London WC1E 7HU.

DEVELOPMENT OF CATIONIC LIPIDS FOR GENE DELIVERY SYSTEMS

A Thesis Presented by

John Bosco Chun-Chung Wong

In Partial Fulfilment of the Requirements
For the Award of the Degree of

Doctor of Philosophy

of the

University of London

**Sir Christopher Ingold Laboratories
Department of Chemistry
University College London
20 Gordon Street
London WC1H 0AJ**

June 2006

UMI Number: U593316

All rights reserved

INFORMATION TO ALL USERS

The quality of this reproduction is dependent upon the quality of the copy submitted.

In the unlikely event that the author did not send a complete manuscript and there are missing pages, these will be noted. Also, if material had to be removed, a note will indicate the deletion.



UMI U593316

Published by ProQuest LLC 2013. Copyright in the Dissertation held by the Author.
Microform Edition © ProQuest LLC.

All rights reserved. This work is protected against
unauthorized copying under Title 17, United States Code.



ProQuest LLC
789 East Eisenhower Parkway
P.O. Box 1346
Ann Arbor, MI 48106-1346

Abstract

This thesis describes investigations into the structural requirements of cationic lipids leading to optimal formulations in a non-viral, ternary lipid/peptide/DNA (LID) delivery system.

Initially, the principles behind current strategies of gene therapy are described. A literature review of the synthesis and effectiveness of cationic lipids used for gene therapy is presented. The principles of utilising antibody fragments and integrins for receptor-mediated gene delivery are also described. The lipid/peptide/DNA vector system is introduced and the advantages it possesses are outlined.

The results and discussion starts in Chapter 2, which outlines the synthetic procedures to generate DOTMA lipid analogues. The results of a systematic investigation into the lipid component in the LID vector formulations are presented and discussed. The influence of lipid structural features on the LID transfection efficiencies and the liposome stabilities are outlined. The synthesis of fluorescently-labelled lipids is also described.

The synthesis and biological activity of lipid analogues bearing short polyethylene glycol (PEG) chains are given in Chapter 3. The development of a novel class pH-sensitive PEG lipids is outlined in Chapter 4, and the lipid stabilities over a pH range as well as its influence on transfection efficiencies is presented and discussed.

Synthetic routes to dicationic lipid analogues bearing erythritol and pentaerythritol backbone are presented in Chapter 5, where several strategies are considered. In Chapter 6 synthetic routes toward lipopeptides and immunoliposomes for receptor-mediated gene delivery are outlined.

An overall summary and possible areas of research in future are discussed in Chapter 7. A formal description of the experimental methods and procedures is presented in Chapter 8.

Contents

Abstract	2
Contents	3
Contents of Figures, Tables, Schemes and Charts	8
Abbreviations	13
Acknowledgements	17
Chapter 1 Introduction	18
1. Introduction to Gene Therapy	19
1.1 Vectors for Gene Therapy	19
1.1.1 Viral Vectors	20
1.1.1.1 Retroviral Vectors	20
1.1.1.2 Adenoviral Vectors	20
1.1.2 Non-Viral Vectors	22
1.1.2.1 Cationic Polymers	22
1.1.2.2 Liposomes	23
1.2 Introduction to Liposome-Mediated Gene Delivery	24
1.2.1 Cationic Lipids for Gene Therapy	24
1.2.1.1 Structures of Cationic lipids	25
1.2.1.2 Polymorphism of Lipid Aggregates in Aqueous Solution	34
1.2.1.3 Structures of Cationic Lipid/DNA Complexes	36
1.2.2 Mechanism of Cationic Lipid-Mediated DNA Transfer	40
1.2.2.1 Cell Uptake and Entry	40

1.2.2.2 Endosomal Release of DNA	41
1.2.2.3 Trafficking of DNA to Nucleus	43
1.3 Synthesis of Cationic Lipids for Gene Therapy	44
1.4 Receptor-Mediated Gene Delivery	54
1.4.1 Immunolipoplexes	54
1.4.2 Integrin-Mediated Gene Delivery	56
1.4.3 Lipid (L)/Peptide (I)/ DNA (D) Delivery System	57
1.4.3.1 Proposed Mechanism of LID-mediated Gene Delivery	59
1.4.3.2 Structural Requirements of the Lipid Component in LID Vector System	61
1.5 Aims of Project	62
Chapter 2 Results and Discussion	63
2. DOTMA Lipid Analogues	63
2.1 Synthesis of DOTMA	64
2.2 Synthesis of Unsaturated DHTMA Analogues	65
2.2.1 Syntheses of Hexadecen-1-ol Analogues	66
2.2.1.1 Synthesis of (Z)-Hexadec-11-en-1-ol via Wittig Methodology	66
2.2.1.2 Synthesis of (Z)- and (E)-Hexadec-11-en-1-ol via Reduction Methodology	67
2.2.1.2 Synthesis of (Z)- and (E)-Hexadec-9-en-1-ol	68
2.2.1.3 Synthesis of (Z)- and (E)-Hexadec-13-en-1-ol	69
2.2.2 Synthesis of DHTMA Analogues	71
2.3 Biological Data for Unsaturated DHTMA Analogues	72
2.3.1 The Effect of Double Bond Position on Activity	73
2.3.2 The Effect of Double Bond Geometry on Activity	74
2.3.3 The Effect of Triple Bond on Activity	76

2.3.4 The Effect of DOPE on Transfection Efficiency	77
2.3.5 The Effect of Lipid Concentration on Transfection Efficiency	78
2.3.6 DOTMA vs. C16:1 Lipid Analogue	79
2.3.7 <i>In Vivo</i> Transfection Studies of C16:1 Lipid	81
2.4 Synthesis of Chiral Lipid Analogues	81
2.5 Biological Results for Chiral Lipids	84
2.6 Synthesis of Labelled Lipid Derivatives	85
2.7 Calcein Leakage Experiments	88
2.8 Conclusion	90
Chapter 3 Results and Discussion	91
3. PEG-Lipid Conjugates	91
3.1 Synthesis of PEG-lipid analogues	93
3.2 Biological Data for PEG-Lipid Conjugates	94
3.2.1 Transfection Data for PEG-Lipid Conjugates	94
3.2.2 PEGylated vs. Non-PEGylated Lipids	95
3.2.3 The Effect of Serum on Activity	96
3.2.4 <i>In Vivo</i> Transfection Studies	97
3.3 Conclusion	98
Chapter 4 Results and Discussion	99
4. pH-Sensitive PEG-Lipid Conjugates	99
4.1 Synthesis of pH-Sensitive PEG Lipids	101
4.1.1 Synthesis of PEG-Acetal Linkers	101
4.1.2 Synthesis of PEG-acetal Lipids and Aldehyde Analogue	105
4.2 Hydrolysis Studies of PEG-Acetal Lipids	106

4.3 Biological Data for PEG-Acetal Lipids	108
4.4 Conclusion	113
Chapter 5 Results and Discussion	114
5. Symmetrical Dicationic Lipid Analogues	114
5.1 Synthesis of Dicationic Lipid Analogues I	116
5.1.1 Synthesis of Erythritol Derivative I	116
5.1.2 Synthesis of Pentaerythritol Derivative I	117
5.1.2.1 Route 1	117
5.1.2.2 Route 2	119
5.1.2.3 Route 3	121
5.2 Synthesis of Dicationic Lipid Analogues II	123
5.2.1 Synthesis of Erythritol Derivative II	124
5.2.1.1 Route 1	124
5.2.1.2 Route 2	125
5.2.1.3 Route 3	127
5.2.1.4 Route 4	129
5.3 Conclusion	131
Chapter 6 Results and Discussion	132
6. Lipopeptides and Immunoliposomes	132
6.1 Lipopeptides	133
6.2 Immunoliposomes	136
Chapter 7 Summary and Future Work	141
7.1 Summary	142
7.2 Future Work	143

Chapter 8 Experimental	145
8.1 General Experimental Procedure	146
8.2 Synthesis of DOTMA	148
8.3 Synthesis of DHTMA Analogues	151
8.4 Synthesis of Chiral Lipid Analogues	178
8.5 Fluorescently-Labelled Lipids	183
8.6 PEG-Lipid Conjugates Synthesis	186
8.7 pH-Sensitive PEG-Lipid Conjugates	191
8.8 Symmetrical Dicationic Lipids	202
8.9 Lipopeptides and Immunoliposomes	220
8.10 Biological Formulation and Methods	227
8.11 Biophysical Methods	228
References	230

Contents of Figures, Tables, Schemes and Charts

Figure 1.1.1	21
Figure 1.1.2	22
Figure 1.1.3	23
Figure 1.2.1	24
Figure 1.2.2	26
Figure 1.2.3	27
Figure 1.2.4	28
Figure 1.2.5	29
Figure 1.2.6	29
Figure 1.2.7	30
Figure 1.2.8	31
Figure 1.2.9	32
Figure 1.2.10	33
Figure 1.2.11	34
Figure 1.2.12	36
Figure 1.2.13	37
Figure 1.2.14	38
Figure 1.2.15	39
Figure 1.2.16	40
Figure 1.2.17	42
Figure 1.4.1	54
Figure 1.4.2	55
Figure 1.4.3	56
Figure 1.4.4	57
Figure 1.4.5	59
Figure 1.4.6	60
Figure 1.4.7	61
Figure 2.2.1	66
Figure 2.3.1	76
Figure 2.5.1	82
Figure 2.7.1	88

Figure 3.1	93
Figure 4.1	100
Figure 4.2.1	107
Figure 4.3.1	112
Figure 5.1	115
Figure 7.2.1	143
Figure 7.2.2	144
Figure 7.2.3	144
Figure 7.2.4	144
Table 2.2.1	70
Table 2.2.2	71
Table 2.2.3	72
Table 2.4.1	84
Table 3.1.1	94
Table 4.1.1	104
Table 4.1.2	104
Table 4.1.3	105
Table 4.2.1	108
Table 5.1.1	117
Table 5.1.2	118
Table 5.1.3	121
Table 5.2.1	124
Table 5.2.2	129
Table 6.1.1	134
Table 6.1.2	136
Table 6.2.1	138
Table 6.2.2	139
Table 6.2.3	140
Scheme 1.3.1	44
Scheme 1.3.2	45
Scheme 1.3.3	45

Scheme 1.3.4	46
Scheme 1.3.5	47
Scheme 1.3.6	47
Scheme 1.3.7	48
Scheme 1.3.8	48
Scheme 1.3.9	49
Scheme 1.3.10	49
Scheme 1.3.11	50
Scheme 1.3.12	51
Scheme 1.3.13	51
Scheme 1.3.14	52
Scheme 1.3.15	53
Scheme 1.3.16	53
Scheme 2.1.1	64
Scheme 2.1.2	65
Scheme 2.2.1	67
Scheme 2.2.2	68
Scheme 2.2.3	68
Scheme 2.2.4	69
Scheme 2.2.5	70
Scheme 2.2.6	70
Scheme 2.2.7	71
Scheme 2.2.8	72
Scheme 2.4.1	83
Scheme 2.4.2	83
Scheme 2.6.1	86
Scheme 2.6.2	87
Scheme 3.1.1	93
Scheme 4.1.1	101
Scheme 4.1.2	102
Scheme 4.1.3	102
Scheme 4.1.4	103
Scheme 4.1.5	104
Scheme 4.1.6	104

Scheme 4.1.7	105
Scheme 4.1.8	106
Scheme 5.1.1	116
Scheme 5.1.2	118
Scheme 5.1.3	119
Scheme 5.1.4	119
Scheme 5.1.5	120
Scheme 5.1.6	120
Scheme 5.1.7	122
Scheme 5.1.8	122
Scheme 5.1.9	123
Scheme 5.2.1	124
Scheme 5.2.2	125
Scheme 5.2.3	126
Scheme 5.2.4	127
Scheme 5.2.5	128
Scheme 5.2.6	129
Scheme 5.2.7	131
Scheme 6.1.1	133
Scheme 6.1.2	134
Scheme 6.1.2	135
Scheme 6.1.3	136
Scheme 6.2.1	137
Scheme 6.2.2	137
Scheme 6.2.3	138
Scheme 6.2.4	139
Scheme 6.2.5	140
Chart 2.3.1	73
Chart 2.3.2	74
Chart 2.3.3	75
Chart 2.3.4	76
Chart 2.3.5	77

Chart 2.3.6	78
Chart 2.3.7	79
Chart 2.3.8	80
Chart 2.3.9	80
Chart 2.3.10	81
Chart 2.5.1	84
Chart 2.5.2	85
Chart 2.7.1	89
Chart 2.7.2	89
Chart 3.2.1	94
Chart 3.2.2	95
Chart 3.2.3	96
Chart 3.2.4	97
Chart 3.2.5	98
Chart 4.3.1	109
Chart 4.3.2	110
Chart 4.3.3	111
Chart 4.3.4	111

Abbreviations

bEND3	Mouse endothelial cells
BGTC	Bis(guanidinium)-tren-cholesterol
Boc	<i>tert</i> -Butyloxycarbonyl group
br	Broad
BTEAC	Benzyltriethylammonium chloride
<i>n</i> BuLi	<i>n</i> -Butyllithium
<i>t</i> Bu	<i>tert</i> -Butyl group
BVEP	(<i>R</i>)-1,2-Di- <i>O</i> -(1 <i>Z</i> ,9 <i>Z</i> -octadecadienyl)-glyceryl-3- <i>ω</i> -methoxy-polyethylene glycolate
C16:1	Lipid containing hexadecenyl (unsaturated) hydrocarbon chains
Cbz	Benzyloxycarbonyl group
CDAN	<i>N</i> -1-Cholesteryloxycarbonyl-3,7-diazanonane-1,9-diamine
CHCl ₃	Chloroform
Chol	Cholesterol
δ	Chemical shift in ppm
d	Doublet
Da	Dalton(s)
Dbe	2-Acetyldimedone group
DCC	Dicyclohexylcarbodiimide
DC-Chol	3β-[<i>N</i> -(<i>N</i> ', <i>N</i> '-Dimethylaminoethane)-carbamoyl]cholesterol
dd	Doublet of doublets
DDAB	Didodecyl dimethylammonium bromide
DHDEAB	<i>N,N</i> -Di-(hydroxyethyl)- <i>N,N</i> -di-(<i>n</i> -hexadecyl)ammonium bromide
DHTMA	2,3-Di-[(<i>Z</i>)-hexadec-11-enyloxy]propyl- <i>N,N,N</i> -trimethylammonium iodide
DMAP	Dimethylaminopyridine
DMF	<i>N,N</i> -Dimethylformamide
DMPC	Dimyristoylphosphatidylcholine
DMRIE	1,2-Dimyristyloxypropyl-3-dimethyl-hydroxyethylammonium bromide
DMSO	Dimethylsulfoxide
DMTM(Gly)	Dimyristoyl bis(<i>N,N,N</i> -trimethylglycyl)tetraester diiodide
DNA	Deoxyribonucleic acid

DOGS	Dioctadecyldimethylammonium bromide
DOHBD	<i>N'</i> -Bis (2-hydroxyethyl)-2, 3-bis (9 <i>Z</i> -octadecenoyloxy)-1, 4-butanediaminium iodide
DOPA	Dioleoylphosphatidic acid
DOPE	Dioleoyl-L- α -phosphatidylethanolamine
DORI	1,2-Dioleoyloxypropyl-3-dimethyl-hydroxyethylammomium bromide
DORIE	1,2-Dioleoyloxypropyl-3-dimethyl-hydroxyethylammomium bromide
DOSPA	2,3-Dioleyloxy- <i>N</i> -[2-(spermine-carboxamido)ethyl]- <i>N,N</i> -dimethyl-1-propanaminiumtrifluoroacetate
DOTAP	1,2-Dioleoyloxy-3-trimethylammonium propane
DOTM(Gly)	Dioleoyl bis(<i>N,N,N</i> -trimethylglycyl)tetraester diiodide
DOTMA	<i>N</i> -[2,3-(Dioleyloxy)propyl]- <i>N,N,N</i> -trimethylammonium chloride
DSPE	Distearoylphosphatidylethanolamine
DSTAP	1,2-Distearoyl-3-trimethylammonium propane
dt	Doublet of triplets
DTBP	2,6-Di- <i>tert</i> -butylpyridine
EDCI·HCl	<i>N</i> -(3-Dimethylaminopropyl)- <i>N'</i> -ethylcarbodiimide hydrochloride
eq	Molar equivalent
ESMS	Electrospray mass spectroscopy
Fab'	Antibody fragment
FAB	Fast atom bombardment
Fmoc	9-Fluorenylmethyloxycarbonyl group
GAP-DLRIE	<i>N</i> -(3-Aminopropyl)- <i>N,N</i> -dimethyl-2,3-bis(dodecyloxy)-1-propanaminium bromide
GAP-DORIE	<i>N</i> -(3-Hydroxypropyl)- <i>N,N</i> -dimethyl-2,3-bis(dodecyloxy)-1-propanaminium bromide
h	Hour(s)
H _{II}	Inverted hexagonal lipid phase
HAE	Human airway epithelial cells
HBE	Human bronchial epithelial cells
HDEAB	<i>N</i> -Hydroxyethyl- <i>N,N</i> -di-(<i>n</i> -hexadecyl)ammonium bromide
HexAce	<i>N,N'</i> -Diacetyl- <i>N,N,N',N'</i> -tetramethyl-1,6-hexanediamine
HMPA	<i>N,N,N',N'</i> -Hexamethylphosphoramide
HOBt	1-Hydroxy-1 <i>H</i> -benzotriazole
HRES	High resolution electrospray

HRFAB	High resolution fast atom bombardment
ID	Peptide/DNA vector
IR	Infra-red
[K] ₁₆	16 Lysine residues
kb	Kilo base(s)
LD	Lipid/DNA vector
LiAlH ₄	Lithium aluminum hydride
LID	Lipid/peptide/DNA vector
Lys	Lysine
L α	Bilayer lipid phase
μ mol	Micromoles
m	Medium intensity (IR)
m	Multiplet (NMR)
mg	Milligram(s)
m.p.	Melting point
<i>m/z</i>	Mass-to-charge ratio
MAb	Monoclonal antibody
Mal	Maleimidyl group
MeI	Iodomethane
mg	Milligram(s)
min	Minute(s)
mmol	Millimole(s)
NHS	<i>N</i> -Hydroxysuccinimide
NLS	Nuclear localisation sequence
nm	Nanometer(s)
NMM	<i>N</i> -Methylmorpholine
NMO	<i>N</i> -Methylmorpholine- <i>N</i> -oxide
NMR	Nuclear magnetic resonance
OEPC	Diorthoester phosphocholine
PAGA	Poly[α -(4-aminobutyl)]-l-glycolic acid
PC	Phosphatidylcholine
PE	Phosphatidylethanolamine
PEG	Polyethylene glycerol
PEG-CerC	PEG-ceramide conjugates
PEI	Polyethyleneimine

PIL	PEGylated immunoliposomes
POD	PEG-diorthoester conjugates
POPC	1-Palmitoyl-2-oleoyl- <i>sn</i> -glycero-3-phosphocholine
PVSMC	Primary porcine vascular smooth muscle cells
RES	Reticuloendothelial system
R _f	Retention factor
RLU	Relative light units
RNA	Ribonucleic acid
rt	Room temperature
s	Singlet (NMR)
s	Strong intensity (IR)
SAINT	Synthetic Amphiphile INTeraction
SAR	Structural-activity relationship
Ser	Serine
SPLP	Stabilised plasmid-lipid particle
t	Triplet (NMR)
TBDPS	<i>tert</i> -Butyldiphenylsilyl group
T _c	Chain-melting phase transition temperature
TFA	Trifluoroacetic acid
THF	Tetrahydrofuran
THP	Tetrahydropyran group
TLC	Thin layer chromatography
TPAP	Tetra- <i>n</i> -propylammonium perruthenate
UV	Ultra-violet
w	Weak (IR)
wt/wt	Weight/weight ratio
λ _{max}	Maximum absorbance (UV)

Acknowledgements

I would like to thank my supervisor, Dr. Helen Hailes, for her guidance, encouragement and support throughout my project. Thanks also to Dr. Alethea Tabor and Dr. Stephen Hart (ICH) for their advice.

I am grateful to Dr. Supti Sarkar (Biomedical Engineering, UCL) who conducted the calcein release experiments, and to Dr. Stephanie Grosse (ICH) and Dr. Aris Tagalakakis (ICH) for carried out the lipid testing. My gratitude also to John Hill (mass spectroscopy, UCL) and Dr. Abil Aliev (NMR, UCL) for their technical support.

Finally extending my thanks to the Hailes and Tabor group past and present, especially Mackie, Val, Jimmy, Firouz and Martin. To Eric and KF for the overnight PS2 game sessions. Finally, I would like to thank my parents and Franz for their love and support.

CHAPTER 1

INTRODUCTION

1. Introduction to Gene Therapy

Since the discovery of DNA and the genetic information it encodes, the treatment of diseases at genetic level has become an attractive alternative to traditional drug and vaccine therapies. With the successful interpretation and annotation of data available from the Human Genome Project,^{1,2} new links can be made between particular genes and diseases. This information should accelerate the utilisation of gene therapy as a therapeutic strategy.

Gene therapy refers to the delivery of genetic material to a cell in order to correct a genetic defect by expressing a specific protein. It has been regarded by many as a potential revolution in medicine, as gene therapy is aimed at treating or eliminating the cause of disease, whereas most current drugs treat the symptoms. Gene therapy offers an exciting therapeutic potential for diseases such as cancer,³ cystic fibrosis,^{4,5} severe immunodeficiency disease,⁶ and acquired immunodeficiency syndrome.⁷ In spite of all the clinical interests, a major challenge for therapeutic gene transfer is the development of safe and viable delivery agents (vectors).⁸ It is clear that gene therapy will become the key therapeutic tool only when such delivery vector systems are fully developed.

1.1 Vectors for Gene Therapy

The delivery of genetic materials (DNA, RNA or oligonucleotides) is problematical for several reasons. Firstly, the electrostatic repulsion between the cell surface and nucleic acid inhibits cell entry. In addition, DNA cannot be administered alone orally or by intravenous injections, due to enzymatic or physical degradation.⁹ To overcome these barriers, gene delivery vectors are needed for genetic information to be transported into the cells and translated in the desired subcellular compartment.¹⁰ Ideally, vectors should be efficacious, non-toxic, and have unlimited packing capacity. It is also desirable to produce vectors in large-scale at low cost, that are sufficiently stable for long-term storage. Most of the current vectors can be divided into two groups, viral and non-viral.

1.1.1 Viral Vectors

Viral vectors are currently the vectors of choice for clinical use, as the transfection efficiency of these vectors is high. Viruses are particularly efficient because they have evolved specific mechanisms to deliver foreign DNA into host cells. However, viral vectors suffer several major disadvantages, such as immunogenicity,¹¹ restriction to dividing cells, and severe problems have been reported in clinical trials.^{11,12} A number of viruses are being developed as gene delivery vectors, with retroviruses and adenoviruses being those most widely used.

1.1.1.1 Retroviral Vectors

Retroviruses are RNA viruses which replicate through a DNA intermediate, where the viral DNA integrates randomly into the host genome.¹³ Retroviral vectors have a wide host range and as a result of their integration into the host genome, allow permanent expression of the transgene without inducing an immune response.^{13,14} Retroviruses are very efficient at gene transfer, with some vectors transfecting close to 100% of the target cells.¹⁵ However, they have a low RNA capacity with maximum insertion of around 8 kilo bases (kb), limiting the size of therapeutic genes to be delivered. In addition, retroviruses will only transduce cells that are proliferating, limiting their potential for *in vivo* gene transfer.¹³ Furthermore, adverse side effects such as insertional mutagenesis could occur.¹² These disadvantages have prompted the need to develop more flexible and much safer vector systems.

1.1.1.2 Adenoviral Vectors

Adenoviruses are double-stranded DNA viruses with a capacity of up to 36 kb. They are ideal for gene therapy because they can be readily purified, grown in large quantities, and can infect a wide range of proliferating and non-proliferating cells.¹⁴ Entry into cells occurs by receptor-mediated endocytosis, with very high transduction efficiency (Figure 1.1.1). Because they replicate into the host cell nucleus without integration into the host genome, expression from adenoviruses is transient, making it ideal for gene delivery where long-term expression is not required.¹⁴

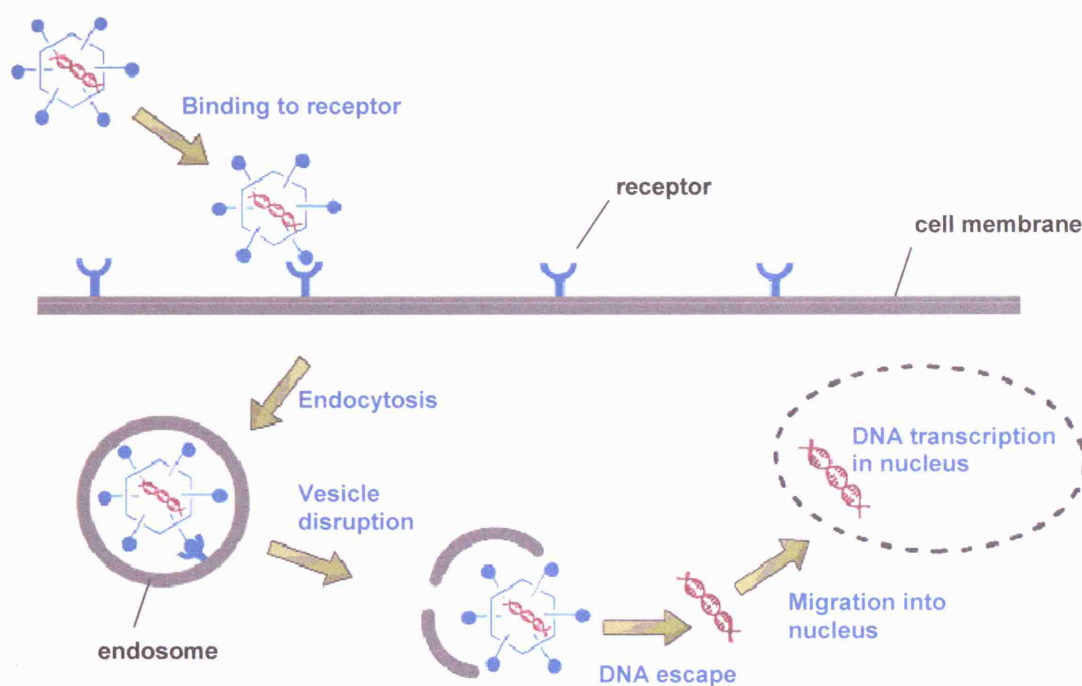


Figure 1.1.1 Schematic representation of adenovirus gene delivery

A major disadvantage of adenoviral vectors for gene delivery is the associated toxic effects induced by the viral proteins.¹⁵ This can cause the destruction of vector-transduced cells, and also lead to local tissue damage and inflammation.^{16,17} Repeat administration of adenoviral vectors also produce strong secondary inflammatory responses.¹⁸ It has been demonstrated that although repeat administration of adenoviruses is possible, the gene transfer becomes progressively less efficacious as a result. Adenoviruses have also been implicated in causing cardiotoxicity and brain damage, as well as causing neurogenic and pulmonary inflammation at high doses.^{19,20} In fact, adenoviral vectors were accounted for the first death in clinical gene therapy trials,²¹ highlighting the potential dangers of gene therapy if the vector chosen is unsuitable for the patients' needs. Limitations of viral vectors, in particular their safety concerns, have led to the evaluation and development of synthetic non-viral vectors.

1.1.2 Non-Viral Vectors

Synthetic non-viral vectors have several advantages over viruses, including significantly lower toxicity and immunogenicity, unlimited packing capacity, and ease of large-scale preparation. An increasing number of clinical trials using non-viral vector systems have been reported, illustrating their potential as viable alternatives to the viral approach.⁸ There are currently two main types of non-viral vectors: cationic polymers and cationic liposomes.

1.1.2.1 Cationic Polymers

Polyamines that are protonatable at physiological pH have been employed as gene carriers.²² They can be combined with the negatively charged DNA molecules to form complexes (polyplexes) that are capable of condensing the DNA to a relatively small size.²³ A variety of polymeric structures have been used as gene delivery vectors, including polylysine (**1**) and branched polyethyleneimine (PEI, **2**) (Figure 1.1.2).²⁴ More recently, multivalent polymers such as dendrimers²⁵ and poly[α -(4-aminobutyl)]-L-glycolic acid (PAGA)²⁶ have also been utilised. Polyplexes prevent the degradation of DNA by serum nucleases,²⁷ and facilitate cell entry *via* endocytosis.²⁸ Their main drawbacks are the lack of mechanisms for releasing the DNA from the endosomes before lysosomal enzymatic degradation,²⁹ and considerable toxicity associated with the synthetic vector.²²

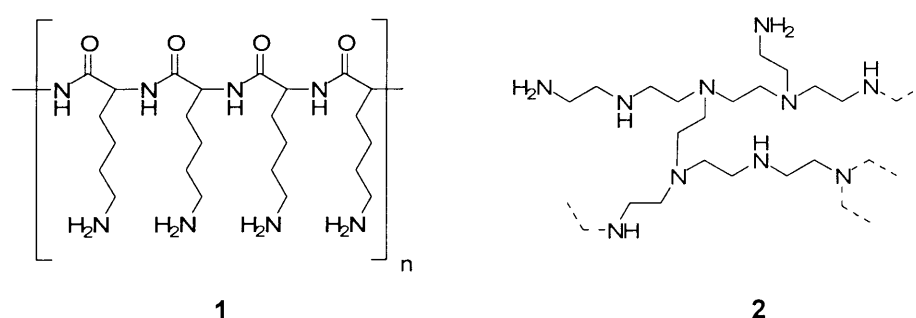


Figure 1.1.2

1.1.2.2 Liposomes

Liposomes are spherical colloidal particles formed from self-aggregated amphiphilic lipid molecules suspended in aqueous solution. These vesicles are curved and self-closed molecular bilayers in which the hydrophobic part of the lipids (e.g. hydrocarbon chains) forms the hydrophobic interior of the bilayer, and the hydrophilic part (polar headgroup) is in contact with the aqueous phase. Liposomes have different morphologies based upon their composition and the formulation method.^{30,31} Formulations frequently used for DNA delivery include lamellar structures such as small unilamellar vesicles (SUVs, ≤ 80 nm) and large unilamellar vesicles (LUVs, 80-400 nm).³¹ Typically, natural occurring lipids are either anionic (e.g. dioleoylphosphatidic acid, DOPA, **3**), neutral (e.g. cholesterol, Chol, **4**), or zwitterionic (e.g. 1-palmitoyl-2-oleoyl-*sn*-glycero-3-phosphocholine, POPC, **5**) (Figure 1.1.3).

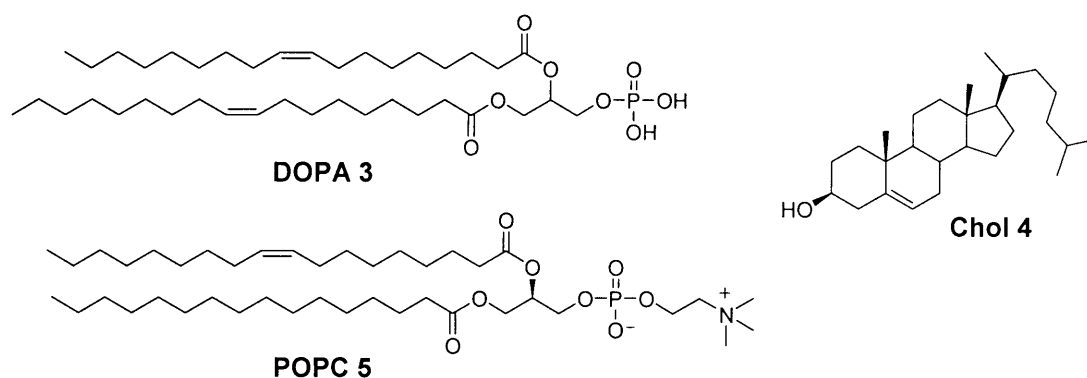


Figure 1.1.3

Liposomes have previously been investigated as a drug carrier for drug delivery systems.³²⁻³⁴ Although conventional liposomes have also been used in gene delivery, their limited efficiency in encapsulating DNA molecules and consequently low transfection levels has limited their potential as gene delivery vectors.^{35,36} The discovery that synthetic cationic liposomes can entrap and complex DNA molecules, led to the pioneering work of using cationic liposomes as gene carrier.³⁷ Since then a large number of cationic lipids, known as cytofectins, have been synthesised and studied for gene delivery.³⁸ Cationic liposomes have several advantages over viral vectors, including the lack of immunogenicity, low toxicity, ability to package large DNA molecules, and ease of preparation. However, cationic liposomes in general

had far lower transfection efficiencies and gene expression levels compared to viral vectors.¹³

1.2 Introduction to Liposome-Mediated Gene Delivery

1.2.1 Cationic Lipids for Gene Therapy

The use of cationic lipids for DNA delivery was initiated by Felgner and co-workers in 1987.³⁷ A combination of two lipids was used to transfect cells: a cationic lipid *N*-[2,3-(dioleoyloxy)propyl]-*N,N,N*-trimethylammonium chloride (DOTMA, **6**), and naturally occurring phospholipid dioleoyl-L- α -phosphatidylethanolamine (DOPE, **7**) (Figure 1.2.1). The formulation has since been commercialised as LipofectinTM.^{37,39} The ability of DOTMA to mediate transfections was attributed to certain properties, including:³⁷

- 1) Electrostatic interactions between the positively charged liposome and the negative charged DNA, which results in an efficient condensation of the nucleic acid;
- 2) The resulting cationic liposome/DNA complexes (lipoplexes) exhibit a net positive charge, promoting their interactions with the anionic or zwitterionic biological membranes;
- 3) Fusogenic properties of lipoplexes induce fusion and/or destabilisation of targeted cell membranes, thus facilitating the intracellular release of complexed DNA.

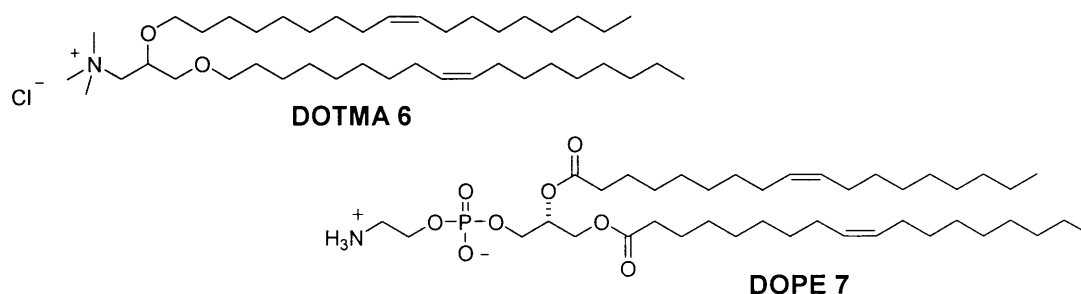


Figure 1.2.1

Cationic lipids are sometimes formulated into liposomes alone, but more often they are mixed with a neutral co-lipid such as DOPE (**7**). The co-lipids play

many roles in lipoplexes gene transfer, including improved fusogenicity and/or endosomolytic activity of the liposome component.⁴⁰⁻⁴² These functions facilitate DNA release into the cytoplasm.

1.2.1.1 Structures of Cationic lipids

Over the last few years a significant amount of work has been devoted to the synthesis of novel cationic lipids, but all have in common a cationic headgroup covalently attached to a hydrophobic moiety through a linker.³⁸ Different cationic lipids have been designed and synthesised with the purpose of increasing gene transfection levels, and were found to exhibit a range of efficiencies when mediating gene transfer.

DOTMA analogues have achieved the most widespread use in cationic liposome formulations. The main analogues are DOTAP (8),⁴³ DMRIE (9),⁴⁰ DORIE (10),⁴⁰ DOSPA (11),⁴⁴ and GAP-DLRIE (12) (Figure 1.2.2).⁴⁴ These lipids are based on the glycerol backbone. Ren *et al.* produced a series of structural analogues of DOTMA and DOTAP to investigate the structural properties for the best level of transfections.^{45,46} The effect of modifying the relative distance between the hydrophobic chains, or between the hydrophobic domain and the cationic headgroup by lengthening the backbone was examined. From their investigations, they concluded that the lipids that gave higher transfection activities *in vivo* were based on the glycerol backbone, where the cationic headgroup and the neighbouring aliphatic chains are in a 1,2-relationship.⁴⁷ However, their *in vitro* activities were not significantly affected by these structural variations.

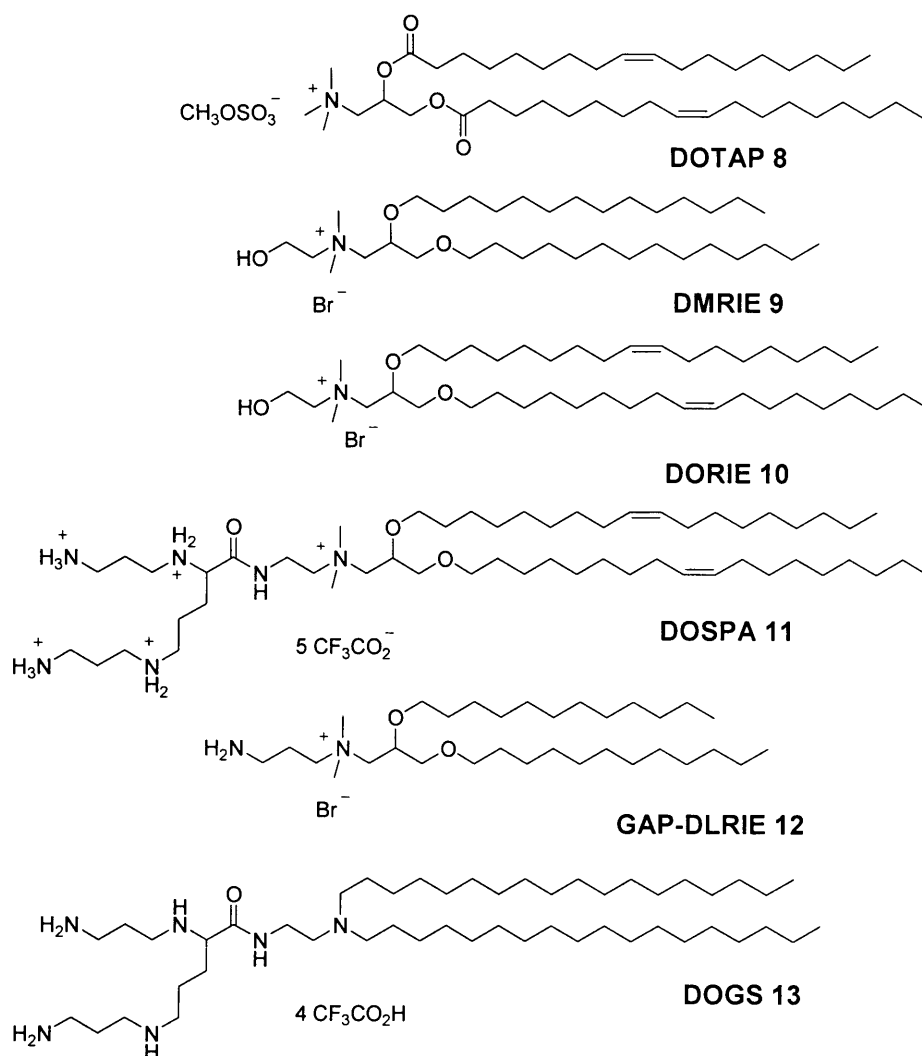


Figure 1.2.2

The cationic lipids DMRIE (9) and DORIE (10) were developed by Felgner *et al.* for a structure-activity relationship (SAR) vector study (Figure 1.2.2).⁴⁰ The hydroxyl group in DMRIE and DORIE is believed to increase the condensation of DNA with liposomes and improve the interaction of the lipoplexes with cellular membranes, leading to greater activity than DOTMA and DOTAP for *in vitro* and *in vivo* applications.⁴⁰ Similarly, lipids that are composed of one or more protonatable amines have pH-buffering properties, which may increase their ability to condense and protect DNA, thus increasing their transfection activities.^{41,48} The lipopolyamine DOGS (13), which was developed by Behr and co-workers, has achieved widespread applications under the tradename LipofectamTM (Figure 1.2.2).⁴⁸ The first cationic lipid containing quaternary amine and protonatable amines in the headgroup is DOSPA (11).⁴⁹ The formulation of DOSPA combined with co-lipid DOPE, called

LipofectAmineTM, showed a high level of transfection activity in different cell types.⁵⁰ Another successful gene delivery cationic lipid GAP-DLRIE (**12**) contains a primary amine, a quaternary amine, and didodecyl chains (Figure 1.2.2).⁴⁴ GAP-DLRIE demonstrated lower toxicity and higher transfection activity than DOSPA and DOTMA in both CFT1 cells and mice lungs.⁴⁴

Another popular hydrophobic moiety for cationic lipids is naturally occurring cholesterol. Huang and co-workers introduced DC-Chol (**14**), which contains a cholesterol skeleton and biodegradable carbamate linker (Figure 1.2.3).⁵¹ The low cellular toxicity of DC-Chol led it to be the first cationic lipid used for clinical trials.⁵² Other cholesterol-based lipids such as BGCT (**15**) and CDAN (**16**) have shown remarkable activities *in vitro* and *in vivo* (Figure 1.2.3).⁵³⁻⁵⁵

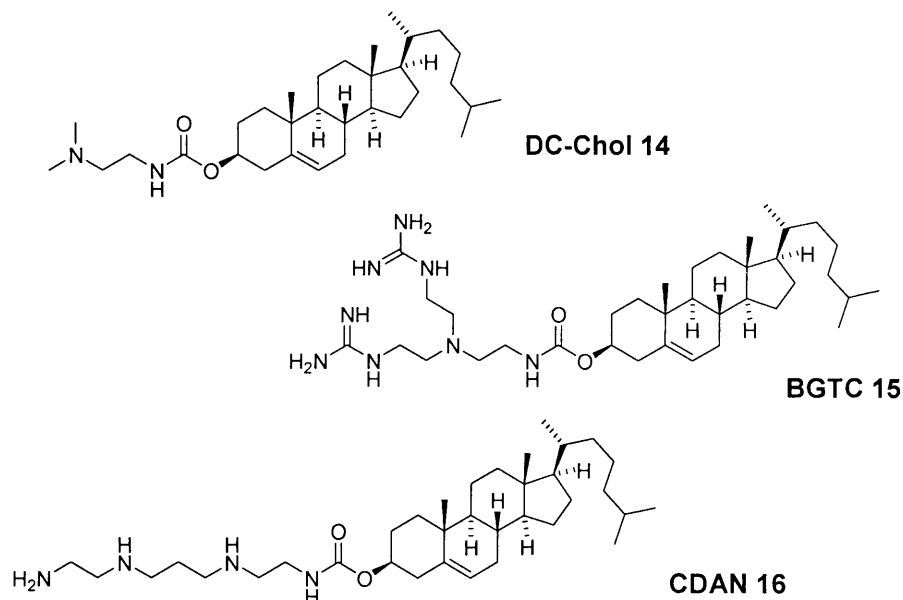


Figure 1.2.3

The vast majority of successful cytofectins employed in gene therapy are based on glycerol or cholesterol backbones, which is perhaps not surprising since many naturally occurring lipids are also based on these carbon-skeletons. However, the production of novel cationic lipids may be advantageous in terms of developing analogue diversity. For example, the formulation of ammonium-based lipid DDAB (**17**) and DOPE has proved successful and has since been commercialised as LipofecAceTM (Figure 1.2.4).⁵⁶ Engberts and co-workers also produced a series of

pyridinium amphiphiles (SAINTs, **18a** and **18b**).⁵⁷ When co-formulated with DOPE, these lipids displayed greater transfection efficiencies and reduced cytotoxicities in COS-7 cells when compared with LipofectinTM.⁵⁸ Furthermore, Chaudhuri and co-workers reported the synthesis of cytofectins bearing a conformationally strained cyclic headgroup (**19**, Figure 1.2.4).⁵⁹ These lipids showed significant enhancement in gene transfections across mouse lungs compared with their open head analogues.⁵⁹

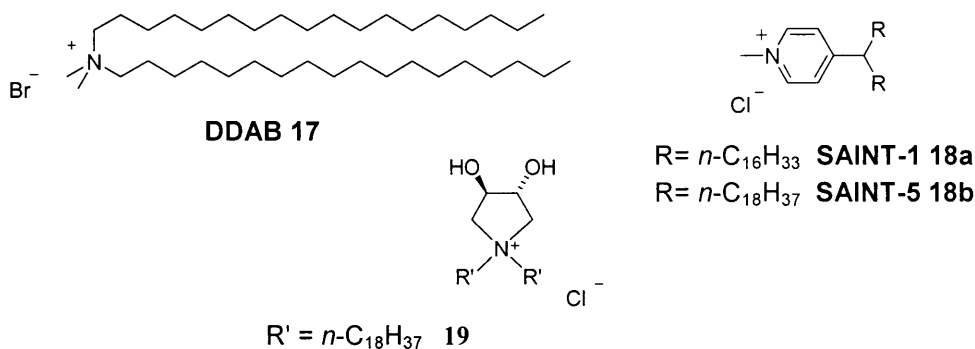


Figure 1.2.4

Most of the lipids with linear hydrocarbons have two symmetrical alkyl chains in the hydrophobic domain. Usually these alkyl chains are either saturated or mono-unsaturated, ranging from C8:0 to C18:1. The effect of chain length and degree of unsaturation on transfection activity has been investigated in several studies. Felgner *et al.* examined the modification of chain length in a homologous series of hydroxyethyl quaternary ammonium derivatives.⁴⁰ They observed that the chain length can influence the transfection activity *in vitro* (DMRIE **9**>DORIE **10**>**20a**>**20b**) (Figure 1.2.5).⁴⁰ Ferrari and co-workers also produced a series of GAP-DLRIE derivatives to study the influence of alkyl chain length and degree of unsaturation, with GAP-DLRIE (**12**) and its C-14 unsaturated derivative GAP-DMORIE (**21b**) being most active *in vitro* (Figure 1.2.5).⁶⁰ Their results suggested that the higher transfection levels of GAP-DMORIE against its saturated analogue **21a** may be attributed to its enhanced membrane fluidity.⁶⁰

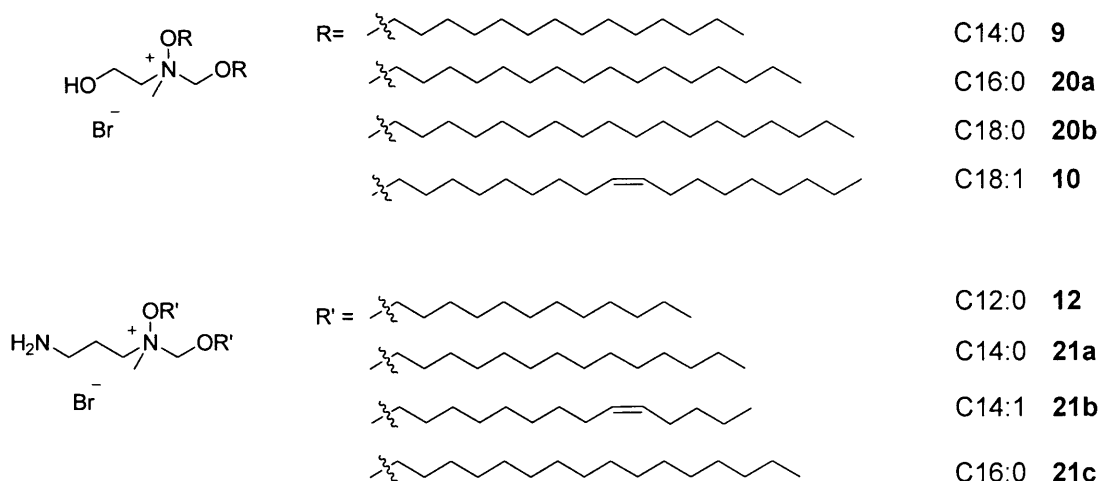


Figure 1.2.5

There are limited systematic reports in the literature surveying the effect of geometry of the unsaturated double bond, although these reports have indicated that the double bond configuration has some influence on the transfection activity. For example, van der Woude and co-workers reported their syntheses of SAINT derivatives **22a** and **22b**, containing oleyl chains with pure *cis* or *trans* double bond orientation (Figure 1.2.6).⁶¹ When co-formulated with DOPE, the *trans* derivative (**22b**) was found to be more favourable at transfecting COS-7 cells.⁶¹ In contrast to this, Obika *et al.* showed that the formulation of DOPE mixed with cationic triglycerides bearing *cis* oleoyl chains (**23a**) was more active in transfecting CHO cells than its *trans* analogue (**23b**).⁶² This contradiction in trends suggested that activities displayed by cationic lipids with different double bond geometry may be system and target dependent.

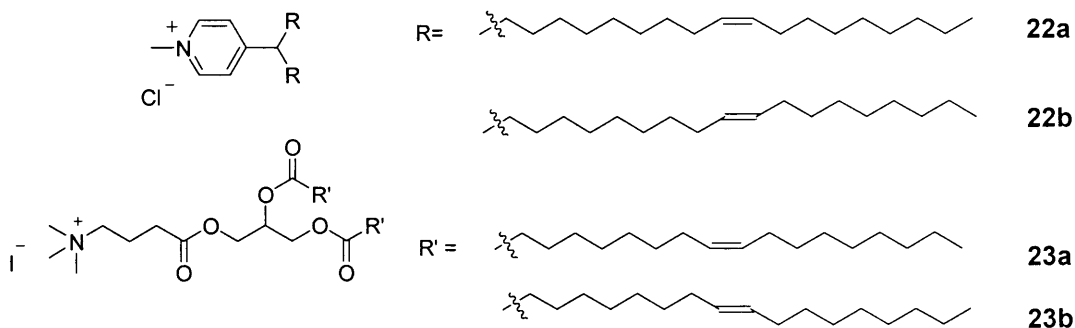


Figure 1.2.6

More recently, Miller and co-workers have demonstrated that modifications to position and degree of unsaturation on alkyl chains can influence activity.⁶³ They synthesised a series of DOTAP analogues with unsaturated fatty acid C18 chains, containing a single alkyne bond at the 4-, 9- and 14-positions (**24a-24c**, Figure 1.2.7). When co-formulated with cholesterol, DS(14-yne)TAP (**24c**) exhibited the highest transfection levels both *in vitro* and *in vivo*, and with less associated toxicity when compared with DOTAP/Chol formulation.⁶³ X-ray diffraction studies suggested that DS(14-yne)TAP formed more stable liposomes and lipoplexes near physiological temperatures compared with DOTAP, making it better to protect the DNA molecules from nuclease degradation during intracellular trafficking. Additionally, this vector system was also designed such that liposomal disruption occurred at physiologically assessable temperatures, so that the transfection efficiency of the lipid was not compromised.⁶³

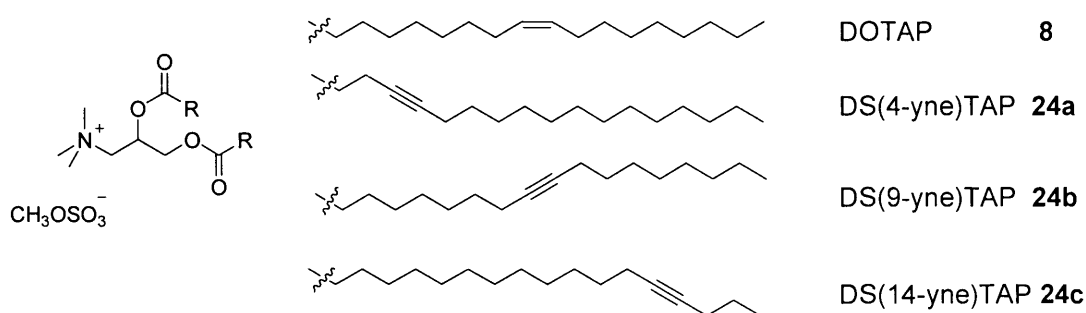


Figure 1.2.7

An increasing number of dicationic ammonium compounds have been reported for gene delivery that possess significant activity.⁶⁴ These bisquaternary lipids, also known as cationic gemini surfactants, usually contain two quaternary ammonium headgroups and two aliphatic chains, linked by a rigid or flexible spacer. In general, bisquaternary ammonium surfactants showed a higher biological activity than the corresponding monomers in a wide range of cell types, which was attributed to their unique physiochemical interactions with DNA molecules.⁶⁴ Rosenzweig *et al.* synthesised a series of gemini vectors, with HexAce (**25**) displaying the greatest activity in BHK-21 cells (Figure 1.2.8).⁶⁵ When co-formulated with DOPE, these bisquaternary compounds exhibited transfection activity comparable to LipofectinTM and LipofecAceTM.⁶⁵ Aberle and co-workers also reported the biodegradable and potentially non-toxic cytofectins DMTM(Gly) (**26a**) and DOTM(Gly) (**26b**).⁶⁶ The

pentaerythritol backbone was introduced in order to utilise biodegradable ester linkages between both headgroups and backbone, and hydrophobic tails and backbone.⁶⁶ The symmetrical dicationic *N,N'*-bis(hydroxyethyl) lipid analogue DOHBD (**27**) developed by Nantz *et al.* was proved to be successful when formulated with DOPE, and is now marketed as TfxTM.^{67,68} More recently, Bombelli *et al.* reported the formulation of gemini surfactant SS-1 (**28**) mixed with co-lipid 1,2-dimeyristoyl-*sn*-glycero-3-phosphocholine (DMPC), and the resulting agent was efficient at transfecting different cell types.⁶⁹ Their results demonstrated that the structure and stereochemistry of the spacer, plays a crucial role in the complexation capability and the transfection efficiency of the liposomes.⁶⁹ Furthermore, in a detailed SAR study, Buijnsters and co-workers synthesised several gemini vectors bearing a tartaric acid backbone.⁷⁰ The lysine-containing surfactant **29** showed activity in CHO-K1 cells, but was accompanied by considerable cytotoxicity (Figure 1.2.8).⁷⁰

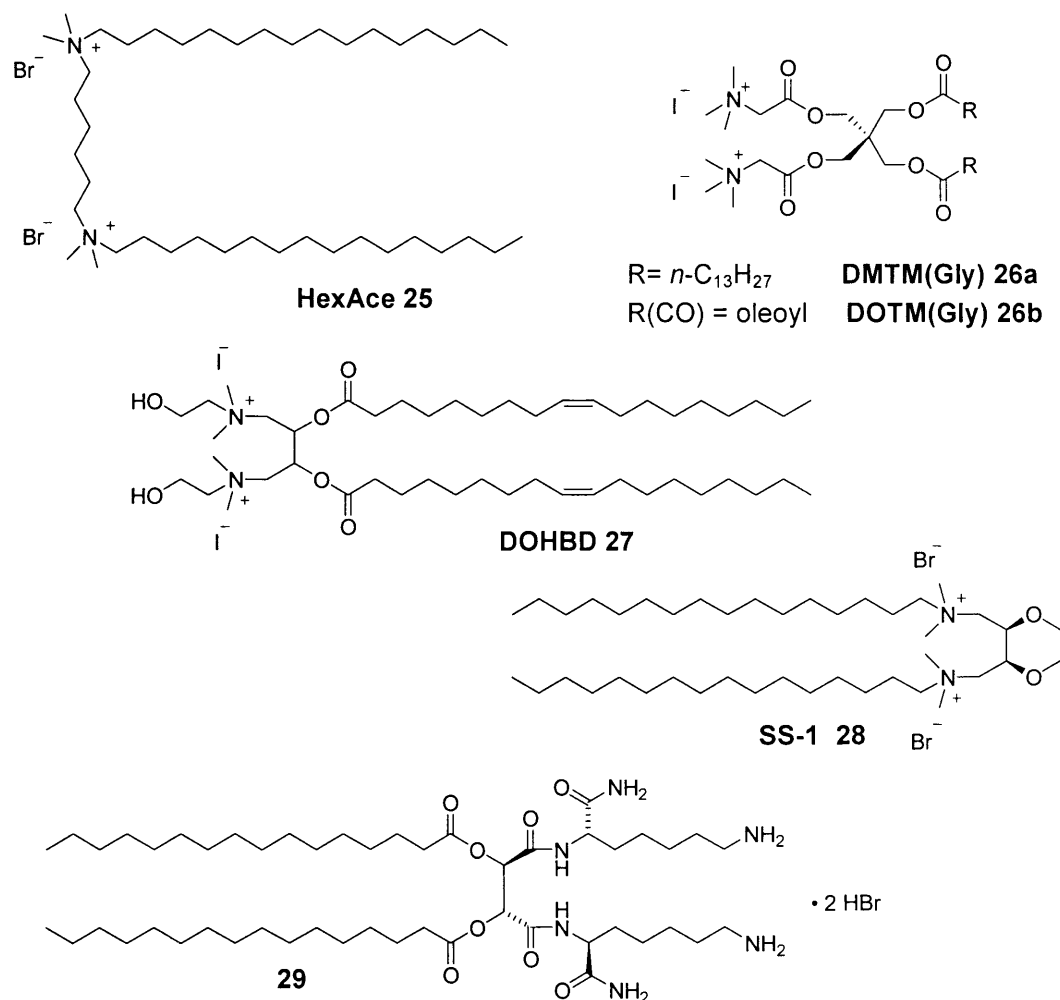


Figure 1.2.8

The conjugation of polyethylene glycol (PEG) polymers to lipids has many advantages compared to conventional lipoplex formulation, including enhanced stability and aqueous solubility, reduced non-specific interactions, improved biodistribution, and increased circulation lifetime for *in vivo* applications.^{71,72} Hong *et al.* reported that the mixing of a small amount (<1 mol%) of PEG-DSPE (**30**) in cationic liposome/DNA complexes resulted in the formation of stealth lipoplexes which were stable to prolonged storage time and had a long circulation time, while maintaining their biological activity.^{73,74} However, it was demonstrated that higher mol% of PEG-lipids would induce steric blocking and poor leakage of lipoplexes leading to reduced cellular uptake and gene expression.⁷⁵ A potential solution to circumvent this problem was to employ PEG-lipid conjugates that would allow the cleavage of PEG polymers in order to re-establish the electrostatic interactions between cell membranes and lipoplexes, thus favouring the transfection. Cullis and co-workers utilised the stabilised plasmid-lipid particle (SPLP) systems, which consists of cationic liposome/DNA complexes mixed with high levels (10 mol%) of PEG-ceramide lipid (**31**) (Figure 1.2.9).⁷⁶ A wide range of circulation half-time (1 min to 13 days) were achieved by modification of the chain length on the hydrophobic moiety (C8 to C24).⁷⁶ The SPLPs were found to be very uniform in size, and could be stored for up to 12 months with no loss in activity. *In vitro* and *in vivo* transfections of SPLPs were comparable or moderately better than cationic liposome/DNA complexes alone.⁷⁷

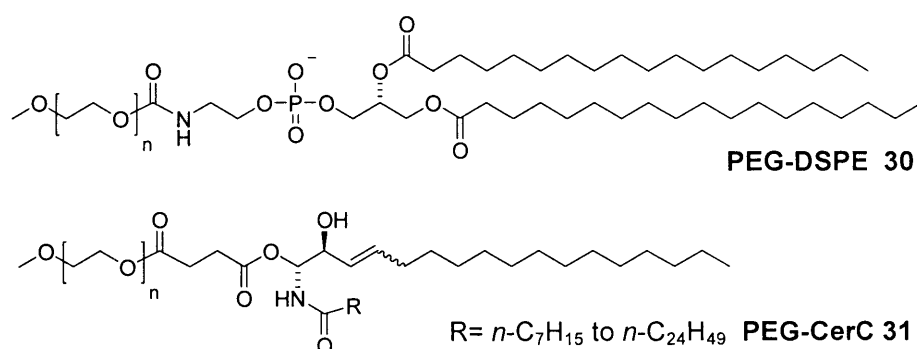


Figure 1.2.9

Several delivery systems employing pH-triggered release of PEG polymers have been described. Thompson and co-workers produced the acid-labile PEG-lipid BVEP (**32**) formulated in stabilised liposomes containing DOPE (Figure 1.2.10).⁷⁸⁻⁸⁰

Acid-catalysed hydrolysis of the vinyl ether bonds at pH 4.5 resulted in removal of the PEG moiety, after which the liposomes become more fusogenic.⁷⁹ However, their biophysical release studies indicated that the release half-time at pH 4.5 was approximately 4 hours, making the formulation too stable for rapid and efficient triggered release in DNA delivery.^{79,80} Szoka and co-workers also reported the synthesis and characterisation of a series of PEG-diorthoester (POD) lipids (**33**) with different PEG chain length or unsaturated lipid chains (Figure 1.2.10).⁸¹⁻⁸³ The PEG-lipid conjugates were found to be stable at neutral pH, but degraded completely within 1 hour at pH 5.5. Biophysical release studies performed with POD-loaded liposomes suggesting that the release half-time at pH 5.5 was approximately 10 minutes.⁸² Gillies and co-workers have investigated the utilisation of acetal-linked PEG-lipid conjugates such as lipid **34** for pH-triggered drug delivery applications, with hydrolysis half-lives ranging from less than 1 minute to several days at pH 5.⁸⁴ Acid-sensitive linkers have also been utilised for liposomes containing cationic headgroups. For example, Nantz *et al.* reported the synthesis of pH-sensitive lipid conjugate **35** containing a dioxazocinium orthoester linker and cationic quaternary headgroup (Figure 1.2.10).⁸⁵ More recently, Skoza *et al.* reported their synthesis of pH-sensitive OEPC (**36**) containing a biocompatible phosphocholine headgroup and an orthoester linker (Figure 1.2.10).⁸⁶

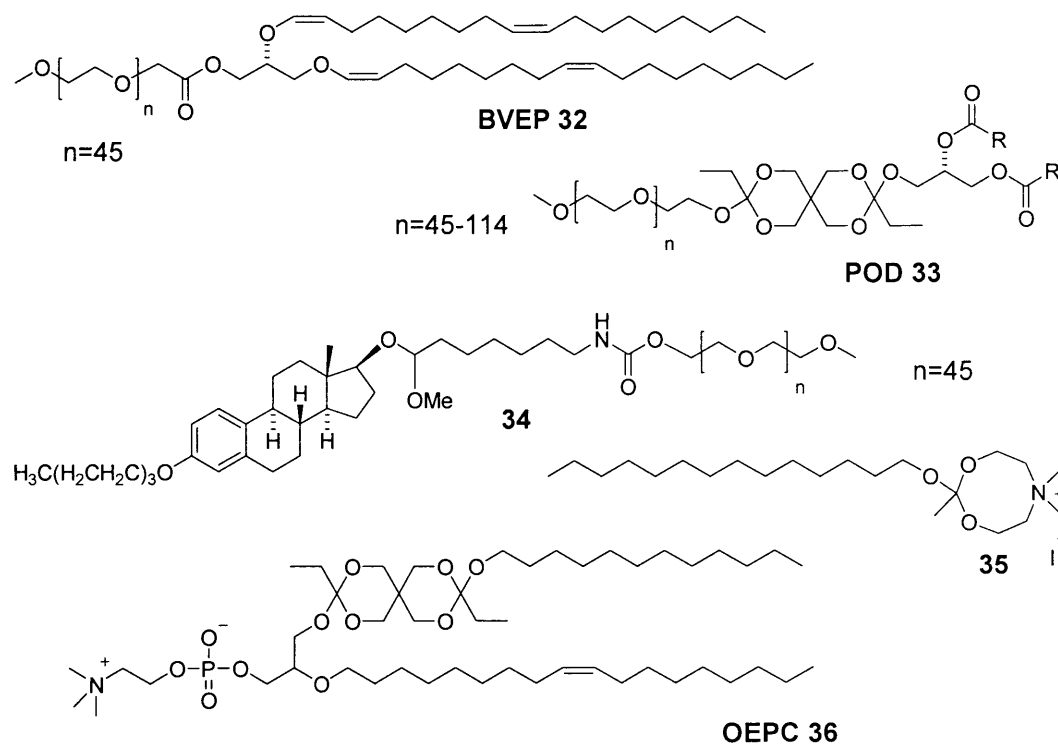


Figure 1.2.10

1.2.1.2 Polymorphism of Lipid Aggregates in Aqueous Solution

The self-assembly of amphiphilic lipids to form complex aggregates in aqueous solution is mainly driven by the hydrophobic effect.⁸⁷ Aggregation of lipids occurs when the concentration of amphiphiles exceeds a certain limit, known as the critical micelle concentration (CMC).³⁰ Depending on their molecular geometries and interactions, the lipids form aggregates of different structures. Cullis and co-workers have correlated the molecular shapes of the lipids to the lipid aggregate phase preferences (Figure 1.2.11).⁸⁸ Conventional spherical micelles are formed when the lipids have a relatively large headgroup area and a small hydrophobic area which exhibits a cone-like shape (Figure 1.2.11a). Alternatively, lipids that have nearly equal headgroup to hydrophobic area are prone to self-assemble into lipid bilayers (L) (Figure 1.2.11b). Lipids with a relatively small headgroup area compared to the hydrophobic area can adopt an inverted micelle or inverted hexagonal (H) phase with a negative membrane curvature (Figure 1.2.11c). Furthermore, the hydrocarbon chains can be described as α (disordered or fluid) or β (untitled ordered or gel). The type of aggregate formed also depends on the temperature and lipid concentration.^{30,88,89} The temperature required to induce the $\beta \rightarrow \alpha$ lipid physical change is defined as the chain-melting phase transition temperature (T_c).⁹⁰ Lipids are more likely to adopt the densely-packed lamellar structure at higher lipid concentration.⁸⁹

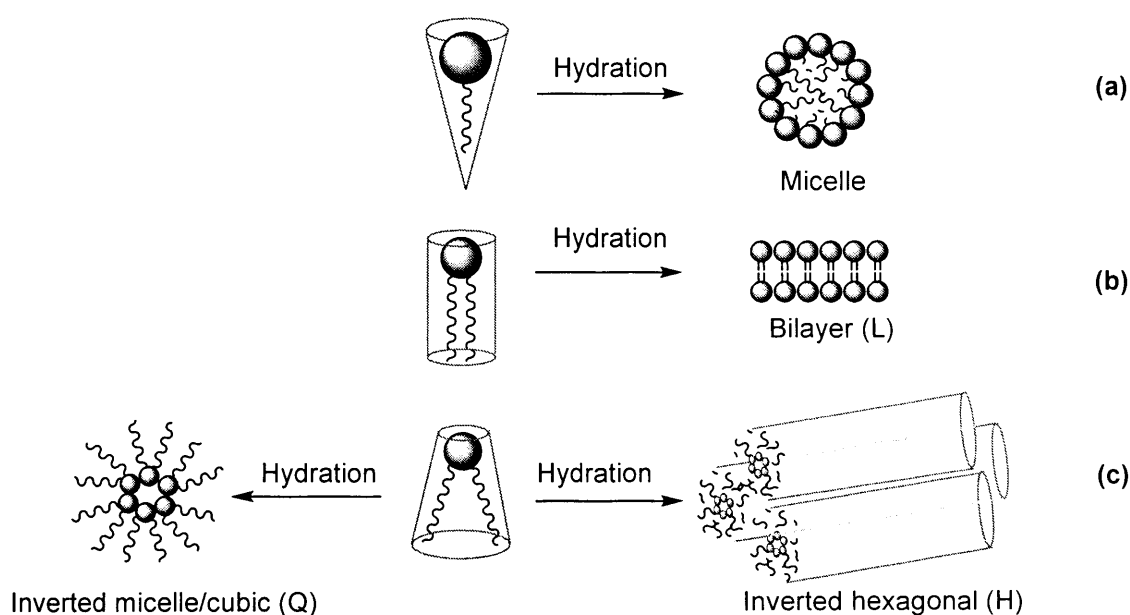


Figure 1.2.11

The molecular shape of the lipid aggregates depends on the effective headgroup size and lipid alkyl tail. For example, surfactants which contain one alkyl chain and a polar headgroup tend to form micelles. Phosphatidylethanolamine (PE) lipids like DOPE (7) that have a smaller headgroup area in comparison to the lipid tail and prefer to adopt a H_{II} phase, whereas phosphatidylcholine (PC) lipids such as POPC (5) tend to pack as bilayer aggregates L_α .⁸⁸ The introduction of the quaternary ammonium moiety in PC lipids increases the effective headgroup size and affects the hydrogen bonding capacity of the lipids, causing the lipids to adopt a cylindrical shape.

Reports have suggested that the length of fatty chain and degree of unsaturation can also influence the packaging and phase preference of the lipids at physiologically relevant temperatures. For example, Seddon *et al.* demonstrated that increasing the chain length of PE lipids causes an increase in T_c .⁹¹ Skoza and co-workers observed a similar chain length dependence for cationic lipid derivatives.⁹² Furthermore, the introduction of the *cis*-alkene moiety in the alkyl chains can induce a significant reduction in T_c and hence favour H_{II} phase packing.⁸⁷ Binder and Gawrisch observed that the introduction of *cis*-alkene moiety into alkyl chains resulted in an increase in the effective cross-sectional area of the lipid, reducing the half-thickness of the lipid membranes formed compared to those which contain saturated alkyl chains.⁹³ Here they attributed these differences to the degree of rotational freedom of the saturated and unsaturated hydrocarbon chain: the *cis*-alkene moiety has a torsion angle of 120° , whereas a saturated chain will prefer *trans* 180° or *gauche* 60° rotational angles. This gives the alkyl chains with the *cis*-alkene moiety a “kink” causing the chains to splay more widely and occupy a larger cross-sectional area, resulting in the lipids preferring to adopt the H_{II} phase.⁸⁸ More recently, Miller and co-workers have reported that the replacement of *cis*-double bonds on DOTAP with triple bonds resulted in liposomes possessing a rigid lamellar gel structure (L_β') near physiological temperatures.⁶³ X-ray diffraction studies indicated that phase transition from L_β' to the less stable fluid lamellar (L_α) phase occurred between 25 and 35 °C, depending on the position of the triple bond (24a-c, Figure 1.2.7). These studies suggested that the introduction of minor structural changes within the lipid can have significant implications on the aggregation properties of the lipid, which in turn influences its biological properties.^{63,87,91-93}

1.2.1.3 Structures of Cationic Lipid/DNA Complexes

Structures of cationic lipid/DNA complexes are often heterogeneous with respect to size, shape and composition. Many different structures have been reported, however, it is unclear which structure is the most active form for transfection. Felgner and co-workers initially observed the complexation between DNA and DOTMA-containing liposomes within an aqueous environment.³⁷ Based on their light scattering results and calculations, they proposed that optimal lipoplex formation could be achieved by electrostatically binding four cationic liposomes to the plasmid DNA (beads-on-strings model) (Figure 1.2.12).³⁷

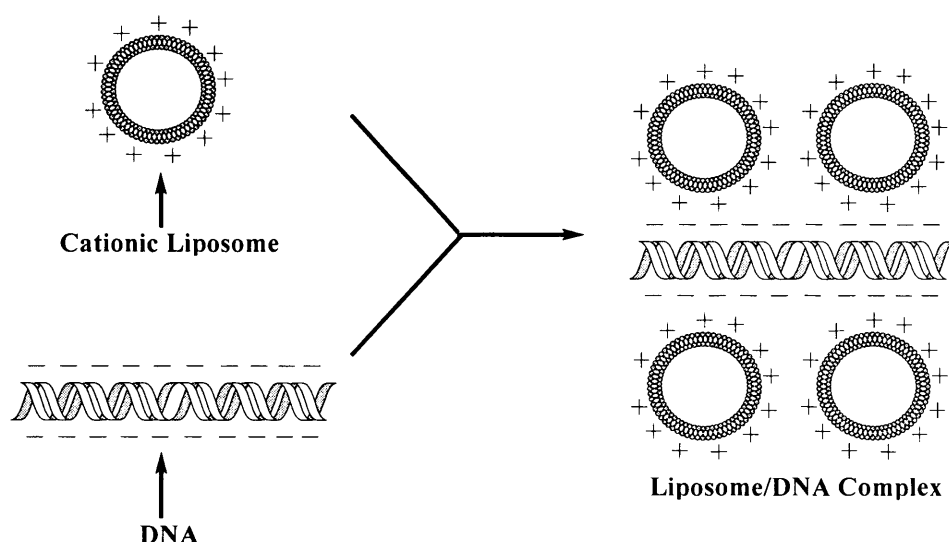


Figure 1.2.12 Beads on strings model proposed by Felgner *et al.*³⁷

Using freeze-fracture electron microscopy, a similar type of structure was observed by Sternberg and co-workers in DC-Chol/DOPE/DNA complexes that gave optimal transfection.⁹⁴ They described the morphology of the lipoplexes as aggregates of cationic liposomes surrounding elongated and intercalated DNA, co-existing with tubular structures composed of the DNA coated by lipid bilayers (spaghetti-meatball model) (Figure 1.2.13).⁹⁴

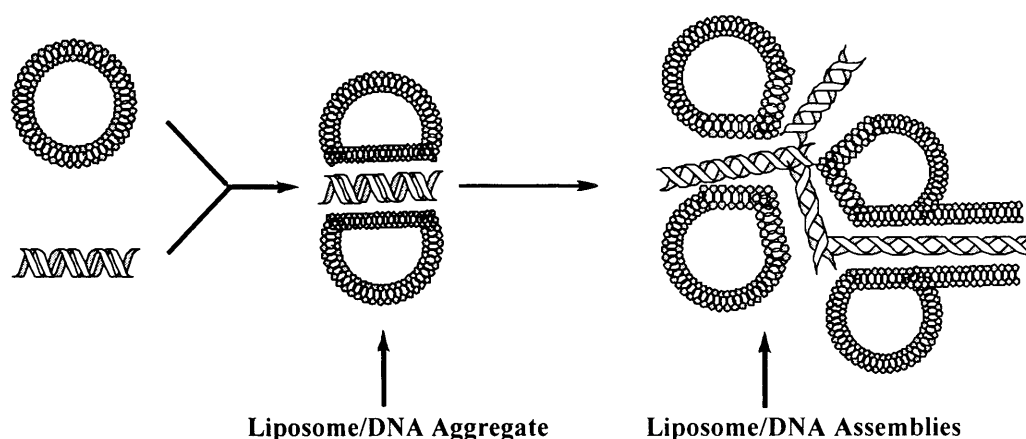


Figure 1.2.13 Spaghetti and meatball model proposed by Sternberg *et al.*⁹⁴

Gustafsson *et al.* obtained cryo-transmission electron microscopy images of DNA complexed with various cationic liposomes.⁹⁵ Their results revealed the presence of small dense particles with loosely bound plasmid DNA when the positive/negative charge ratio was less than one. Once the lipid/DNA charge ratio exceeded this value, large aggregate structures (>100 nm) were observed, and the group proposed that multilamellar structures were formed inside which the DNA was entrapped.⁹⁵ The exact nature of this encapsulation was revealed by a combination of *in situ* optical microscopy and X-ray diffraction data obtained by Rädler and co-workers in studying cationic liposomes complexed with λ -phage DNA.⁹⁶ They observed the mixing of cationic liposomes with DNA results in a topological transition from a liposome structure to a liquid-crystalline, condensed globular structure (Figure 1.2.14a). The regular multilamellar structure L_α was comprised of parallel strands of DNA sandwiched between fluid cationic lipid bilayers. This phase was stabilised by the electrostatic interactions between the negatively charged DNA molecules and the cationic lipid bilayers, driven by the release of DNA-associated counterions.⁹⁶

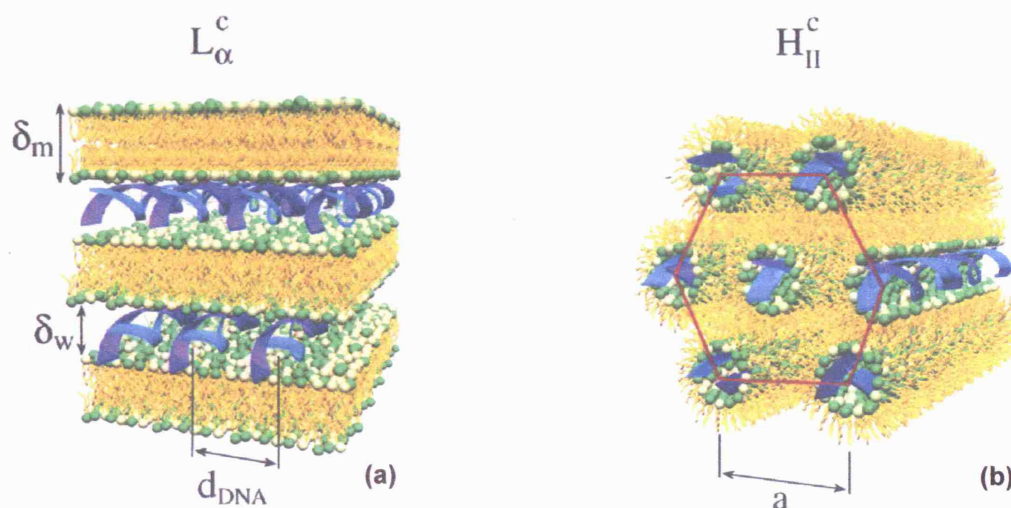


Figure 1.2.14 Schematic representation of the arrangement of DNA and lipids in (a) sandwich lamellar (L_{α}^c) and (b) honeycomb inverted hexagonal (H_{II}^c) phase. Taken from Koltover *et al.*⁴²

Rädler *et al.* reported a dramatic change in the structure of lipid/DNA complexes when DOPE was added at a certain ratio.⁴² Using small-angle X-ray scattering and optical microscopy, they observed a phase transition from a multilamellar structure L_{α} to a tubular inverted hexagonal liquid crystalline state H_{II} , with the DNA strands condensed by lipid molecules in a micellar fashion (Figure 1.2.14b). Lipids such as DOPE are known to prefer the formation of the H_{II} phase under physiological pH and temperature.⁸⁸ The tendency for lipoplexes to undergo $L_{\alpha} \rightarrow H_{II}$ transition plays an important role in the delivery of DNA molecules across cell membranes, as this will facilitate the formation of highly curved intermediates that are necessary for membrane fusion and endosomal disruption. Hence the inclusion of DOPE in cationic liposome/DNA complexes is likely to facilitate endosomal escape of DNA through the induced $L_{\alpha} \rightarrow H_{II}$ destabilisation.⁴² The phase diagram of the system was complex, revealing a multitude of phase transitions and coexistence.⁹⁷

An invaginated bilayer structure of extruded lipid/DNA complexes was reported by Templeton *et al.*⁹⁸ Based on experimental evidence provided by cryo-electron microscopy and light scattering analysis, they suggested that the initial interactions of DNA molecules with the outer surface of a unilamellar vesicle induced a contraction of its outer lipid layer due to charge neutralisation (Figure

1.2.15). This led to an inversion of the vesicle around the DNA, and so a bilamellar invaginated vesicle BIV is formed (Figure 1.2.15). The DNA can be engulfed in the innermost compartment where it appears to be well protected and highly effective in transfection.⁹⁸

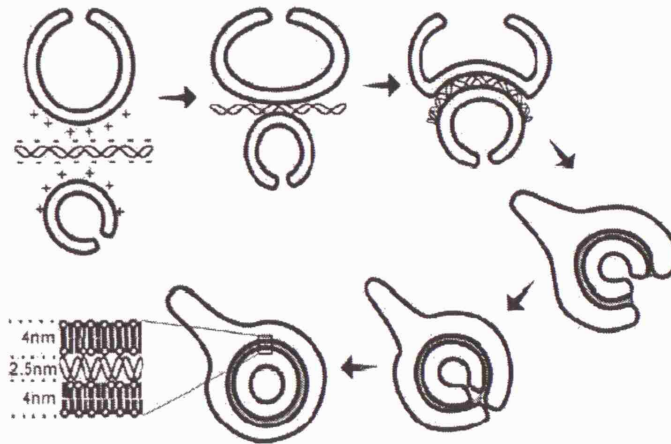


Figure 1.2.15 Schematic representation of the BLV structure. Taken from Templeton *et al.*⁹⁸

1.2.2 Mechanism of Cationic Lipid-Mediated DNA Transfer

Successful intracellular delivery of DNA by cationic lipid-based gene carriers involves four main steps: (A) initial binding of lipoplexes to the cell surface; (B) endocytotic cellular uptake by cell membranes; (C) escape of DNA molecules from the endosome compartment to the cell cytoplasm; (D) transport of the endosomally released DNA to the cell nucleus followed by its transgene expression (Figure 1.2.16). Despite the extensive use of cationic lipids for gene therapy *in vitro* and *in vivo*, the exact mechanism by which DNA delivery occurs in cells is not well understood.

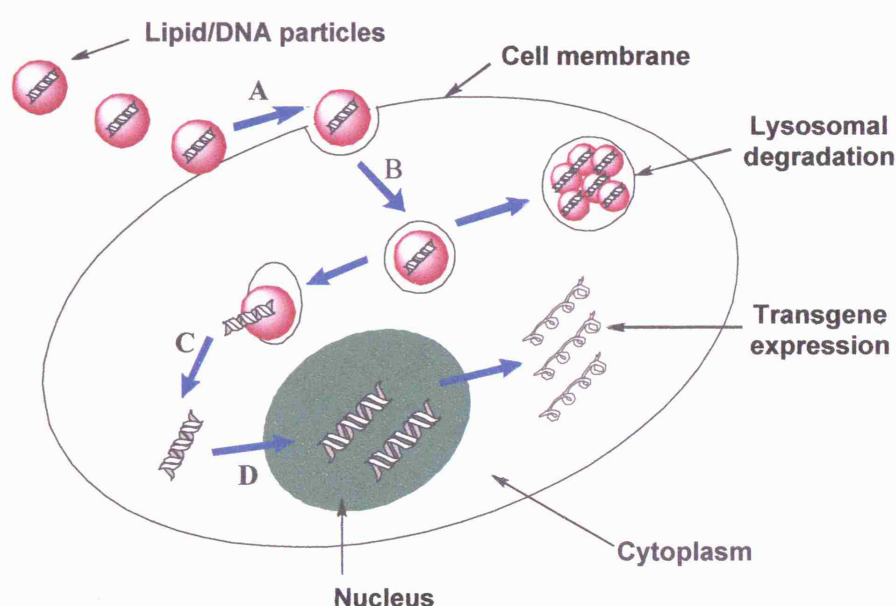


Figure 1.2.16 Diagram to show the cationic lipid-mediated DNA delivery pathway

1.2.2.1 Cell Uptake and Entry

The initial binding of cationic lipoplexes on the cell surface can be initiated by non-specific electrostatic interactions (Figure 1.2.16, step A). Cells are negatively charged on the surface with specific cell types varying in charge density, which can influence the ability of cells to be transfected. Different formulations of lipoplexes are likely to interact with cell surfaces *via* a variety of mechanisms.⁹⁹⁻¹⁰¹ Previously, it was thought that membrane fusion was the primary means of cell entry.^{102,103} However, investigations carried out by Wrobel *et al.* suggested that endocytosis plays a major role in the cellular uptake of liposomes.⁹⁹ Zabner *et al.* followed the

cell entry of gold-labelled DNA complexed to DMRIE/DOPE liposomes using electron microscopy.¹⁰⁰ They observed the initial association of the complexes followed by endocytotic uptake at the cell surface. Once inside the cytoplasm, the complexes were bound within vesicles of endosomes. It is now widely accepted that endocytosis is the major pathway by which lipoplexes enter cells (Figure 1.2.16, step B).

1.2.2.2 Endosomal Release of DNA

The endosomal release of DNA into the cell cytoplasm is one of the major barriers to cationic lipid-mediated gene therapy (Figure 1.2.16, step C). The escape in the early phase of the endosome is thought to be essential as this would evade lysosomal degradation of the endosomes.^{99,100} Zabner *et al.* investigated the dissociation of cationic lipid/DNA complexes inside different cells.¹⁰⁰ They identified that 80% of cells were successfully endocytosed with liposomes, however, gene expression to those cells only occurred at a level of less than 50%. They attributed the poor transduction efficiency to insufficient escape of DNA from the endosome, and suggested that endosomal escape mostly relies on destabilisation of the endosome membranes.¹⁰⁰

Xu and Szoka observed that DNA became exposed when lipoplexes interacted with anionic liposomes that resembled the cell membranes.¹⁰⁴ They proposed a model for endocytosis cell entry and early endosomal breakdown in which lipoplexes destabilise the endosome membranes to allow DNA release (Figure 1.2.17). Initially, the cationic lipid/DNA complex is endocytosed (Step 1), and within the early endosome, disruption of the endosome membrane occurs (Step 2). Anionic lipids from the endosomal membrane diffuse into the complex, leading to the formation of charge neutral ion pair with cationic lipids (Step 3). The electrostatic interactions between DNA and cationic lipids are thus disrupted, allowing the DNA to diffuse freely into the cytoplasm (Step 4).¹⁰⁴

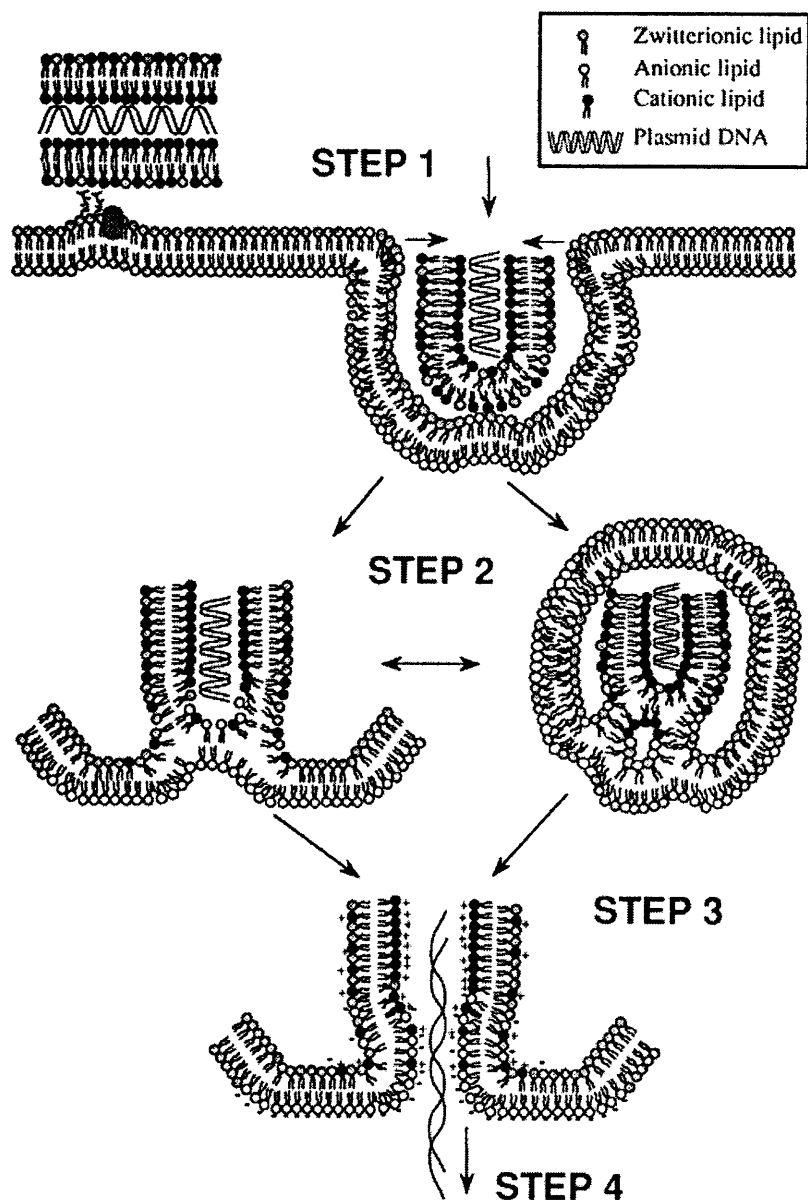


Figure 1.2.17 Proposed mechanism of uptake and release of plasmid DNA from the cationic lipid/DNA complex. Taken from Xu *et al.*¹⁰⁴

This mechanistic hypothesis from Xu and Szoka was supported by experimental data reported by Bhattacharya *et al.*¹⁰⁵ They observed that the release of DNA from cationic lipid/DNA complexes could be induced by several anionic additives. The release of DNA was attributed to the ion-pairing interactions between cationic and anionic amphiphiles, and that this interaction was stronger than the electrostatic forces involved in the cationic lipid-DNA complexation.¹⁰⁵ Furthermore, it was revealed that DNA release was most effective around the phase transition temperature of the cationic lipids used for lipoplex formation, implying that the

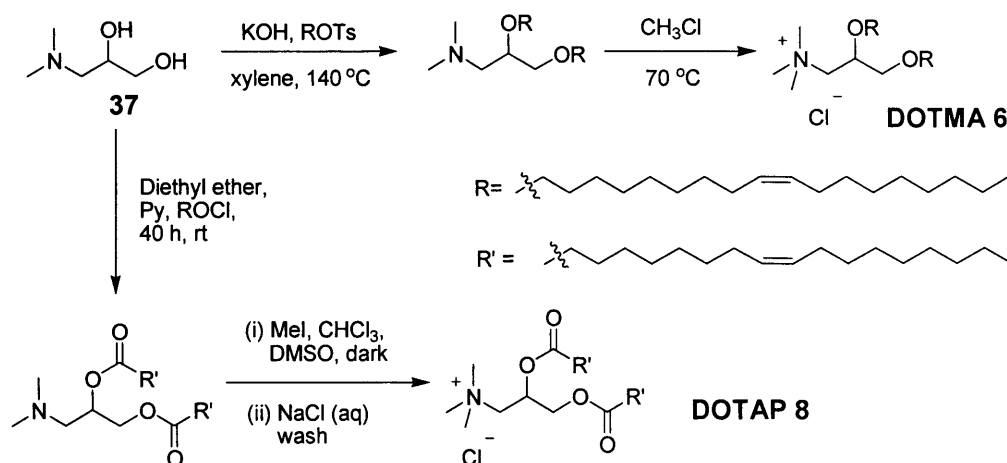
phase transition of cationic lipids plays an important role in the endosomal release of DNA.¹⁰⁵

1.2.2.3 Trafficking of DNA to Nucleus

Once in the cytoplasm, DNA must make its way into the nucleus in order to be expressed (Figure 1.2.16, step D). The passage of DNA to the nucleus is unclear, however, Zander *et al.* suggested that the size of DNA is an important factor to determine whether it will reach the nucleus or not.¹⁰⁰ Capecchi *et al.* demonstrated that the efficiency of such nuclear trafficking is very low, with less than 1 in 10000 plasmids taken up by the cell eventually being expressed.¹⁰⁶ The major reason that a majority of DNA failed to reach the nucleus is the presence of cytoplasmic nucleases that act to degrade the free DNA molecules.^{107,108} One approach to overcome the barriers was to try to increase the nuclear localisation of DNA molecules for enhanced gene delivery and expression. Zanta *et al.* used a nuclear localisation sequence (NLS) peptide to increase DNA entry into the nucleus.¹⁰⁹ It was suggested that nuclear import machinery can recognise the peptide sequence and was responsible for increased transfection levels of between 10 to 10000-folds. Several NLS-containing peptides have been incorporated onto gene delivery vectors, and many of these peptides contain lysine and arginine motifs.¹¹⁰ Once the DNA molecules successfully enter the nucleus, the final step in transfection is the transgene expression.

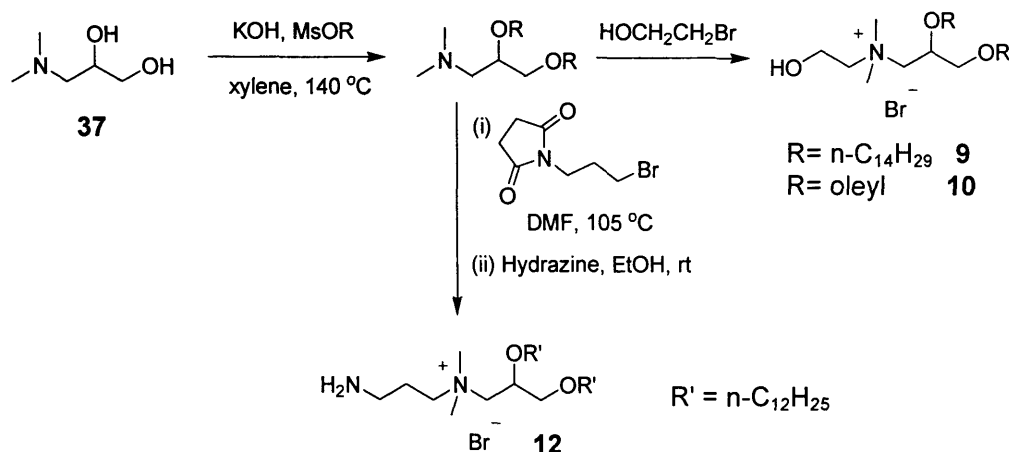
1.3 Synthesis of Cationic Lipids for Gene Therapy

The syntheses of cationic lipids for gene therapy should be short, facile, high yielding, and versatile for the production of structural analogues. Felgner and co-workers produced the first cationic lipid for gene therapy.³⁷ DOTMA (**6**) was prepared from dietherification of racemic 3-dimethylamino-1,2-propanediol (**37**) with tosylated oleyl alcohol, followed by subsequent quaternisation with chloromethane at 70 °C (Scheme 1.3.1). Similarly structural analogue DOTAP (**8**) was synthesised *via* diesterification of aminodiol **37** using oleoyl chloride, followed by quaternisation with iodomethane. The iodide salt was repeatedly washed with sodium chloride solution to afford chloride counter ion-containing DOTAP (Scheme 1.3.1).⁴³



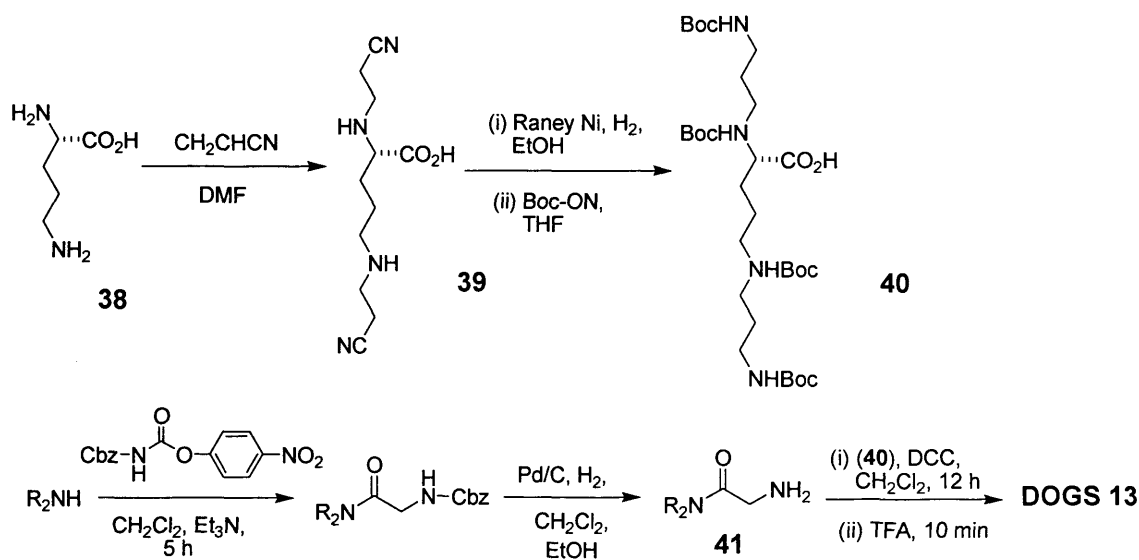
Scheme 1.3.1

DOTMA analogues DMRIE (**9**) and DORIE (**10**) were synthesised by Felgner *et al.*⁴⁰ The aminodiol **37** was first dietherified with mesylated alcohols, followed by quaternisation with 2-bromoethanol to yield *N*-hydroxyethyl ammonium lipids **9** and **10** (Scheme 1.3.2). The *N*-aminopropyl ammonium lipid GAP-DLRIE (**12**) was synthesised in an analogous manner.⁴⁴



Scheme 1.3.2

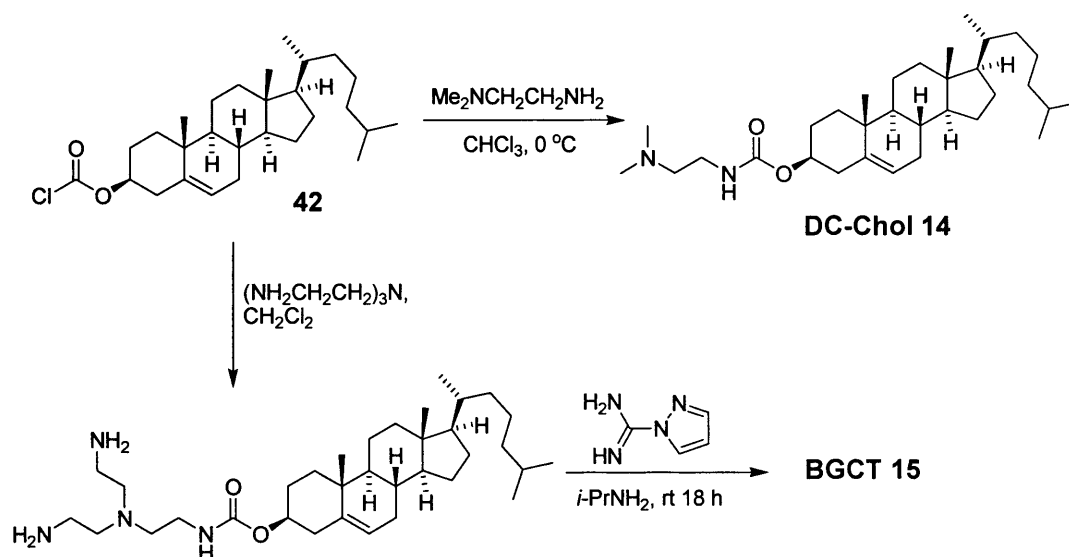
The cationic lipid DOGS (**13**) was synthesised by Behr *et al.* in a multi-step convergent fashion (Scheme 1.3.3).⁴⁸ Initially, (*S*)-2,5-diaminopentanoic acid (**38**) was converted to the di-*N*-ethylnitrile derivative **39**, which was subsequently reduced and *t*-butyloxycarbonyl (Boc)-protected to afford spermine derivative **40**. The diesterification coupling of compound **40** and glycine derivative **41** followed by acidic deprotection afforded **13** (Scheme 1.3.3).⁴⁸



Scheme 1.3.3

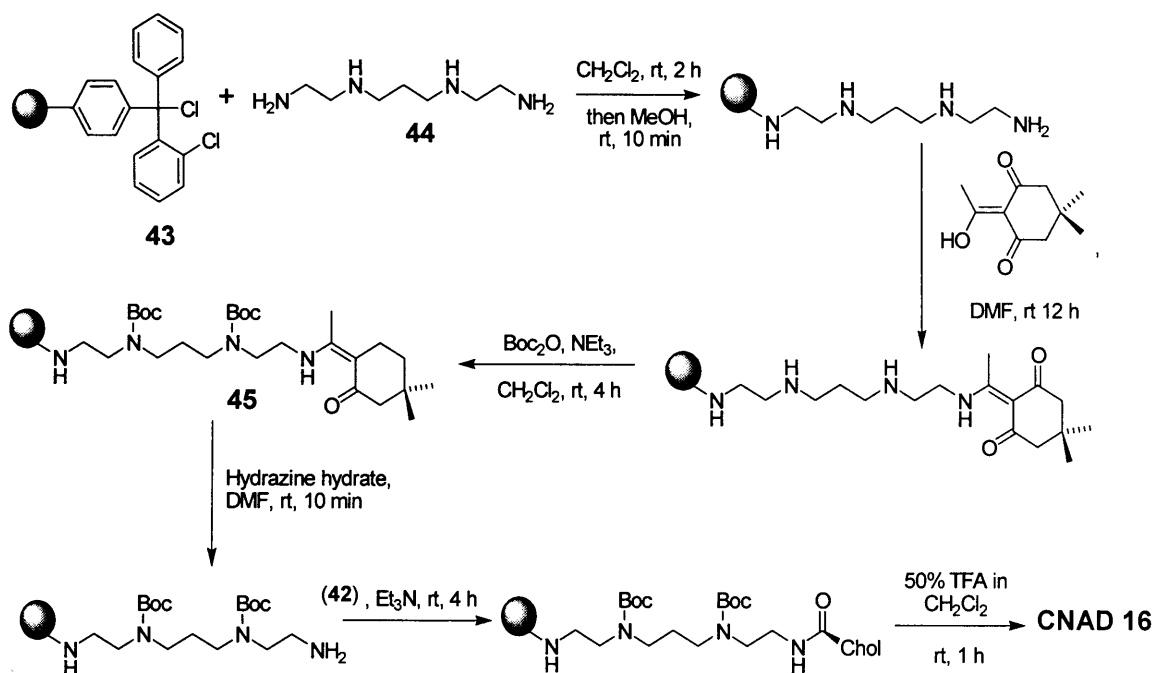
The cholesterol-derived lipid DC-Chol (**14**) was synthesised in a one-step procedure by aminolysis of commercial available cholesterol chloroformate (**42**) (Scheme 1.3.4).⁵¹ A similar procedure was used for the production of BGTC (**15**).⁵³

Aminolysis of **42** followed by guanidinylation of the product afforded **15** (Scheme 1.3.4).



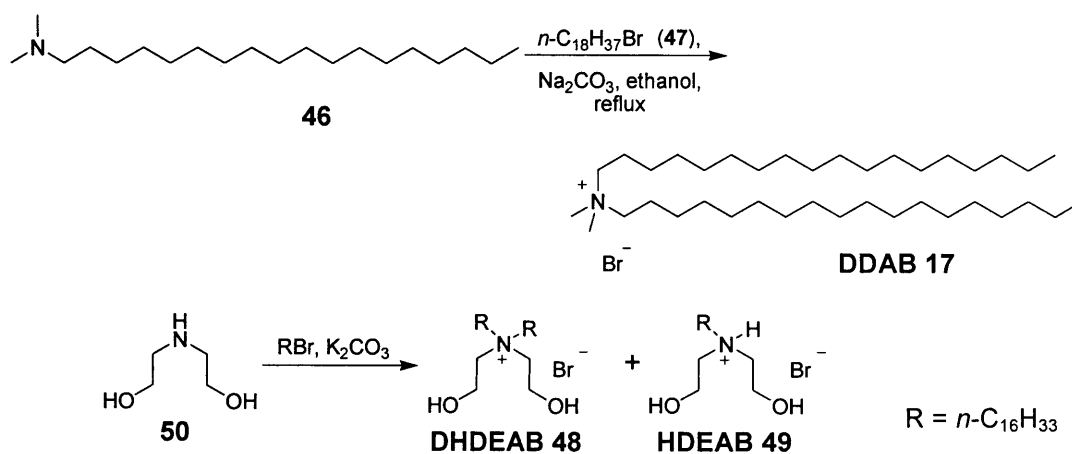
Scheme 1.3.4

Recently, Miller and co-workers reported a new synthetic strategy for the production of cationic lipid CNAD (**16**) utilising a solid-phase methodology (Scheme 1.3.5).¹¹¹ The 2-chlorotrityl chloride resin (**43**) was employed to protect one primary amine on starting material **44**, while its second primary amine was protected by 2-acetyldimedone (Dde), allowing selective Boc-protection of the secondary amine to yield **45**. Dde-deprotection of **45** and subsequent coupling with cholesterol chloroformate (**42**), followed by Boc-deprotection and resin removal afforded the lipid **16** in 93% yield over six steps (Scheme 1.3.5).¹¹¹



Scheme 1.3.5

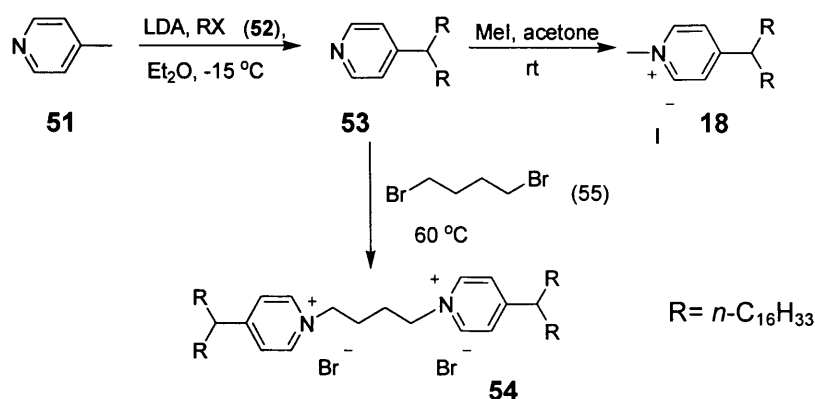
The synthesis of DDAB 17 has been reported by Kunitake and co-workers, using *N,N*-dimethyloctadecan-1-amine (46) and 1-bromooctadecane (47) (Scheme 1.3.6).¹¹² The hydrophilic analogues DHDEAB (48) and HDEAB (49) were generated *via* quaternisation of diethanolamine (50) (Scheme 1.3.6).¹¹³



Scheme 1.3.6

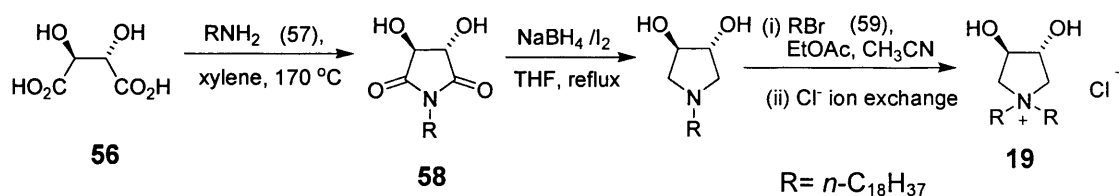
Pyridinium-derived amphiphiles SAINTs (18) were synthesised by van der Woude and co-workers, using 4-methylpyridine (51) as a starting material (Scheme 1.3.7).⁶¹ Double alkylation on the methyl group with lithium diisopropylamide (LDA) and an alkyl halide 52 yielded compound 53, followed by subsequent quaternisation

with iodomethane afforded **18**. The dipyridinium SAINT derivative **54** was obtained by refluxing alkylpyridine **53** with dibromide **55** (Scheme 1.3.7).⁶¹



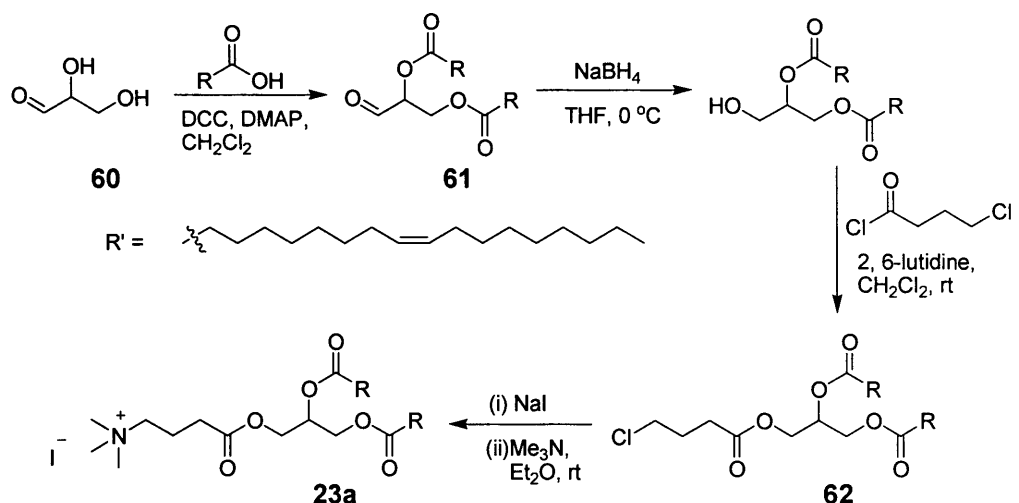
Scheme 1.3.7

The cyclic-head cationic lipid **19** was produced *via* dehydrative coupling of L(+)-tartaric acid **56** and amine **57** to give the cyclic imide intermediate **58** (Scheme 1.3.8).⁵⁹ Compound **58** was then reduced by sodium borohydride/iodine mixture, and subsequently quaternised with bromide **59** followed by Cl^- ion exchange to afford the target lipid **19** in 18% yield over three steps.

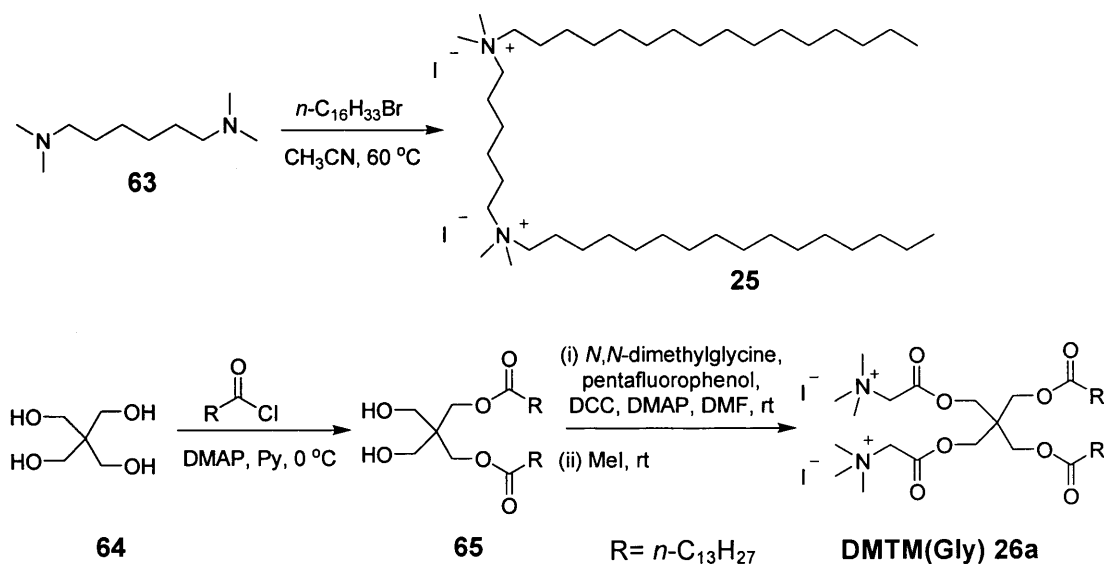


Scheme 1.3.8

The symmetrical triglyceride **23a** was synthesised *via* a four-step strategy (Scheme 1.3.9).⁶² 1,3-Dihydroxyacetone (**60**) was coupled with the oleoyl acid to afford the diester derivative **61**. Carbonyl reduction of **61** and acylation with 4-chlorobutyryl chloride afforded **62**. Finally, conversion to the iodide derivative followed by quaternisation with trimethylamine afforded **23a** in 39% yield over 4 steps (Scheme 1.3.9).

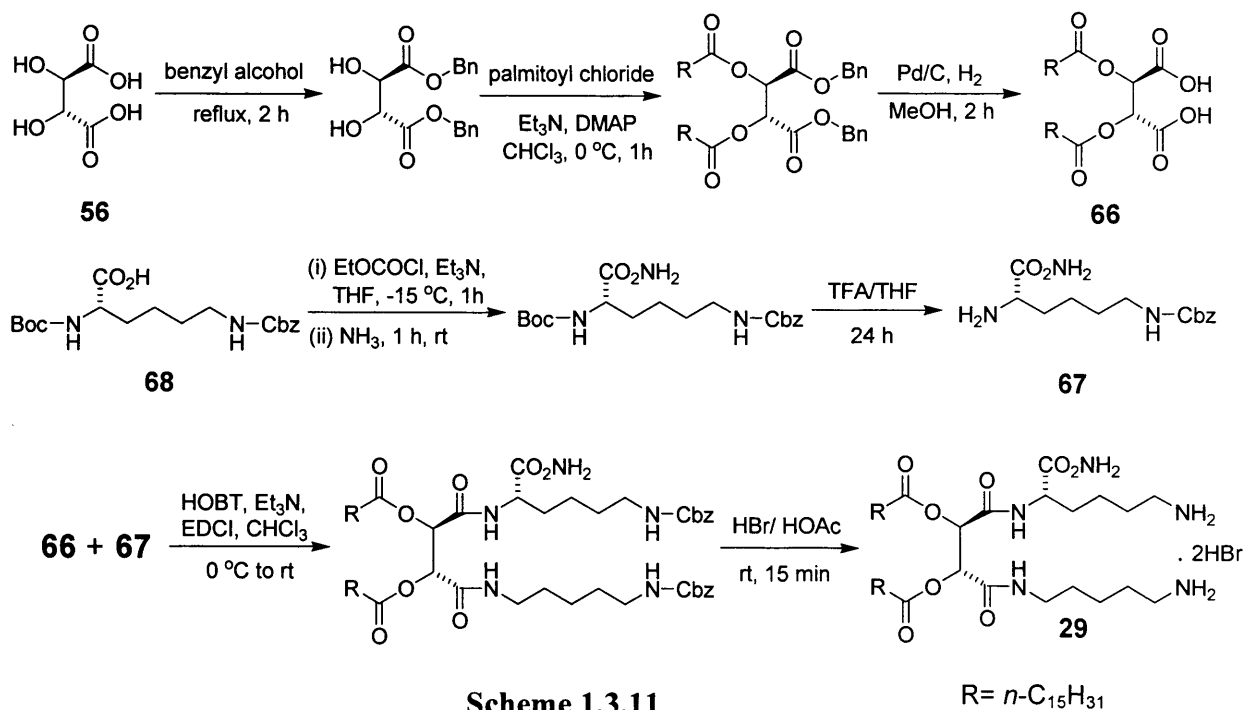


Rosenzweig *et al.* described a short and facile synthesis of gemini surfactant HexAce (**25**) *via* the diquaternisation of diamine **63** (Scheme 1.3.10).⁶⁵ The gemini surfactant DMTM(Gly) (**26a**) was produced by diesterification of pentaerythritol (**64**) with myristoyl chlorides.⁶⁶ The diester derivative **65** was then further diesterified with *N,N*-dimethylglycine followed by quaternisation with iodomethane to yield **26a** in 30% yield over two steps (Scheme 1.3.10).

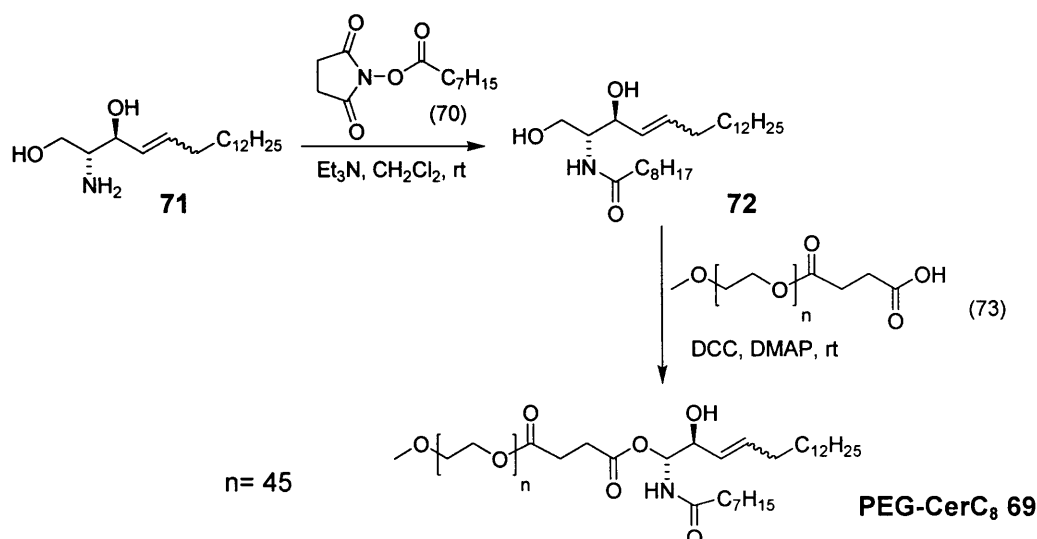


Buijnsters and co-workers have described a convergent methodology for the synthesis of surfactant **29** utilising L(+)-tartaric acid (**56**) and Boc-Lys(Cbz)-OH (**66**) as starting materials (Scheme 1.3.11).⁷⁰ Benzyl protection of **56** and acyl coupling with palmitoyl chloride, followed by benzyl deprotection gave the backbone **66**. The

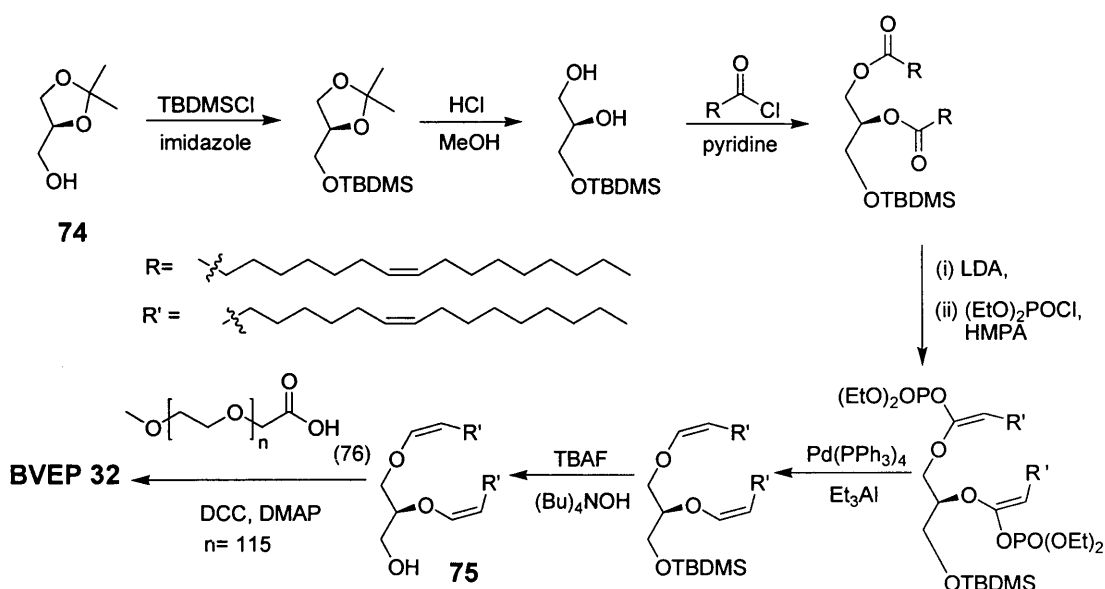
protected headgroup **67** was produced by treatment of **68** with ethyl chloroformate and ammonia, followed by removal of the Boc group. Coupling of **66** and **67** followed by subsequent Cbz-deprotection generated the desired lipid **29** (Scheme 1.3.11).⁷⁰



Webb *et al.* reported the synthesis of a series of PEG-ceramide lipid analogues including PEG-CerC₈ (**69**).⁷⁶ The freshly-prepared *N*-hydroxysuccinimide (NHS) ester of myristic acid **70** was coupled with D-sphingosine (**71**) to afford amide derivative **72**. Subsequent coupling of **72** with PEG-ceramide (**73**) afforded **69** (Scheme 1.3.12).

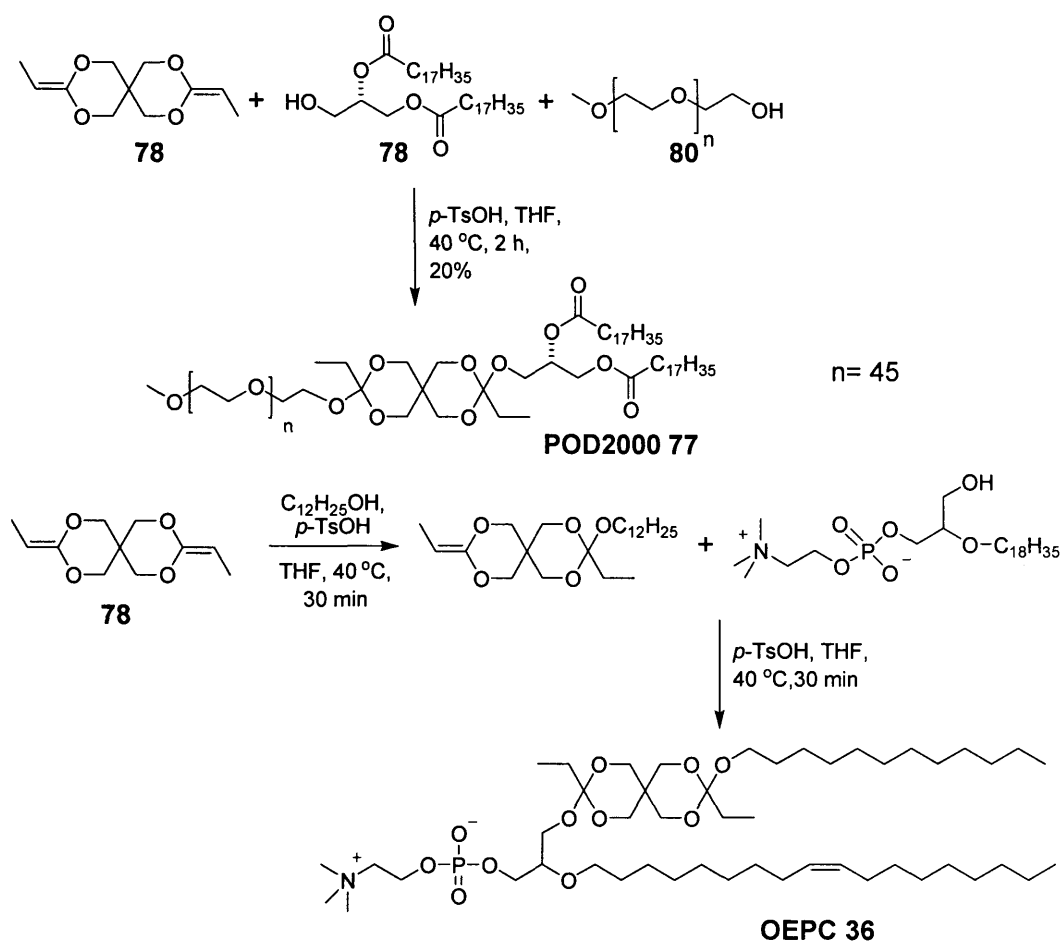


The optically active PEG-lipid BVEP (**32**) was generated in moderate yield (26%) *via* a seven-step strategy from the chiral acetal **74**, culminating in the *N,N'*-dicyclohexylcarbodiimide (DCC)-mediated coupling of glycerol derivative **75** and methoxy-poly(ethyleneoxide)-carboxymethyl (MPEGA) of PEG5000 **76** (Scheme 1.3.13).⁷⁸



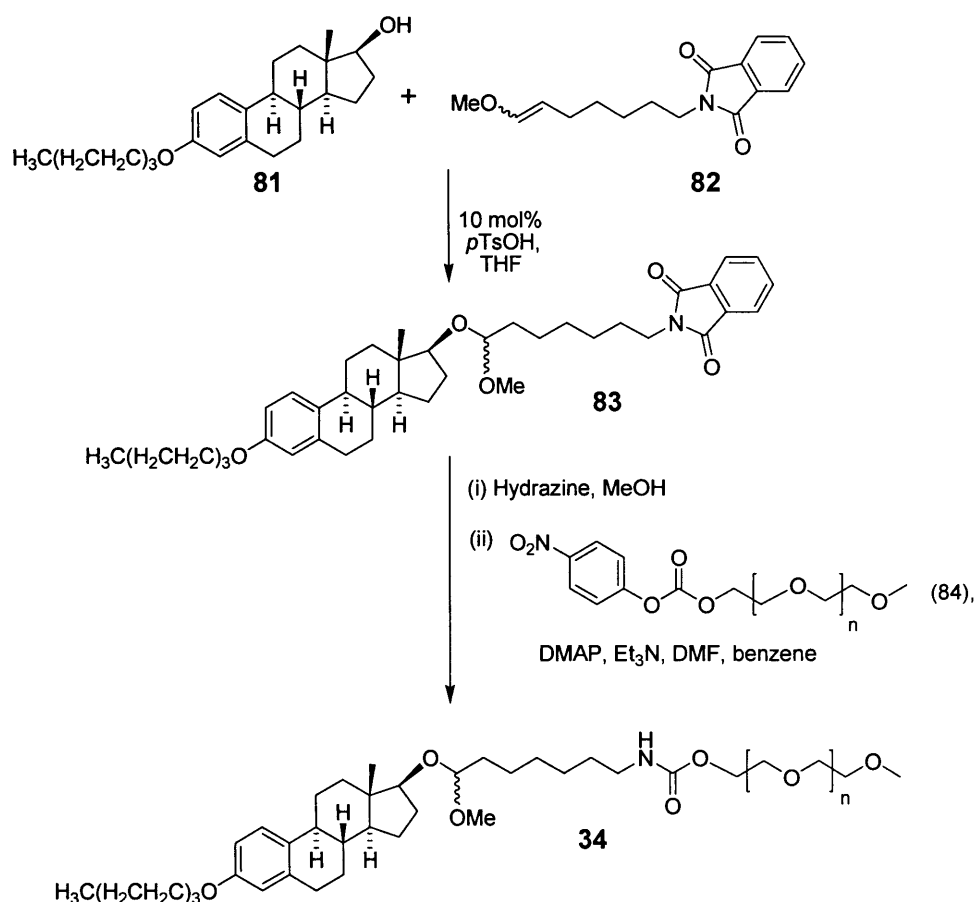
Guo and Szoka devised a one-step synthesis for PEG-lipid POD2000 (**77**), involving the coupling of diketene acetal **78** to distearoyl glycerol (**79**) and PEG2000

monomethyl ether (**80**) (Scheme.1.3.14), in 20% yield.⁸¹ pH-Sensitive lipid OEPC (**36**) was produced by Nantz and co-workers in a similar fashion.⁸⁶



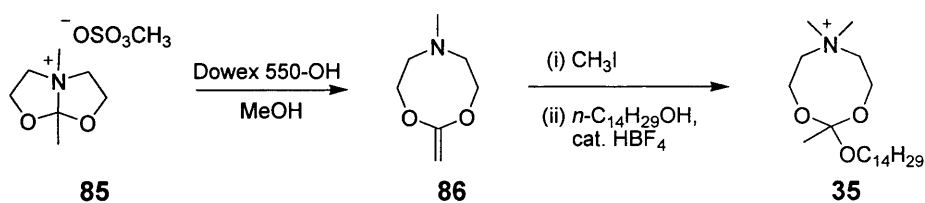
Scheme 1.3.14

Gilles *et al.* have reported the synthesis of acetal-linked PEG-lipid **34** (Scheme 1.3.15).⁸⁴ The highlight of their strategy was the conjugation of estradiol derivative **81** with enol ether **82**, in the presence of acid, to provide the acetal **83** as a mixture of two diastereomers. The phthalamide protecting group of **83** was then removed, and the resulting amine was conjugated to activated-PEG derivative **84** to provide the target lipid **34**.



Scheme 1.3.15

The dioxazocinium lipid **35** was generated *via* a three-step procedure.⁴² Eluting a methanol solution of ammonium salt **85** through an anion exchange resin Dowex 550-OH afforded the ketene acetal **86** (Scheme 1.3.16). Quaternisation of **86** followed by conjugation with myristyl alcohol in the presence of tetrafluoroboric acid gave the **35** in 85% yield.



Scheme 1.3.16

1.4 Receptor-Mediated Gene Delivery

The initial binding and internalisation of lipoplexes are crucial steps for intracellular gene delivery (see Figure 1.2.16, step A & B). Much effort has been made to improve the efficacy and selectivity of non-viral vector systems by mimicking the cell-binding mechanisms utilised by viruses.¹¹⁴ In particular, synthetic vectors have been incorporated with targeting ligands that can attach to membrane receptors for site-specific cell entry. Several targeting moieties including vitamins,¹¹⁵ antibodies,¹¹⁶ and peptide^{18,117} have been utilised for active-targeting gene transfer. Receptor-mediated gene delivery can alter the biodistribution of lipoplexes *in vivo* so that non-specific gene transfer is reduced, while the expression level in the target tissue is maintained or even increased. For example, Hofland *et al.* studied gene transfer by lipoplexes containing a small amount (<3 mol%) of folate-targeted PEG-liposome DSPE-PEG₃₄₀₀-folate (**87**) after intravenous administration on mice (Figure 1.4.1).¹¹⁵ Their data showed that while DSPE-PEG₃₄₀₀-folate showed significantly reduced gene expression on mice lungs compared with non-PEGylated lipoplexes, the gene transfer activity was maintained in folate-active tumor cells. This specificity in gene expression was attributed to the presence of folate receptors on tumor cell membranes, which favours lipoplex internalisation *via* receptor-mediated endocytosis.¹¹⁵

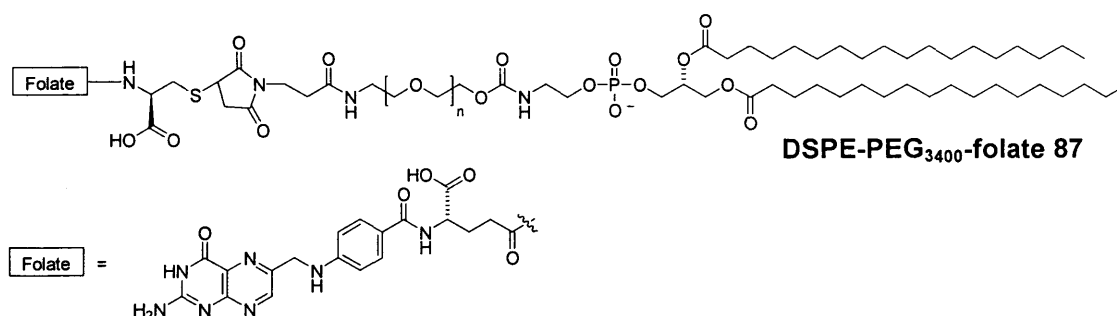


Figure 1.4.1

1.4.1 Immunolipoplexes

Antibody-mediated targeted liposomes, or immunoliposomes, represent a novel strategy for drug and gene delivery. The first reported case of antibody-mediated cell entry was revealed in the 1970s, when Gregoriadis *et al.* demonstrated the specific

cellular uptake of an immunoliposome entrapping a radiolabelled antitumor drug.¹¹⁸ Since then, several coupling techniques have been described for conjugating monoclonal antibodies (MAb) or their fragments (Fab') to liposomes, each with their own advantages and drawbacks.¹¹⁹⁻¹²¹ Previous studies have revealed that immunoliposomes were taken up by cells *via* a receptor-mediated endocytotic pathway.^{122,123}

Recent advances in immunoliposome research have been focused on developing PEGylated immunoliposomes (PILs) that are conjugated to Fab' fragments for active-targeting cancer therapy (Figure 1.4.2).^{116,124} Fab' fragments are usually conjugated *via* the free thiol group in the hinge region to maleimidyl (Mal) groups at the terminus of the PEG chains. Kirpotin *et al.* devised the PIL anti-HER2-SL, comprising a PEG-phospholipid DPSE-PEG-Mal (**88a**) conjugated to the anti-HER2 Fab' fragments, as a drug carrier targeting HER2-overexpressing cancer cells *in vitro* (Figure 1.4.3).¹²³ Similarly, Maruyama and co-workers generated a PIL with lipid DPPE-PEG-Mal (**89**) conjugated to the anti-21B2 Fab' fragments for targeting solid tumor in mice.¹²⁵ Compared with DPPE-PEG-Mal that conjugated to a whole antibody, the linkage of the Fab' fragment to the lipid allowed the immunoliposome to evade the reticuloendothelial system (RES) uptake and remained in the circulation for a longer period, resulting in enhanced accumulation in the solid tumor.¹²⁵

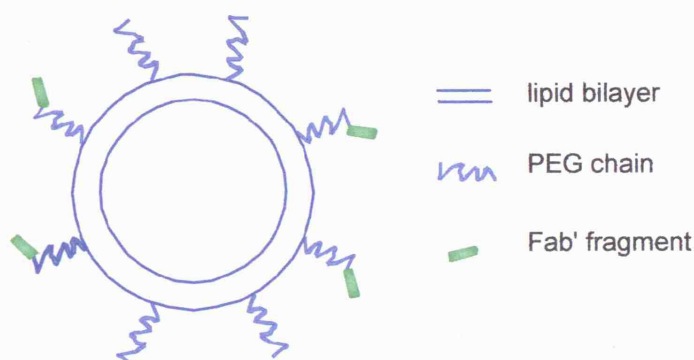


Figure 1.4.2 Schematic representation of Fab'-PEG-immunoliposomes

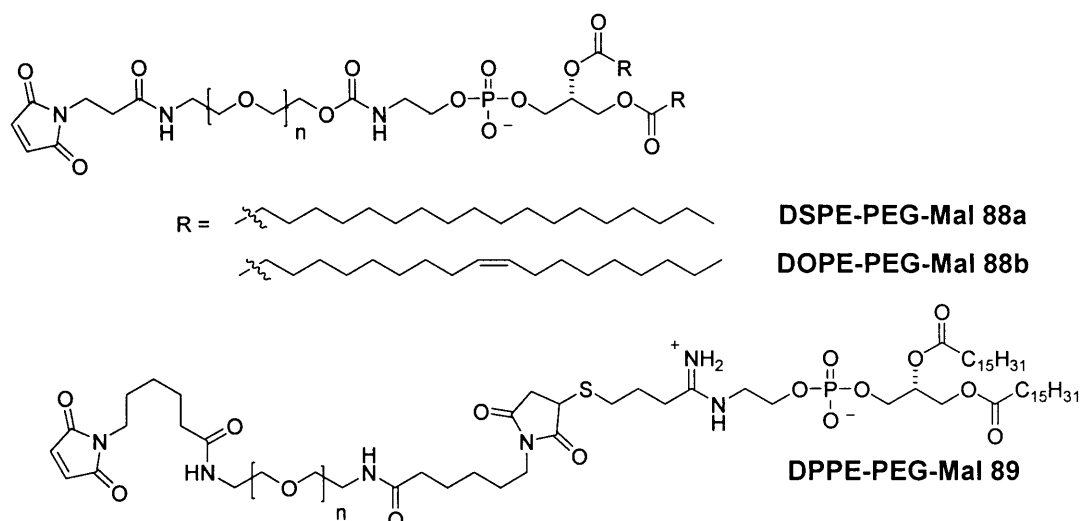


Figure 1.4.3

Several groups have attempted to construct immunolipoplexes for gene therapy by incorporating antibody- and Fab'-conjugated lipids into liposome/DNA complexes. For example, Zhang *et al.* reported the *in vitro* delivery of plasmid DNA to human glioma cells with lipid DPSE-PEG-Mal conjugated to the murine 83-14 MAb that targeted human insulin receptors.¹²⁶ Their highly condensed immunolipoplexes (~ 85 nm) showed persistent gene expression in rhesus monkey brains *in vivo*, with low levels of associated systemic toxicity.¹²⁷ Lee *et al.* have developed an anti-HER2 Fab'-targeted PIL formulation comprised of lipids DOTAP (8), Chol (4), and DOPE-PEG-Mal (88b) (Figure 1.4.3).¹²⁸ The resulting immunolipoplex was able to achieve high specificity *in vitro* on human breast cancer SK-BR3 cells with HER2 overexpressions. More recently, Chang and co-workers utilised an immunolipoplex conjugated to the anti-transferrin receptor single-chain antibody fragment (TfRscFv) for efficient and specific delivery of siRNA to tumor cells in mice after intravenous administration.¹²⁹ Although the utilisation of immunoliposomes is a promising approach for targeted gene delivery, there is a lack of SAR study on the structures of PEG-phospholipids for achieving optimal gene transfections.

1.4.2 Integrin-Mediated Gene Delivery

Integrins are heterodimeric membrane proteins found on all cells that mediate cell adhesion to extracellular matrices.¹³⁰ They are exploited as cell-surface receptors by

a number of intracellular pathogens including bacteria and viruses.^{131,132} In particular, adenoviruses are known to require an arginine-glycine-aspartic acid (RGD) tripeptide sequence for cell binding and internalisation.¹³³ The RGD motif has a high binding affinity for several different integrins including $\alpha_5\beta_1$ and most α_v -containing proteins.^{130,134} $\alpha_5\beta_1$ Integrins are expressed on many cells including epithelial cells, airway fibroblasts, smooth muscle cells and hematopoietic cells. Integrin-mediated internalisation allows multipoint attachment to cell-surface receptors, and has no specific size limitation for cell entry.¹³⁵ These properties are desirable for active-targeting gene delivery.

The integrin-binding ability of natural proteins can be easily reproduced by synthetic peptides that mimic the integrin-binding sequence. Hart and co-workers synthesised two bifunctional peptides **90** and **91**, each comprising a cyclic targeting domain and a short stretch of 16 lysine ([K]₁₆) residues for DNA compaction (Figure 1.4.4).^{136,137} Peptide **90** features an integrin-binding domain which possesses the conserved RGD motif, whereas peptide **91** is based on a cyclic domain CRRETAWAC isolated from a phage display library and specific for the $\alpha_5\beta_1$ integrin.¹³⁴ The highly-condensed peptide/DNA complexes protected the plasmid DNA from nuclease degradation and transfected a wide range of cell lines. Several other synthetic peptides have since been synthesised to facilitate both *in vitro* and *in vivo* gene delivery, however, low transfection efficiencies were observed due to insufficient endosomal escape.¹³⁶⁻¹³⁹

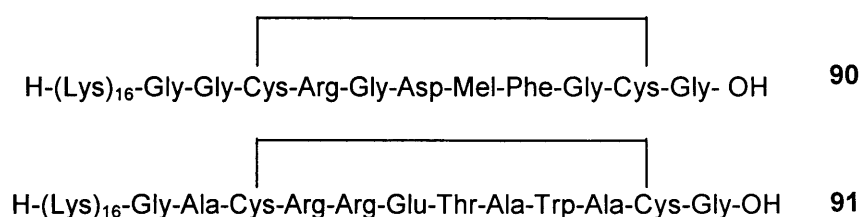


Figure 1.4.4

1.4.3 Lipid (L)/Peptide (I)/ DNA (D) Delivery System

The novel ternary LID vector comprising a cationic liposome (L), an integrin-binding peptide (I) with a [K]₁₆ tail, and a plasmid DNA (D), has been described by Hart *et al.*¹⁴⁰ The first generation LID vector utilising LipofectinTM (1:1 mixture of

DOTMA and co-lipid DOPE) as cationic liposome, has significant advantages over the lipid/DNA (LD) and peptide/DNA (ID) systems used for gene transfer, transfecting a range of non-dividing cells with high efficiencies.¹⁴⁰ The delivery of luciferase reporter genes to bronchial epithelium and parenchymal cells with this system was achieved with a similar efficiency to an adenoviral vector.¹⁸ Repeat administration of the LID vector system exhibited a negligible toxicity or inflammatory response *in vitro*. The LID particles were also found to transfect lung airway epithelium in mice, rats and piglets with high efficiencies, displayed negligible histological or biochemical evidence of inflammation.^{18,141,142} Furthermore, *in vitro* tests indicated that the LID vector system was able to transfect human keratinocytes with DNA molecules larger than 100 kb.¹⁴³ The LID vector was initially identified for the possible treatment of respiratory diseases such as cystic fibrosis. The integrin-binding peptides **90** and **91** in the LID vector have previously been utilised for LID formulations.¹⁴⁰ Other lipopolyplex vector systems utilising cytofectins such as DOTAP and DOSPA have also been reported.^{144,145}

Based on our preliminary biophysical studies, a model for the macromolecular structure of the LID complex has been postulated (Figure 1.4.5).^{140,146} The polylysine part of the peptide interacts with the plasmid DNA to form a tightly condensed DNA/polylysine inner core. The lipid component may have secondary interactions with the DNA/polylysine core resulting in further condensation of the complex. The lipids DOTMA and DOPE are likely to form a disordered coating to encapsulate the complex. Furthermore, the cyclic domain of the peptide should be at least partially exposed at the lipid surface to facilitate integrin binding of the LID complex (Figure 1.4.5).¹⁴⁶ Particle sizing studies indicated that discrete particles are formed upon self-assembly of the LID components with diameters of 100-150 nm.^{140,146,147}

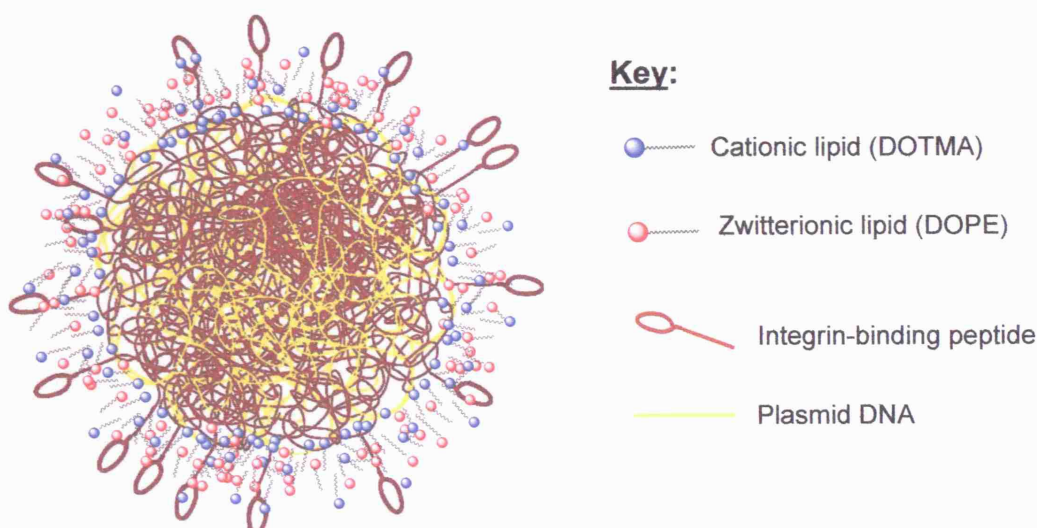


Figure 1.4.5 Model of LID delivery system¹⁴⁶

1.4.3.1 Proposed Mechanism of LID-mediated Gene Delivery

It is believed that the LID vector complex enters cells *via* a receptor-mediated endocytotic pathway. Hart *et al.* have proposed a mechanism for cell entry and the intracellular fate of the LID delivery system (Figure 1.4.6).¹⁴⁰ The LID complex has a very high surface concentration of integrin-binding ligands and thus a high affinity for the cell-surface receptors (Step 1). Once bound to the cell surface, the complex is can be invaginated into the cell membrane and internalised by integrin-mediated endocytosis (Step 2), resulting in vesicle formation and encapsulating the LID complex within an endosome (Step 3). The lipid component can induce endosomal disruption leading to the release of the peptide/DNA complex into the cytoplasm (Step 4).¹⁴⁰ The peptide can then mediate DNA transport into the nucleus, followed by unpackaging of the peptide/DNA complex and transcription of the DNA.¹⁴⁸

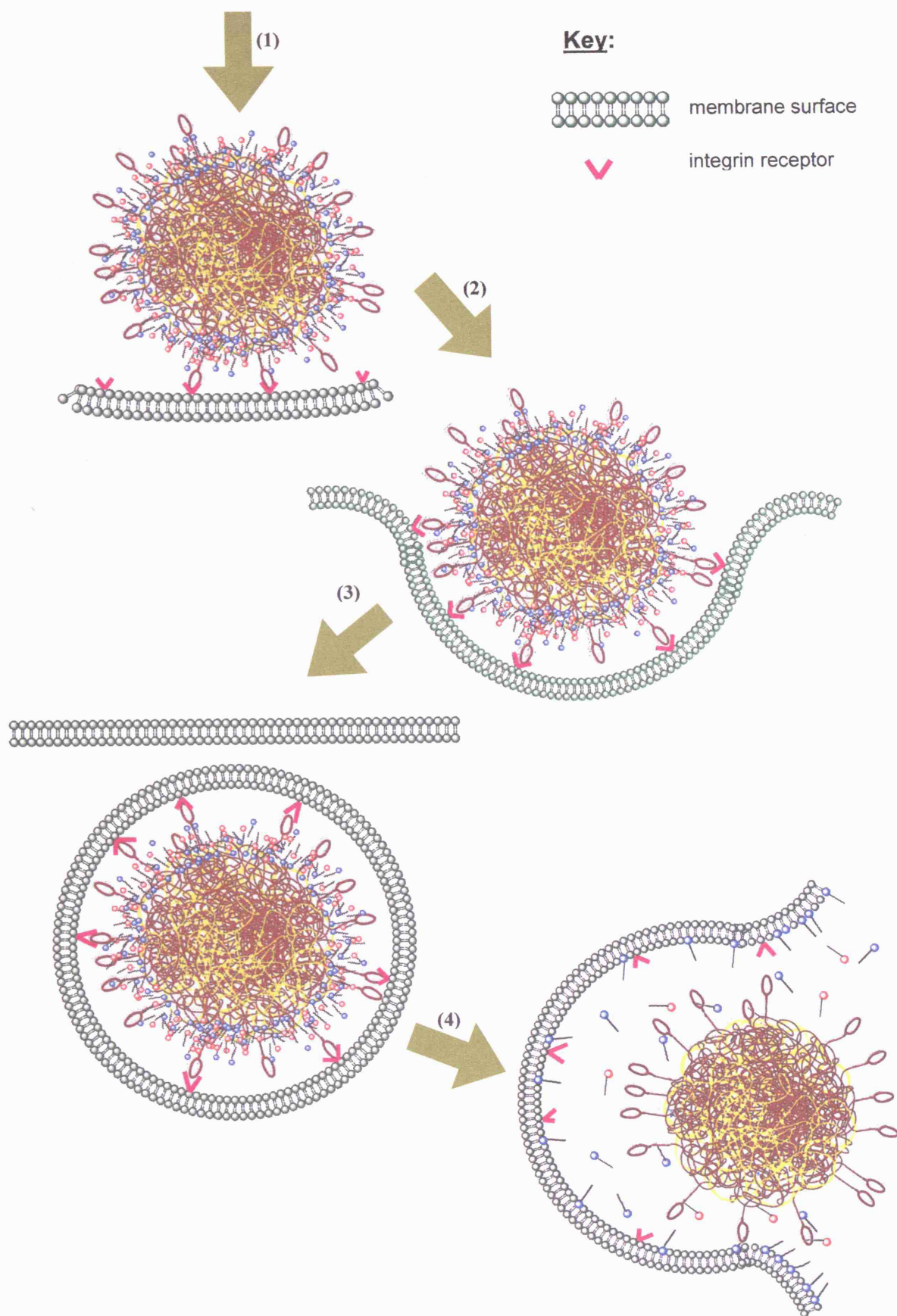


Figure 1.4.6 Proposed mechanism for LID-mediated cell entry

1.4.3.2 Structural Requirements of the Lipid Component in LID Vector System

The lipid component in the initial LID vector studied contained the cationic lipid DOTMA (6) and co-lipid DOPE (7). The cationic lipid DOTMA is comprised of three main structural components: i) a cationic quaternary amine headgroup; ii) glycerol skeleton possessing ether linkages; iii) two 18-carbon (C18) lipid chains with *cis*-alkene moiety. Each of these elements is known to influence the transfection efficiency of LD systems and therefore may also affect the transfection efficiency of LID formulations.^{40,47}

Previous preliminary investigations within our group explored the influence of lipid chain length and their degree of unsaturation on LD and LID vector transfection activities (Figure 1.4.7).¹⁴⁹ It was found that varying the alkyl chain length within the two series of saturated and unsaturated lipids had specific and different effects on the transfection efficiency of LD and LID systems. In particular, the shortening of the unsaturated lipid chain from C18 to C16 generated cationic lipid DHTMA, which displayed significantly improved transfection activity in the LID vector system, with high transfection levels observed in human airway epithelial (HAE) cells and primary human skin fibroblasts *in vitro*.¹⁴⁹ The addition of DOPE was beneficial when formulated into liposomes with saturated lipids but more variable in its effects with unsaturated lipids, and the effect of DOPE here may depend on the target cell.

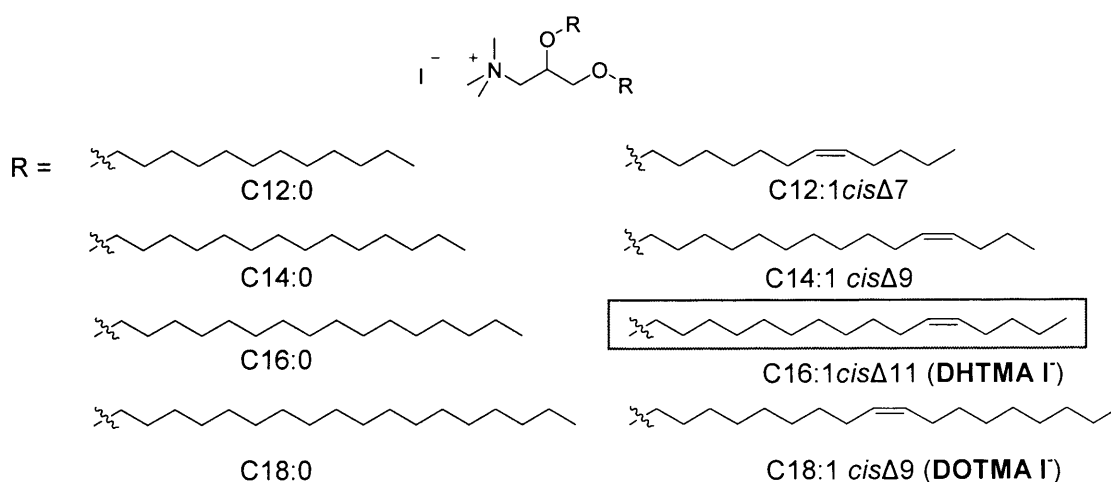


Figure 1.4.7

1.5 Aims of Project

The aim of this project was to explore the structural requirements of the lipid component which leads to optimal formulation for the LID delivery system. Our previous preliminary structure-activity relationship (SAR) study on 1,2-dialkoxo-3-trimethylammonium propane cationic lipids (DOTMA analogues) demonstrated that different lipid chain lengths and the degree of unsaturation had a major influence on the activity of the LD and LID systems (see Section 1.4.3.2).¹⁴⁹ Nevertheless, other structural elements such as the position and geometry of double bond on the lipid chain, as well as the optical activity of lipids, could also have a significant influence on vector transfection activity. A modular study of these structural components was therefore carried out to further optimise cationic lipids for lipopolyplex gene transfection. Also the synthesis of fluorescently-labelled lipids would enable investigations into the role of cationic lipids in the LID complex.

The attachment of PEG to lipids has been found to enhance stability of other LD systems. It was hoped that the synthesis and use of PEG-lipid conjugates would improve LID vector stability and hence enhance transfections for both *in vitro* and *in vivo* delivery. In particular, the development of novel cationic lipids bearing acid-cleavable PEG moieties was desirable as this might facilitate endosomal release of the DNA molecules once internalised in the cell. The acid sensitivity of these lipids as well as their biological activities would be assessed.

Furthermore, it was hoped that the introduction of a secondary cationic charge on the lipids would be beneficial for LID formulations. Having the targeting ligands conjugated directly to the lipids could be a useful strategy for active-targeting in gene delivery. Designing lipids that are covalently attached to integrin-binding peptides or antibody fragments would therefore be advantageous for receptor-mediated liposomal gene delivery.

CHAPTER 2

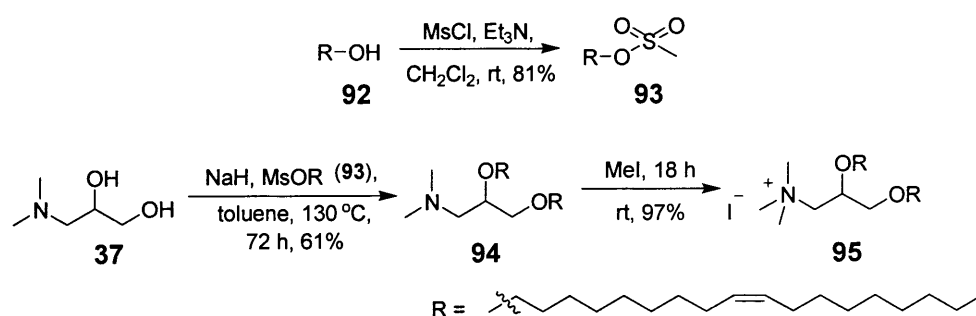
RESULTS AND DISCUSSION

DOTMA Lipid Analogues

2.1 Synthesis of DOTMA

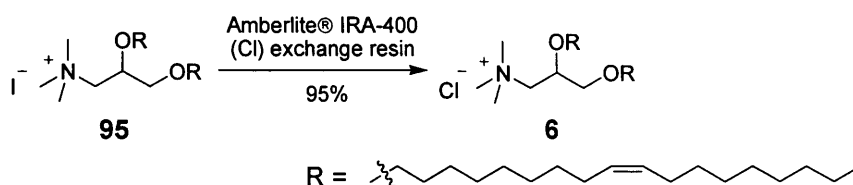
Investigations into the structural requirements of the lipid component in the LID vector formulation were initiated with the synthesis of DOTMA (**6**). DOTMA is commercially available, but has a poor availability and is very expensive.¹⁵⁰ A direct route to DOTMA has been reported by Felgner *et al.*, involving the dietherification of racemic 3-dimethylamino-1,2-propanediol (**37**) with activated oleyl alcohol and subsequent quaternisation with chloromethane (Figure 1.3.1).³⁷ Our initial aims were to produce DOTMA for use in control transfection experiments, and an optimised synthetic condition established could then be adapted in the syntheses of analogues.

The preparation of DOTMA was carried out through modifications of Felgner's method.^{37,151} Initially, commercially available oleyl alcohol (**92**, *cis/trans* \approx 85:15) was activated using methanesulfonyl chloride and triethylamine, to yield the mesylated alcohol **93** in 81% yield (Scheme 2.1.1).¹⁵² Dietherification of diol **37** was first attempted with **93** in anhydrous THF, using sodium hydride as base, by heating the reaction mixture at 80 °C. The desired diether derivative **94** was formed after 72 h, and was isolated by flash column chromatography in a low yield of 18%. In an attempt to optimise the reaction conditions, the preparation of **94** was repeated using anhydrous toluene as a solvent. Heating the reaction mixture at reflux resulted in the formation of **94** in an enhanced yield of 61%, after purification by column chromatography. Finally, the dietherified derivative **94** was successfully converted to the iodide salt of DOTMA (**95**) in 97% yield, by stirring with excess iodomethane at rt (Scheme 2.1.1).



Scheme 2.1.1

The chlorinated salt of DOTMA was obtained by passing the iodide derivative **95** through an Amberlite® IRA-400 (Cl) ion exchange resin column, to afford the chloride derivative **6** in 95% yield (Scheme 2.1.2). A notable colour change was observed in this transition: the iodide salt **95** was a dark yellow oil, whereas the chloride salt **6** was a pale yellow oil.



Scheme 2.1.2

2.2 Synthesis of Unsaturated DHTMA Analogues

The influence of lipid structural features on the activity of lipid/DNA vector systems has previously been reported;^{40,47,61-63} however, results from these studies suggested that the effect of structural variation on activity is both vector and cell-type dependent. We have previously tested a series of 1,2-dialkoxy-3-trimethylammonium propane cationic lipids (DOTMA analogues) and demonstrated that lipid chain length variations and degree of unsaturation had a significant influence on the transfection activity of lipoplex and lipopolyplex formulations (see Section 1.4.3.2).¹⁴⁹ Specifically, the DOTMA analogue with 16-carbon alkyl chain and a *cis*-alkene moiety (DHTMA I⁻) was found to be superior in targeting human airway epithelial (HAE) cells and human skin fibroblasts. It was therefore decided to further investigate the structural requirements of the lipid component by a systematic modification of the hydrophobic region in the glycerol based lipids, and to synthesise a structurally related series of unsaturated DHTMA analogues. The selected modifications involved varying the geometry and position of the double bonds on lipid chains by incorporating a *cis*- or *trans*-alkene moiety at the C-9, C-11 or C-13 positions (Figure 2.2.1). Furthermore, the degree of unsaturation was also investigated by replacing the double bonds with an alkyne moiety.

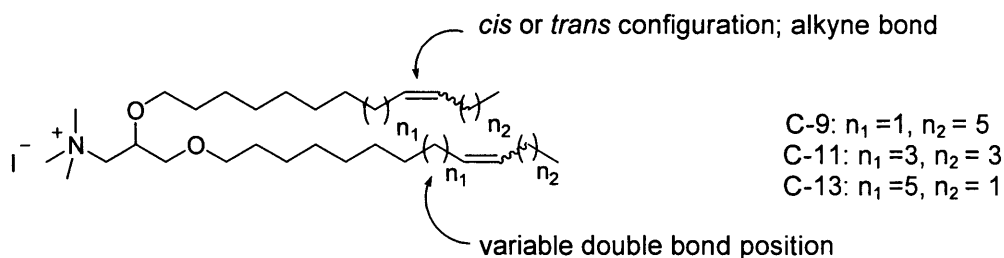


Figure 2.2.1 Proposed structural variations on DHTMA

Structural variations on cytofectins can influence the transfection process in several ways. For example, different lipid packaging preferences could alter the stability of LID complexes and their abilities to promote endosomal escape under physiological conditions. In addition, the amount of integrin-binding motif exposed on the surface of LID vector could be altered, thus affecting the transfection efficacy of the lipopolyplexes.

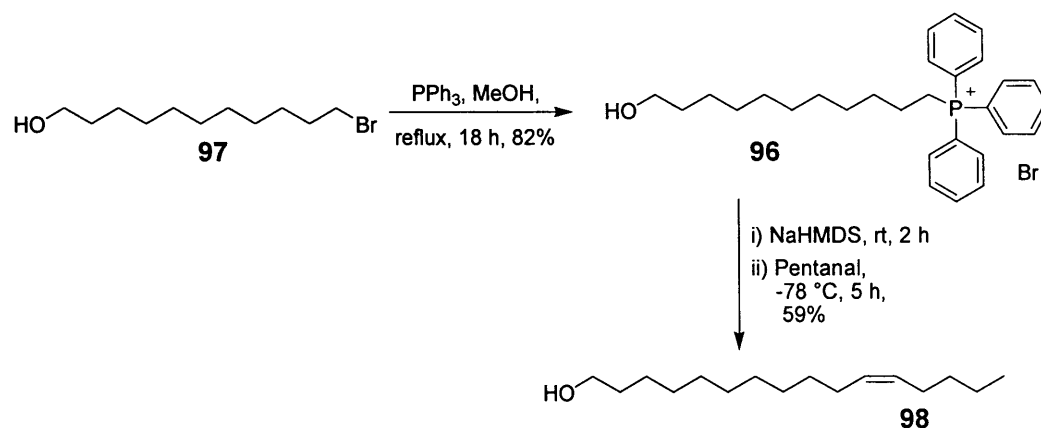
2.2.1 Syntheses of Hexadecen-1-ol Analogues

The syntheses of hexadecen-1-ol derivatives were initially investigated to prepare geometric isomers of the unsaturated alcohols, which were later utilised to produce DHTMA analogues.

2.2.1.1 Synthesis of (Z)-Hexadec-11-en-1-ol via Wittig Methodology

Synthesis of (Z)-hexadec-11-en-1-ol was first investigated utilising Wittig methodology. Formation of the phosphonium bromide salt **96** was achieved in 82% yield, by heating 11-bromo-1-undecanol (**97**) and triphenylphosphine in methanol at reflux (Scheme 2.2.1).¹⁵³ The Wittig coupling of **96** and pentanal was initially attempted in anhydrous THF at $-78\text{ }^{\circ}\text{C}$, using *n*-butyllithium (*n*-BuLi) as base.¹⁵⁴ ^1H NMR spectroscopic analysis of the crude reaction mixture indicated that the alkene **98** was formed with a *cis:trans* ratio of approximately 1:3, and was isolated by column chromatography in 60% yield. In an attempt to increase the stereospecificity of alkene formation, the coupling reaction was performed under salt-free conditions, using sodium hexamethyldisilylamide (NaHMDS) as base.¹⁵⁵ After pre-mixing **96** and NaHMDS for 1 h, addition of pentanal led to the formation of **98** in 59% isolated yield, after purification by column chromatography. The alkene formed was roughly

a *cis:trans* mixture (9:1) of the two inseparable geometric isomers, as indicated by ^1H NMR spectroscopic analysis of the isolated product.^{156,157}



Scheme 2.2.1

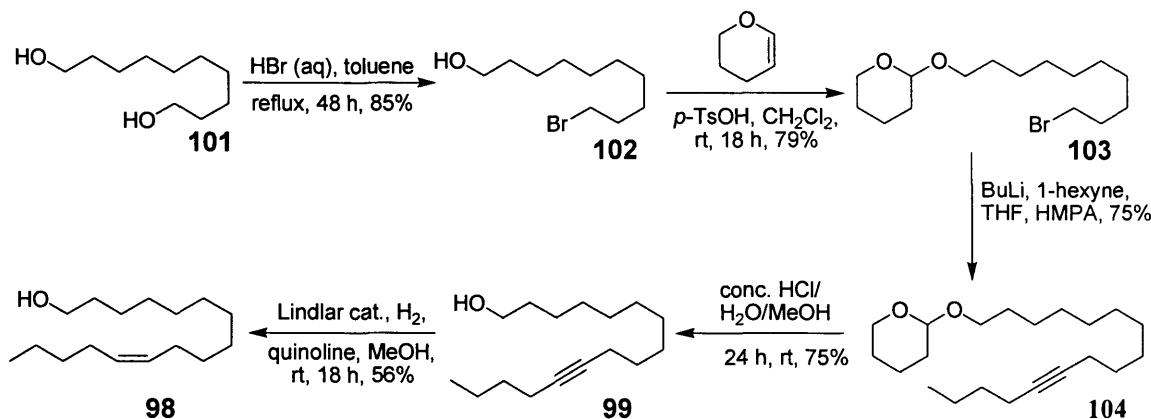
The Wittig strategy has the advantage that only two steps were required to form the unsaturated alcohol. In addition, the alkene formed using NaHMDS as base has a *cis:trans* ratio similar to the oleyl alcohol used for DOTMA formation (see Section 2.1); however, the stereoselectivity of the reaction was not sufficiently high enough for the SAR study. At this stage an alternative strategy was considered.

2.2.1.2 Synthesis of (Z)- and (E)-Hexadec-11-en-1-ol via Reduction

Methodology

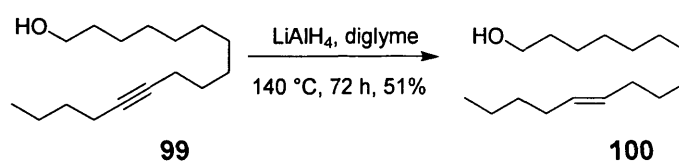
The second strategy investigated involved the stereoselective reduction of alkyne intermediate 99 to afford the *cis*- and *trans*-alkene 98 and 100, respectively. (Scheme 2.2.2 & 2.2.3).¹⁵⁸ Initially, commercially available undecane-1,11-diol (101) was mono-brominated using aqueous hydrobromic acid, to give the bromo alcohol 102 in 75% yield after purification by column chromatography.¹⁵⁹ Compound 102 was converted to the corresponding tetrahydropyran ether (THP) 103 in 79% yield, using 3,4-dihydro-2H-pyran and *p*-toluenesulfonic acid (*p*TsOH) as catalyst. The coupling of 103 and 1-hexyne was carried out using *n*-butyllithium (*n*-BuLi), in the presence of hexamethylphosphoramide (HMPA) as a co-solvent, to give 104 in 75% yield after column purification.¹⁵⁸ THP-deprotection of 104 was carried out using a concentrated hydrochloric acid/water/methanol mixture (1:1:5), to furnish 99 in 75% yield. The *cis*-reduction of 99 was undertaken utilising a Lindlar catalyst with quinoline under a hydrogen atmosphere.¹⁵⁸ Purification by flash column

chromatography afforded the *cis* alkene **98** in 56% yield (Scheme 2.2.2). The formation of the *trans* alkene was not detected by ^1H NMR spectroscopy, suggesting that the *cis*-reduction by Lindlar catalyst was >97% stereoselective.



Scheme 2.2.2

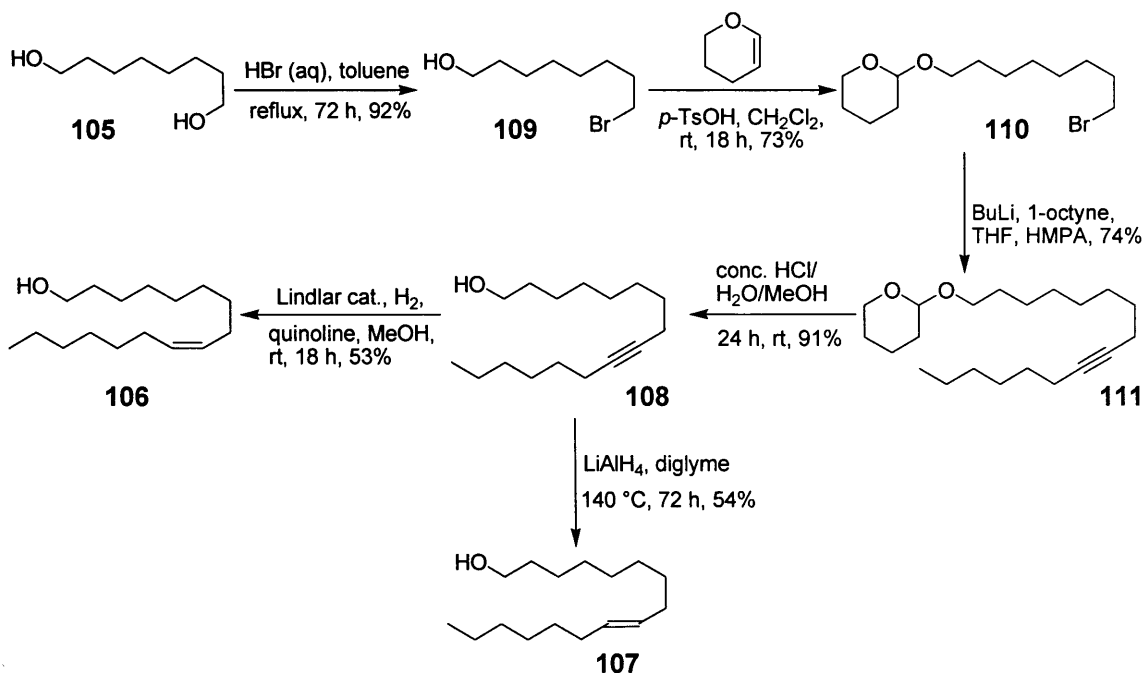
Sorochinskaya *et al.* have reported the stereoselective reduction of **99** to its corresponding *trans* alkene **100** with lithium aluminium hydride (LiAlH_4).¹⁶⁰ Using this method, a solution of **99** and LiAlH_4 in anhydrous diglyme was heated at $140\text{ }^\circ\text{C}$ (Scheme 2.2.3). ESMS analysis of the crude reaction mixture indicated that the alkyne was completely consumed after 72 h, with no over-reduction product observed. The *trans* alkene **100** was isolated and purified by flash column chromatography in 51% yield. No *cis* isomer was detected by ^1H NMR spectroscopy.



Scheme 2.2.3

2.2.1.2 Synthesis of (*Z*)- and (*E*)-Hexadec-9-en-1-ol

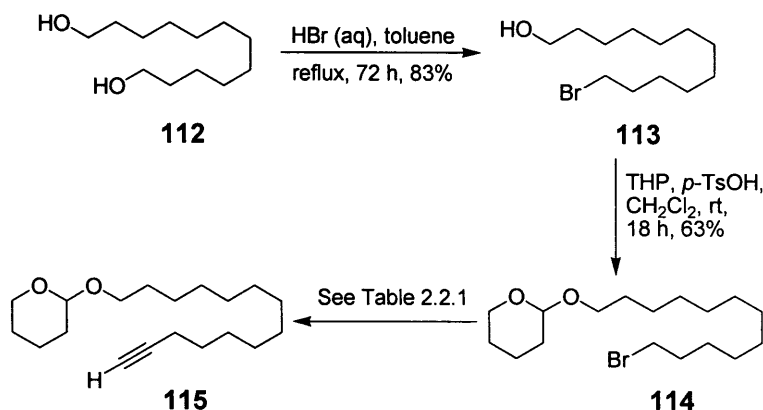
The synthesis of *cis* and *trans* isomers of hexadec-9-en-1-ol were carried out following the alkyne reduction methodology established previously (see Section 2.2.1.1). The synthetic route investigated is summarised in Scheme 2.2.4. Starting from 1,8-octandiol (**105**), the (*Z*)- and (*E*)-hexadec-9-enol, **106** and **107**, were readily prepared by the stereoselective reduction of the alkyne intermediate **108**, both with yields of 25% over five steps (Scheme 2.2.4).



Scheme 2.2.4

2.2.1.3 Synthesis of (Z)- and (E)-Hexadec-13-en-1-ol

The synthetic route for preparing (Z)- and (E)-hexadec-13-en-ol is summarised in Scheme 2.2.5 and 2.2.6. 1,12-Dodecandiol (**112**) was first mono-brominated using aqueous hydrobromic acid, followed by THP-protection of the resulting bromo alcohol **113**, to give the THP-protected bromide **114** in 52% yield over two steps (Scheme 2.2.5). Due to the poor availability and high cost of 1-butyne, a two-step approach was investigated as an alternative route to introduce the alkyne moiety. The conversion of **114** to alkyne **115** was initially attempted using ethynylmagnesium bromide in anhydrous THF and HMPA, but only the starting materials were recovered after 72 h (Table 2.2.1, entry 1). Following the methodology described by Hanack *et al.*, the alkylation of **114** was re-attempted using sodium acetylide (Table 2.2.1, entry 2).¹⁶¹ Examination of the ¹H NMR spectrum of the crude mixture indicated that the alkyne **115** was formed after 72 h, but approximately 50% of **114** was left unreacted. The isolation of **115** by column chromatography was not attempted as TLC analysis indicated that **114** and **115** have very similar R_f values. Finally, complete conversion of **114** to **115** was achieved using lithium acetylide-ethylenediamine complex in anhydrous DMSO, following the methodology described by Nieuwenhuizen *et al.* (Table 2.2.1, entry 3).¹⁶² Compound **115** was isolated and purified by flash column chromatography in 60% yield.

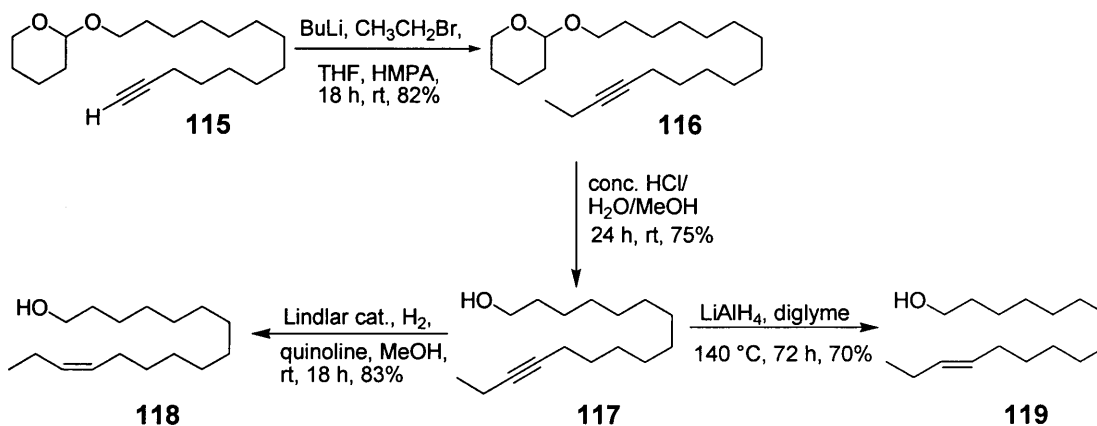


Scheme 2.2.5

Entry	Alkyne reagent (eq)	Conditions	Yield (%)
1	$\text{HC}\equiv\text{CMgBr}$ (1.6)	THF, HMPA, 72 h, rt	0
2	$\text{HC}\equiv\text{CNa}$ (2.6)	THF, HMPA, 72 h, rt	—
3	$\text{HC}\equiv\text{CLi} \cdot \text{EDA}$ (1.2)	DMSO, HMPA, 72h, rt	60

Table 2.2.1

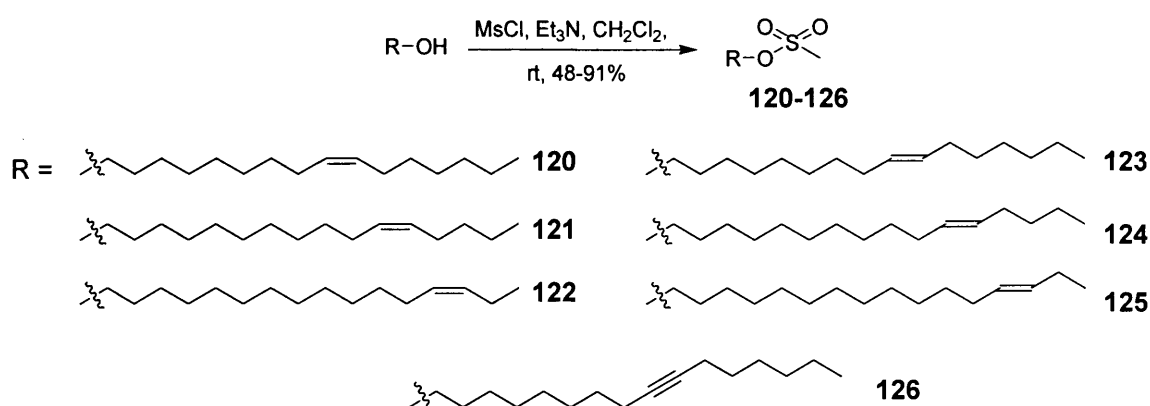
The coupling of **115** and bromoethane was readily achieved, using *n*-BuLi as base, to afford **116** in 82% yield (Scheme 2.2.6). Subsequent THP-deprotection followed by stereoselective reductions of the alkyne intermediate **117** yielded the (*Z*)- and (*E*)-hexadec-13-en-1-ol (**118** and **119**) in high yields.



Scheme 2.2.6

2.2.2 Synthesis of DHTMA Analogues

Formation of mesylate derivatives of the unsaturated alcohols (**98**, **100**, **106**, **107**, **118** and **119**) and an alkyne analogue (**108**) were achieved using methanesulfonyl chloride and triethylamine (Scheme 2.2.7). The conversion of **108** to its corresponding C16 lipid analogue was undertaken to examine the effect of alkyne bonds on LID vector transfections compared to its alkene analogues. Compounds **120-126** were purified by flash column chromatography and the conversions occurred in moderate to high yields (Table 2.2.2).



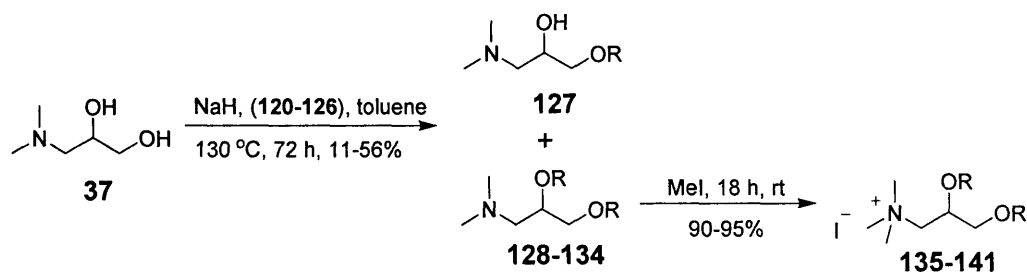
Scheme 2.2.7

Entry	Alcohol	Product (yield, %)
1	106	120 (71)
2	98	121 (48)
3	118	122 (60)
4	107	123 (55)
5	100	124 (71)
6	119	125 (76)
7	108	126 (91)

Table 2.2.2

Following the procedure optimised for DOTMA synthesis (see Section 2.1), the dietherification of amine **37** was undertaken by stirring with sodium hydride in anhydrous toluene, followed by addition of the selected mesylate (**120-126**) (Scheme 2.2.8). In general, ESMS and ^1H NMR spectroscopic analysis of the crude reaction mixtures suggested that the mono-etherified derivative **127** and dietherified products

(128-134) were formed. The desired compounds **128-134** were isolated and purified by column chromatography in low to modest yields (Table 2.2.3). The dietherified derivatives were subsequently quaternised with excess iodomethane, to furnish the DHTMA analogues **135-141** in moderate to high yields (Scheme 2.2.8).



Scheme 2.2.8

Entry	Mesylate	Amine (Yield, %)	C1-16 DOTMA analogues (Yield, %)	Alkene position (geometry)
1	120	128 (44)	135 (95)	C-9 (<i>cis</i>)
2	121	129 (34)	136 (95)	C-11 (<i>cis</i>)
3	122	130 (11)	137 (93)	C-13 (<i>cis</i>)
4	123	131 (20)	138 (64)	C-9 (<i>trans</i>)
5	124	132 (25)	139 (95)	C-11 (<i>trans</i>)
6	125	133 (19)	140 (90)	C-13 (<i>trans</i>)
7	126	134 (56)	141 (65)	C-9 (alkyne)

Table 2.2.3

2.3 Biological Data for Unsaturated DHTMA Analogues

In these structure-activity relationship (SAR) studies we aimed to:

- Investigate the influence of lipid chain double bond position on the transfection efficiency of LID vector systems;
- Explore the influence of alkene geometry within the lipid chain;
- Establish the effect of triple bond on lipid chain;
- Investigate the effect of DOPE in the systems;
- Estimate the influence of lipid concentration on transfection with the compounds.

Testing was undertaken following the methodology described by Hart *et al.* and carried out by Dr. Stephanie Grosse (ICH).¹⁴⁰ Human airway epithelial (HAE) cell lines were investigated for transfection with standard and modified LID vector formulations unless otherwise stated. Standard LID vector formulations used of cyclic peptide **91** ([K]₁₆GACRETAWACG), plasmid DNA (pCILuc luciferase reporter gene), and cytofectin (LipofectinTM or cationic lipid synthesised). Modified lipid formulations were comprised of cationic lipid/DOPE at a 1:1 ratio (*wt/wt*) or cationic lipids alone. The following weight ratios were tested for each lipid/peptide/DNA formulation, 0.75:4:1, 2:4:1 or 4:4:1. Results for lipids at 2:4:1 and 4:4:1 ratios are presented unless otherwise stated. Transfection activity has been expressed as relative light units per milligrams of protein produced (RLU/mg).

2.3.1 The Effect of Double Bond Position on Activity

The effect of varying the double bond position (C-9, C-11, C-13) of *cis*- and *trans*-alkene (C16:1) lipids on transfection activity with HAE cells was determined and is summarised in Chart 2.3.1 and 2.3.2, respectively. For C16:1 lipids having the *cis*-alkene moiety (**135-137**), the transfection efficiencies varied in the order C-11 (**136**) > C-13 (**137**) > C-9 (**135**). At constant peptide and DNA concentrations, the C-11 analogue (**136**) was more active than its C-9 (**135**) and C-13 (**137**) counterparts (**135**) by more than 8 and 3 fold, respectively (Chart 2.3.1).

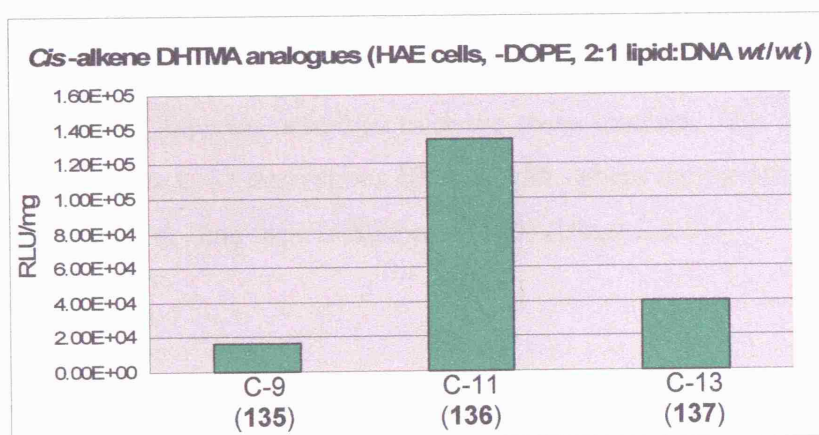


Chart 2.3.1

Interestingly, the activities of C16:1 lipids bearing the *trans*-alkene moiety gave a different pattern: C-13 (**140**) > C-9 (**138**) > C-11 (**139**) with C-11 analogue

(**139**) being the least active (Chart 2.3.2). Variations in the *trans*-alkene position had less influence on activities than their *cis* counterparts, which was demonstrated by only small differences in their efficiencies (~2 fold).

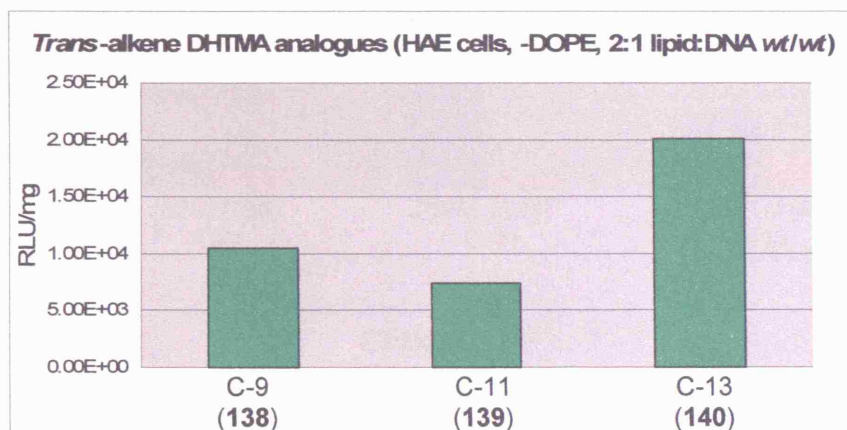


Chart 2.3.2

The influence of lipid double bond position on transfection activity has been demonstrated for the first time within the LID vector system. These results indicate that a significant variation in activity can be achieved by simply changing the position of the double bond, while keeping the geometry and degree of unsaturation constant.

2.3.2 The Effect of Double Bond Geometry on Activity

Generally it was found that at a fixed double bond position the *cis*-alkene lipid derivatives displayed superior activities over the *trans*-isomers. This is exemplified by a comparison of the C-11 derivatives **136** and **139**, where the *cis*-alkene lipid (**136**) was 18 fold more active than the *trans*-isomer (**139**) (Chart 2.3.3).

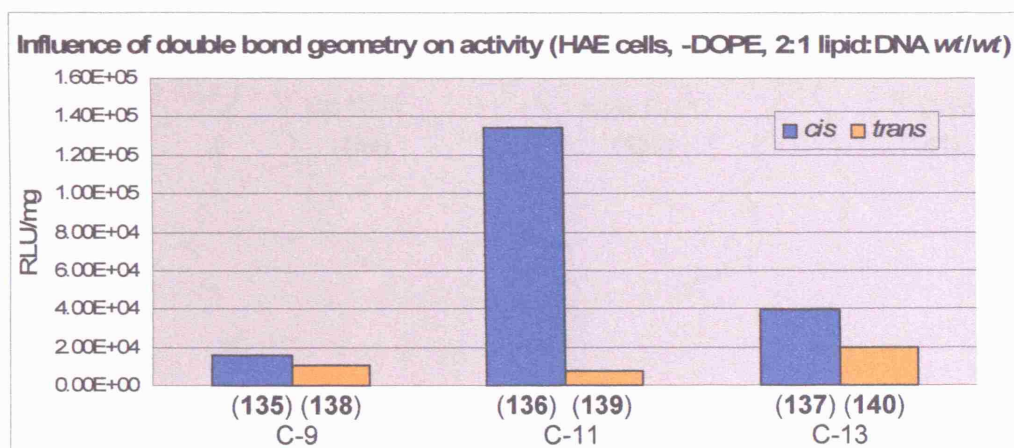


Chart 2.3.3

The effect of double bond geometry on activity has been reported in only a few other vector systems,^{61,62} but this is the first time that it has been observed within the LID vector systems. The difference in activity between the *cis*- and *trans*-alkene lipids may be rationalised in terms of their differing abilities to promote endosomal escape. It was previously suggested that the *cis*-alkene moiety generates a “kink” in the lipid chain, resulting in lipids which prefer to adopt a cone-like molecular shape (Figure 2.3.1a).^{88,93} The cone-like structure was shown to favour membrane fusion, by promoting the H_{II} lipid phase at lower temperatures.^{87,88,93} In addition, the H_{II} lipid phase may promote endosomal escape of the encapsulated contents *via* liposome-endosome membrane fusion, leading to enhanced DNA release into the cytoplasm. In addition, the *cis*-alkene lipids (135-137) are likely to have lower chain-melting phase transition temperatures (T_c) than their *trans* counterparts, leading to greater disruption on the liposomal membranes. By contrast, the *trans*-alkene lipids (138-140) contain the *trans*-alkene moiety with a torsion angle of 180°. These lipids are likely to occupy less volume than their *cis* counterparts and have a more-cylindrical shape (Figure 2.3.1b). These lipids are more likely bilayer in nature and less likely to promote endosomal disruption at physiological temperatures, resulting in reduced activity compared to their *cis* counterparts.

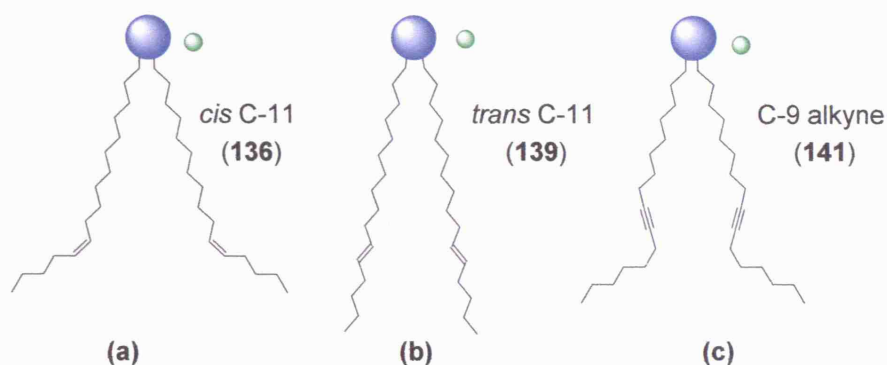


Figure 2.3.1

2.3.3 The Effect of Triple Bond on Activity

The transfection efficiencies were determined for the alkene and alkyne lipid analogues (Chart 2.3.4). For C16 lipids that have unsaturated bonds at the C-9 position, the alkyne analogue (**141**) showed the greatest activity with the following pattern observed: alkyne (**141**) > *cis* (**135**) > *trans* (**138**).

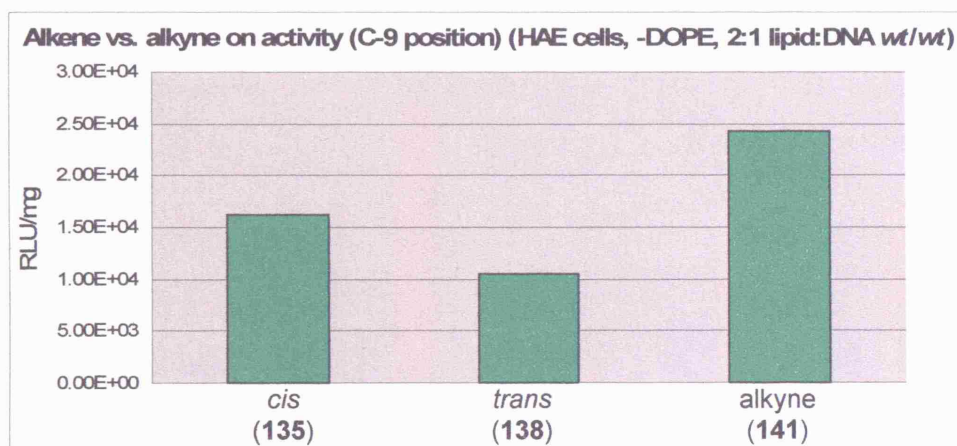


Chart 2.3.4

The superior activity of alkyne lipid over its alkene counterparts has been observed in another system. Miller and co-workers have rationalised that the presence of triple bonds can significantly reduce the “kink” on the lipid chains present in the *cis* analogue, leading to lipids occupying less volume (Figure 2.3.1c).⁶³ Hence the alkyne lipid (**141**) may prefer to adopt a more rigid lamellar liposome structure and exhibit a higher phase transition temperature than the *cis*-alkene lipid (**138**). As suggested by Miller and co-workers, the additional liposomal and lipoplex

stability formed by an alkyne lipid such as **141** may enhance the lipopolyplex activity, by providing enhanced protection to DNA from extracellular nuclease degradation and prevent particle aggregation in serum during its pathway to the endosome.⁶³ Ideally, a cytofectin should undergo phase transition near 37 °C so as to promote endosomal escape. Optimised transfection activity could be achieved by lipopolyplexes that have the right balance between the extracellular protection and intracellular endosomal release of the encapsulated contents.⁶³

2.3.4 The Effect of DOPE on Transfection Efficiency

It was found that the co-formulation of DOPE had specific and different effects on LID vector transfections. Firstly, the addition of DOPE to most of the *cis*- and *trans*-alkene lipids led to enhanced activities (Chart 2.3.5). This was exemplified by the presence of DOPE with the *trans* C-9 lipid (**138**), resulting in a formulation which was 14 times more active than utilising **138** alone.

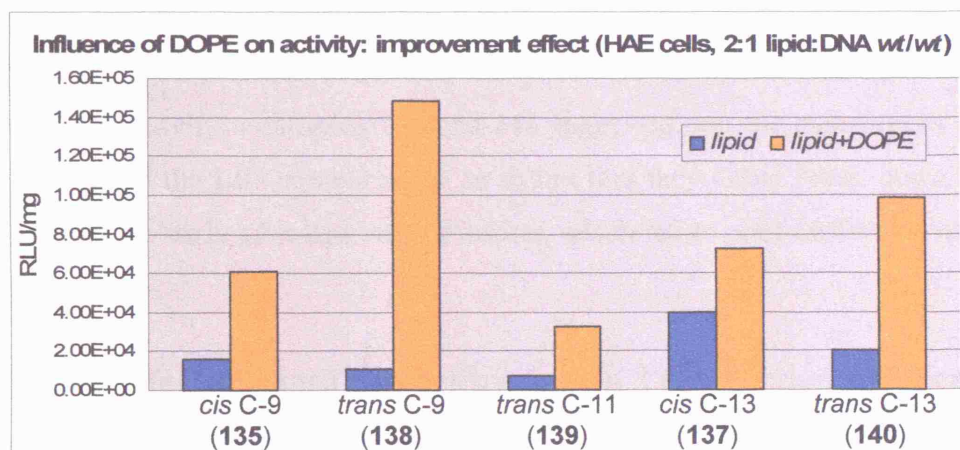


Chart 2.3.5

Conversely, addition of DOPE (1:1 *wt/wt*) with the *cis* C-11 (**136**) and alkyne (**141**) lipids resulted in reduction of activities by up to 4 fold compared to formulations utilising cationic lipids alone (Chart 2.3.6).

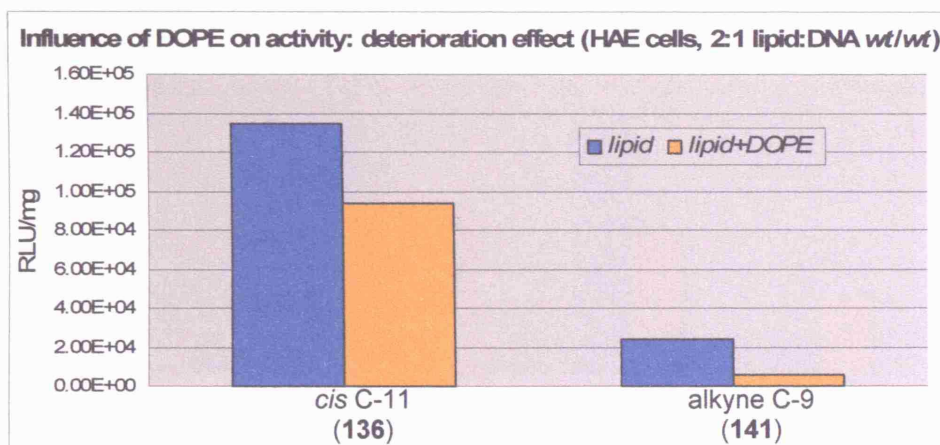


Chart 2.3.6

DOPE has been widely used as a helper lipid and was shown to enhance transfection activity in many vector systems.³⁸ DOPE forms an inverted hexagonal (H_{II}) phase at physiological temperature, and in combination with cationic lipids may force the $L_{\alpha} \rightarrow H_{II}$ phase transition.⁴² The resulting liposomes would be more fusogenic leading to greater endosomal escape, thus expected to enhance the transfection efficacy of LID complexes. However, the unexpected detrimental effect of DOPE on activity with lipids **136** and **141** suggested that the inclusion of DOPE may destabilise the LID complexes to an extent that they either break down before cell entry or too early after cell internalisation, which led to poor trafficking of DNA to the nucleus.

2.3.5 The Effect of Lipid Concentration on Transfection Efficiency

The transfection efficiencies of DHTMA analogues were determined for LID vector systems with lipid/DNA ratios at 2:1 and 4:1 (*wt/wt*). With the DNA and peptide ratios kept constant, different transfection activities were observed at different lipid concentrations. Generally the activities of unsaturated lipid analogues were found to decrease at increasing lipid concentration, however, the alkyne lipid (**141**) achieved an enhanced activity by increasing the lipid:DNA ratio to 4:1 (Chart 2.3.7). It was observed that lipid **136** gave the optimal transfection efficiencies in the absence of DOPE, both in 2:1 and 4:1 lipid/DNA weight ratios.

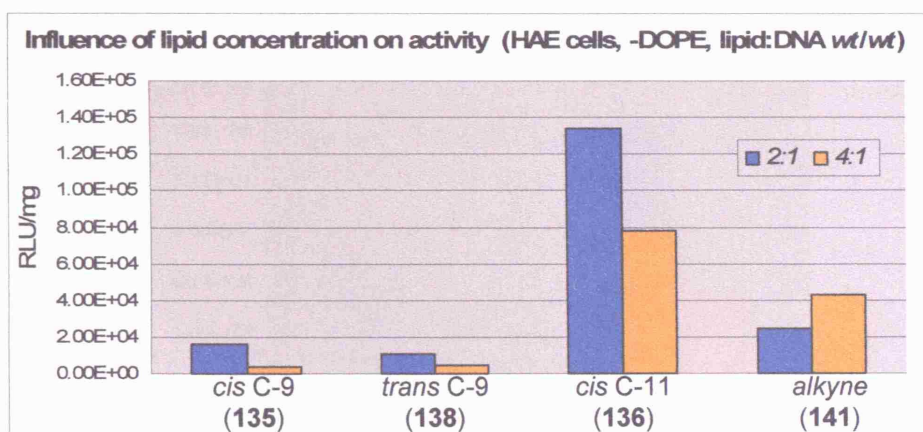


Chart 2.3.7

There are several ways in which increasing the lipid concentration can affect the biophysical properties of LID complexes. Firstly, increasing the number of positively charged lipids will enhance the electrostatic repulsions between the lipid headgroups, which can affect the aggregation phase structures in aqueous solution.³⁸ In addition, a higher lipid density can force the lipids into forming more rigid lamellar aggregates.⁸⁹ Furthermore, increasing the positive charge on the lipid compartment will increase its interactions with naturally occurring anionic lipids, thereby facilitating the endosomal escape. The differences in transfection efficiencies for DHTMA lipid analogues at different lipid concentrations were likely to be a result of combinations of these effects.

2.3.6 DOTMA vs. C16:1 Lipid Analogue

The transfection activity of DOTMA (**6**) and C16:1 lipid **136** with HAE cells and primary human skin fibroblasts, in the presence and absence of DOPE, was determined at lipid/peptide/DNA weight ratio of 4:2:1 (Chart 2.3.8 & 2.3.9). The LID vector transfections with HAE cells displayed the following order: **136** > **6** > **136**+DOPE > **6**+DOPE (Chart 2.3.8). It was demonstrated that the lipid **136** and DOTMA displaying reduced activity when co-formulated with DOPE. The optimal lipopolyplex formulation utilising lipid **136** as a cytofectin was 9 times more efficient than LipofectinTM (**6**+DOPE), the most widely used non-viral vector for gene delivery.^{37,39}

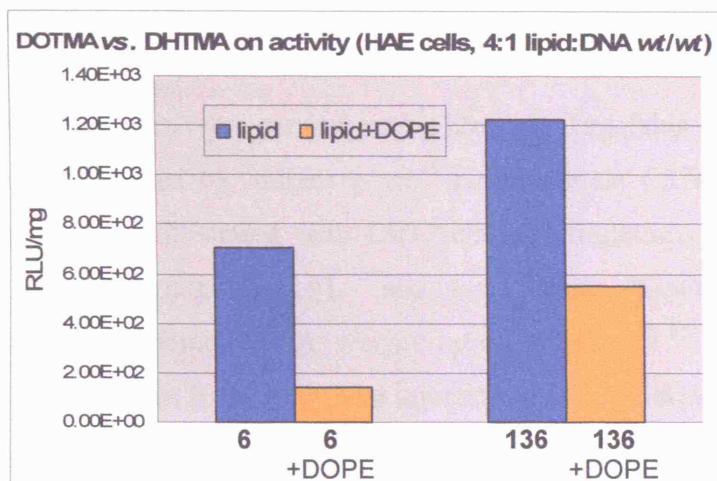


Chart 2.3.8

Transfections performed with human skin fibroblasts demonstrated some similarities in the trends of transfections with HAE cells. The most effective formulation again contained the lipid **136**, but it required co-formulation with DOPE to achieve greatest activity (Chart 2.3.9). The changing preference of DOPE on activity suggested that the dependence of DOPE in lipopolyplex transfections are probably cell-type dependent.

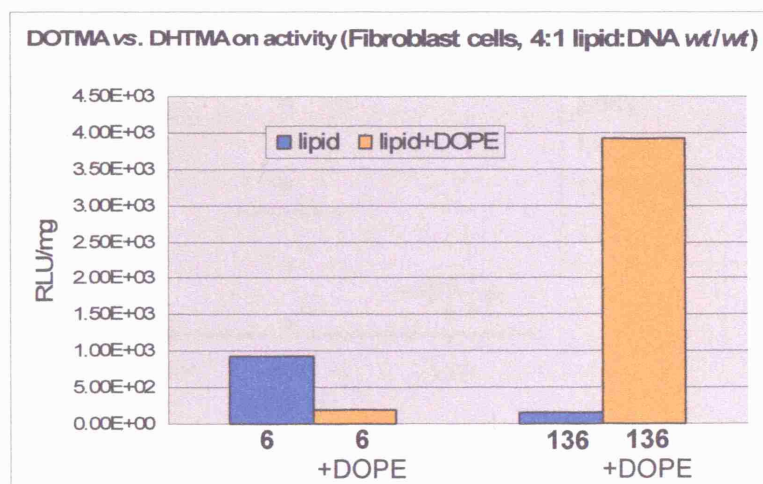


Chart 2.3.9

2.3.7 *In Vivo* Transfection Studies of C16:1 Lipid

In vivo transfection studies were carried out by Dr. Aris Tagalakakis (ICH), following the methodology described by Jenkins *et al.*¹⁸ Briefly, male C57Bl/6 mice at 4-5 weeks of age were administrated with LID vector formulations comprised of a luciferase gene (pCILuc), peptide **91**, and a cytofectin (LipofectinTM, **136** or **136**+DOPE) at a lipid/peptide/DNA weight ratio of 0.75:4:1.¹⁸ All transfection formulations were installed by intratracheal injection in a single dose. The mice were euthanized 24 h after instillation. Lung tissues were processed and the samples analysed in luciferase assays, with transfection activity expressed as RLU/mg.¹⁸

Transfection with mice lungs indicated that the lipopolyplex formulation comprised of cytofectin **136**+DOPE displayed superior activity over other formulations being tested, and was almost 10 fold better than the original LipofectinTM formulation (Chart 2.3.10). The LID vector containing lipid **136** alone was also slightly more active than LipofectinTM. The enhancement in activity observed *in vivo* by lung airway delivery with lipid **136** (\pm DOPE) is consistent with the results of the *in vitro* transfections with HAE cells and fibroblasts.

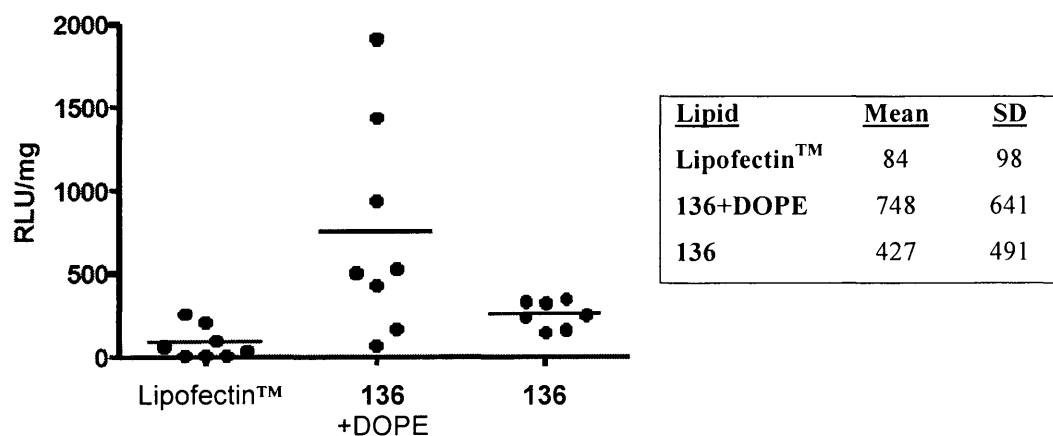


Chart 2.3.10

2.4 Synthesis of Chiral Lipid Analogues

Within the original LID vector formulations, three of the four components are in optically active form: the peptide, plasmid DNA and co-lipid DOPE (**7**), which is naturally available as the (*R*)-isomer (Figure 1.2.1). However, the cationic lipid DOTMA (**6**) is commercially used in LipofectinTM as a racemic mixture. The

synthesis of the (*R*)- and (*S*)-lipid analogues is therefore important to establish whether the enantiomers have different transfection properties. Few cationic lipids utilised for gene therapy are produced and used as stereochemically-defined isomers. Nantz and co-workers have reported their synthesis of optically active lipid (*R*)-DORI (**142**) (Figure 2.4.1).¹⁶³ When co-formulated with cholesterol, lipid **142** was found to facilitate transfections in both the respiratory epithelial cells and mouse fibroblasts.¹⁶⁴ Nazih *et al.* have also described the synthesis of optically active pcTG201 (**143**) as gene transfer agent, although no transfection data was reported.¹⁶⁵

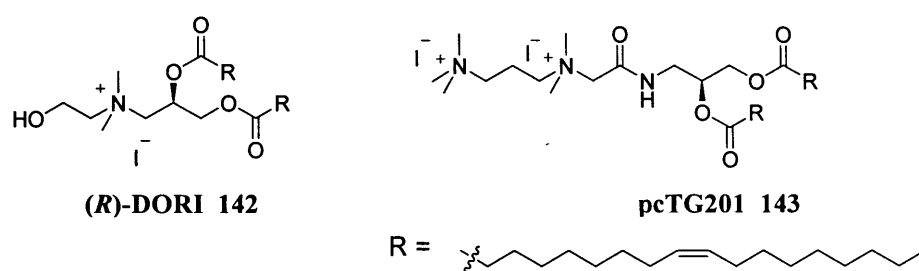
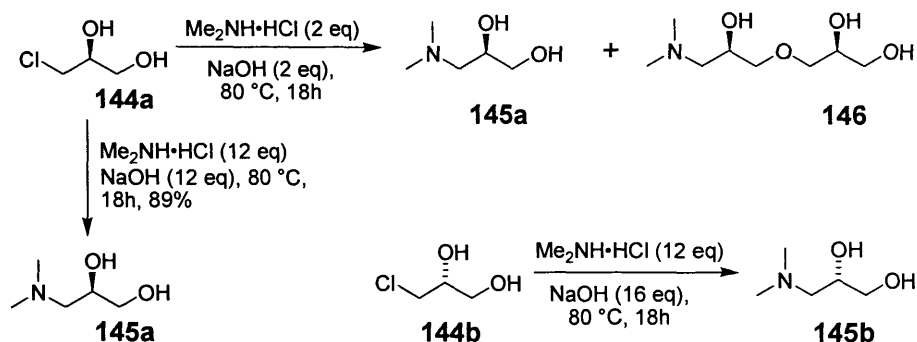


Figure 2.5.1

Most synthetic routes to optically active lipids utilised epoxy alcohol derivatives derived from the Sharpless asymmetric epoxidation.^{163,165} In his original patent, Felgner and co-workers described the synthesis of (*S*)-DOTMA in five steps from D-mannitol-3,4-acetonide; however, this route from the chiral pool would not readily afford the (*R*)-isomer.¹⁶⁶ Our aim was therefore to establish a direct and versatile route to produce (*S*)- and (*R*)-enantiomers of DOTMA (C18:1) and DHTMA (C16:1), for a SAR vector study.

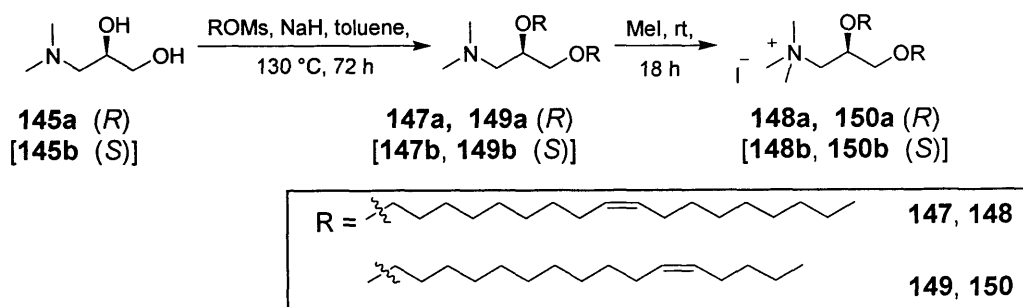
A three-step procedure was devised to prepare optically active C18:1 and C16:1 lipids, starting from commercially available (*S*)- and (*R*)-3-chloro-1,2-propanediol **144a** and **144b**, respectively.¹⁵¹ Initially, the conversion of **144a** to its corresponding amine **145a** was attempted according to the method described by Alquist and Slagh,¹⁶⁷ using two equivalents of dimethylamine hydrochloride and sodium hydroxide (Scheme 2.4.1). Examinations of ESMS and ¹H NMR spectra of the reaction mixture suggested that **145a** and the triol **146** were formed, with TLC analysis indicated that the mixtures have very similar *R_f* values. To avoid the formation of **146**, the reaction was re-attempted using a large excess (12 equivalents) of dimethylamine hydrochloride and sodium hydroxide.¹⁵¹ After heating at 80 °C for

18 h, compound **145a** was formed and separated from all impurities by extraction into chloroform, in 89% isolated yield. The (*R*)-enantiomer **145b** was produced by an analogous route (Scheme 2.4.1).



Scheme 2.4.1

The synthetic strategy employed to produce racemic DOTMA was utilised to generate the enantiomers of C18:1 and C16:1 lipids. Dietherification of **145a** utilising oleyl mesylate (**93**) and sodium hydride gave the dietherified derivative **147a** in 61% yield (Scheme 2.4.2). Quaternisation of **147a** with excess iodomethane and purification by column chromatography afforded (*R*)-C18:1 lipid **148a** in nearly quantitative yield (Table 2.4.1, entry 1). Using a similar strategy, the (*S*)-enantiomer **148b** was generated from amine **145b** in 58% yield over two steps (Table 2.4.1, entry 2). The optical rotation data for **148b** (-21.7 ; c 0.5, CHCl_3) were consistent with that reported by Felgner for the chloride salt of (*S*)-DOTMA (-20 ; no c value, CHCl_3) (Table 2.4.1, entry 2), indicating that no racemisation occurred during the synthesis of **148b**.¹⁶⁶ Similarly, the enantiomers of C16:1 lipids were prepared, starting from the dietherification of **145a** and **145b** using mesylated hexadec-11-en-1-ol (**121**) (see Section 2.2), to afford the tertiary amines **149a** and **149b** (Scheme 2.4.2). Subsequently quaternisation using excess iodomethane gave the (*R*)- and (*S*)-enantiomers of C16:1 lipids **150a** and **150b**, respectively (Table 2.4.1, entry 3 & 4).



Scheme 2.4.2

Entry	Mesylate	Amine (yield, %), $[\alpha]_D^{20}$	I ⁻ salt (yield, %), $[\alpha]_D^{20}$
1	93	147a (47), +2.40	148a (97), +22.2
2	93	147b (61), -2.70	148b (95), -21.6
3	121	149a (13), +4.80	150a (95), +17.4
4	121	149b (17), -3.90	150b (95), -17.1

Table 2.4.1

2.5 Biological Results for Chiral Lipids

The synthesis of optimally active C18:1 and C16:1 lipids were conducted primarily to investigate differences in activities between the enantiomers, in the presence and absence of L- α -DOPE (7, *R*-isomer). The testing of these lipids were conducted with HAE cells, formulated as LID vector complexes at a lipid/peptide/DNA weight ratio of 2:4:1, using a luciferase reporter gene and peptide **151** ([K]₁₆GACLP HKSMPCG), which have previously shown to facilitate plasmid DNA delivery and specifically target HAE cells with high affinity.¹⁶⁸

The transfection efficiencies of the (*R*)- and (*S*)-enantiomers of C18:1 lipids revealed enantiomeric dependent activities when formulated within LID complexes. The (*R*)-C18:1 lipid **148a** was 3 fold more active than the (*S*)-enantiomer (**148b**) in the absence of DOPE, but **148b** was almost 3 times more active than **148a** when tested in the presence of DOPE (Chart 2.5.1). Interestingly, the effect of DOPE on activity is also enantiomeric dependent. When formulated with DOPE, the activity of (*R*)-C18:1 lipid (**148a**) was reduced by up to 4 fold, whereas the addition DOPE increased the activity of the (*S*)-enantiomer **148b** by nearly 3 times (Chart 2.5.1).

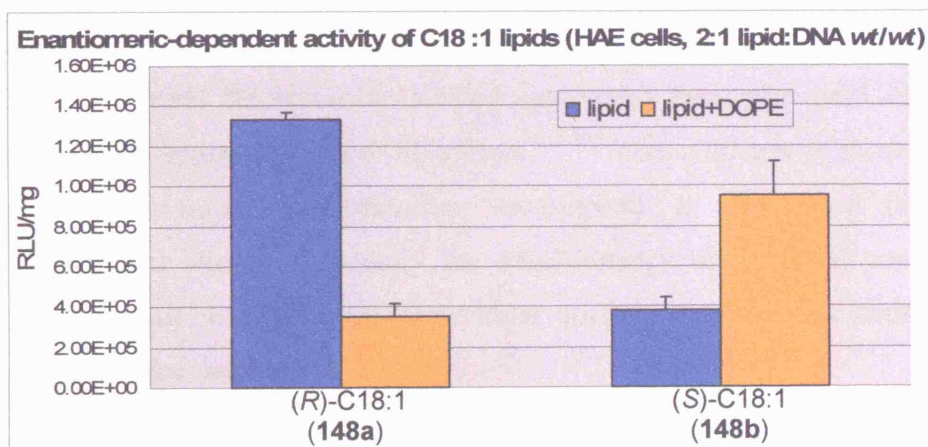


Chart 2.5.1

However, the trends for (*R*)- and (*S*)-C16:1 lipids **150a** and **150b** are less straightforward. The enantiomers of C16:1 lipids displayed no enantiomeric dependent activity in the absence of DOPE (Chart 2.5.2). LID complexes containing the (*R*)-enantiomer (**150a**) demonstrated similar transfection efficiencies regardless of its DOPE content; however, the activity of (*S*)-enantiomer (**150b**) was increased by almost 5 times when formulated with DOPE.

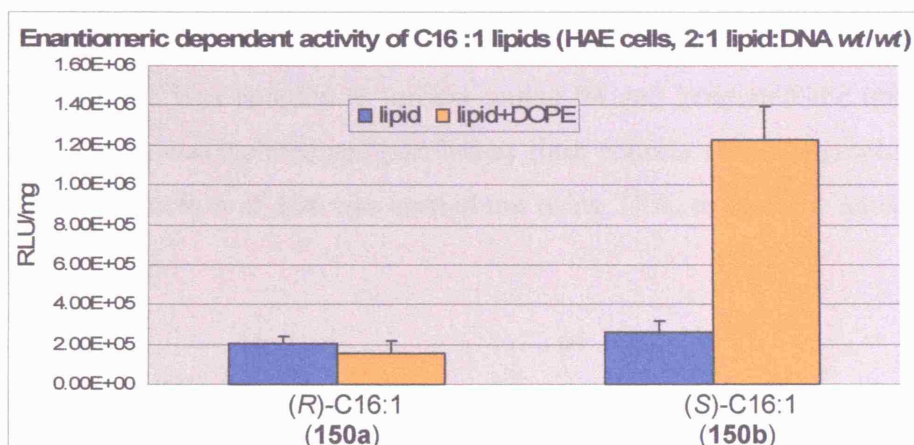
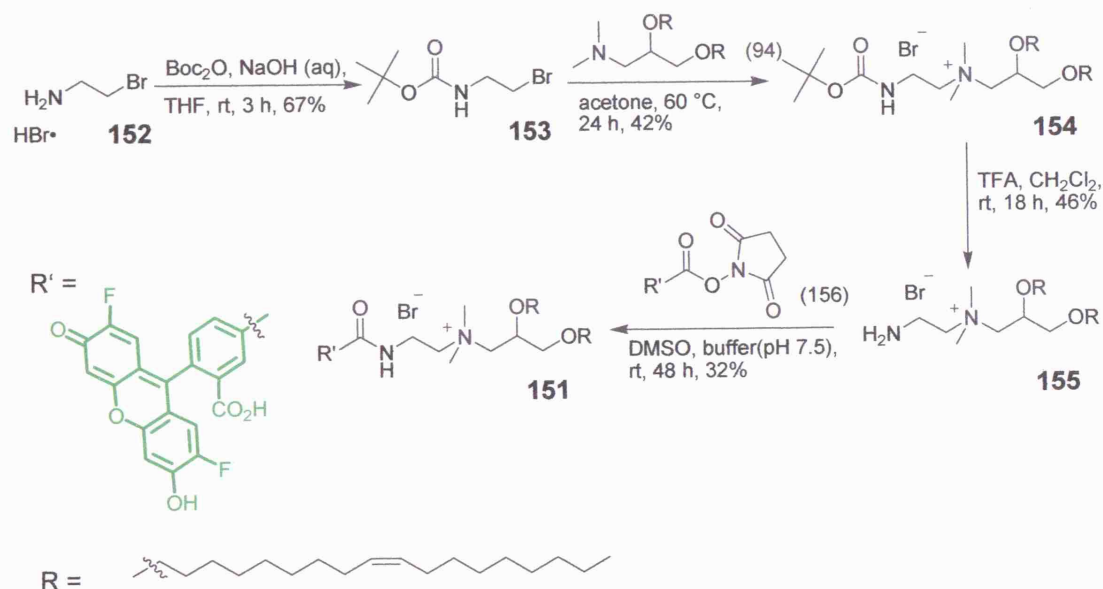


Chart 2.5.2

2.6 Synthesis of Labelled Lipid Derivatives

The use of fluorophores that are either electrostatically or covalently attached to the components of a synthetic gene vector, enable the structure and intracellular fate of the vector complexes to be investigated. For example, ethidium bromide has been used as a DNA intercalating agent to assess the condensation efficiency of lipoplex formulations.¹⁶⁹ Fluorescence techniques such as fluorescence correlation spectroscopy (FCS) have been employed to monitor the association of lipid/DNA complexes.¹⁷⁰ Several fluorescently-labelled cytofectins have also been utilised to examine the transfection process of lipoplexes.¹⁷¹⁻¹⁷³ The synthesis of fluorescently-labelled lipid derivatives was therefore investigated. It was hoped that these compounds would allow us to study the stoichiometry of the lipid components contained in the LID complex and intracellular trafficking of the cytofectins, using various fluorescence methods.

The synthesis of Oregon Green[®]-labelled DOTMA **151** was undertaken, with the fluorophore attached on the headgroup *via* a short linker. The Oregon green[®] label was utilised because of the near match of its absorption (~498 nm) and emission (~512 nm) maxima to the strong spectral lines of an argon-ion laser, making it a versatile fluorophore for several fluorescence imaging applications.¹⁷⁴ Initially, 2-bromoethylamine hydrobromide (**152**) was protected with the *tert*-butyloxycarbonyl (Boc) group, using Boc anhydride in a mixture of THF/sodium hydroxide (2 M) solution, to give **153** in 67% yield (Scheme 2.6.1).¹⁷⁵ The Boc-protected bromide was coupled to tertiary amine **94** and generated the quaternised amine **154**, which was isolated and purified by flash column chromatography in 42% yield. Boc-deprotection of **154** was carried out using TFA, to give the amine **155** in 46% isolated yield.

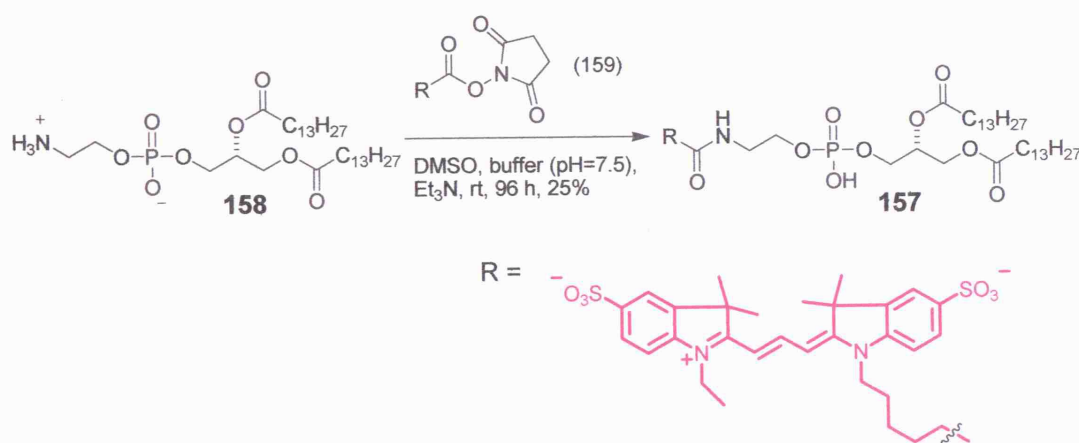


Scheme 2.6.1

The synthesis of labelled lipid **151** was carried out on a 1 mg scale, using Oregon Green[®] succinimidyl ester (**156**) and amine **155**, in the presence of DMSO and phosphate buffer at pH 7.5 (Scheme 2.6.1). Initially, the isolation of **151** was attempted by reverse phase HPLC, using a solvent gradient (100% water to 100% acetonitrile) over 90 minutes; however, the desired product was not afforded, possibly due to product decomposition during its isolation. Purification of **151** was finally achieved using preparative TLC, to afford the labelled lipid in 32% isolated

yield. The formation of **151** was confirmed by ESMS analysis ($m/z = 1058$, $[M-Br]^+$), and UV spectroscopic analysis of the isolated product consistent with the attachment of the Oregon Green[®] label ($\lambda_{\text{max}} = 500.3$ nm).

The synthesis of fluorescently-labelled lipid **157** was undertaken to explore the role and structural organisation of phospholipid derivatives such as DOPE in the LD and LID vector complexes. Cyanine reagents such as CyTM3 and CyTM5 have been widely employed as fluorophores for investigating biological systems, due to their intense fluorescence and high water solubility.¹⁷⁶ These cyanine labels have previously been utilised as DNA probes to monitor the structural organisation and gene delivery of lipid/DNA complexes.^{177,178} The conversion of phospholipid **158** to the CyTM3-labelled lipid **157** with CyTM3 succinimidyl ester (**159**) was initially carried out in a mixture of DMSO and phosphate buffer at pH 7.5 (Scheme 2.6.2). However, examination of ESMS spectrum of the crude reaction mixture suggested that no desired product was formed after stirring for 24 h. At this stage an excess of triethylamine was added, and the mixture stirred for a further 96 h. Finally, the Cy3-labelled phospholipid **157** was formed and purification by preparative TLC afforded **157** in 25% isolated yield. Again, the formation of **157** was confirmed by ESMS spectroscopy ($m/z = 1249$, $[M+2H]^+$), with UV spectroscopic analysis showing the attachment of the Cy3 label ($\lambda_{\text{max}} = 553.5$ nm). Both lipids **151** and **157** were relatively stable for long-term storage (>6 months in refrigerator), but appeared to be very hygroscopic.



Scheme 2.6.2

2.7 Calcein Leakage Experiments

We have demonstrated that substituting the C18:1 hydrocarbon chains for C16:1 lipid chains in glycerol based lipids has a dramatic influence on the transfection efficiency of the LID complexes *in vitro* and *in vivo* (see Section 2.3); however, the reason for this enhanced activity is not clear. It is known that the length of alkyl chains of a lipid can affect its packaging and phase preference.^{91,92} We have previously observed that DOTMA (**6**) and the C16:1 lipid **136** exhibited a $L_{\beta} \rightarrow L_{\alpha}$ phase transition at temperature below 0 °C.¹⁴⁶ In order to establish further the influence of lipid chain length variation on activity, calcein leakage experiments were performed to investigate the stability of liposomes at different pH. The calcein leakage experiments were designed as a model system to mimic the pH change experienced by LID complexes during its path through to the endosome. The level of calcein (**160**) released from the lipid, measured by the relative percentage of fluorescence detected, was taken as an indicative of DNA molecules released from the liposomes. As the liposome bilayers were disrupted in response to the lowering pH, the membranes become leaky and calcein was released into the surrounding medium (Figure 2.7.1).

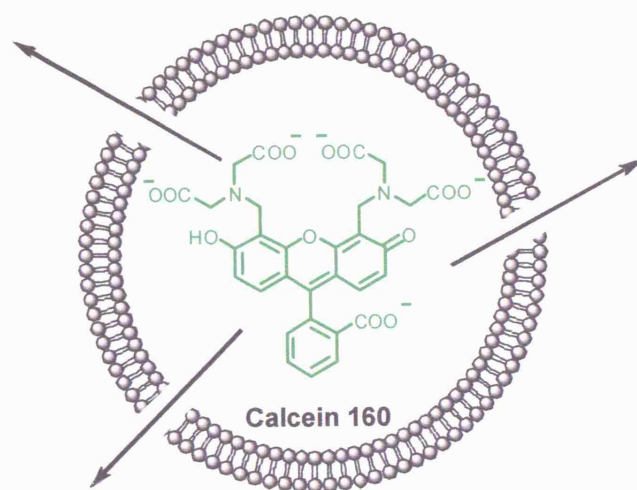


Figure 2.7.1

The calcein release assays were performed using liposomes of DOTMA and C16:1 lipid **136**, formulated with and without DOPE, buffered in MES-saline solution at various pH values (pH 5.0-7.5).¹⁷⁹ Liposomes prepared from DOTMA

were stable across the whole pH range, regardless of the DOPE content (Chart 2.7.1). The level of calcein released with DOTMA (\pm DOPE) was consistently low ($> 15\%$).

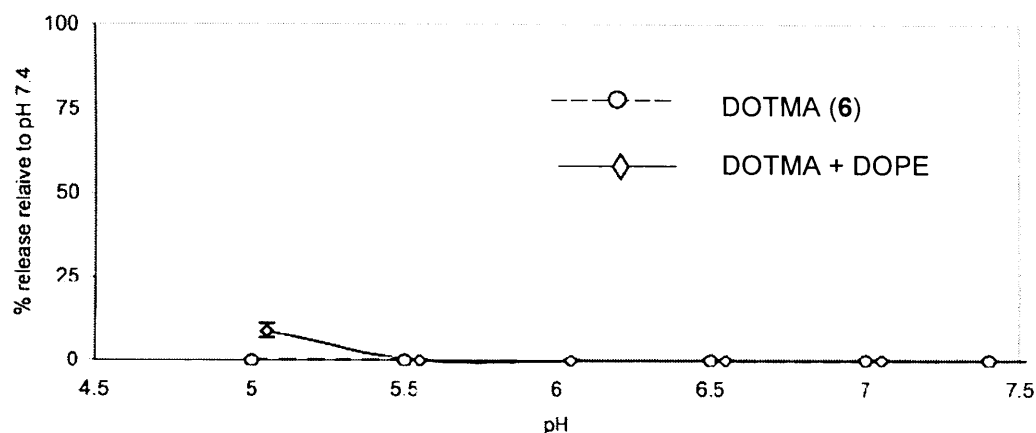


Chart 2.7.1

By contrast, liposomes prepared from lipid **136** displayed a plateau level of fluorescence in the range pH5-6 (Chart 2.7.2). Indeed, there was a greater level of calcein released at pH 5.5 from liposomes containing **136**+DOPE ($>50\%$) compared to that of lipid **136** alone ($\sim 30\%$). The presence of DOPE in liposome formulation is likely to enhance the electrostatic repulsions due to protonation at lower pH, thus leading to liposomal breakdown. This data suggested that liposomes prepared from lipid **136** had greater fluidity than DOTMA at acidic conditions, regardless of their DOPE contents, leading to enhanced membrane fusion and thus give rise to greater rate of calcein release. These observations correlated well with our transfection results obtained *in vitro* and *in vivo*, suggesting that the disruption of liposomal membranes inside the endosomes plays an important role in enhancing the activity of lipid **136** compared to DOTMA (see Section 2.3.6 & 2.3.7).

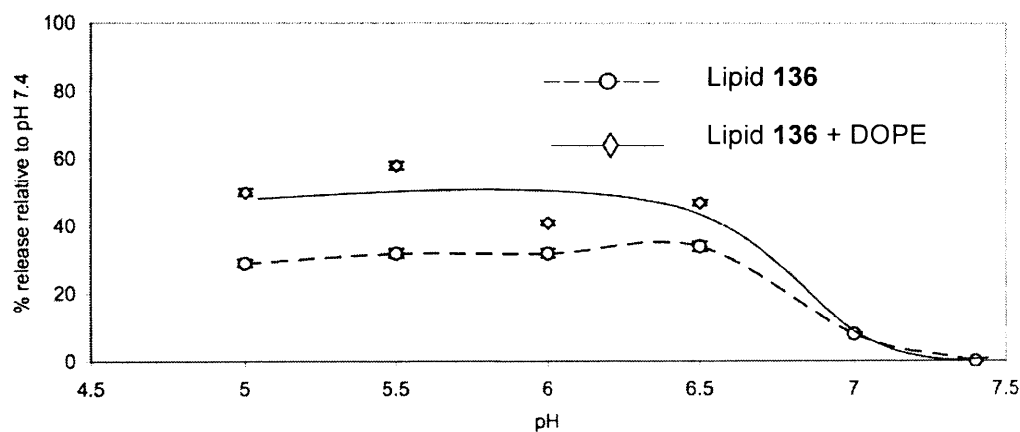


Chart 2.7.2

2.8 Conclusion

In summary, we have described a systematic optimisation of the lipid component in the LID vector system. Structural features including the position and geometry of the unsaturated moiety on lipid tail as well as the chirality of the lipid molecules were considered, along with the effect of DOPE co-formulation. We have shown that all these features are important in determining the optimal formulation for a specific cell type but that consistent trends were apparent. Specifically, formulation of LID complexes containing the C16:1 lipid **136** was found to greatly enhance transfection efficacy compared to that containing DOTMA, and was better at transfecting HAE cells and primary human skin fibroblasts *in vitro* as well as murine lung airway *in vivo*. Furthermore, calcein release experiments suggested that the optimal liposome component for lipopolyplex transfection is likely to be a compromise between structural and functional requirements for complex formation and endosomal membrane destabilisation.

CHAPTER 3

RESULTS AND DISCUSSION

PEG-Lipid Conjugates

3. PEG-Lipid Conjugates

A crucial problem with the *in vivo* administration of non-viral delivery systems is that cationic lipid/DNA complexes are bound by plasma proteins and rapidly eliminated from the bloodstream, hence limiting their circulation lifetime.¹⁸⁰ In addition, such formulations are unstable in buffers and serum, and tend to aggregate.¹⁸¹ Previous works in this area have suggested that these problems can be reduced by shielding the complexes with polyethylene glycol (PEG) polymers.^{71,72} PEG polymers with molecular weights between 2000-5000 Da have been attached onto the lipids for use in several systems, and added to the formulations at a relatively low concentration (1-10 mol%). This results in the formulation of lipoplexes with enhanced blood circulation lifetime and particle stability in the presence of serum.^{74,76,182} However, the grafting of long PEG polymers on the liposome surface interferes with the ability of liposomes to undergo membrane fusion and destabilisation.⁷⁵ It has been suggested by Hui *et al.* that shorter PEG chains may significantly increase particle fusion as a result of reduced steric bulk of the PEG units.¹⁸² In addition, a slight increase in activity was observed when a shorter PEG polymer, PEG750, was incorporated into the PEG-ceramide, compared to that utilising PEG2000 and PEG5000 polymers.¹⁸³

Our aim was to develop a series of PEG-lipid conjugates that could be utilised for LID vector formulations and would enhance particle stability and transfection activity for *ex vivo* or *in vivo* applications. In the LID vector system, exposure of the integrin-binding domain on the peptide is required for interaction with cell surface proteins. Since long PEG chains would obstruct the targeting domain accessing the cell surface, we envisaged that the use of a shorter PEG chain lipid would induce a shielding layer on the LID complex without hindering its targeting capacity. Indeed, Bianco-Peled *et al.* have investigated the headgroup length of a PEG-lipid, incorporated into a membrane containing a peptide amphiphile, and determined that shorter PEG chains were required for accessibility of the peptide ligand to cell surface receptor.¹⁸⁴ In addition, the PEG-lipids would increase the aqueous solubility of LID complexes compared to the non-PEGylated analogues synthesised previously. It would be desirable to incorporate the short PEG chains onto the quaternary headgroup of glycerol based lipids and to formulate these lipids

at a high mol%. The influence of the size of PEG unit and lipid chain length variation would also be assessed (Figure 3.1).

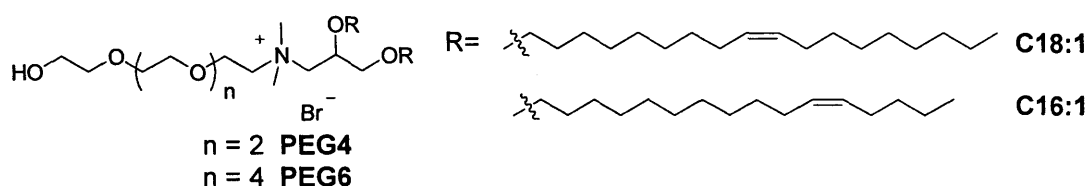
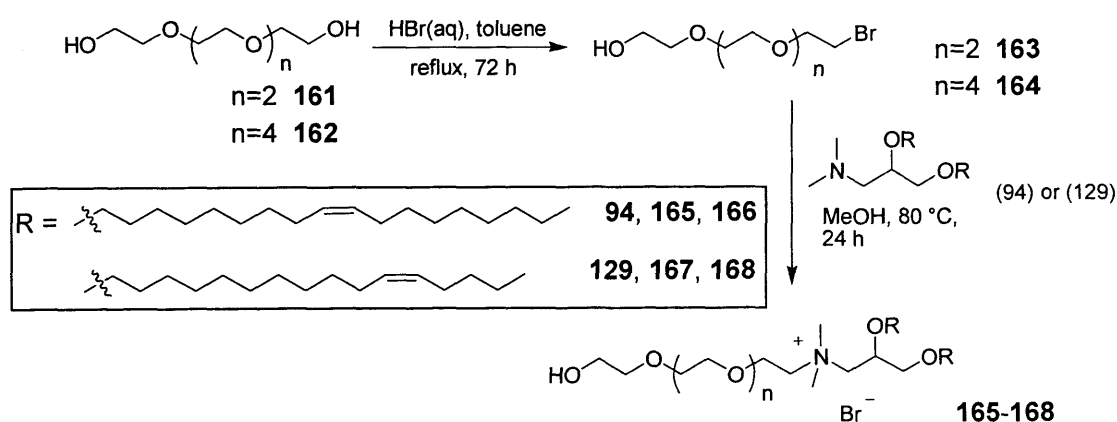


Figure 3.1

3.1 Synthesis of PEG-lipid analogues

Initially the mono-bromination of tetra(ethylene) glycol (**161**) and hexa(ethylene) glycol (**162**) was carried out using aqueous hydrobromic acid, following the methodology described by Herve *et al.* (Scheme 3.1.1).¹⁸⁵ The PEG bromides **163** and **164** were isolated in moderate yields after purification by reverse-phase column chromatography. Subsequent quaternisation of tertiary amine **94** with the PEG bromides afforded the C18:1 PEG-lipids **165** and **166** (Table 3.1.1, entry 1 & 2). The PEG-lipids were readily recrystallised from ethyl acetate at low temperature (-15 °C). Alternatively, purification by column chromatography on silica (10% methanol in dichloromethane) isolated these lipids in moderate yields. In a similar manner, the quaternisation of C16:1 tertiary amine **129** with bromides **163** and **164**, afforded the C16:1 PEG-lipids **167** and **168**, respectively (Table 3.1.1, entry 3 & 4). Overall this is a short and facile procedure, ideal for accessing PEG-lipid conjugates with different PEG unit and lipid length.



Scheme 3.1.1

Entry	Ternary amine	PEG-Br	PEG-lipid	Yield (%)
1	94	163	165	58
2	94	164	166	32
3	129	163	167	43
4	129	164	168	44

Table 3.1.1

3.2 Biological Data for PEG-Lipid Conjugates

Lipids **165-169** were synthesised to study the effect of short PEG chains on LID vector transfections *in vitro* and *in vivo*. Testing of **165-168** and their non-PEGylated counterparts (**6** and **136**) were carried out, formulated as LID complexes at lipid/peptide/DNA weight ratios of 2:4:1 and 4:4:1, with peptide **169** ([K]₁₆GACSERSMNFCG), which has previously displayed high binding affinity for HAE cells.¹⁶⁸

3.2.1 Transfection Data for PEG-Lipid Conjugates

The lipids were initially tested to establish the influence of PEG unit length and lipid/DNA ratio on activity. The transfection efficiencies of **165-168** were determined for LID vector systems with HAE cells, at 2:1 and 4:1 lipid/DNA weight ratios. With the DNA and peptide ratios kept constant, transfection efficiencies of the lipids were found to be higher at a 4:1 lipid/DNA weight ratio (Chart 3.2.1).

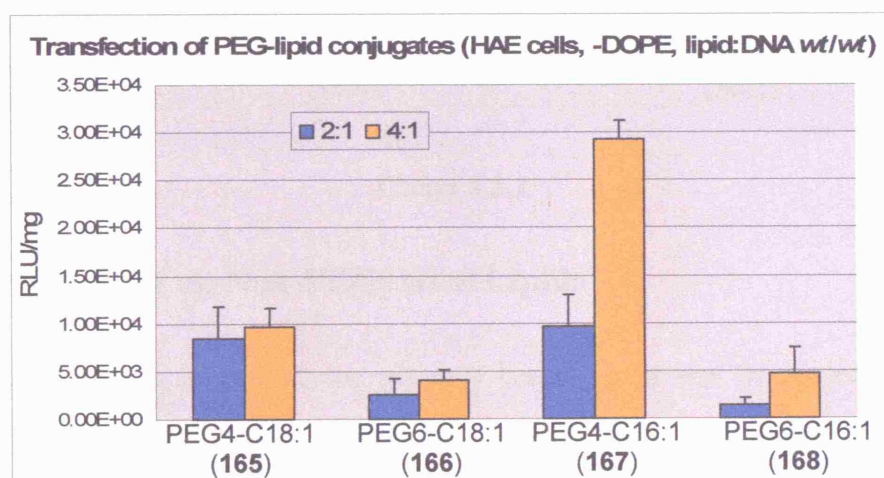


Chart 3.2.1

For a fixed lipid anchor the shorter PEG4 derivative displayed higher activity compared to its PEG6 counterpart. This is highlighted by the C16:1 lipids, in which the PEG4 derivative (**167**) was 6 fold more active than its PEG6 counterpart (**168**) at a 4:1 lipid/DNA ratio (Chart 3.2.1). With the lipid anchor of these lipids being identical, the observed increase in activity must be as a result of a decrease in hydration and a decrease in the steric bulk of the lipid headgroup. Interestingly, for a fixed PEG unit length the C16:1 lipids (**167** and **168**) were more active than their C18:1 counterparts (**165** and **166**). This was highlighted by the transfection efficiency of PEG4-C16:1 lipid (**167**) which was three times more active than its C18:1 counterpart (**165**) at a 4:1 lipid/DNA ratio (Chart 3.2.1). The results indicate that the activity of the PEG-lipids were dependent on the length of PEG unit as well as the lipid chain length.

In the presence of DOPE the transfection efficiencies of PEG4 lipid derivatives **165** and **167** were altered, with the formulation of **167**+DOPE displaying the greatest activity at a 4:1 lipid/DNA ratio (Chart 3.2.2).

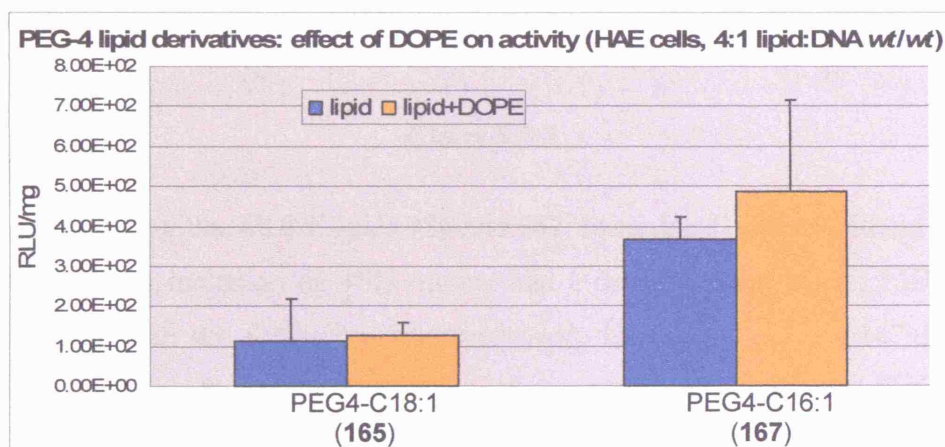


Chart 3.2.2

3.2.2 PEGylated vs. Non-PEGylated Lipids

The effect of short PEG units on glycerol based lipids was determined for LID complexes, formulated with or without DOPE, at a lipid/peptide/DNA weight ratio of 2:4:1. Testing of the PEG-lipids compared with their non-PEGylated counterparts revealed that inclusion of the PEG moiety had different effects on activity of the LID

vectors. For lipids with a C18:1 lipid anchor (DOTMA **6** and PEG4 derivative **165**) the transfection efficiencies with HAE cells varied in the following order: **165** \simeq **6**+DOPE \simeq **6** > **165**+DOPE (Chart 3.2.3a). Indeed, the activity of **165** was nearly halved when co-formulated with DOPE. The PEG4-C18:1 lipid (**165**) and DOTMA displayed similar transfection efficiency in the absence of DOPE. When formulated with DOPE, lipid **165** was slightly less active than its non-PEGylated counterpart (**6**). The lipid anchor is identical for DOTMA and **165**, therefore the observed differences in activities must be as a result of the incorporation of PEG unit.

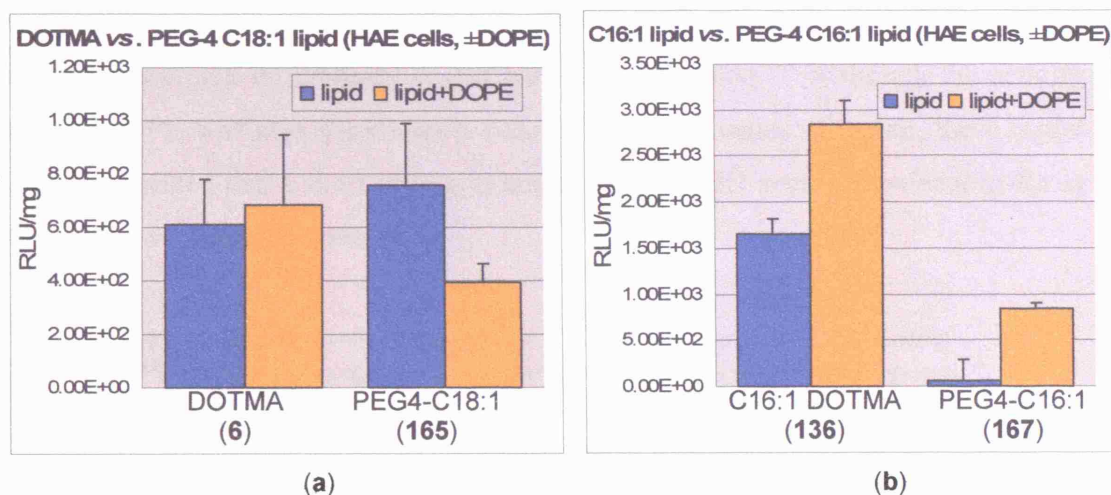


Chart 3.2.3

Conversely, the C16:1 lipids **136** and **167**, formulated with or without DOPE, revealed that the inclusion of PEG moiety had a detrimental effect on LID vector transfections, with the following order observed: **136**+DOPE > **136** > **167**+DOPE > **167** (Chart 3.2.3b). In contrary to their C18:1 counterparts, the PEG4-C16:1 lipid (**167**) was up to 30 fold less active than its non-PEGylated counterpart (**136**) in the absence of DOPE, and up to 4 times less active when formulated with DOPE.

3.2.3 The Effect of Serum on Activity

The effect of serum on transfection activity was determined and is summarised in Chart 3.2.4. Lipopolyplex formulations comprised of **165**+DOPE at a 6:1 lipid/DNA weight ratio and its non-PEGylated counterpart DOTMA (**6**) at a 4:1 lipid/DNA ratio were tested. These formulations were previously established to be optimal for HAE

cell transfections.¹⁸⁶ Foetal calf serum (FCS) was included in the transfection incubation step in the range 0-10%.

Both the LID vector formulations with cytofectins **165**+DOPE and DOTMA displayed lower transfections in the presence of serum (Chart 3.2.4). Formulations with **165**+DOPE gave higher expression levels in the absence of serum, which dropped markedly in the presence of 1-10% serum. When incubated with 5% serum, the activity of DOTMA was inhibited to 0.5% of its efficiency without serum, while the efficiency of **165**+DOPE was reduced to about 10%. It is well known that serum in the medium inhibits the transfection efficiency of cationic lipoplexes *in vivo* by means of complex destabilisation and particle aggregation.¹⁸¹ Although the activity of **167**+DOPE was also significantly reduced in the presence of serum, these initial results suggested that a short PEG unit might enhance LID vector transfections for *in vivo* and *ex vivo* applications.

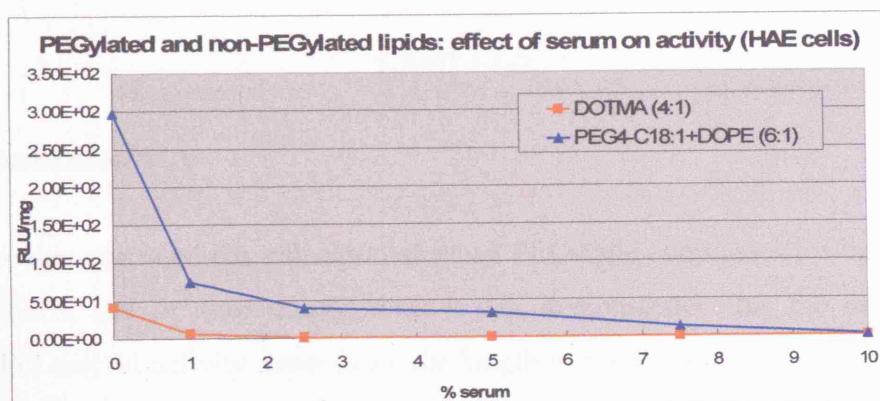


Chart 3.2.4

3.2.4 *In Vivo* Transfection Studies

In vivo transfection studies were carried out by intratracheal administration of mice, following the methodology described by Jenkins *et al.*¹⁸ LID vector complexes comprised of luciferase reporter gene and peptide **169**, formulated with different cytofectins (**136**, **165**+DOPE and branched PEI 25 kDa) at a lipid/peptide/DNA weight ratio of 0.75:4:1, were tested on C57Bl/6 mice at 6-8 weeks of age. *In vivo* transfection results indicated that LID complexes formulated with **165**+DOPE and **136** had similar activities on mice lungs, and were more active than branched PEI 25

kDa, a commercial gene transfer reagent (Chart 3.2.5). We have previously demonstrated that lipopolyplexes containing lipid **136** displayed higher activity than Lipofectin™ in mice lungs (see Section 2.3.7). Hence the apparent enhanced activity of lipid **165** over Lipofectin™, both have a C18:1 lipid anchor, can be attributed to the inclusion of PEG unit on the lipid headgroup, resulting in increased serum resistance and enhanced LID particle stability.

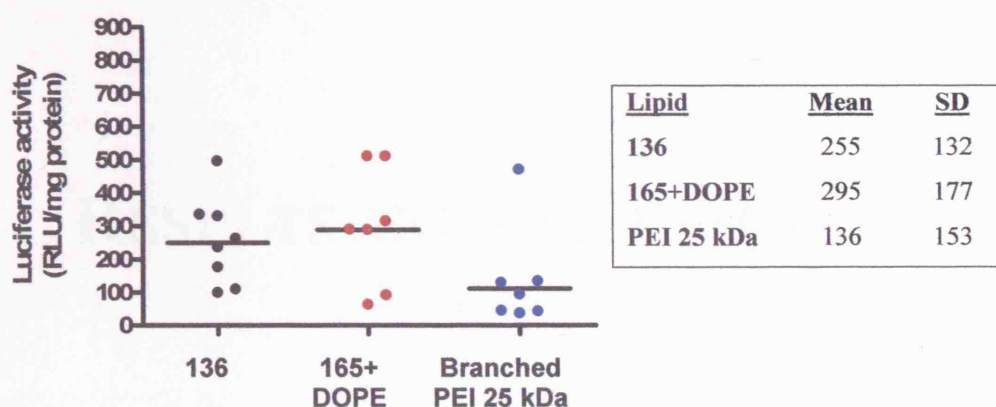


Chart 3.2.5

3.3 Conclusion

We have demonstrated the utilisation of novel PEG-lipid conjugates for lipopolyplex formulations. For *in vitro* transfections it was demonstrated that the influence of short PEG unit on activity depends on the length of the PEG unit as well as the lipid chain length. The PEG-lipid **165** displayed some serum resistance compared to its DOTMA, and showed reasonable transfection efficiency on mice lungs. Furthermore, the PEGylated C16:1 lipid **167** displayed lower transfections compared to its non-PEGylated counterpart, suggesting that the coating of liposomal surface with PEG moiety may inhibit the integrin-binding ability of the peptide and/or make the complex too stable for membrane fusion and destabilisation. Investigations such as the size of LID complexes as well as particle stability in the presence of serum should be carried out in future to elucidate further the influence of lipid PEGylation.

CHAPTER 4

RESULTS AND DISCUSSION

pH-Sensitive PEG-Lipid Conjugates

4. pH-Sensitive PEG-Lipid Conjugates

The previous chapter outlined the synthesis of a series of novel PEG- lipid conjugates utilised in the lipopolyplex formulations (see Section 3). Ideally, a PEGylated liposome should remain stable until it reaches the target site, and release its payload from the endosome after cell internalisation. However, many non-viral vectors with PEG coatings have exhibited poor gene expressions as a consequence of lacking an active release mechanism, leading to high levels of lysosomal degradation.⁷³⁻⁷⁵ Different strategies have been proposed to accomplish the triggered release of DNA molecules into the cytoplasm, in particular, acid-triggered release has been extensively studied for drug and gene delivery.^{187,188} The rationale for the design of pH-sensitive PEG-liposomes is to exploit the intrinsic low pH (pH 5.0-6.5) within endosomes, to induce hydrolysis of the acid-sensitive linkages and trigger the shedding of the PEG moieties. Such liposomes should be stable under neutral conditions but undergo destabilisation and become fusogenic under acidic conditions, thus leading to release of the encapsulated contents.

It was previously demonstrated that pH-sensitive PEG liposomes have prolonged circulation lifetimes, and are as stable as conventional PEG-grafted liposomes at neutral pH.^{81,83} In addition, membrane fusion can be induced under mildly acidic conditions, leading to rapid release of the encapsulated contents.^{83,189} Different headgroups, lipid tails, linker groups, and linkage configurations have been utilised to render pH-sensitive PEG lipids of different properties.¹⁸⁸ Our goal was to develop a series of pH-sensitive PEG liposomes that are easy to handle and would undergo hydrolysis under distinct physiological conditions. We focused on preparing a novel class of lipids that possess acetal linkages between the cationic headgroups and PEG moieties (Figure 4.1). The effect of varying the PEG unit length, the length of the spacer, lipid chain length, as well as the nature of the PEG units was evaluated.

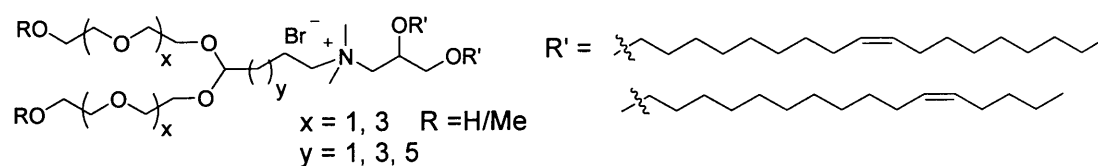
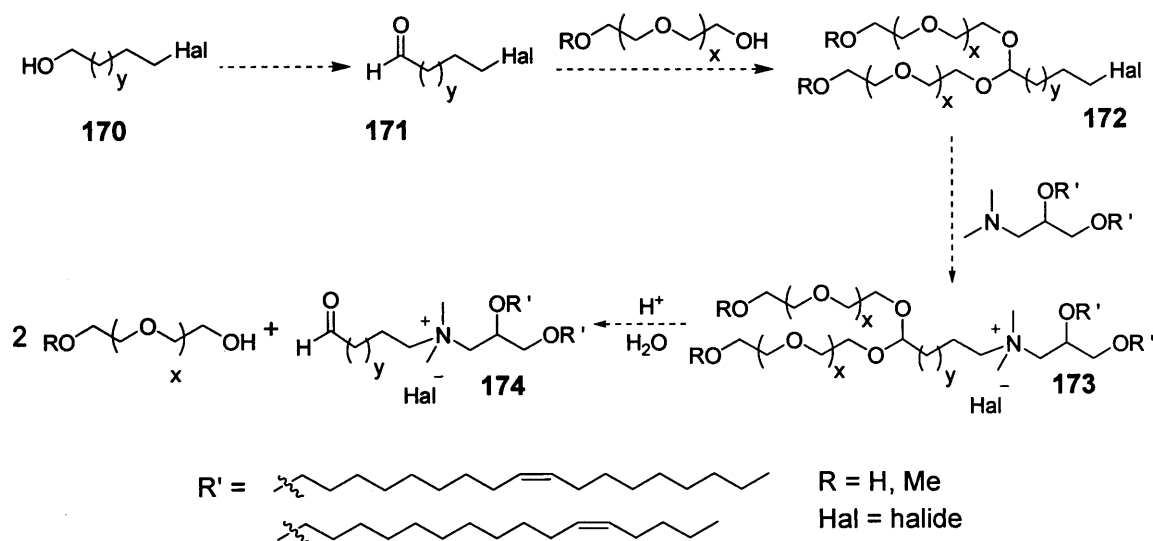


Figure 4.1

4.1 Synthesis of pH-Sensitive PEG Lipids

Formation of the acid-labile linkers was initially carried out. An acetal moiety was selected as the acid-cleavable linkage between the headgroup and the PEG units (Figure 4.1). Acetals are ideal readily cleavable, acid-sensitive linkers as the rate of hydrolysis is proportional to the acidity of the medium, and is expected to increase 10 times with every unit of pH decrease.¹⁹⁰ The synthesis of pH-sensitive PEG lipids was investigated starting with the selective oxidation of primary alcohol **170** to yield the corresponding aldehyde **171** (Scheme 4.1.1). This was followed by acetal formation with PEG chains to give the PEG-acetal linker **172**, and subsequent coupling with the lipid anchor to generate the desired PEG-acetal lipid derivative **173**. It was anticipated that acid-catalysed hydrolysis of the acetal linkage would trigger dePEGylation to produce the corresponding aldehyde lipid analogue **174** and the PEG chain as major fragments.

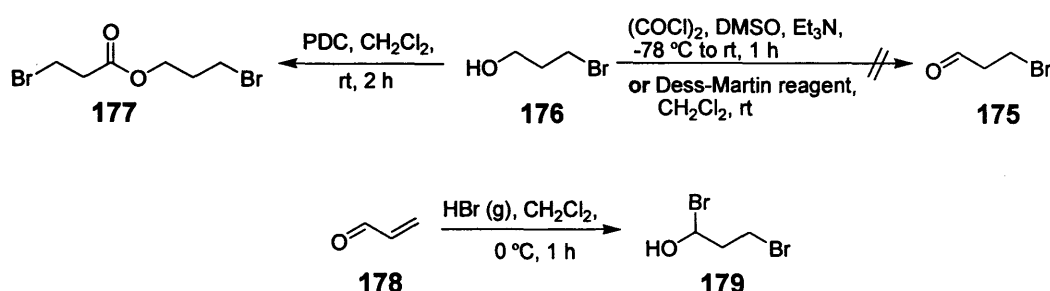


Scheme 4.1.1

4.1.1 Synthesis of PEG-Acetal Linkers

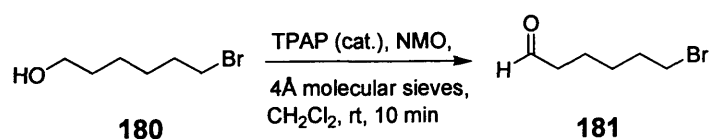
The synthesis of 3-bromopropan-1-al (**175**) was initially attempted to establish the synthetic strategy for aldehyde formation. Oxidation of 3-bromopropan-1-ol (**176**) was first attempted *via* Swern oxidation methodology, following the methodology described by Bunce *et al.*¹⁹¹ However, TLC analysis of the crude mixture indicated that only the starting material was recovered (Scheme 4.1.2). Formation of **175** was

then attempted using Dess-Martin periodinane.¹⁹² TLC and ^1H NMR spectroscopic analysis of the crude reaction mixture indicated that **175** was generated but a significant amount of unreacted **176** remained. The oxidation of alcohol **176** was also attempted utilising pyridinium dichromate (PDC) as oxidant, but examination of the ^1H NMR spectrum indicated that the ester **177** was yielded as the major product. Furthermore, the formation of **175** was attempted using an alternative strategy, by bubbling hydrogen bromide gas into a solution of 2-propenal (**178**) in anhydrous dichloromethane.^{193,194} Unfortunately, ESMS and ^1H NMR spectroscopic analysis indicated that the dibromide **179** was formed (Scheme 4.1.2).



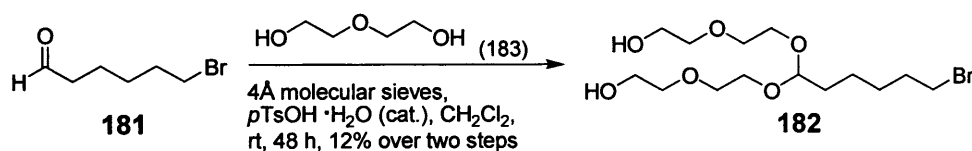
Scheme 4.1.2

Due to difficulties in generating **175**, the synthesis of aldehyde derivatives with longer alkyl chains was explored. It was also envisaged that aldehydes with longer hydrocarbon chains might be more stable and easier to handle in further reaction steps. The oxidation of primary alcohols to the corresponding aldehydes using tetra-*n*-propylammonium perruthenate (TPAP) and *N*-methylmorphine-*N*-oxide (NMO) has previously been reported by Ley *et al.*^{195,196} Using this method, 6-bromohexan-1-ol (**180**) was added into a solution of TPAP/NMO/activated molecular sieves (4Å) in anhydrous dichloromethane (Scheme 4.1.3). TLC analysis of the crude mixture indicated that the aldehyde **181** was formed after stirring for 10 min at rt, and the product isolated by filtering the crude mixture through a short pad of silica (~2 cm). After ^1H NMR spectroscopic analysis to confirm that the aldehyde was formed, the crude product was subsequently utilised for acetal formation.



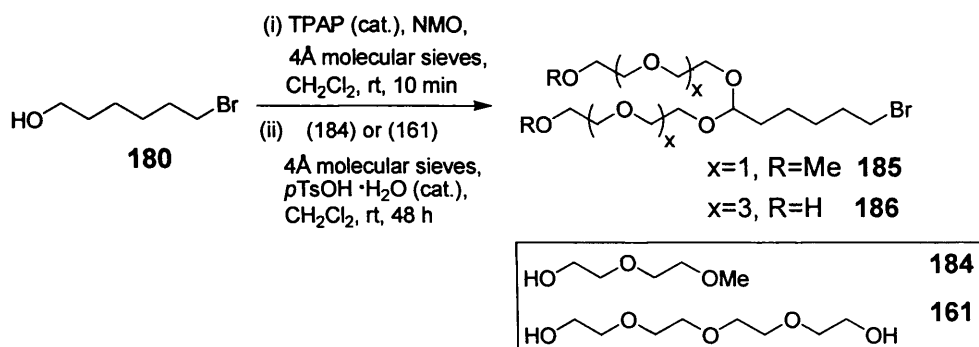
Scheme 4.1.3

The conversion of **181** to acetal **182** was first attempted with an excess of di(ethylene)glycol (**183**), using *p*TsOH as catalyst (Scheme 4.1.4). It is well known that water generated in acetal formation can promote the reverse reaction, so activated molecular sieves were added to the reaction mixture to remove any water formed. The glycol **183** was also pre-dried over molecular sieves to minimise its water content. After stirring the mixture for 48 h, ESMS analysis of the crude reaction mixture indicated that the desired product **182** had been formed. Examination of the ^1H NMR spectrum suggested that the conversion of **181** to **182** was approximately 50%, as indicated by the integration of peaks corresponding to the *CH* proton on acetal (δ_{H} 4.54 ppm) compared to that of the aldehyde $\text{O}=\text{CH}$ proton (δ_{H} 9.79 ppm). Compound **182** was isolated and purified by flash column chromatography in 12% yield over two steps (Scheme 4.1.4). The low yield reflects a moderate conversion rate to the acetal, but also that isolation of the product by column chromatography was extremely difficult, due to very similar R_{f} values of **182** and the glycol **183**. In an attempt to improve the reaction yield, reaction times of 24 h and 72 h were used for the acetal conversion, but this failed to increase the production of **182**. Although the yield of the reaction was modest, we used this synthetic route further because only two steps were required, and the method is quick and the reagents relatively inexpensive.



Scheme 4.1.4

We had previously observed that variation in the PEG length can have significant effects on the transfection activity of PEG-lipid conjugates (see Section 3.2). The synthesis of acetal linker derivatives with varying PEG units was therefore undertaken. The oxidation of alcohol **180** and subsequent acetal formation with diethyleneglycol methyl ether (**184**) and tetra(ethylene)glycol (**161**) gave the acetal linkers **185** and **186**, respectively (Scheme 4.1.5). Formation of the acetal linkers was confirmed by ESMS and ^1H NMR spectroscopic analysis (Table 4.1.1).

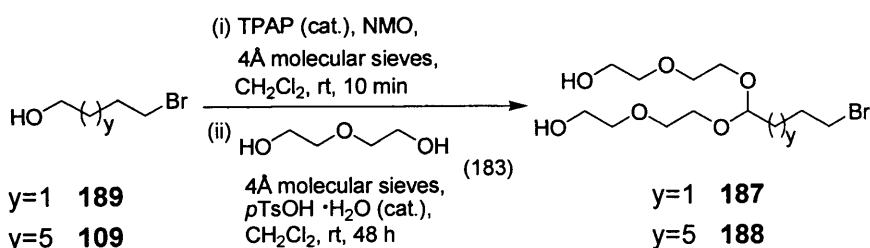


Scheme 4.1.5

Entry	Alcohol (Eq)	PEG chain (Eq)	Acetal (yield, %)	<i>m/z</i> , ([M+Na] ⁺)	δ_{H} (OCHO)/ ppm
1	180 (1)	183 (4)	182 (12)	396	4.51
2	180 (1)	184 (4)	185 (35)	423	4.56
3	180 (1)	161 (4)	186 (9)	572	4.51

Table 4.1.1

The synthesis of acetal derivatives **187** and **188** was carried out to provide reagents for the preparation of acetal lipid analogues with different linkers (Scheme 4.1.6). The oxidation of 4-bromobutan-1-ol (**189**) and 8-bromooctan-1-ol (**109**), followed by subsequent acetal formation with diethyleneglycol (**183**), afforded the corresponding acetal linkers **187** and **188** in 40% and 39% yield, respectively (Table 4.1.2).



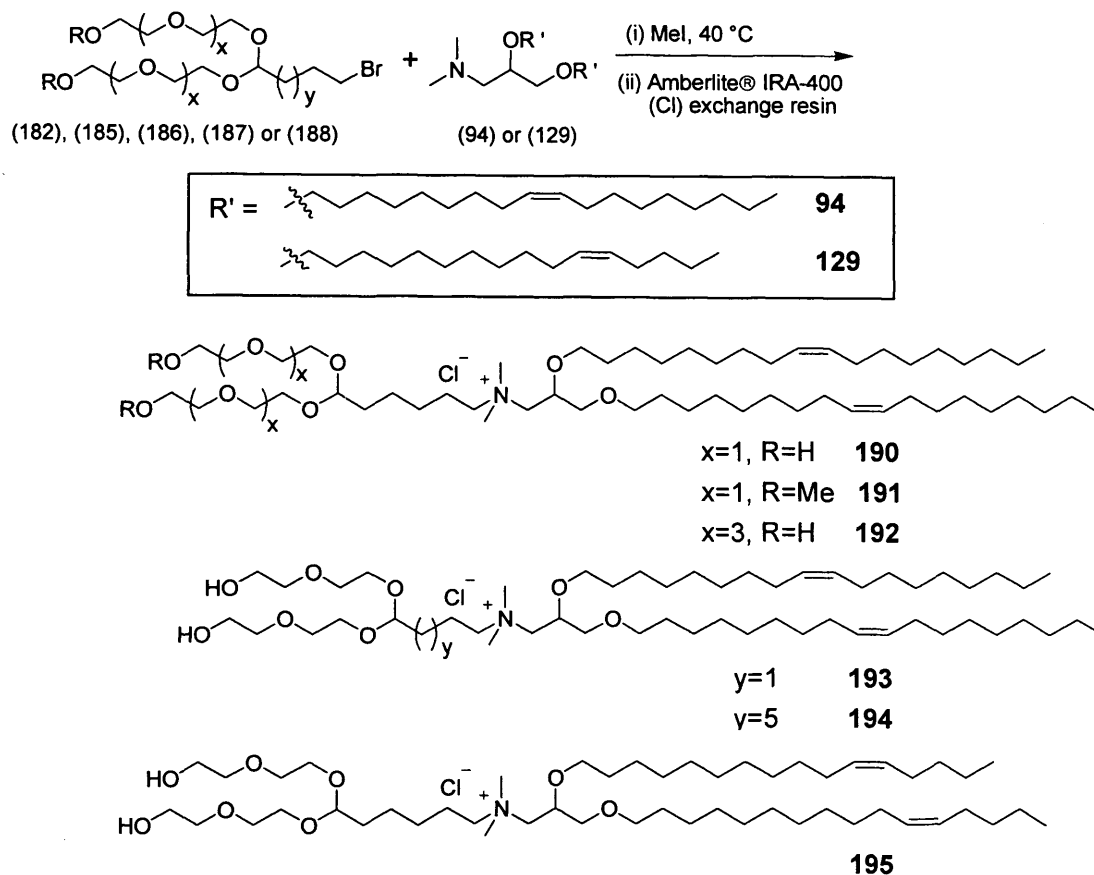
Scheme 4.1.6

Entry	Alcohol (Eq)	PEG chain (Eq)	Acetal (Yield, %)	<i>m/z</i> , ([M+Na] ⁺)	δ_{H} (OCHO)/ ppm
1	189 (1)	183 (4)	187 (40)	367	4.58
2	109 (1)	183 (4)	188 (39)	423	4.56

Table 4.1.2

4.1.2 Synthesis of PEG-acetal Lipids and Aldehyde Analogue

Synthesis of the pH-sensitive PEG-acetal lipids **190-194** was carried out *via* quaternisation of the C18:1 tertiary amine **94** with selected acetal linkers (**182**, **185-188**) at 40 °C (Scheme 4.1.7). The crude mixtures were then passed through an Amberlite® IRA-400 (Cl) ion exchange resin column, to furnish the corresponding PEG-acetal lipids (**190-194**) as the chloride salts in moderate yields (Table 4.1.3). An analogous route to the C16:1 lipid analogue **195** was carried out using the C16:1 tertiary amine **129** and acetal linker **182** as starting materials.

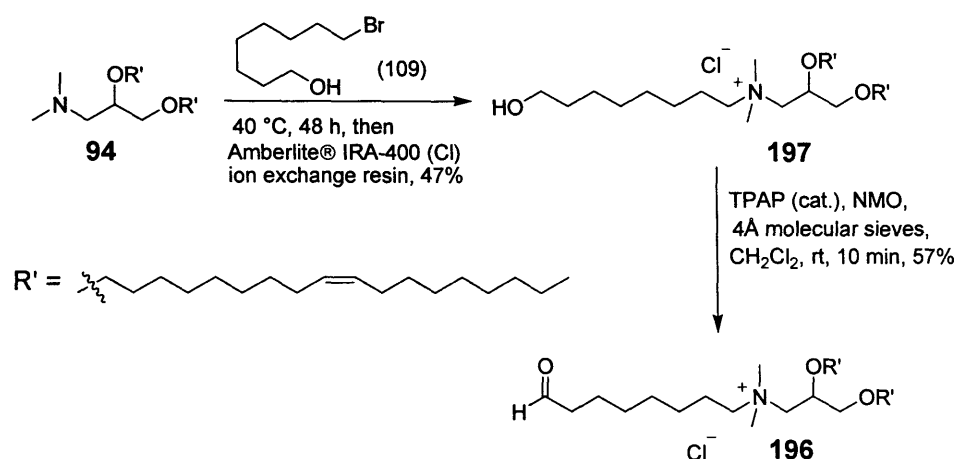


Scheme 4.1.7

Entry	Amine (Eq)	Acetal (Eq)	Product (Yield, %)	$m/z, ([M-Cl]^+)$
1	94 (1)	182 (1)	190 (29)	914
2	94 (1)	185 (1)	191 (44)	941
3	94 (1)	186 (1)	192 (33)	1090
4	94 (1)	187 (1)	193 (21)	885
5	94 (1)	188 (1)	194 (21)	857
6	129 (1)	182 (1)	195 (34)	941

Table 4.1.3

In order to determine the effect of PEG units of PEG-acetal lipids on transfection efficiencies, we also synthesised a non-PEGylated aldehyde lipid **196**, which mimics the product from the hydrolysis of lipid **194**. Initially, the coupling of amine **94** and 8-bromooctanol (**105**) followed by subsequent ion exchange using an Amberlite® IRA-400 (Cl) ion exchange resin column, to give **197** in 47% yield (Scheme 4.1.8). Finally, oxidation of the hydroxyl moiety on **197** with TPAP and NMO as oxidant, afforded the aldehyde lipid **196** in 57% yield.



Scheme 4.1.8

4.2 Hydrolysis Studies of PEG-Acetal Lipids

One of the major reasons for the production of PEG-acetal lipids **190-195** was to investigate the influence of lipid structure on acid sensitivity of the acetal linkages. To quickly evaluate the lipid stability over a small pH change, we employed a TLC assay to monitor the hydrolysis and degradation of the lipids. In a typical procedure, 0.15 mg of lipid was diluted in HMA buffers of pH ranging from 3 to 7.5, to achieve a final lipid concentration between 0.19-0.23 mM. The resulting lipid solutions were incubated at 37 °C for 30 minutes to 3 hours, after which small amounts were removed and neutralised. The degradation of lipids was monitored by TLC and ESMS analysis.

The hydrolysis of lipid **193** was initially examined between pH 3 and 7.5 at 0.5 pH intervals, after 30 min of incubation at 37 °C. TLC analysis of the aliquots demonstrated that **193** was partially degraded in buffers of pH 3.5 to 5.5, as indicated

by the appearance of degraded fragment di(ethylene)glycol (**183**) at $R_f \approx 0.36$ (Figure 4.2.1a). ESMS analysis of the aliquot confirmed that the lipid was partially hydrolysed (Figure 4.2.1b). Products with m/z values of 691, 779, 797 and 885 could correspond to the degraded products **198-200** and lipid **193** (Figure 4.2.1c).

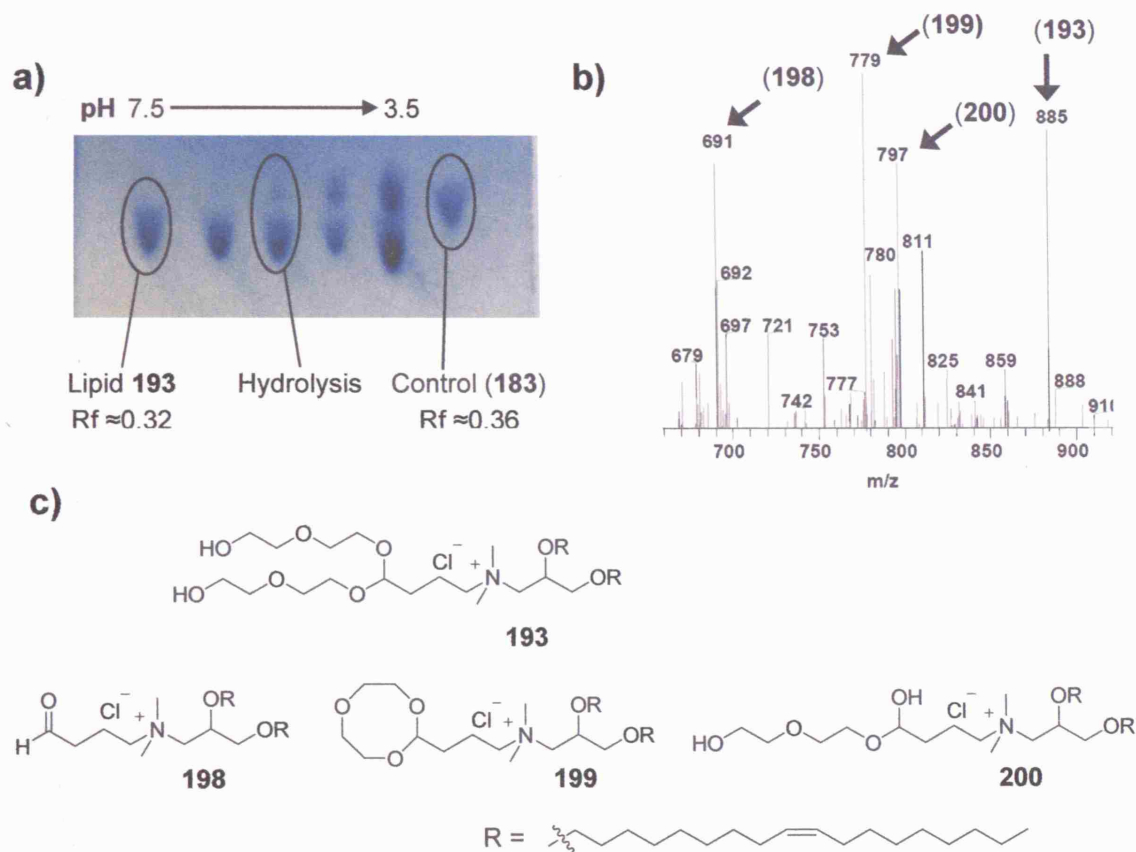


Figure 4.2.1 (a) TLC monitored hydrolysis of lipid **193** at different pH; (b) ESMS confirmed degradation of **193** at pH 5.5; (c) structures of degraded products from hydrolysis of **193**.

Hydrolyses of the PEG-acetal lipids were monitored in similar fashion and the results are summarised in Table 4.2.1. The lipids **190-195** were shown to degrade between pH 3.0 and 5.5 after 30 min of incubation, with the acid sensitivity of the acetal linkages in the following order: **193** \geq **191** $>$ **194** \geq **190** $>$ **192** \approx **195** (Table 4.2.1). The effect of PEG chain variation on acid sensitivity was first examined by comparing the hydrolysis pH of lipids **190-192**. The methoxyPEG (mPEG) lipid derivative **191** was hydrolysed at pH 5.0, being more acid-labile than its hydroxyPEG counterpart **190** (Table 4.2.1, entry 1 & 2). With the lipid anchor and acetal linkage spacing kept constant, the greater acid sensitivity of **191** must be as a result of the

mPEGylation, which favours the hydrolysis of acetal linker at higher pH. The lipid **190** and its PEG4 lipid analogue **192** were degraded in similar pH range (3.0-3.5), indicating that variation of the short PEG chain length had little influence on lipid stability under acidic conditions (Table 4.2.1, entry 1 & 3).

Entry	Acetal Lipid	Degradation pH
1	190	3.5
2	191	5.0
3	192	3.0
4	193	5.5
5	194	4.0
6	195	3.0

Table 4.2.1

Altering the linkage spacing between the acetal moiety and the cationic headgroup was shown to affect lipid stability under mildly acidic conditions. At a fixed lipid anchor and PEG chain length, the shorter C-4 spacer lipid **193** was more acid-labile than its C-6 (**190**) and C-8 (**194**) counterparts (Table 4.2.1, entry 1, 4 & 5). Indeed, hydrolysis of **193** was initiated at approximately pH 5.5, analogous to the physiological pH within the endosome.¹⁸⁸ Finally, similar pHs for cleavage were observed for C18:1 lipid **190** and its C16:1 analogue **195** (pH 3.0-3.5), indicating that varying the lipid chain length had little influence on acid sensitivity of the acetal linkages in this case (Table 4.2.1, entry 1 & 6)

TLC analysis of the aliquots indicated that the lipids **190-195** remained intact over 3 h at a HMA buffer of pH 7.5. ESMS analysis of the aliquots confirmed that none of the lipids were completely degraded after 3 h of incubation, within the pH range being tested.

4.3 Biological Data for PEG-Acetal Lipids

Encouraged by our results on the hydrolysis of PEG-acetal lipids, we proceeded to study the effect of lipid structure on activity *in vitro*. The acetal lipids **190-195** and aldehyde lipid **196**, mixed with DOPE at a 1:1 ratio (*wt/wt*), were formulated as LID complexes at a 2:4:1 lipid/peptide/DNA weight ratio. Peptide **169** and luciferase

reporter gene (pCILuc) were utilised for lipopolyplex formulations. Transfections were studied with three different cell types: human bronchial epithelial (HBE), mouse endothelial (bEND3) and primary porcine vascular smooth muscle cells (PVSMCs). Initial studies indicated that formulations with these lipids did not transfect well in the absence of DOPE. This was exemplified by the transfection efficiency of lipid **190** with HBE cells at 2:1 and 4:1 lipid/DNA ratios (Chart 4.3.1). Transfection activity was highest when **190** was formulated with DOPE. Indeed, the lipid was 25 times more active when formulated with DOPE at a 2:1 lipid/DNA ratio.

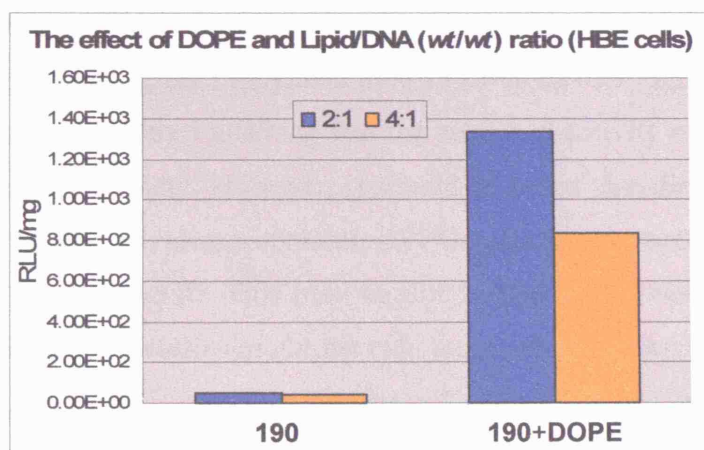


Chart 4.3.1

The effect of DOPE may be twofold. Firstly, the enhancement in activity may be as a result of DOPE capacity to promote H_{II} lipid phase formation and facilitate endosomal escape.⁴² Secondly, formulation with DOPE decreases the amount of PEG-acetal lipids in LID complexes, which in turn could alter the phase behaviour and aggregate structures of the lipid component. Using cryo-transmission electron microscopy, Johnson and Edwards have demonstrated that a mixture of PEG(750)-DSPE and DOPE preferred to adopt the lamellar $L\alpha$ phase at low mol% of PEG-lipids (>35%).¹⁹⁷ At high PEG-lipid mol% (~80%) most of the liposomes underwent phase transition to form spherical micelles. In addition, they observed the coexistence of liposomes and spherical micelles at intermediate PEG-lipid concentrations.¹⁹⁷ Based on these results, we postulated that the PEG-acetal lipid/DOPE mixtures may prefer to form bilayer aggregates at a 1:1 ratio (wt/wt), hence provided sufficient protection to the LID complexes before endocytosised into cells. Conversely, cytofectins

containing PEG-acetal lipids alone are more likely to form spherical micelles, which may provide limited protection to the lipopolyplexes formed.

The transfection efficiencies of lipopolyplexes containing PEG-acetal lipids **190-195** have been tested with different cell lines and compared with that of the aldehyde lipid (**196**) and DOTMA (**6**). With human bronchial cell (HBE) transfections the PEG-acetal lipids displayed activities in the following order: **193** ≥ **191** > **194** > **190** > **195** > **192** (Chart 4.3.2). There appeared to be a correlation between the activity and lipid stability under mildly acidic conditions. Indeed, the most acid-labile lipid **193** was ~20 fold more active than the least acid-labile lipid (**192**) (see Section 4.2). Interestingly, the PEGylated lipid **194** was up to 3 fold more active than its aldehyde analogue (**196**), indicating that the enhanced activity of **194** was due to inclusion of the PEG moiety. However, it should be noted that the general level of transfections with lipopolyplexes containing PEG-acetal lipids were lower than that of DOTMA (**6**) (Chart 4.3.2). This may be due to incomplete hydrolysis of PEG-acetal lipids. The PEG moieties might provide too much shielding to the complexes formed, leading to less efficient entry into the cell and/or poor endosomal escape.

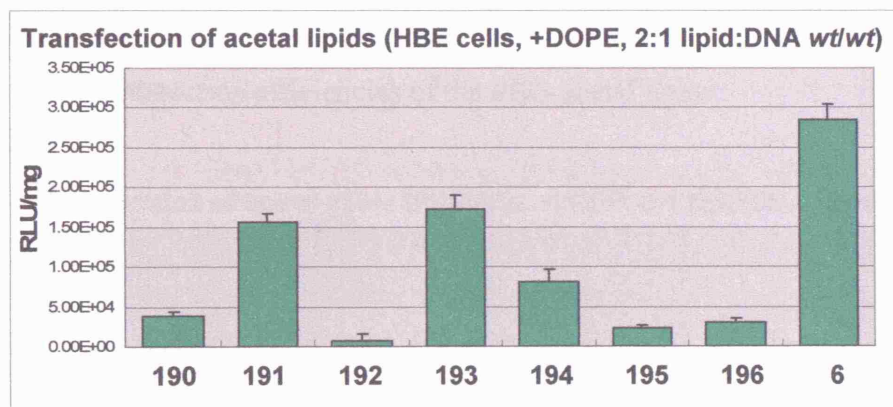


Chart 4.3.2

With mouse endothelial cell (bEND) transfections the most active lipopolyplexes were those containing lipids **191**, **193** and **194**, which were significantly hydrolysed at pH 5.0, 5.5 and 4.0, respectively (Chart 4.3.3). In addition, lipopolyplexes with these lipids were shown to transfect better than that containing DOTMA, indicating that the activities of the lipids are cell type-dependent.

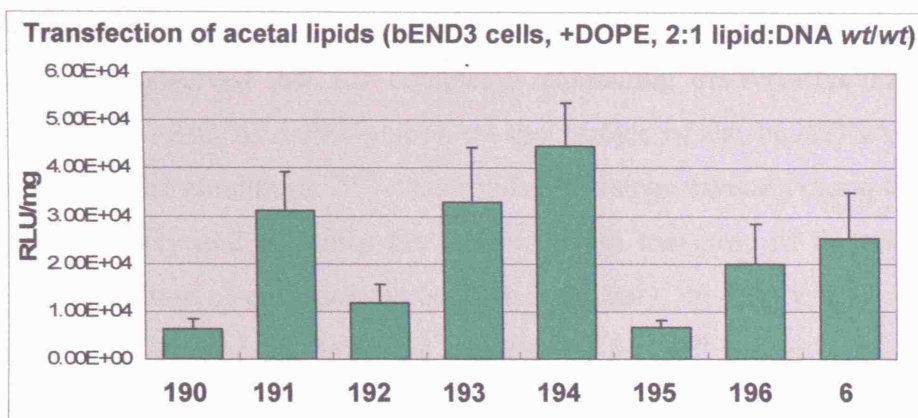


Chart 4.3.3

Transfections performed with primary porcine vascular smooth muscle cells (PVSMCs) using PEG-acetal lipids demonstrated some similarities to the trends with bEND3 transfections. For example, the most effective formulation again contained lipid **194**, with the following pattern observed: **194** > **190** \approx **191** \approx **193** > **192** (Chart 4.3.4). When formulated with DOPE, lipopolyplexes containing lipids **191**, **193** or **194** displayed transfections efficiency similar to or better than that containing DOTMA. Furthermore, the aldehyde lipid **196** was 4 times less active than its PEGylated analogue (**194**), indicating that the PEG units plays an important role in enhancing the transfection efficiencies of the PEG-acetal lipids.

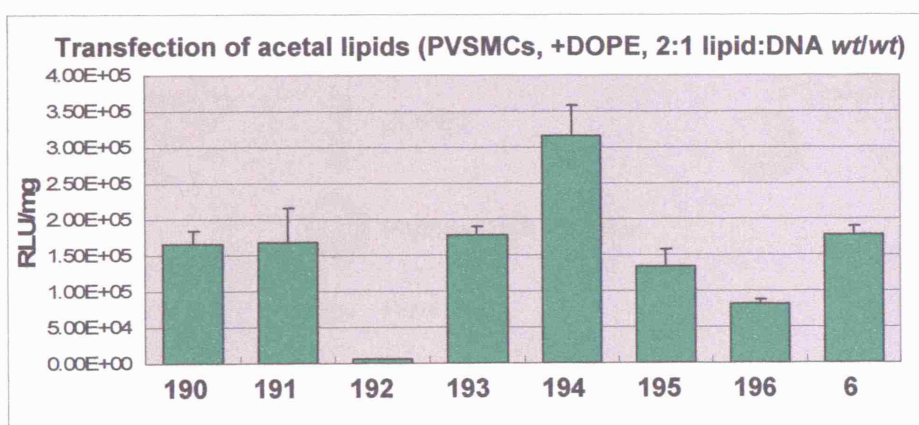


Chart 4.3.4

The transfection results obtained from the cell types tested were in good agreement with lipid stability observed under mildly acidic conditions. Indeed, the highest levels of lipopolyplex transfections were achieved with lipids **191**, **193** and

194, which undergo hydrolysis at physiological accessible pHs (see Section 4.2). It was previously observed that LD complexes containing pH-sensitive PEG lipids destabilised as a result of dePEGylation on the surface of the lipid/DNA complex under mildly acidic conditions.^{79,198} This solubility change causes a disruption of the liposomal assembly and promotes the $L_{\alpha} \rightarrow H_{II}$ phase transition of liposomes, thus triggering the release of encapsulated contents. Similarly, the LID vector complexes formulated with PEG-acetal lipids are expected to be dePEGylated once they are internalised into endosomal vesicles, where the pH is mildly acidic (Figure 4.3.1).¹⁸⁸ This may induce the $L_{\alpha} \rightarrow H_{II}$ phase transition in a similar fashion, leading to membrane destabilisation and increases the amount of plasmid DNA release into the cytoplasm, thus enhancing the transfection efficacy. The incorporation of fusogenic lipid DOPE into lipopolyplex formulations is also expected to facilitate the $L_{\alpha} \rightarrow H_{II}$ phase transition at physiologically accessible pHs.

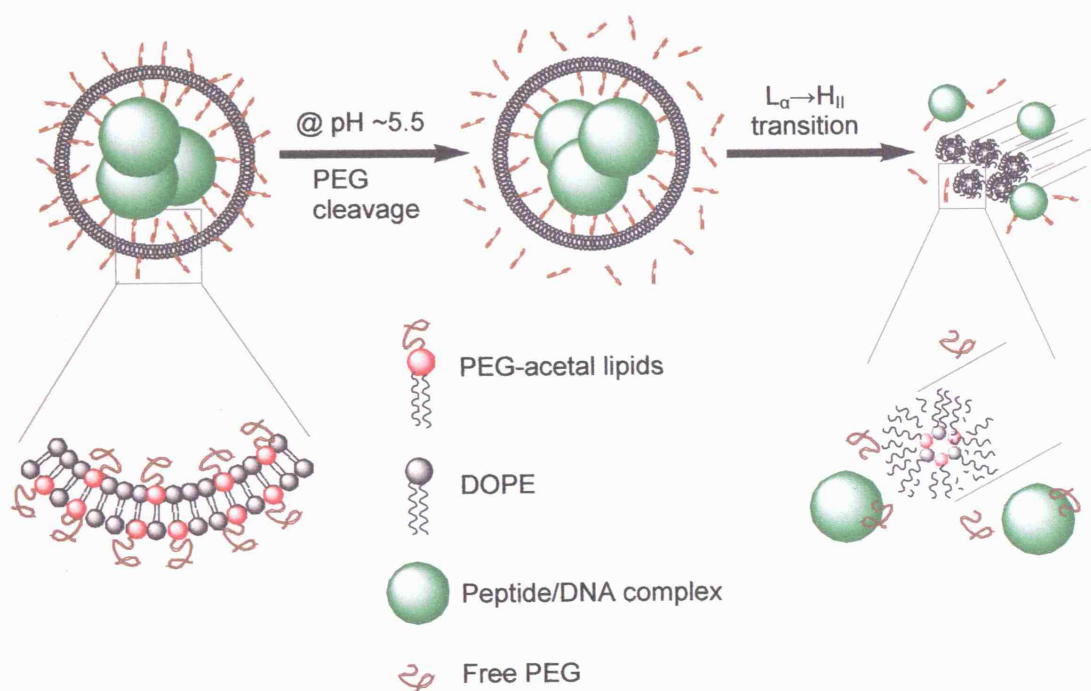


Figure 4.3.1 Proposed $L_{\alpha} \rightarrow H_{II}$ phase transition induced by dePEGylation of PEG-acetal lipids

4.4 Conclusion

We have designed and prepared a novel class of pH-sensitive PEG lipids bearing acid-cleavable acetal linkages and short PEG chains. It has proven possible to alter the degradation pH of these lipids by varying lipid structural properties including the PEG chain length, nature of the PEG chains, the spacing of the linkage, and the lipid chain length. Hydrolysis studies demonstrated that these lipids are readily hydrolysed at a pH range 3.0-5.5 after incubation at 37 °C for 30 min. In addition, lipopolyplexes formulated with PEG-acetal lipids and DOPE at a 1:1 weight ratio have been utilised to transfect different cell types *in vitro*, and displayed cell-type dependent activity. Generally, the transfection results indicated a strong correlation between the transfection efficiency and lipid stability under mildly acidic conditions. The best candidates for LID formulations are lipids that undergo hydrolysis at physiologically accessible pHs. Furthermore, PEG-acetal lipid **194** displayed higher transfection efficiency than its non-PEGylated aldehyde analogue (**196**), indicating that PEGylation on the lipids enhances transfection activity of the LID vector complexes. These observations suggest that pH-sensitive PEG lipids are good candidates for lipopolyplex formulations that may protect the LID complexes before cell internalisation and induce endosomal fusion, thus enhancing the transfection efficacy. Work is in progress to validate the use of these lipids for *in vivo* applications.

CHAPTER 5

RESULTS AND DISCUSSION

Symmetrical Dicationic Lipid Analogues

5. Symmetrical Dicationic Lipid Analogues

Symmetrical cationic lipids that possess two positively charged headgroups were recently prepared and tested for non-viral gene delivery.^{64,65,69} These dicationic lipid derivatives, also known as cationic gemini surfactants, are usually comprised of two ammonium headgroups and aliphatic chains linked *via* a spacer.¹⁹⁹ The dicationic lipids were found to bind and compact DNA efficiently, and displayed high transfection efficiency with a variety of cell types.^{64,65,200} It was previously demonstrated that the introduction of a secondary quaternary amine increased the strength of interaction with plasmid DNA and as a result improved the lipoplex transfection.⁶⁴ In addition, high transfection efficiencies were achieved at low lipid concentrations, thus diminishing any lipid-associated toxic effects.^{201,202}

This chapter describes investigations into the synthesis of novel symmetrical dicationic lipids utilised for LID vector formulations. The formation of lipids bearing an erythritol backbone (**201**) was initially studied, as this would enable dicationic lipids to be constructed with the amine functionality in a 1,2-relationship to the lipid chains, analogous to structural relationship of the glycerol based lipids we had synthesised previously (see Section 2-4) (Figure 5.1). The structural requirements of symmetrical dicationic lipids will be further investigated with bisquaternary ammonium lipids bearing the pentaerythritol backbone (**202**). In the literature there are limited examples of bisquaternary ammonium lipids with erythritol and pentaerythritol backbones being utilised as gene transfer agent.^{66,68,69,203} Interestingly, the diesterified lipid DOHBD (**27**) with erythritol backbone and hydroxyethyl ammonium headgroups was proved to be successful in transfecting a wide range of cell types when mixed with DOPE.^{67,68} Our aim was to establish synthetic strategies that are suitable for preparing headgroup derivatives of erythritol and pentaerythritol lipids, for a detailed SAR vector study.

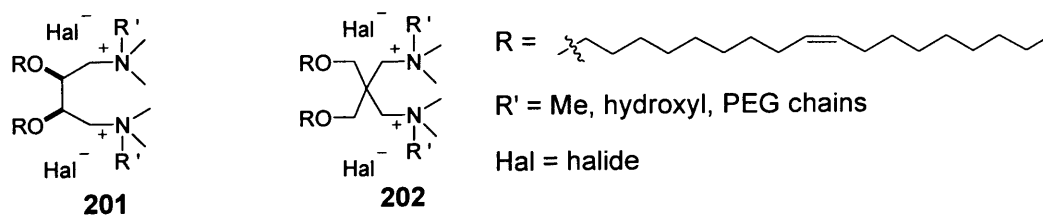
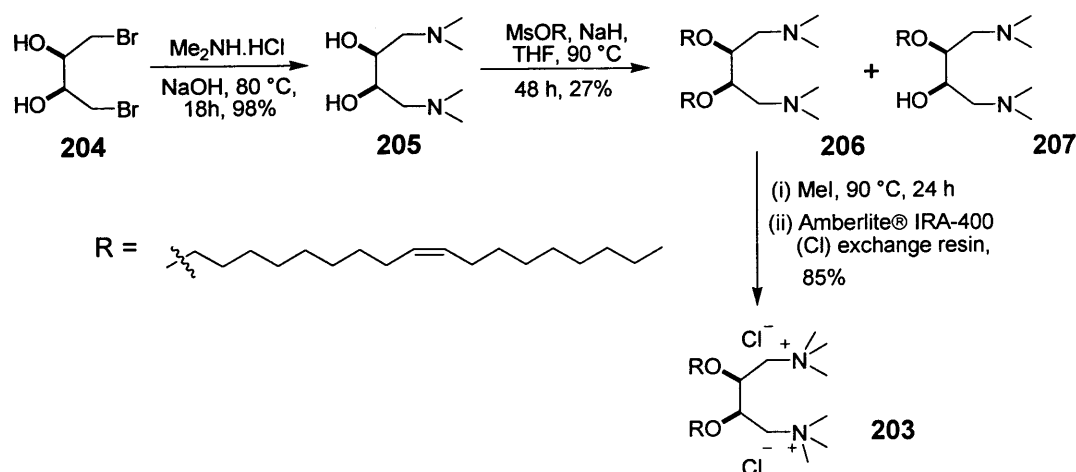


Figure 5.1

5.1 Synthesis of Dicationic Lipid Analogues I

5.1.1 Synthesis of Erythritol Derivative I

The synthesis of erythritol lipid analogue **203** was initially investigated using *meso*-1,4-dibromo-2,3-diol (**204**) as a starting material. Conversion of **204** to its corresponding diamine **205** was readily achieved, using excess of dimethylamine hydrochloride and sodium hydroxide (Scheme 5.1.1). Compound **205** was then separated from all other impurities by extraction into chloroform, to give **205** in near quantitative yield. Dietherification of **205** was then attempted using oleyl mesylate (**93**) and sodium hydride in anhydrous toluene, by heating the reaction mixture at reflux for 48 h. However, no dietherification product was detected by ESMS and NMR analysis of the crude mixture (Table 5.1.1, entry 1). When repeating the reaction using anhydrous THF as solvent the dietherified product **206** was formed, but ESMS and ^1H NMR analysis indicated that the mono-ether **207** was generated as a major product ($\sim 40\%$ conversion). Nevertheless, **206** was isolated and purified by flash column chromatography in 27% yield (Table 5.1.1, entry 2). In an attempt to optimise the synthetic conditions, the reaction was repeated by increasing the reaction time to 72 h, but the reaction yield of **206** decreased to 14% (Table 5.1.1, entry 3). Finally, compound **206** was quaternised with excess iodomethane and subsequently passed through an Amberlite[®] IRA-400 (Cl) ion exchange resin column, to furnish the bisquaternary ammonium chloride salt **203** in 85% yield. Although the overall yield was only modest, this methodology provides a direct route for preparing the erythritol lipid analogue over three steps.



Scheme 5.1.1

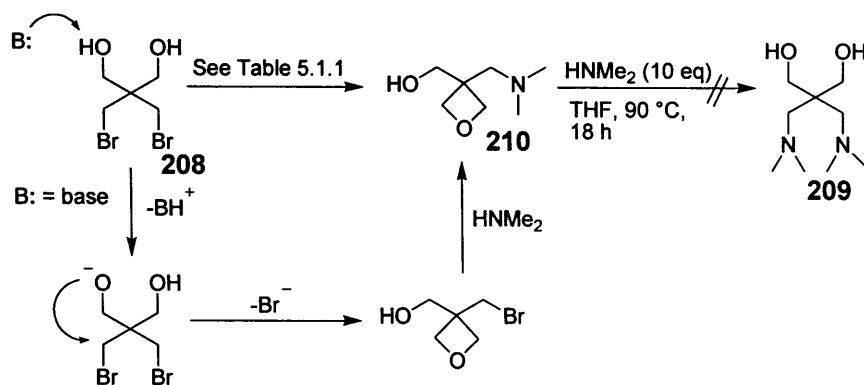
Entry	Mesylate (eq)	Amine (eq)	Base (eq)	Solvent	Conditions	Yield (%)
1	93 (3)	206 (1)	NaH (3)	Toluene	110 °C, 48 h	0
2	93 (3)	206 (1)	NaH (3)	THF	90 °C, 48 h	27
3	93 (3)	206 (1)	NaH (3)	THF	90 °C, 72 h	14

Table 5.1.1

5.1.2 Synthesis of Pentaerythritol Derivative I

5.1.2.1 Route 1

With the synthetic route to the bisquaternary erythritol lipid **203** established, an analogous route was initially attempted to prepare the pentaerythritol lipid analogue, using the dibromide **208** as a starting material. The conversion of **208** to its corresponding diamine **209** was first attempted using an excess of dimethylamine hydrochloride (12 eq) and sodium hydroxide (16 eq) (Scheme 5.1.2). Rather, the oxetane **210** was formed and isolated by column chromatograph in 72% yield (Table 5.1.2, entry 1). It was initially thought that an excess of sodium hydroxide in the reaction mixture deprotonated the hydroxyl group and the alkoxide formed underwent an intramolecular nucleophilic cyclisation reaction (Scheme 5.1.2). Hence the reaction was repeated using equimolar amount of dimethylamine hydrochloride and sodium hydroxide (12 eq), but ^1H NMR spectroscopic analysis of the crude mixture indicated that the oxetane **210** was again formed as the major product (Table 5.1.2, entry 2). Finally, conversion of **208** to **209** was attempted by treatment with commercially available dimethylamine solution in THF at rt (Table 5.1.2, entry 3); however, ESMS and ^1H NMR analysis indicated that a mixture of compounds was formed, with **210** being the major product. In an attempt to generate **209** *via* oxetane ring-opening, compound **210** was heated in an excess of dimethylamine in anhydrous THF (Scheme 5.1.2). However, the formation of **209** was not detected by ESMS analysis or it was produced in very low yield (typically <1%).



Scheme 5.1.2

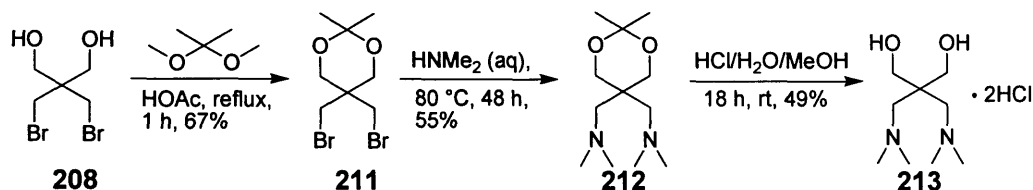
Entry	Amine (Eq)	Base (Eq)	Solvent	Conditions	Product
1	HNMe ₂ ·HCl (12)	NaOH (16)	H ₂ O	90 °C, 18 h	210
2	HNMe ₂ ·HCl (12)	NaOH (12)	H ₂ O	90 °C, 18 h	210
3	HNMe ₂ (12)	—	THF	rt °C, 24 h	210

Table 5.1.2

Oxetanes are relatively stable towards nucleophilic addition, but ring-opening with nucleophiles can be achieved in the presence of protic or Lewis acids such as aluminium chloride and titanium tetrachloride.^{204,205} However, this approach was not feasible for the ring-opening of **209** using dimethylamine, as the amine can act as a strong Lewis base that will complex with any acid present. At this stage an alternative route to generate **209** was considered.

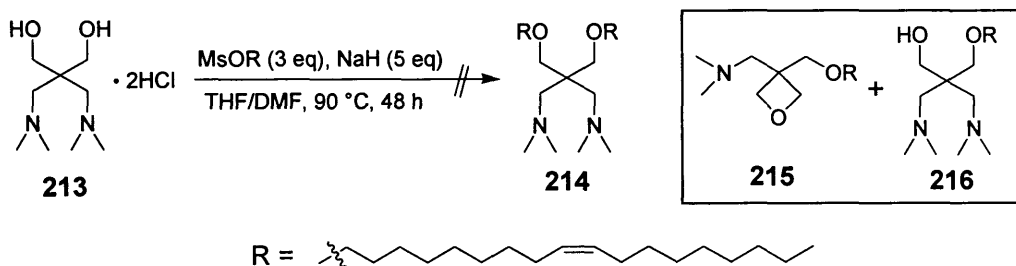
The synthesis of acetal-protected dibromide **211** was then undertaken. It was envisaged that acetal protection of the diol would exclude the possibility of oxetane formation during amination, and the acetal could then be cleaved under mildly acidic conditions. The diol protection of **208** using 2,2-dimethoxypropane and glacial acetic acid has been previously described by Bitha *et al.*²⁰⁶ Using this method, compound **211** was formed in 67% yield after purification by column chromatography (Scheme 5.1.3). The conversion of **211** to its corresponding diamine **212** was carried out using aqueous dimethylamine solution, to afford **212** in 55% yield. Removal of the acetal group was initially attempted by stirring **212** in a mixture of water/methanol (1:10) solution for 72 h, using *p*TsOH as catalyst, but ESMS analysis of the crude mixture indicated that a significant amount of **212** was left unreacted. Finally, deprotection

was achieved by stirring **212** in a mixture of hydrochloric acid/water/methanol (1:1:5) solution at room temperature for 18 h. Isolation of the diamine **209** had proved to be difficult due to its high aqueous solubility; therefore the corresponding dihydrochloride salt **213**, which was extracted from the reaction mixture using dichloromethane and recrystallised from diethyl ether, to afford **213** in 49% yield (Scheme 5.1.3).



Scheme 5.1.3

Conversion of **213** to the diether derivative **214** was then attempted with oleyl mesylate (**94**), utilising an excess of sodium hydride as base (Scheme 5.1.4). It was envisaged that the dihydrochloride salt **213** could be converted to the free amine by stirring with excess sodium hydride prior to mesylate addition. However, examination of the ESMS and ¹H NMR spectroscopy indicated that the oxetane **215** and monoether **216** were formed as major products, with **216** being isolated and purified by flash chromatography in 44% yield.

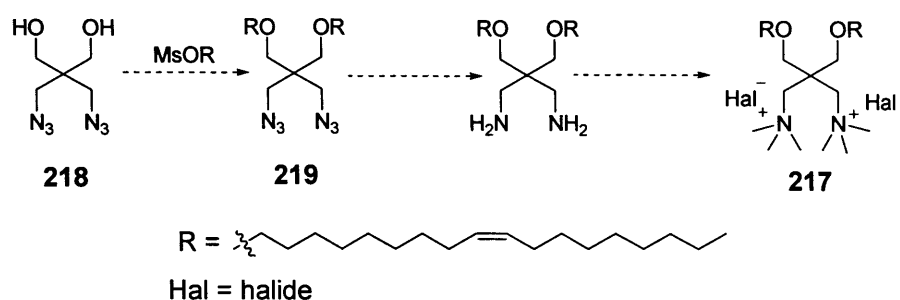


Scheme 5.1.4

5.1.2.2 Route 2

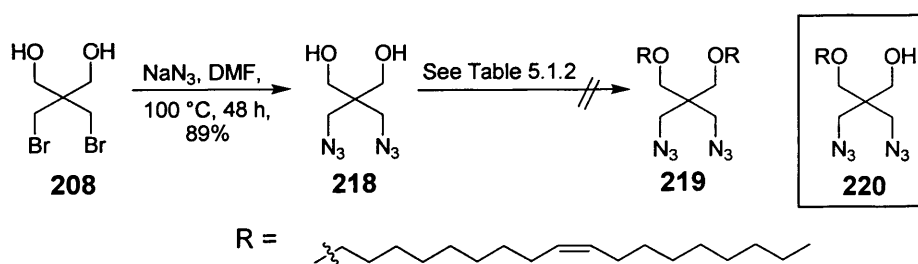
Due to the problems associated with the dietherification of **214**, an alternative strategy to yield the pentaerythritol lipid analogue **217** was then considered. It has been reported that the diazide **218** can undergo dietherification with mesylated alcohol, with the azides acted as ‘masked’ amine groups (Scheme 5.1.3).²⁰⁷ It was

hoped that compound **219** could then be reduced to its corresponding diamine and subsequently quaternised to yield the pentaerythritol lipid **217**.



Scheme 5.1.5

Diazidation of dibromide **208** with sodium azide was carried out following the methodology described by Bitha *et al.*, to afford the diazide **218** in 89% yield (Scheme 5.1.6).²⁰⁸ The dietherification of **218** with mesylated alcohol in anhydrous toluene, using potassium *tert*-butoxide as base, has been previously reported.²⁰⁷ Several attempts were made to convert **218** into the corresponding diether **219** with oleyl mesylate (**93**) (Table 5.1.3). Initially the reaction was carried out in anhydrous toluene for 24 to 48 hours; however, only starting materials were recovered from the reaction mixtures (Table 5.1.3, entry 1 & 2). At this stage the use of toluene was questioned due to the poor solubility of potassium *tert*-butoxide in this solvent, despite the fact that similar conditions were reported for the dietherification of **218**.²⁰⁷ The reaction was then repeated in anhydrous THF (Table 5.1.3, entry 3), but ESMS and ¹H NMR analysis of the crude reaction mixture indicated that the monoether **220** was formed as the major product. The reaction was repeated by increasing the reaction time to 48 h, but the desired product **219** was not yielded (Table 5.1.3, entry 4). This suggested that the second etherification on **218** was limited, possibly as a result of steric hindrance.



Scheme 5.1.6

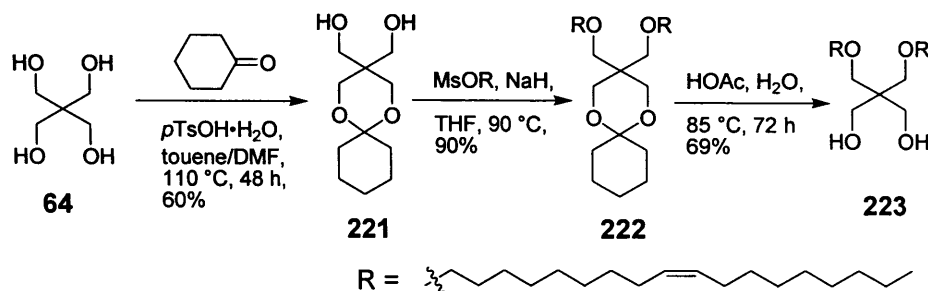
Entry	Diol (eq)	Mesylate (eq)	Base (eq)	Solvent	Conditions
1	218 (1)	93 (2.5)	KO ^t Bu (2.4)	toluene	70 °C, 24 h
2	218 (1)	93 (3)	KO ^t Bu (3)	toluene	70 °C, 48 h
3	218 (1)	93 (3)	KO ^t Bu (3)	THF	90 °C, 24 h
4	218 (1)	93 (3)	KO ^t Bu (3)	THF	90 °C, 48 h

Table 5.1.3

5.1.2.3 Route 3

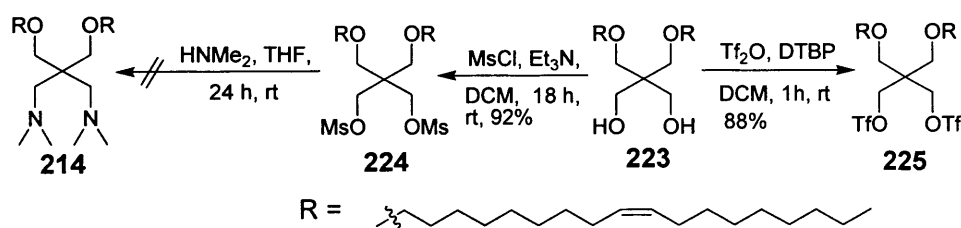
With the unsuccessful strategy to form the diether **219**, an alternative route was examined to generate the pentaerythritol lipid analogue. The use of the mono-acetal pentaerythritol derivative was then explored, utilising pentaerythritol (**64**) as a starting material. Pentaerythritol has very limited solubility in non-polar solvents, but its di-protected derivatives are soluble in a range of organic solvents, making them useful for synthetic transformations. By protecting two of the hydroxyl groups as cyclic acetal, the lipid chains can then be introduced to the pentaerythritol backbone, with minimised steric effect induced from the pendant groups.

Murgufa *et al.* has described the mono-acetal protection of pentaerythritol with an equimolar amount of cyclohexanone, in a mixture of benzene and DMF, heated at 130 °C, using *p*TsOH as catalyst.²⁰⁹ The reaction was set up using a Soxhlet trap for azeotropic removal of water formed. A mixture of toluene and DMF was utilised as the reaction solvents. Using this approach, the conversion of **64** to diol **221** was achieved in 60% yield (Scheme 5.1.7). The dietherification of **221** with oleyl mesylate, using sodium hydride as base, was then readily achieved in anhydrous THF. The dietherified derivative **222** was isolated and purified by flash column chromatography in a high yield of 90%, suggesting that the dietherification of **221** was not too sterically hindered. Removal of the acetal protection was initially attempted by stirring **222** in a mixture of HCl/water/methanol (1:1:5) solution at room temperature for 18 h, but TLC analysis of the crude mixture indicated that diol **223** was formed but a significant amount of **222** left unreacted. In an attempt to optimise the deprotection, compound **222** was heated in a mixed solution of acetic acid/water (4:1) at 85 °C, to furnish **223** in 69% yield (Scheme 5.1.7).²⁰⁹



Scheme 5.1.7

With the diol **223** in hand, activation of the hydroxyl groups was required in order that the amines could be attached by nucleophilic substitution. Initially compound **223** was activated with methanesulfonyl chloride, using triethylamine as base, to afford the dimesylate **224** in near quantitative yield (Scheme 5.1.8). The conversion of **224** to diamine **214** by reacting with dimethylamine in anhydrous THF was initially attempted at rt, but this failed to give any product and dimesylate **224** was recovered. As mesylate activation did not appear to give sufficiently reactive leaving groups to promote diamination, the use of trifluoromethanesulfonate (triflate) ethers as leaving groups was then explored. Conversion of **223** to its corresponding ditriflate **225** was carried out with triflic anhydride in anhydrous dichloromethane, using 2,6-di-*tert*-butylpyridine (DTBP) as base, following the methodology described by Ambrose *et al.*²¹⁰ Purification of the ditriflate was straightforwardly achieved by filtering the crude reaction mixture through a short pad (~2 cm) of silica, to afford **225** in 88% yield.



Scheme 5.1.8

Initially, the diamination of **225** was attempted using 5 eq of dimethylamine in anhydrous THF (Scheme 5.1.9). However, ESMS and ¹H NMR spectroscopic analysis of the crude product indicated that the azetidinium salt was formed as the major product, which was isolated and converted to the chloride salt, giving **226** in

(i) HNMe_2 (20 eq), THF, rt, 24 h
 (ii) Amberlite® IRA-400 (Cl) exchange resin, 82%

227

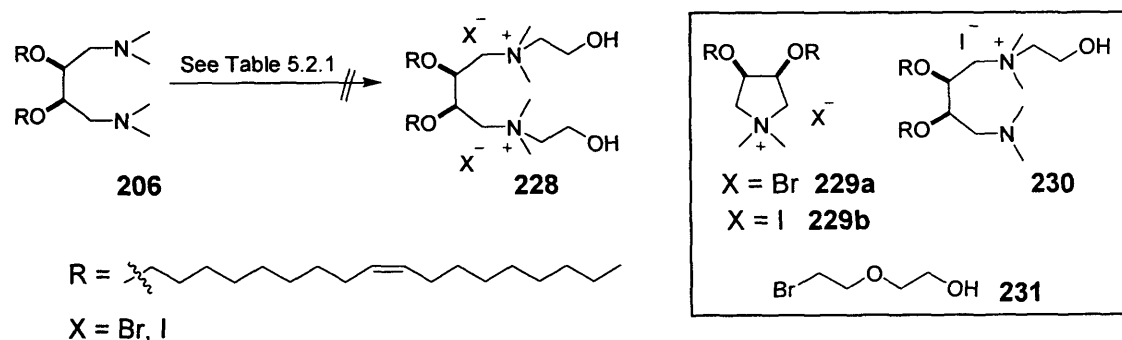
In summary, a successful route to a pentaerythritol lipid analogue was established, starting from commercially available pentaerythritol. The lipid **227** was formed in 15% yield over six steps. Although the overall yield was low, we envisaged that this methodology could be applied to generate pentaerythritol lipid derivatives with different headgroup functionalities.

While preparing the erythritol lipid **203** for vector formulations it was revealed that it had poor aqueous solubility, which could possibly lead to inconsistent formulations and poor vector transfections. It was proposed that the attachment of a hydrophilic moiety such as a hydroxyl group or PEG units could increase the aqueous solubility of the dicationic lipids as well as improve the vector stability in serum, thus leading to enhanced transfection activities *in vitro* and *in vivo*. The synthesis of erythritol and pentaerythritol lipid derivatives containing headgroups with hydrophilic moieties was therefore explored.

5.2.1 Synthesis of Erythritol Derivative II

5.2.1.1 Route 1

The synthesis of erythritol lipids with hydrophilic headgroup functionalities was initially explored using diamine **206** as a key intermediate (Scheme 5.2.1). It was hoped that direct quaternisation of the amine groups would afford the desired products. Conversion of **206** to lipid **228** was initially attempted using 2-bromoethanol, by stirring the reaction mixture in anhydrous acetone (Table 5.2.1, entry 1). While TLC analysis of the crude reaction mixture indicated that the starting material had been converted to another species, ESMS and ¹H NMR analysis of the crude reaction mixture indicated that the pyrrolidinium bromide salt **229a** was formed as the major product. Compound **229a** was isolated and purified by flash column chromatography in 63% yield.



Scheme 5.2.1

Entry	Diamine (eq)	Alcohol (eq)	Solvent	Conditions	Product
1	206 (1)	2-bromoethanol (4)	acetone	rt, 18 h	229a
2	206 (1)	2-iodoethanol (4)	acetone	rt, 18 h	229b
3	206 (1)	2-iodoethanol (600)	—	rt, 18 h	229b
4	206 (1)	2-iodoethanol (600)	—	0 °C, 5 h	229b+230
5	206 (1)	231 (4)	acetone	rt, 18 h	229a

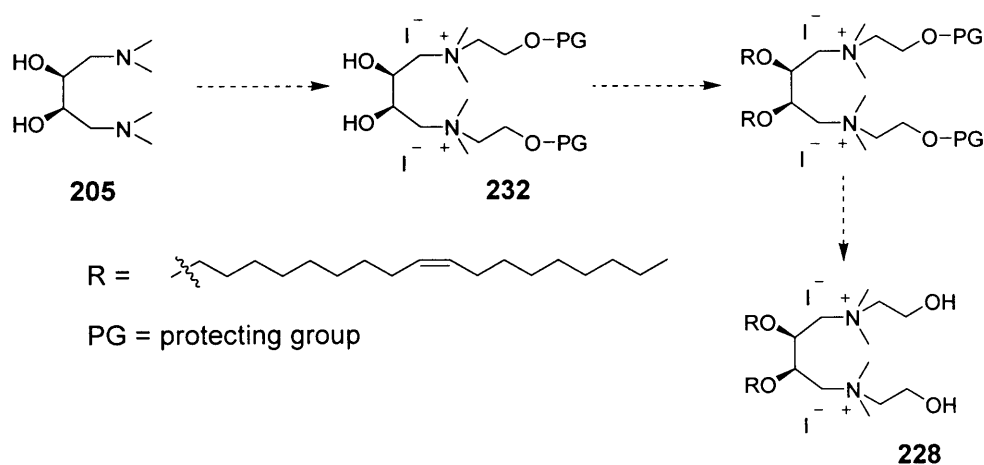
Table 5.2.1

In an attempt to promote the diquaternisation process, compound **206** was stirred with the more reactive 2-iodoethanol in anhydrous acetone, but the iodide salt **229b** was again afforded as the major product (Table 5.2.1, entry 2). The diquaternisation was re-attempted in the absence of solvent, using a large excess of

2-iodoethanol, at room temperature and 0 °C (Table 5.2.1, entry 3 & 4). ESMS and TLC analysis of the crude mixtures indicated that the formation of **229b** dominated, with traces of the mono-quaternised salt **230** found when the reaction was carried out at 0 °C. This suggested that compound **228** preferred to undergo cyclisation rather than a second quaternisation under the reaction conditions being tested. The quaternisation of **206** using 2-(2-bromoethoxy)ethanol (**231**) was also explored, but this again generated the bromide salt **229a** as the major product (Table 5.2.1, entry 5). At this stage an alternative synthetic approach was considered.

5.2.1.2 Route 2

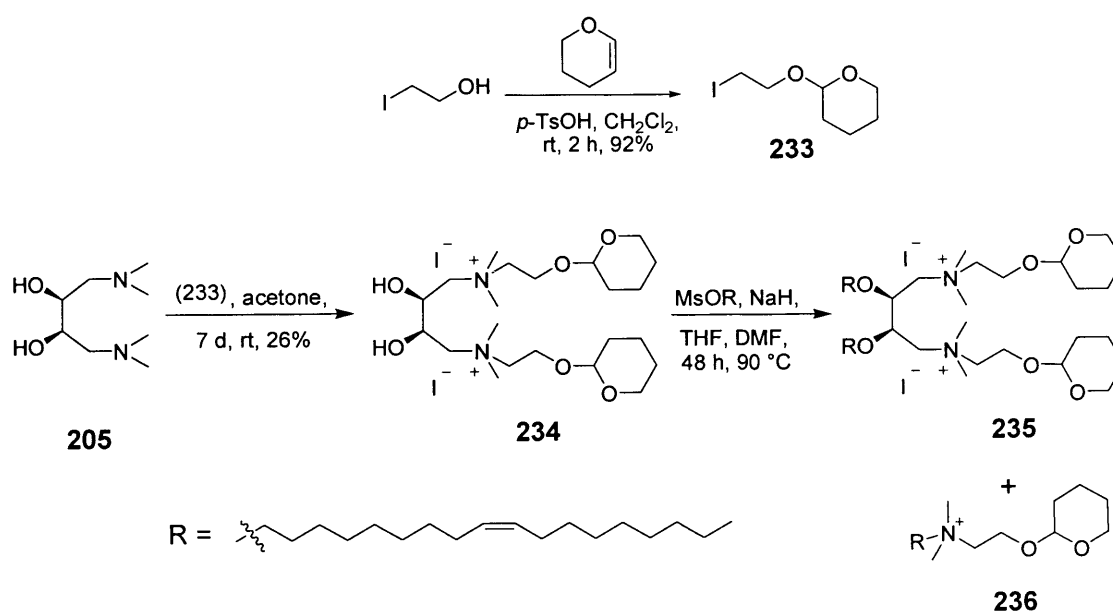
The second synthetic route considered to access the dicationic lipid **228** involved the utilisation of diamine **205** as a reaction intermediate (Scheme 5.2.2). The key steps involved quaternisation of **205** with protected 2-iodoethanol, to form the bisquaternary ammonium salt **232**. Dietherification of **232** using oleyl mesylate and subsequent deprotection would afford the lipid **228**.



Scheme 5.2.2

Initially, THP-protection of 2-iodoethanol was undertaken to provide a reagent for quaternisation. The synthesis of THP-protected iodide **233** proceeded smoothly by stirring 3,4-dihydro-2H-pyran with *p*-toluenesulfonic acid (*p*TsOH) as the catalyst (Scheme 5.2.3).²¹¹ The conversion of diamine **205** to the diquaternised salt **234** was then carried out by treatment with **233** in anhydrous acetone. ESMS analysis of the crude reaction mixture indicated that the conversion to **234** was complete after seven days, as evidenced by the disappearance of the peak

corresponding to **205** ($m/z = 177$, MH^+) and the appearance of the peak corresponding to **234** ($m/z = 436$, $[M-2I]^+$). Purification of **234** was not straightforward, as the product was highly soluble in aqueous solution and very polar. Low-temperature recrystallisation was attempted using several solvent systems but was unsuccessful. Purification by fractional distillation was not attempted as the product was a gum. Since the crude reaction mixture was mostly made up of unreacted **233**, as evidenced by ESMS analysis, the isolation of **234** using two immiscible organic solvents was explored. It was hoped that, by dissolving the mixture in a more polar solvent, extraction with a less polar solvent would remove any unreacted **233** from the mixture, leaving the diquaternised salt **234** in the polar solvent. Using this approach, the crude mixture was dissolved in methanol, and was repeatedly washed (<10 times) with hexane and petroleum ether to ensure that all unreacted **233** was removed. After concentrated *in vacuo*, the bisquaternary salt **234** was isolated as a yellow gum in 26% yield. Although the conversion of **205** to **234** was likely to be high yielding, some of the product was probably lost during the extraction steps.



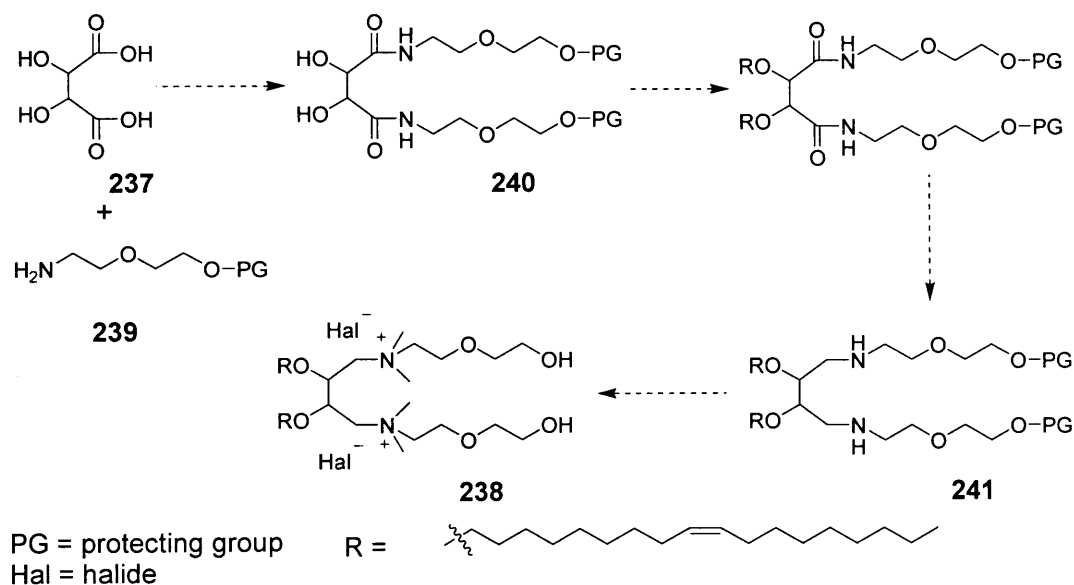
Scheme 5.2.3

Dietherification of **234** with oleyl mesylate was attempted in a mixture of anhydrous THF and DMF, using sodium hydride as base (Scheme 5.2.3). Analysis of the crude reaction mixture by ESMS and ^1H NMR spectroscopy indicated that a complex mixture of products was formed. Peaks with m/z values of 436 ($\frac{1}{2}[M-2I]^+$) and 425 ($[M-I]^+$) was observed which could correspond to the products **235** and **236**,

respectively. The formation of **236** was thought to be due to cleavage of the amine moiety and subsequently quaternised with oleyl mesylate. Several attempts were made to separate the mixture by flash column chromatography, but were unsuccessful since the products had very similar R_f values. Due to the mixture of products formed the yield of **235** was likely to be low, a different strategy to form headgroup derivatives of diquaternised erythritol lipid was considered.

5.2.1.3 Route 3

The third synthetic route investigated involved using DL-tartaric acid (**237**) as a starting material, to generate the PEGylated lipid analogue **238** (Scheme 5.2.4). It was hoped that the coupling of **237** with amine **239** would generate the diamide **240**, which would then be dietherified with activated oleyl alcohol followed by amide reduction to give **241**. Quaternisation with iodomethane and subsequent deprotection should generate the desired lipid analogue **238**. This synthetic approach has the advantage that the amine moiety will be masked as an amide, which is unlikely to undergo the unwanted cyclisation reaction previously observed.



Scheme 5.2.4

Initially, *tert*-butyldiphenylsilyl (TBDPS) protection of commercially available 2-(2-aminoethoxy)ethanol was carried out, using TBDPS chloride and imidazole, to afford **242** in 62% yield (Scheme 5.2.5).²¹² The coupling of **237** and **242** was readily achieved in anhydrous DMF, using *N*-(3-dimethylaminopropyl)-*N'*-



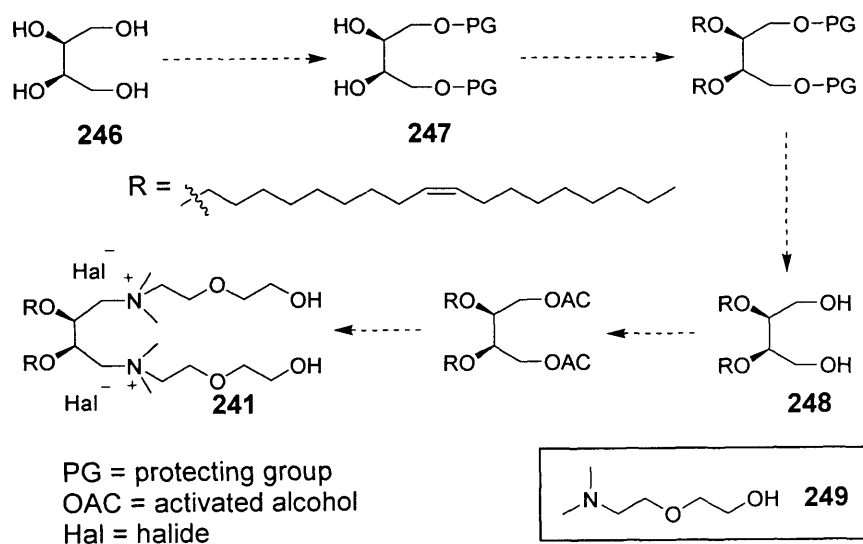
128

Entry	Diol (eq)	Mesylate (eq)	Base (eq)	Solvents (ratio)	Conditions
1	243 (1)	93 (3)	NaH (3)	DMF/THF (1: 10)	70 °C, 24 h
2	243 (1)	93 (3)	NaH (5)	DMF/THF (1: 10)	70 °C, 48 h
3	243 (1)	93 (3)	NaH (5)	DMF/toluene (1: 10)	90 °C, 48 h
4	243 (1)	93 (3)	NaH (5)	DMF/toluene (1: 10)	110 °C, 72 h

Table 5.2.2

5.2.1.4 Route 4

A synthetic route to generate compound **241** utilising *meso*-erythritol (**246**) as a starting material was explored (Scheme 5.2.6). Initially, the primary hydroxyl groups on **246** could be selectively protected to afford the diol **247**. Dietherification of **247** and subsequent deprotection will give the diol **248**. Finally, alcohol activation followed by quaternisation with amine **249** would generate the lipid **241**. This synthetic approach has the advantage that the activated diol can be utilised as reaction intermediate to synthesise lipid analogues with modified headgroup functionalities.



Scheme 5.2.6

Selective protection of primary hydroxyl groups can be readily achieved by using the triphenylmethyl (trityl, Trt) group. The trityl group offers stability under basic conditions but is easily removed under mildly acidic conditions. Paaov *et al.* reported the selective protection of **246** to the corresponding diol **250** in the presence

of pyridine.²¹³ Using this method, compound **250** was isolated and purified by flash column chromatography in 57% yield (Scheme 5.2.7). Dietherification of **250** with oleyl mesylate was carried out in anhydrous DMF, using sodium hydride as base, to afford **251** in 38% yield. The moderate yield of **251** could be attributed to unfavourable steric hindrance of the neighbouring trityl groups. Deprotection of **251** was carried out with trifluoroacetic acid (TFA), using triethylsilane (Et₃SiH) as a scavenging agent, to give the diol **248** in 57% yield.²¹⁴ Compound **248** was then converted to its corresponding ditriflate ether **252** using triflic anhydride and DTBP, and was isolated by passing through a short pad (~2 cm) of silica, in near quantitative yield.²¹⁰ The isolated ditriflate was stirred with amine **249** in anhydrous acetone, and subsequently passed through an Amberlite[®] (Cl) ion exchange resin column. ESMS analysis of the crude reaction mixture indicated that a mixture of products was formed. Products with an *m/z* of 428 ($\frac{1}{2}[\text{M}-2\text{Cl}]^+$) could correspond to the desired product **241**, with peaks at 739 ($[\text{M}-\text{Cl}]^+$) and 624 (MH^+) possibly indicating alternative side products **253** and the diol **248**, due to hydrolysis of the triflate. Several attempts were made to isolate **241** by silica column chromatography and reverse phase chromatography but were unsuccessful, since the products in the mixture were amphiphilic and had very similar *R_f* values. It was envisaged that the amine **249** could be hydroxyl-protected and subsequently reacted with **252** to yield the corresponding diquaternised amine **254**, which could be more readily isolated. However, the conversion to **254** was not undertaken due to insufficient time in the last stages of the PhD.



The syntheses of symmetrical dicationic lipids with erythritol and pentaerythritol backbones were explored. A direct synthetic methodology to erythritol lipid **203** with *N,N,N*-trimethylammonium headgroups was established, but the formation of headgroup analogues using an analogous route had failed. Several synthetic routes to headgroup derivatives were then explored; however, the formation of side products and purification problems limited the application of these routes. The synthetic route to pentaerythritol lipid analogue **227** has also been established. It was hoped that the same methodology can be adapted to generate dicationic lipid analogues with modified headgroups. Lipids with conformationally strained headgroups have previously been tested and displayed enhanced gene transfection activity *in vivo* than their open head analogues.⁵⁹ The testing of cyclic lipids **226** and **229a** for lipopolyplex formulations was therefore desirable. These lipids, together with the symmetrical dicationic lipids synthesised, are now being tested for lipopolyplex transfections *in vitro*.

CHAPTER 6

RESULTS AND DISCUSSION

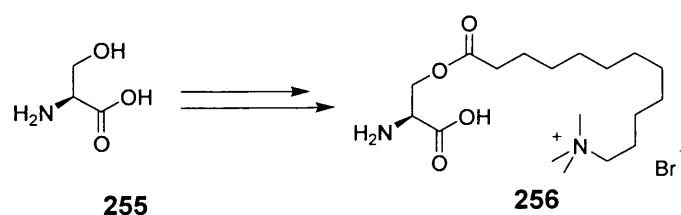
Lipopeptides and Immunoliposomes

6. Lipopeptides and Immunoliposomes

The syntheses of cationic lipids that were utilised in lipopolyplex formulations, together with their transfection results, are described in Chapters 2 to 5. It was demonstrated that the structure of the cytofectin had a significant effect on the activity of the resulting LID complex. Moreover, the targeting capacity provided by the integrin-binding peptide is necessary for high levels of transfection to be achieved.¹⁴⁶ It may therefore be desirable to combine the structural features of the peptide and lipid components, to develop cytofectins that are able to condense and encapsulate the plasmid DNA as well as provide receptor-targeting ability. In this chapter synthetic strategies investigated to generate lipopeptides and PEG-immunoliposomes are outlined.

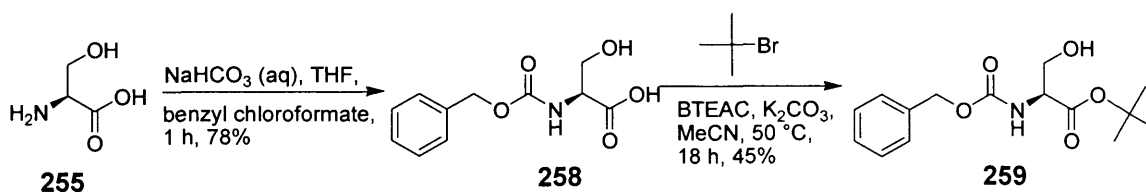
6.1 Lipopeptides

The synthesis of lipopeptides was undertaken to explore the possibility of incorporating an integrin-binding peptide with lipophilic residues attached. The use of (*S*)-serine (**255**) as the lipid anchor was investigated, as it contains three functional groups that can be readily attached to the lipophilic and peptide moieties. In addition, the serine backbone provides a chiral building block, which can be utilised to access stereochemically defined molecules to study the effect of lipid optical activity on transfection activity. Previous preliminary investigations within the group have explored the synthesis of amino acid derivative **256** (Scheme 6.1.1); however, it was noted that **256** was almost completely insoluble in a wide range of organic solvents, making it impossible to use in further reactions. It was therefore desirable to generate soluble derivatives of **256** that could be utilised for the attachment of the peptide moiety.



Scheme 6.1.1

The synthesis of cationic lipophilic amino acid derivative **257** was considered as this provides a cationic lipophilic moiety with an easily cleavable ester linkage (Scheme 6.1.2 & 6.1.3). (*S*)-Serine was initially benzyloxycarbonyl (Cbz) protected by treatment with benzyl chloroformate and aqueous sodium hydrogencarbonate to give **258**, after recrystallisation from chloroform/hexane, in 78% yield.²¹⁵ It was envisaged that subsequent carboxylate protection of **258** as *tert*-butyl (*t*-Bu) ester would provide an orthogonal protection strategy, so that the selective deprotection of the amine could be accomplished at later stage. The conversion of **258** to the *t*-Bu ester **259** was carried out with 2-bromo-2-methyl propane, in the presence of benzyltriethylammonium chloride (BTEAC) and a large excess of potassium carbonate, in 45% yield.²¹⁶ No racemisation was detected during the synthesis of **258** and **259**, as confirmed by comparison of their optical rotations with those reported in the literature (Table 6.1.1).^{217,218}



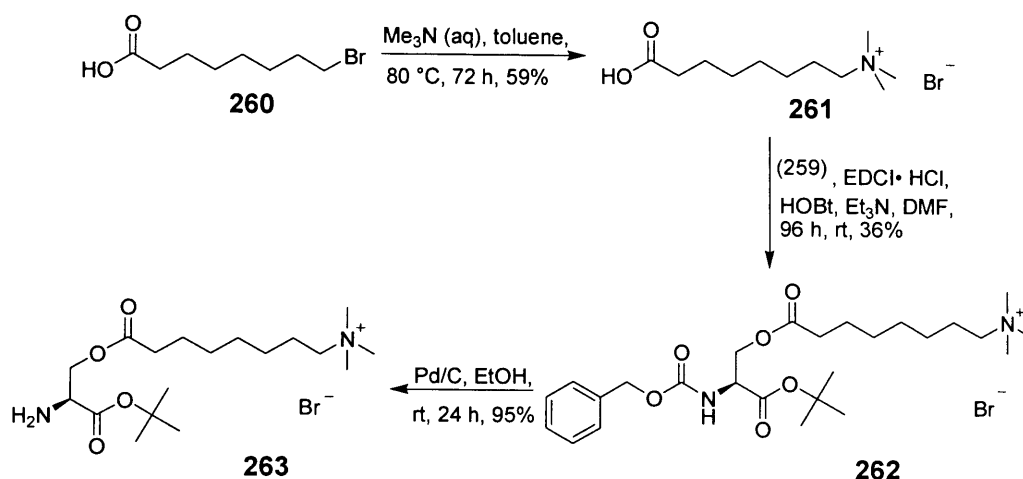
Scheme 6.1.2

Entry	Product, yield (%)	$[\alpha]_D^{15}$ [c, solvent] (lit. value)
1	258 (78)	+2.30 [1.41, MeOH] (+2.45 [0.42, MeOH])
2	259 (45)	-15.5 [1.13, EtOH] (-15.9 [1.10, EtOH])

Table 6.1.1

Initially, the synthesis of ammonium salt **261** was undertaken to provide the starting material for esterification (Scheme 6.1.3). Davey *et al.* have described a methodology for the amination of the bromo acid, $\text{Br}(\text{CH}_2)_{13}\text{CO}_2\text{H}$, by heating with aqueous trimethylamine solution in toluene at 80 °C.²¹⁹ Using this method, 8-bromooctanoic acid (**260**) was successfully converted to the corresponding ammonium salt **261**, which was isolated by recrystallisation in 59% yield. With the ammonium salt in hand, the esterification of **259** and **261** was achieved in the presence of EDCI·HCl, HOBt and triethylamine, to furnish compound **262** in 36% yield. Although the yield of the coupling reaction was not high, this procedure

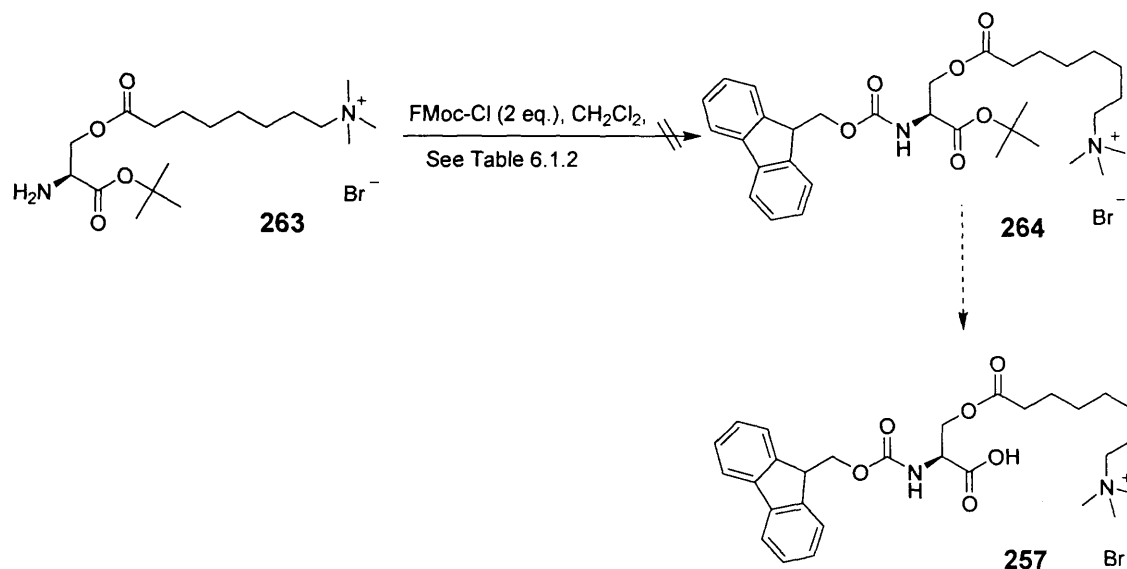
provided a convenient means to remove the urea by-products by aqueous work-up, and the product could be readily isolated and purified by flash column chromatography. Cbz-Deprotection of **262** was achieved by catalytic hydrogenolysis, using 10 mol% of palladium on carbon (Pd/C) under a hydrogen atmosphere. ESMS and ^1H NMR spectroscopic analysis of the crude reaction mixture indicated that deprotection was complete after 24 h. The amine **263** was isolated by passing through a short pad (~2 cm) of Celite[®], and was soluble in a wide range of organic solvents. It was believed that stereochemistry on the serine backbone was conserved during the synthesis, but the optical purities of **262** and **263** were not confirmed at this stage of the investigation.



Scheme 6.1.3

The 9-fluorenylmethyloxycarbonyl (Fmoc) protection of **263** was then explored, as this was required for the production of peptides using solid-phase synthetic methods (Scheme 6.1.3). The conversion of **263** to **264** was initially attempted with Fmoc chloroformate (FmocCl) in anhydrous dichloromethane, using *N*-methylmorphine (NMM) as base (Table 6.1.2, entry 1); however, this failed to give the desired product, as indicated by the TLC and ESMS analysis of the crude mixture. In addition, recovery of the amine **263** by flash column chromatography was also problematical. Attempts to introduce the protecting group using pyridine as base failed to afford **264** (Table 6.1.2, entry 2). The Fmoc-protection of **263** was then attempted using triethylamine as base, however, the formation of **264** was not observed (Table 6.1.2, entry 3). It was thought that **263** might form micellar aggregates in the reaction mixture, thus limiting the availability of its primary amine

for Fmoc-protection. Future synthetic investigations into the production of lipid-amino acid conjugates should focus on preparing derivatives of **257** that can be utilised for solid-phase peptide synthesis.



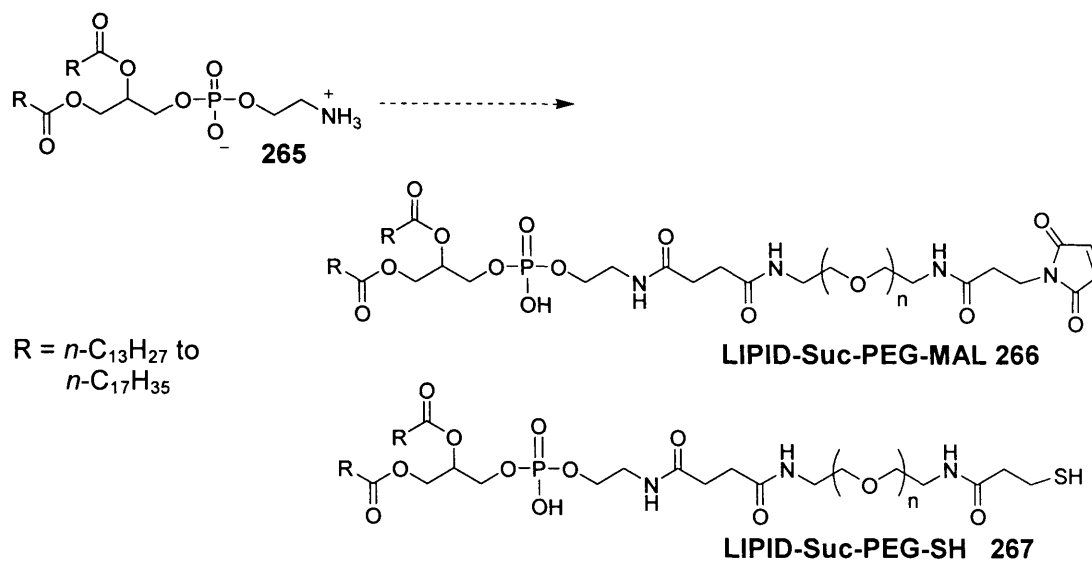
Scheme 6.1.3

Entry	Base (eq)	Conditions
1	NMM (2)	-15 °C→rt, 5 h
2	Pyridine (1.5)	-15 °C→rt, 18 h
3	Et ₃ N (1.5)	0 °C→rt, 24 h

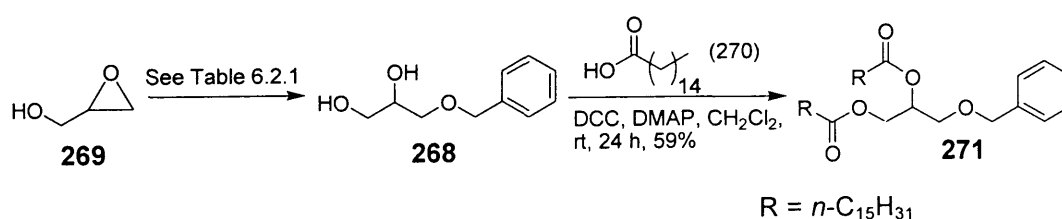
Table 6.1.2

6.2 Immunoliposomes

The synthesis of phospholipid **265** was initially tackled. Although compound **265** is commercially available,²²⁰ due to its high cost a synthetic route to **265** was required before it could be used in subsequent reactions, to generate PEG-phospholipids such as LIPID-Suc-PEG-MAL (**266**) and LIPID-Suc-PEG-SH (**267**) (Scheme 6.2.1). These PEG-phospholipid derivatives have previously been used for the attachment of targeting antibody fragments to generate immunoliposomes. With the synthetic pathway to **265** established, it was hoped that lipid chain length analogues could be synthesised in analogous routes to investigate the effect of lipid chain length on the transfection activity of immunolipoplexes.



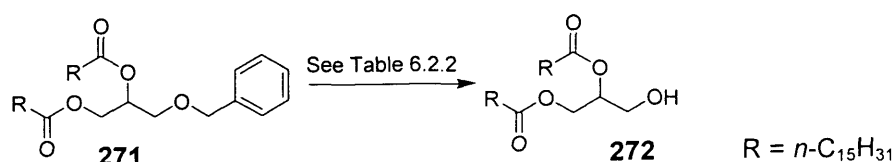
The synthesis of mono-protected glycerol **268** was explored by the ring-opening of (\pm)-glycidol (**269**) with benzyl alcohol, using caesium fluoride as catalyst (Scheme 6.2.2). Following the methodology described by Kitaori *et al.*, the formation of diol **268** was initially attempted using 2 mol% of caesium fluoride;²²¹ however, TLC analysis of the crude reaction mixture indicated that the desired product was not formed (Table 6.2.1, entry 1). The reaction was then repeated using 10 mol% caesium fluoride, but again no trace of **268** was observed (Table 6.2.1, entry 2). Finally, the ring-opening of **269** was carried out using an equimolar amount of caesium fluoride, by stirring the reaction mixture from 24 to 96 hours (Table 6.2.1, entry 3 & 4). The highest yield was obtained when heating the reaction mixture at 120 °C for 96 h, to furnish **268** in 71% yield (Table 6.2.1, entry 4). The acylation of **268** was readily achieved using hexadecanoic acid (**270**), in the presence of *N,N*-dicyclohexylcarbodiimide (DCC) and 4-dimethylaminopyridine (DMAP).²²² The diester derivative **271** was isolated and purified by flash column chromatography in 59% yield (Scheme 6.2.2).



Entry	Epoxide (eq)	Catalyst (eq)	Conditions	Product (yield, %)
1	269 (1)	CsF (0.02)	120 °C, 6 h	—
2	269 (1)	CsF (0.1)	120 °C, 6 h	—
3	269 (1)	CsF (1)	120 °C, 24h	268 (30)
4	269 (1)	CsF (1)	120 °C, 96 h	268 (71)

Table 6.2.1

Several conditions had been explored to carry out the benzyl deprotection of **271** to yield the corresponding alcohol derivative **272** (Scheme 6.2.3). Initially, the removal of the benzyl group was attempted under standard hydrogenolysis conditions (10 mol% Pd/C catalyst, ethanol and a hydrogen atmosphere), but **271** had poor solubility in ethanol, causing it to precipitate out of solution when stirred at room temperature (Table 6.2.2, entry 1). By reviewing the literature it was revealed that Martin *et al.* have carried out the hydrogenolysis of **271** in a mixed solution of acetic acid/ethanol (1:10) at 45 °C.²²³ Using this method, the debenzylation of benzyl ether was re-attempted (Table 6.2.2, entry 2); however, ESMS and ¹H NMR spectroscopic analysis suggested that a complex mixture of products was yielded without the formation of **272**. Removal of the benzyl group was also attempted using the Pearlman's catalyst, but again the formation of **272** was not observed (Table 6.2.2, entry 3). At this stage an alternative strategy for debenzylation was considered. Xia and Hui have reported the successful debenzylation of 3-benzyl-1,2-diacylglycerol derivatives, using boron trichloride at low temperatures.²²⁴ Using this method, the conversion of **271** to **272** was readily achieved in 68% (Table 6.2.2, entry 4). Compound **272** was readily isolated and purified by column chromatography with no undesired acyl migration, as confirmed by NMR analysis of the isolated product.

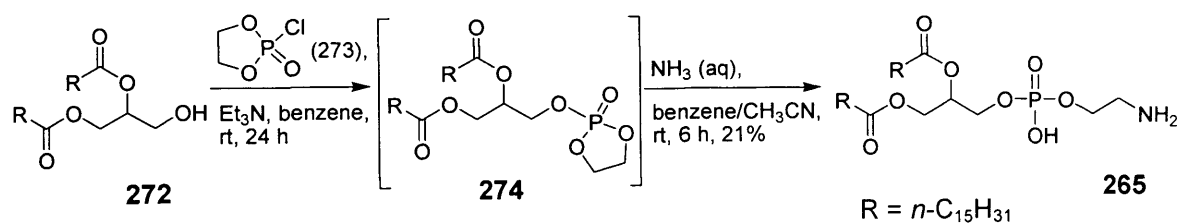


Scheme 6.2.3

Entry	Reagent (eq)	Solvent (ratio)	Conditions	Product (yield, %)
1	Pd/C (0.1)	EtOH	rt, 18 h	—
2	Pd/C (0.1)	EtOH/AcOH (10:1)	45 °C, 96 h	—
3	Pd(OH) ₂ /C (0.1)	EtOH	40 °C, 18h	—
4	BCl ₃ (1)	CH ₂ Cl ₂	-78 °C → rt, 40 min	272 (68)

Table 6.2.2

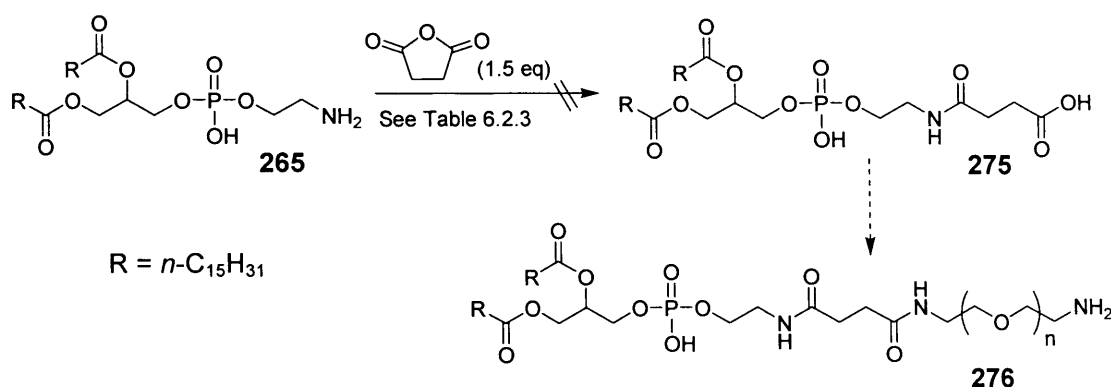
A two-step procedure was then utilised to synthesise the phospholipid **265** (Scheme 6.2.4). Initially, compound **272** was stirred with 2-chloro-2-oxo-1,3,2-dioxaphospholane (**273**) in anhydrous benzene at room temperature, to generate the reaction intermediate **274**.²²⁵ The conversion of **272** to **274** was complete after 24 h, as indicated by TLC analysis of the reaction mixture. The five-membered heterocyclic ring on **274** was then subjected to nucleophilic ring-opening with ammonia in anhydrous benzene/acetonitrile (1:1) mixture. The product **265** was crystallised on cooling and obtained in high yield; however, as flash column chromatography on phospholipids frequently results in losses on recovery, the product yield after column purification was 21%. Compound **265** was a waxy solid and appeared hygroscopic; NMR spectroscopic analysis proved to be difficult as it was almost completely insoluble in all deuterated solvents tested. As a result, only the ¹H NMR spectrum in deuterated methanol was obtained. Nevertheless, ESMS and TLC analysis as well as the melting point of the isolated product, was in good agreement with those reported in the literature, confirming that phospholipid **265** was indeed formed.^{226,227}



Scheme 6.2.4

With the phospholipid **265** in hand, the synthesis of succinimidyl amide **275** was explored, to generate a precursor for preparing PEG-Suc-Lipid **276** (Scheme 6.2.5). Schmitt *et al.* have previously reported a procedure for the generation of Suc-DPPE (**275**) with **265** and succinic anhydride in a mixed solution of

chloroform/methanol (9:1), using triethylamine as base (Table 6.2.3, entry 1).²²⁷ However, TLC and ESMS analysis of the crude reaction mixture indicated that the succinimide **275** was not afforded. The reaction was also investigated using pyridine and DMAP as base, but again the formation of **275** was not observed (Table 6.2.3, entry 2 & 3).



Scheme 6.2.5

Entry	Base (eq)	Solvent (ratio)	Conditions
1	Et ₃ N (1.5)	CHCl ₃ /MeOH (9:1)	rt, 4 h
2	pyridine (1.5)	CHCl ₃ /MeOH (9:1)	rt, 18 h
3	DMAP (1.5)	CHCl ₃ /MeOH (9:1)	rt, 18h

Table 6.2.3

The synthetic investigation of compound **275** was not pursued further due to insufficient time in the last stages of the PhD, but these initial investigations provide a starting point for the preparation of PEG-immunoliposomes. Additionally, the route to **265** should provide access to the chain-length analogues of the phospholipids that can be utilised for the synthesis of immunoliposomes as well as lipopolyplex formulations.

CHAPTER 7

SUMMARY AND FUTURE WORK

7. Summary and Future Work

7.1 Summary

Overall the synthesis and biological activity of cationic lipid analogues have been evaluated. We have demonstrated that the transfection activity of the LID vector is influenced by the structure of the cytofectin utilised. In Chapter 2, we observed structure dependent activity for 1,2-dialkoxy-3-trimethylammonium propane lipids (DOTMA analogues). In particular, the double bond geometry and position on lipid chains had a significant affect on the LID vector transfection activity. The synthesis of optically active lipid analogues was successfully achieved, with enantiomeric dependent activity observed in LID vector transfections. Results from calcein leakage experiments indicated that liposomes containing C16:1 lipid (**136**) were less stable than its C18:1 lipid analogue (DOTMA, **6**) under mildly acidic conditions. In addition, the successful synthesis of fluorescently-labelled lipids was also achieved.

The synthesis and biological activity of novel PEG-lipid conjugates was presented in Chapter 3. We observed that the PEG unit length and lipid chain length influence the LID vector transfection activity *in vitro*. Specifically, a PEG-lipid (**165**) displayed serum resistance compared to its non-PEGylated analogue (**6**), and showed *in vivo* activity superior to a commercial gene transfer reagent. In Chapter 4, the synthesis and lipid stability study of pH-sensitive PEG-lipids bearing acetal linkages have been presented. The PEG chain length, nature of the PEG chains, the spacing of the linkage, and the lipid chain length affect lipid stability under mildly acidic conditions. Hydrolysis studies demonstrated that these lipids are readily degraded at physiological accessible pHs. Furthermore, transfections with several cell types indicated a strong correlation between acid sensitivity of the lipids and LID vector activities *in vitro*.

Investigations into the synthesis of dicationic lipids with erythritol and pentaerythritol backbones were described in Chapter 5. Synthetic routes to dicationic lipids with *N,N,N*-trimethylammonium headgroups have been established. Synthetic routes to lipid-amino acid conjugates and PEG-phospholipids were explored in

Chapter 6. These routes investigated should provide access to lipopeptides and PEG-immunoliposomes for receptor-mediated gene delivery.

7.2 Future Work

We have demonstrated that changes in the structural features of 1,2-dialkoxo-3-trimethylammonium propane lipids significantly affect the efficiencies of lipopolyplex formulations (Chapter 2). An initial calcein leakage study of the lipid analogues has indicated possible liposome-stability dependent activity. It will be desirable to elucidate further the structural and functional requirements of lipid components, by studying various parameters such as the size and zeta potential of the LID vector complexes. The fluorescently-labelled lipids synthesised could be utilised for biophysical studies such as fluorescence quenching and confocal microscopy, to assess the structure and intracellular fate of the LID vector system.

The attachment of short PEG units to a glycerol based backbone produced lipid analogues with increased serum resistance (Chapter 3). For further derivatisation of the lipids, synthesis of methoxy-PEG analogues such as **277** and **278** should be undertaken, to establish possible effect of ‘PEG-capping’ on transfection activity *in vitro* and *in vivo* (Figure 7.2.1).

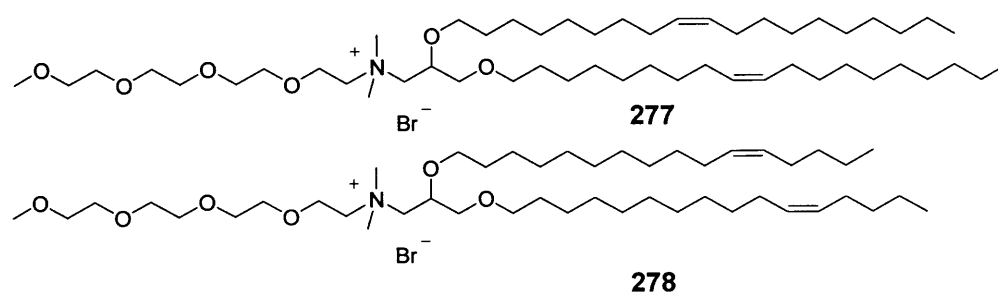
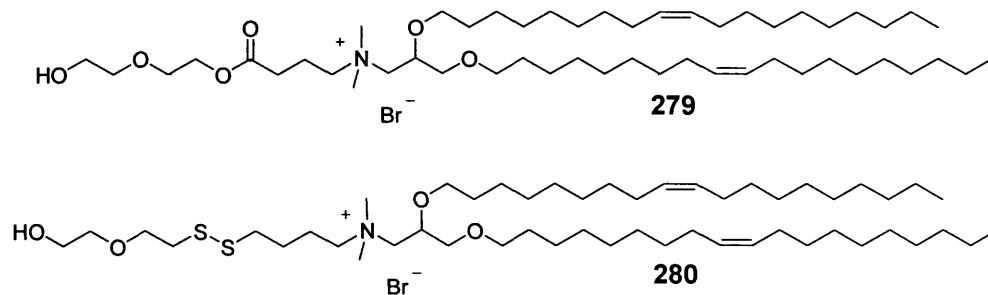
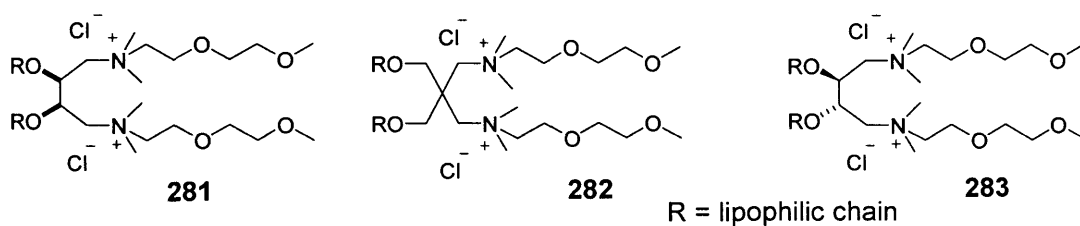


Figure 7.2.1

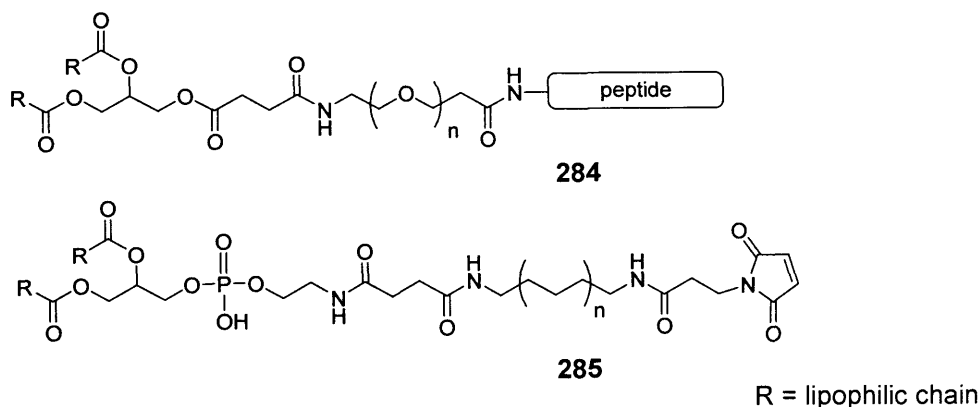
Lipopolyplexes formulated with pH-sensitive PEG-lipid analogues displayed *in vitro* activity similar to or better than that of DOTMA (Chapter 4). The activity of these lipids *in vivo* needs to be established. Fluorescence leakage studies should be utilised to establish the liposomal stability of these lipids when co-formulated with DOPE. PEG-lipid conjugates such as **279** and **280** could be constructed to generate cytofectins that are sensitive to different biological environments (Figure 7.2.2).

**Figure 7.2.2**

The development of an extensive series of dicationic lipid analogues needs to be accomplished (Figure 7.2.3). For example, erythritol and pentaerythritol lipid analogues (**281** and **282**) with methoxy-PEG derivative on the headgroups might provide lipids with increased aqueous solubility, and can be readily isolated and purified by column chromatography. Furthermore, if the synthesis of this structural series proves successful, the formation of lipid chain length analogues along with diastereochemically defined erythritol lipids **283** could be undertaken (Figure 7.2.3).

**Figure 7.2.3**

The investigations of lipopeptides and immunoliposomes are also worth pursuing (Chapter 6). For example, the diacylglycerol derivatives synthesised could be utilised to construct more “lipid-like” lipid-peptide conjugates (**284**) (Figure 7.2.4). Furthermore, the synthesis of phospholipid analogues with a hydrophobic spacer (**285**) will provide information on PEG-dependent activity.

**Figure 7.2.4**

CHAPTER 8

EXPERIMENTAL

8.1 General Experimental Procedure

Chemical and general reagents were purchased from Sigma-Aldrich Co. Ltd., BDH laboratory supplies, Fisher Scientific UK and Lancaster synthesis, and used without further purification. Fluorescent probes were purchased from Molecular Probes Ltd., Oregon Green, USA.

Anhydrous solvents were HPLC grade and distilled over calcium hydride (dichloromethane and toluene), phosphorus pentoxide (acetonitrile), sodium hydroxide pellets (triethylamine), sodium with benzophenone (THF), and 4Å activated molecular sieves (acetone), under a nitrogen atmosphere. Anhydrous benzene, DMF and methanol were purchased distilled from Sigma-Aldrich Co. Ltd. and used without further purification. Ethanol refers to absolute ethanol (>99.7%) and brine refers to saturated sodium chloride solution.

For all air and moisture sensitive reactions, glassware was dried in a hot oven (120 °C) and a nitrogen atmosphere was used.

The term *in vacuo* refers to the removal of solvents by means of evaporation at a reduced pressure, provided by the in-house vacuum or an oil pump, using a Buchi® rotary evaporator.

Thin layer chromatography (TLC) was performed in pre-coated, aluminium backed Merck 60 F₂₅₄ silica plates for normal phase TLC, Merck 60 F₂₅₄ neutral alumina plates for neutral alumina TLC, and Merck RP-18 F₂₅₆ silica plates for reverse-phase TLC. Visualisation was done by absorption of UV light or by dipping with phosphomolybdic acid (PMA) solution [PMA hydride (12 g), conc. sulphuric acid (10 mL), ethanol (250 mL)], potassium permanganate solution [KMnO₄ (1.25 g), Na₂CO₃ (6.25 g), water (250 mL)] and anisaldehyde solution [anisaldehyde (6.00 g), conc. H₂SO₄ (2.50 mL), ethanol (250 mL)]. Normal phase flash chromatography was carried out using silica gel (40-63 µm), and reverse phase flash chromatography was carried out using silicagel 60 silanized (60-200 µm), both supplied by Merck. Flash chromatography on neutral alumina was carried out using aluminium oxides (activated, neutral, Brockmann I) purchased from Sigma-Aldrich Co. Ltd.

Melting points (m.p.) were determined using a gallenkamp apparatus and are uncorrected.

IR spectra were recorded using a FT-IR Shimidazu 8700 instrument. Only selected peaks were reported (cm^{-1}). All UV-vis spectra were recorded using a Shamadzu UV-2401PC spectrophotometer.

^1H NMR and ^{13}C spectra were recorded on Bruker[®] AMX300 MHz, AMX400 MHz and AVANCE500 MHz machines. ^{31}P NMR and ^{19}F NMR were recorded on a Bruker[®] AMX300 MHz machine. The chemical shifts (δ) were given in units ppm relative to tetramethylsilane (TMS), where δ (TMS) = 0 ppm. Coupling constants (J) were measured in Hertz. Multiplicities for ^1H are shown as s (singlet), d (doublet), t (triplet), m (multiplet), or a combination of these. Deuterated chloroform (CDCl_3) solution used to record NMR spectra of acid-sensitive compounds was filtered through basic alumina prior to use.

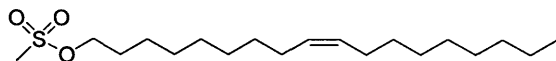
Mass spectra (+ES) were recorded on a Micromass Quattro LC spectroscopy (MassLynx software) (+ES and -ES), a UG70FE (FAB), and a MAT 900XP spectrometer (+HRFAB and +HRES). Major peaks were reported with intensities quoted as percentages of the base peak. Microanalyses were determined using a Perkin Elmer 2400 Elemental Analyser (CHN) and Perkin Elmer 240 Elemental Analyser (halogen). However, for a majority of compounds, the purity was determined by accurate mass spectrometry and NMR spectroscopic analysis.

Optical rotations were recorded on Optical Activity:PolAAR2001 polarimeter at 589 nm and the solvents used are stated when applicable, with concentration (c) in g/100 mL.

For liposome preparations, water (sterile-filtered, cell culture tested) was purchased from Sigma-Aldrich Co. Ltd. Glass vials were sterilised by soaking in ethanol for 5 min and subsequently heated at 140 °C for 2 h. A Kerry sonicator was used to produce the lipid vesicles.

8.2 Synthesis of DOTMA

(Z)-Octadec-9-enyl mesylate (**93**)¹⁵²



A solution of (Z)-octadec-9-en-1-ol (2.35 g, 7.45 mmol) and methanesulfonyl chloride (0.58 mL, 7.45 mmol) in anhydrous dichloromethane (30 mL) was stirred at rt for 30 min. After cooling to 0 °C, triethylamine (1.57 mL, 11.2 mmol) was added dropwise and the mixture stirred at rt for 18 h. Dichloromethane (20 mL) was added, and the mixture washed with water (20 mL), saturated sodium hydrogencarbonate solution (20 mL) and brine (20 mL), dried over magnesium sulfate, and then concentrated *in vacuo*. Purification by flash chromatography on silica (50% dichloromethane in hexane) yielded the titled compound as a pale yellow oil (2.90 g, 81%).

R_f 0.70 (dichloromethane);

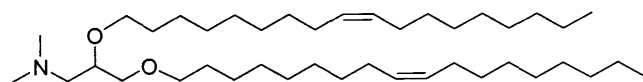
ν_{\max} (neat)/ cm^{-1} 2926s, 1466m, 1356m;

δ_H (300 MHz; CDCl_3) 0.88 (3H, t, J 6.9 Hz, CH_3) 1.27-1.30 (22H, m), 1.74 (2H, m, OCH_2CH_2), 2.00 (4H, m, $\text{CH}_2\text{CH}=\text{CHCH}_2$), 3.01 (3H, s, CH_3SO_2), 4.22 (2H, t, J 6.6 Hz, OCH_2), 5.37 (2H, m, $\text{CH}=\text{CH}$);

δ_C (75.4 MHz; CDCl_3) 14.5 (CH_3), 23.1, 25.8, 27.6 (overlap), 29.4, 29.5, 29.6, 29.7, 29.9, 30.0, 30.1, 30.2, 32.3, 37.8 (CH_3SO_2), 70.5 (OCH_2CH_2), 130.1 and 130.4 ($\text{CH}=\text{CH}$);

m/z (+ES) 347 (MH^+ , 100%).

2,3-Di-[(Z)-octadec-9-enyloxy]propyl-*N,N*-dimethylamine (**94**)¹⁵¹



Sodium hydride (60%; 0.38 g, 10.1 mmol) was stirred in anhydrous toluene (20 mL) at rt for 15 min. 3-(Dimethylamino)propane-1,2-diol (**37**) (0.40 g, 3.36 mmol) was added and the mixture stirred at 50 °C for 30 min. After addition of the mesylate **93** (3.20g, 10.1 mmol), the reaction mixture was heated at reflux for 72 h. Water (30 mL)

was added and the product extracted with ethyl acetate (3×20 mL), the combined organic extracts were washed with saturated sodium hydrogencarbonate (25 mL) and brine (25 mL), dried over magnesium sulfate, and then concentrated *in vacuo*. Purification by flash chromatography on silica (5% methanol in dichloromethane) yielded the titled compound as a pale yellow oil (1.13 g, 57%).

R_f 0.38 (5% methanol in dichloromethane);

ν_{\max} (neat)/ cm^{-1} 2925s, 2854m, 1459m;

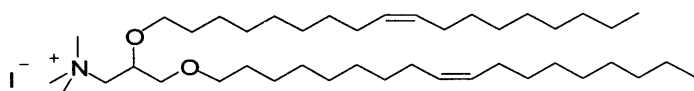
δ_H (300 MHz; CDCl_3) 0.86 (6H, t, J 7.3 Hz, CH_3CH_2) 1.15–1.33 (44H, m), 1.48 (4H, m, $2 \times \text{OCH}_2\text{CH}_2$), 1.93 (8H, m, $2 \times \text{CH}_2\text{CH}=\text{CHCH}_2$), 2.27 (6H, s, $\text{N}(\text{CH}_3)_2$), 2.33 (2H, m, NCH_2CH), 3.32–3.67 (7H, m, CHOCH_2 , CH_2OCH_2), 5.35 (4H, m, $2 \times \text{CH}=\text{CH}$);

δ_C (75.4 MHz; CDCl_3) 14.4 (CH_3CH_2), 23.1, 26.3, 27.6, 29.4–30.7 (signal overlap), 32.3, 46.7 ($\text{N}(\text{CH}_3)_2$), 61.5 (NCH_2CH), 70.6 (CHCH_2O), 72.1 and 72.5 (OCH_2CH_2), 77.3 (CHOCH_2), 130.1 and 130.3 ($\text{CH}=\text{CH}$);

m/z (+HRFAB) 620.6333 (MH^+ , $\text{C}_{41}\text{H}_{82}\text{NO}_2$ requires 620.6346);

m/z (+ES) 621 (MH^+ , 100%).

2,3-Di-[(*Z*)-octadec-9-enyloxy]propyl-*N,N,N*-trimethylammonium iodide (95)¹⁵¹



The amine **94** (0.10 g, 0.18 mmol) and iodomethane (2.50 mL) were stirred in a sealed tube at rt for 12 h. Excess iodomethane was evaporated *in vacuo*. Purification by flash chromatography on silica (5% methanol in dichloromethane) yielded the titled compound as a yellow oil (0.12 g, 97%).

R_f 0.35 (5% methanol in dichloromethane);

ν_{\max} (neat)/ cm^{-1} 2925s, 2854s, 1459m;

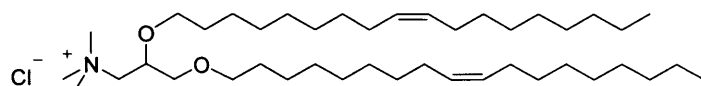
δ_H (300 MHz; CDCl_3) 0.87 (6H, m, $2 \times \text{CH}_3\text{CH}_2$) 1.20–1.35 (44H, m), 1.54 (4H, m, $2 \times \text{OCH}_2\text{CH}_2$), 2.01 (8H, m, $2 \times \text{CH}_2\text{CH}=\text{CHCH}_2$), 3.42 (4H, t, J 6.8 Hz, $2 \times \text{OCH}_2\text{CH}_2$), 3.47 (9H, s, $\text{N}^+(\text{CH}_3)_3$), 3.55–3.72 (3H, m, $\text{CHCH}_2\text{OCH}_2$), 4.05 (2H, m, N^+CH_2), 5.35 (4H, m, $2 \times \text{CH}=\text{CH}$);

δ_{C} (75.4 MHz; CDCl_3) 14.0 (CH_3CH_2), 23.0, 26.5, 27.6, 29.5-30.6 (signal overlap), 32.3, 33.0, 55.6 ($\text{N}^+(\text{CH}_3)_3$), 68.5 (N^+CH_2), 70.6 and 72.5 ($\text{CHCH}_2\text{OCH}_2$, CHOCH_2 ; overlap), 73.3 (CHCH_2O), 130.3 and 130.7 ($\text{CH}=\text{CH}$);

m/z (+HRFAB) 634.6479 ($[\text{M}-\text{I}]^+$, $\text{C}_{42}\text{H}_{84}\text{NO}_2$ requires 634.6502);

m/z (+ES) 635 ($[\text{M}-\text{I}]^+$, 100%).

2,3-Di-[(Z)-octadec-9-enyloxy]propyl-*N,N,N*-trimethylammonium chloride (6)³⁷



The iodide salt **95** (0.10 g, 0.13 mmol) was passed through an Amberlite[®] IRA- 400 (Cl) ion exchange column eluting with dichloromethane/methanol (1:1). The solvents were removed *in vacuo* to give the titled compound as a pale yellow oil (82 mg, 95%).

R_f =0.35 (5% methanol in ethyl acetate);

ν_{max} (neat)/ cm^{-1} 2924s, 2854s, 1465w;

δ_{H} (300 MHz; CDCl_3) 0.88 (6H, m, $2 \times \text{CH}_3\text{CH}_2$) 1.20-1.35 (44H, m), 1.60 (4H, m, $2 \times \text{OCH}_2\text{CH}_2$), 2.03 (8H, m, $2 \times \text{CH}_2\text{CH}=\text{CHCH}_2$), 3.40-3.52 (13H, m, $2 \times \text{OCH}_2\text{CH}_2$, $\text{N}^+(\text{CH}_3)_3$), 3.54-3.75 (3H, m, CHOCH_2 , $\text{CHCH}_2\text{OCH}_2$), 4.08 (2H, m, N^+CH_2), 5.37 (4H, m, $2 \times \text{CH}=\text{CH}$);

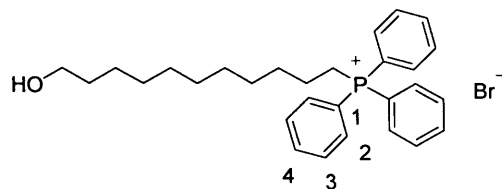
δ_{C} (75.4 MHz; CDCl_3) 14.0 (CH_3CH_2), 22.3, 26.1, 27.2, 29.3-30.2 (signal overlap), 32.3, 33.0, 55.6 ($\text{N}^+(\text{CH}_3)_3$), 68.4 (N^+CH_2), 70.3, 72.2 and 73.0 (CHCH_2O , CHCH_2O , OCH_2CH_2 ; overlap), 130.1 and 130.5 ($\text{CH}=\text{CH}$);

Anal. ($\text{C}_{42}\text{H}_{84}\text{ClNO}_2 \cdot \text{H}_2\text{O}$) found C, 73.59; H, 12.41; N, 1.89; Cl, 5.77; requires C, 75.26; H, 12.59; N, 2.03; Cl, 5.15;

m/z (ES+) 634.79 ($[\text{M}-\text{Cl}]^+$, 100%);

8.3 Synthesis of DHTMA Analogues

(11-Hydroxyundecyl)triphenylphosphonium bromide (**96**)¹⁵³



A solution of 11-bromo-1-undecanol (20.0 g, 79.2 mmol) and triphenylphosphine (20.9 g, 79.2 mmol) in methanol (60 mL) was heated at reflux for 18 h. The solvent was removed *in vacuo* and the product recrystallised from acetone to give the titled compound as a white solid (33.4 g, 82%).

m.p. 88 °C (acetone) (lit., 90-91 °C);¹⁵³

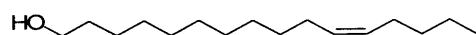
ν_{\max} (chloroform)/ cm^{-1} 3364m, 2932s, 2866m, 1709w;

δ_{H} (300 MHz; CDCl_3) 1.19-1.25 (16H, m), 1.47-1.61 (4H, m, $\text{P}^+\text{CH}_2\text{CH}_2\text{CH}_2$), 3.60 (2H, t, J 6.5 Hz, CH_2OH), 7.68-7.75 (15H, m, $3 \times \text{Ph}$);

δ_{C} (75.4 MHz; CDCl_3) 23.0, 23.6, 26.0, 29.4, 29.6, 29.6, 29.7, 30.6, 30.8, 33.1, 63.1 (CH_2OH), 118.2 and 119.4 (C-1), 130.8 and 131.0 (C-2), 134.0 and 134.1 (C-3), 135.4 (C-4; overlap);

m/z (+ES) 433 ($[\text{M}-\text{Br}]^+$, 100%).

(*Z*)-Hexadec-11-en-1-ol (**98**) *via* Wittig Route¹⁵³



The phosphonium salt **96** (2.00 g, 3.90 mmol) and sodium hexamethyldisilylamide (1 M in THF; 7.80 mL, 7.80 mmol) were stirred at rt for 2 h. After cooling to -78 °C, pentanal (0.90 mL, 3.90 mmol) was added and the mixture stirred at this temperature for 5 h. Hexane (20 mL) and dichloromethane (20 mL) were added, and the mixture washed with hydrochloric acid solution (1 M, 20 mL) and brine (50 mL), dried over magnesium sulfate, and then concentrated *in vacuo*. Purification by flash chromatography on silica (50% dichloromethane in hexane) yielded the titled compound as a yellow oil (0.55 g, 59%).

cis:trans; 9:1 (determined by ^1H NMR);

R_f 0.25 (dichloromethane);

ν_{max} (neat)/ cm^{-1} 3333br s, 2925, 1665w;

δ_{H} (300 MHz; CDCl_3) 0.90 (3H, t, J 6.8 Hz, CH_3) 1.19-1.57 (20H, m), 2.02 (4H, m, $\text{CH}_2\text{CH}=\text{CHCH}_2$), 3.62 (2H, t, J 6.6 Hz, CH_2OH), 5.35 (2H, m, $\text{CH}=\text{CH}$);

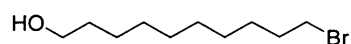
δ_{C} (75.4 MHz; CDCl_3) 14.3 (CH_3), 22.7, 26.1, 27.3, 27.6, 28.4, 29.4, 29.8, 29.9, 30.0, 30.1, 32.4, 33.2, 63.5 (CH_2OH), 130.3 ($\text{CH}=\text{CH}$; overlap);

m/z (+ES) 241 (MH^+ , 20%), 55 (100).

General procedure for preparing bromo alcohols

A solution of the diol (1 eq) and aqueous hydrobromic acid solution (48%; 1.2 eq) in toluene was heated at reflux for 48-72 h. The mixture was neutralised by saturated sodium hydrogencarbonate and the product extracted with dichloromethane (3 \times 50 mL). The combined organic extracts were washed with brine (100 mL), dried over magnesium sulfate, and then concentrated *in vacuo*.

10-Bromodecan-1-ol (102)¹⁵⁹



The above procedure was carried out using the following quantities: 1,10-decandiol (9.00 g, 51.7 mmol), aqueous hydrobromic acid (10.45 mL, 62.0 mmol) and toluene (180 mL), for 48 h. Purification by dry-column flash chromatography on silica (30% diethyl ether in hexane) yielded the titled compound as a yellow oil (10.4 g, 85%).

R_f 0.60 (30% diethyl ether in hexane);

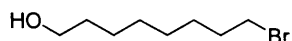
ν_{max} (neat)/ cm^{-1} 3395br s, 2927s;

δ_{H} (300 MHz; CDCl_3) 1.26-1.44 (12H, m), 1.55 (2H, tt, J 6.6, 6.8 Hz, $\text{CH}_2\text{CH}_2\text{OH}$), 1.85 (2H, tt, J 6.9, 7.2 Hz, $\text{CH}_2\text{CH}_2\text{Br}$), 3.41 (2H, t, J 6.9 Hz, CH_2Br), 3.64 (2H, t, J 6.6 Hz, CH_2OH);

δ_{C} (75.4 MHz; CDCl_3) 25.5, 28.1, 28.5, 29.4, 30.1, 30.5, 32.7 ($\text{CH}_2\text{CH}_2\text{OH}$), 32.9 (CH_2Br), 33.8 ($\text{CH}_2\text{CH}_2\text{Br}$), 62.9 (CH_2OH);

m/z (+ES) 239 ($MH^+[^{81}Br]$, 97%), 237 ($MH^+[^{79}Br]$, 100%).

8-Bromooctan-1-ol (109)¹⁵⁹



The above procedure was carried out using the following quantities: 1,8-octandiol (8.00 g, 54.8 mmol), aqueous hydrobromic acid (11.1 mL, 65.8 mmol) and toluene (160 mL), for 72 h. Purification by dry-column flash chromatography on silica (30% diethyl ether in hexane) yielded the titled compound as a yellow oil (10.5 g, 92%).

R_f 0.60 (30% diethyl ether in hexane);

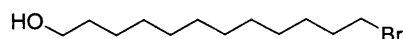
ν_{max} (neat)/ cm^{-1} 3394br s, 2926s;

δ_H (300 MHz; $CDCl_3$) 1.21-1.59 (10H, m), 1.86 (2H, tt, J 6.9, 7.1 Hz, CH_2CH_2Br), 3.40 (2H, t, J 6.9 Hz, CH_2Br), 3.64 (2H, t, J 6.7 Hz, CH_2OH);

δ_C (75.4 MHz; $CDCl_3$) 25.5, 28.4, 29.4, 30.4, 32.4 (CH_2CH_2OH), 32.8 (CH_2Br), 33.7 (CH_2CH_2Br), 63.0 (CH_2OH);

m/z (+ES) 212 ($MH^+[^{81}Br]$, 100%), 210 ($MH^+[^{79}Br]$, 100%).

12-Bromododecan-1-ol (113)¹⁵⁹



The above procedure was carried out using the following quantities: 1,12-dodecandiol (5.00 g, 24.8 mmol), aqueous hydrobromic acid (5.00 mL, 29.7 mmol) and toluene (160 mL), for 72 h. Purification by flash chromatography on silica (30% diethyl ether in hexane) yielded the titled compound as a yellow oil (5.41 g, 83%).

R_f 0.60 (30% ether in hexane);

ν_{max} (neat)/ cm^{-1} 3418br s, 2928s;

δ_H (300 MHz; $CDCl_3$) 1.18-1.45 (16H, m), 1.57 (2H, m, CH_2CH_2OH), 1.85 (2H, tt, J 6.9, 7.3 Hz, CH_2CH_2Br), 3.41 (2H, t, J 6.9 Hz, CH_2Br), 3.64 (2H, t, J 6.6 Hz, CH_2OH);

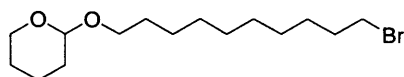
δ_C (75.4 MHz; $CDCl_3$) 25.9, 26.6, 27.4, 28.7, 29.4, 30.0, 30.4, 32.2, 32.6 (CH_2CH_2OH), 33.2 (CH_2Br), 34.0 (CH_2CH_2Br), 62.5 (CH_2OH);

m/z (+ES) 290 ($MH^+[^{81}Br]$, 96%), 288 ($MH^+[^{79}Br]$, 100%).

General procedure for THP-protection of bromo alcohols

To a solution of bromo alcohol (1 eq) and 3,4-dihydro-2H-pyran (1.2 eq) were stirred in anhydrous dichloromethane at rt. *p*-Toluenesulfonic acid monohydrate (*p*TsOH·H₂O) (0.1 eq) was added and the mixture stirred at rt for 18 h. Dichloromethane (100 mL) was added and the mixture washed with water (80 mL), saturated sodium hydrogencarbonate solution (80 mL) and brine (80 mL), dried over magnesium sulfate, and then concentrated *in vacuo*.

2-(10-Bromodecyloxy)-tetrahydro-2H-pyran (103)²²⁸



The above procedure was carried out using the following quantities: alcohol **102** (10.0 g, 42.4 mmol), 3,4-dihydro-2H-pyran (4.55 mL, 50.83 mmol), *p*TsOH·H₂O (0.81 g, 4.24 mmol) and dichloromethane (67 mL). Purification by dry-column flash chromatography on silica (5% ethyl acetate in hexane) yielded the titled compound as a yellow oil (10.7 g, 79%).

R_f 0.29 (5% ethyl acetate in hexane);

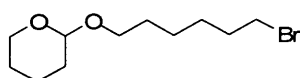
ν_{max} (neat)/cm⁻¹ 2924s, 1120m, 1035s;

δ_H (300 MHz; CDCl₃) 1.30-1.91 (22H, m), 3.41 (3H, m, OCHH, BrCH₂), 3.53 (1H, m, OCHH), 3.75 (1H, m, OCHH), 3.89 (1H, m, OCHH), 4.60 (1H, m, OCHO);

δ_C (75.4 MHz; CDCl₃) 20.1, 25.9, 26.6, 27.4, 28.0, 28.6, 29.1, 29.8, 30.1, 31.2, 32.2 (CH₂CH₂Br), 34.3 (CH₂Br), 62.7 (OCH₂), 68.1 (THPOCH₂), 99.3 (OCHO);

m/z (+ES) 345 ($[M(^{81}Br)+Na]^+$, 95%), 343 ($[M(^{79}Br)+Na]^+$, 100%).

2-(8-Bromooctyloxy)-tetrahydro-2H-pyran (110)²²⁹



The above procedure was carried out using the following quantities: alcohol **109** (10.5 g, 50.2 mmol), 3,4-dihydro-2H-pyran (5.39 mL, 60.3 mmol), *p*TsOH·H₂O

(0.95 g, 5.02 mmol) and dichloromethane (200 mL). Purification by flash chromatography on silica (5% ethyl acetate in hexane) yielded the titled compound as a yellow oil (10.8 g, 73%).

R_f 0.30 (5% ethyl acetate in hexane);

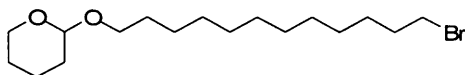
ν_{\max} (neat)/ cm^{-1} 2924s, 1119m, 1034s;

δ_H (300 MHz; CDCl_3) 1.33-1.90 (18H, m), 3.38 (3H, m, OCHH, CH_2Br), 3.50 (1H, m, OCHH), 3.73 (1H, m, OCHH), 3.85 (1H, m, OCHH), 4.57 (1H, t, J 3.5 Hz, OCHO);

δ_C (75.4 MHz; CDCl_3) 19.7, 24.3, 25.5, 26.1, 27.5, 28.7, 29.7, 30.9, 32.8 ($\text{CH}_2\text{CH}_2\text{Br}$), 36.0 (CH_2Br), 62.4 (OCH_2), 67.6 (THPOCH_2), 98.9 (OCHO);

m/z (+ES) 318 ($[\text{M}(^{81}\text{Br})+\text{Na}]^+$, 95%), 316 ($[\text{M}(^{79}\text{Br})+\text{Na}]^+$, 100%).

2-(12-Bromododecyloxy)-tetrahydro-2H-pyran (114)²³⁰



The above procedure was carried out using the following quantities: alcohol **113** (6.53 g, 24.8 mmol), 3,4-dihydro-2H-pyran (2.66 mL, 29.7 mmol), $p\text{TsOH}\cdot\text{H}_2\text{O}$ (0.47 g, 2.48 mmol) and dichloromethane (130 mL). Purification by flash chromatography on silica (5% ethyl acetate in hexane) yielded the titled compound as a colourless oil (5.46 g, 63%).

R_f 0.35 (5% ethyl acetate in hexane);

ν_{\max} (neat)/ cm^{-1} 2937s, 1135m, 1035s;

δ_H (300 MHz; CDCl_3) 1.27-1.70 (24H, m), 1.84 (2H, m, BrCH_2CH_2), 3.38 (3H, m, OCHH, BrCH_2), 3.50 (1H, m, OCHH), 3.73 (1H, m, OCHH), 3.96 (1H, m, OCHH), 4.57 (1H, m, OCHO);

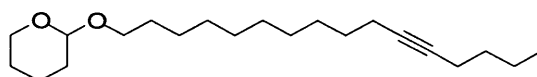
δ_C (75.4 MHz; CDCl_3) 19.7, 25.5, 26.2, 28.2, 28.7, 29.5, 29.8, 30.1, 32.9 ($\text{CH}_2\text{CH}_2\text{Br}$), 33.9 (BrCH_2), 62.3 (OCH_2), 67.7 (THPOCH_2), 98.8 (OCHO);

m/z (+ES) 349.33 ($\text{MH}^+[^{79}\text{Br}]$, 100%).

General procedure for alkyne coupling to THP-protected bromides

A solution of the alkyne (1.6 eq) in anhydrous THF and hexamethylphosphoramide (HMPA) was cooled to -10 °C. *n*-Butyllithium (*n*BuLi) (2.5 M solution in hexane; 1.9 eq) was added dropwise and the mixture stirred for 2 h. THP-protected bromide (1 eq) in anhydrous THF was added dropwise, and the mixture stirred at rt for 18 h. Water (40 mL) and saturated ammonium chloride solution (40 mL) were added, and the product extracted with dichloromethane (2 × 50 mL), the combined organic extracts washed with brine (50 mL), dried over magnesium sulfate, and then concentrated *in vacuo*.

2-(Hexadec-11-ynoxy)tetrahydro-2H-pyran (**104**)²³¹



The above procedure was carried out using the following quantities: 1-hexyne (2.80 mL, 25.0 mmol), THF (20 mL), HMPA (5 mL), *n*BuLi (11.9 mL, 29.7 mmol), and bromide **103** (5.00 g, 15.6 mmol) in THF (10 mL). Purification by flash chromatography on silica (10% ethyl acetate in hexane) yielded the titled compound as a pale yellow oil (3.78 g, 75%).

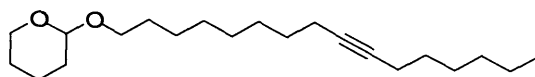
R_f 0.40 (10% ethyl acetate in hexane);

ν_{\max} (neat)/ cm^{-1} 2925s, 2134w, 1121m, 1035m;

δ_H (300 MHz; CDCl_3) 0.91 (3H t, J 6.4 Hz, CH_3), 1.22-1.83 (26H, m), 2.13 (4H, m, $\text{CH}_2\text{C}\equiv\text{CCH}_2$), 3.37 (1H, m, OCHH), 3.50 (1H, m, OCHH), 3.72 (1H, m, OCHH), 3.85 (1H, m, OCHH), 4.58 (1H, m, OCHO);

δ_C (75.4 MHz; CDCl_3) 14.0 (CH_3), 18.8, 19.1, 20.1, 25.9, 26.5, 29.1, 29.9, 30.2, 31.2, 31.7, 62.7 (OCH_2), 68.1 (THPOCH₂), 80.4 and 80.5 ($\text{C}\equiv\text{C}$), 99.5 (OCHO);

m/z (+ES) 345 ($[\text{M}+\text{Na}]^+$, 100%).

2-(Hexadec-9-ynyloxy)tetrahydro-2H-pyran (111)²³²

The above procedure was carried out using the following quantities: 1-octyne (5.00 mL, 25.6 mmol), THF (14.0 mL), HMPA (4.2 mL), *n*BuLi (12.2 mL, 30.7 mmol), and bromide **110** (5.00 g, 17.1 mmol) in THF (14 mL). Purification by flash chromatography on silica (10% ethyl acetate in hexane) yielded the titled compound as a pale yellow oil (4.06 g, 74%).

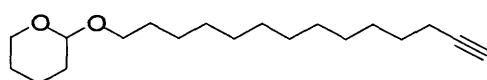
R_f 0.40 (10% ethyl acetate in hexane);

ν_{max} (neat)/cm⁻¹ 2925s, 1120m, 1034s;

δ_H (300 MHz; CDCl₃) 0.88 (3H t, *J* 6.9 Hz, CH₃CH₂), 1.22-1.82 (26H, m), 2.13 (4H, m, CH₂C≡CCH₂), 3.38 (1H, m, OCHH), 3.49 (1H, m, OCHH), 3.73 (1H, m, OCHH), 3.87 (1H, m, OCHH), 4.57 (1H, m, OCHO);

δ_C (75.4 MHz; CDCl₃) 14.2 (CH₃), 18.6, 19.0, 19.9, 25.6, 26.4, 29.2, 29.9, 30.1, 31.1, 31.8, 62.6 (OCH₂), 68.5 (THPOCH₂), 80.5 and 81.1 (C≡C), 99.7 (OCHO);

m/z (+ES) 346 ([M+Na]⁺, 100%).

2-(Tetradec-13-ynyloxy)tetrahydro-2H-pyran (115)¹⁶²

Lithium acetylide-ethylenediamine complex (0.14 g, 1.55 mmol) in anhydrous DMSO (1 mL) was stirred at 0 °C for 10 min. A solution of bromide **114** (0.40 g, in 1.15 mmol) in DMSO (1 mL) was added dropwise, and the mixture stirred at rt for 72 h. Water (10 mL) was added, the product extracted with dichloromethane (10 mL) and ethyl acetate (10 mL), and the combined organic extracts washed with brine (20 mL), dried over magnesium sulfate, and then concentrated *in vacuo*. Purification by flash chromatography on silica (10% ethyl acetate in hexane) yielded the titled compound as a colourless oil (0.20 g, 60%).

R_f 0.35 (5% ethyl acetate in hexane);

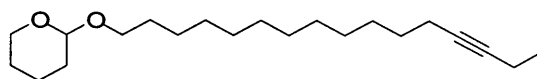
ν_{max} (neat)/cm⁻¹ 3312m, 2926s, 1121w, 1023w;

δ_{H} (300 MHz; CDCl_3) 1.25-1.84 (26H, m), 1.92 (1H, t, J 2.6 Hz, $\text{C}\equiv\text{CH}$), 2.16 (2H, dt, J 2.6, 7.1 Hz, $\text{CH}_2\text{C}\equiv\text{CH}$), 3.39 (1H, m, OCHH), 3.49 (1H, m, OCHH), 3.71 (1H, m, OCHH), 3.86 (1H, m, OCHH), 4.57 (1H, t, J 4.4 Hz, OCHO);

δ_{C} (75.4 MHz; CDCl_3) 18.4, 19.7, 25.6, 26.3, 28.6, 28.8, 29.1, 29.2, 29.4, 29.9, 30.3, 31.2, 30.9, 62.3 (OCH_2), 66.4 ($\text{C}\equiv\text{CH}$), 67.7 (THPOCH_2), 84.7 ($\text{C}\equiv\text{CH}$), 98.9 (OCHO);

m/z (+ES) 296 (MH^+ , 100%).

2-(Hexadec-13-ynoxy)tetrahydro-2H-pyran (116)



A solution of alkyne **115** (2.50 mL, 8.49 mmol) in anhydrous THF (16 mL) and HMPA (1.8 mL) was cooled to -10°C . $n\text{BuLi}$ (2.5 M solution in hexane; 5.09 mL, 12.7 mmol) was added dropwise and mixture stirred for 2 h. Bromoethane (0.95 mL, 12.7 mmol) in anhydrous THF (16 mL) was added dropwise, and the mixture stirred at rt for 18 h. Water (40 mL) and saturated ammonium chloride solution (40 mL) were added and the product extracted with dichloromethane (2×50 mL), the combined organic extracts washed with brine (50 mL), dried over magnesium sulfate, and then concentrated *in vacuo*. Purification by flash chromatography on silica (10% ethyl acetate in hexane) yielded *the titled compound* as a pale yellow oil (2.25 g, 82%).

R_f 0.40 (10% ethyl acetate in hexane);

ν_{max} (neat)/ cm^{-1} 2925s, 1121m, 1034m;

δ_{H} (400 MHz; CDCl_3) 1.08 (3H m, CH_3CH_2), 1.20-1.87 (26H, m), 2.16 (4H, m, $\text{CH}_2\text{C}\equiv\text{CCH}_2$), 3.37 (1H, m, OCHH), 3.50 (1H, m, OCHH), 3.72 (1H, m, OCHH), 3.86 (1H, m, OCHH), 4.57 (1H, m, OCHO);

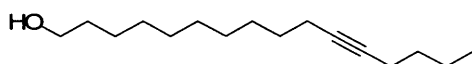
δ_{C} (75.4 MHz; CDCl_3) 12.4 (CH_3CH_2), 14.4 (CH_3), 18.7, 19.0, 19.7, 25.5, 26.3, 28.9-30.8 (signal overlap), 31.1, 62.3 (OCH_2), 67.7 (THPOCH_2), 80.3 and 80.5 ($\text{C}\equiv\text{C}$), 98.8 (OCHO);

m/z (+ES) 345 ($[\text{M}+\text{Na}]^+$, 100%).

General procedure for THP deprotection

THP-protected alcohol (1 eq) was stirred in concentrated HCl/water/methanol (1:1:5) solution at rt for 24 h. Water (100 mL) was added and the product extracted with dichloromethane (3×50 mL), the combined organic extracts washed with brine (75 mL), dried over magnesium sulfate, and then concentrated *in vacuo*.

Hexadec-11-yn-1-ol (99)¹⁶⁰



The above procedure was carried out using the following quantities: **104** (3.78 g, 11.7 mmol) and concentrated HCl/water/methanol (165 mL). Purification by flash chromatography on silica (dichloromethane) yielded the titled compound as a pale yellow oil (2.09 g, 75%).

R_f 0.25 (dichloromethane);

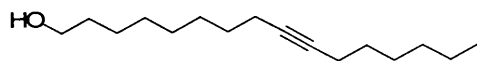
ν_{\max} (neat)/ cm^{-1} 3333br m, 2927s, 2245w;

δ_H (300 MHz; CDCl_3) 0.91 (3H t, J 6.8 Hz, CH_3), 1.22-1.63 (20H, m), 2.14 (4H, m, $\text{CH}_2\text{C}\equiv\text{CHCH}_2$), 3.64 (2H, t, J 6.6 Hz, CH_2OH);

δ_C (75.4 MHz; CDCl_3) 14.0 (CH_3), 18.8, 19.1, 22.3, 26.1, 29.2, 29.5, 29.6, 29.7, 29.8, 29.9, 31.7, 33.2, 63.5 (CH_2OH), 80.1 and 80.4 ($\text{C}\equiv\text{C}$);

m/z (+ES) 261 ($[\text{M}+\text{Na}]^+$, 40%), 147 (100%).

Hexadec-9-yn-1-ol (108)²³³



The above procedure was carried out using the following quantities: **111** (4.00 g, 12.4 mmol) and concentrated HCl/water/methanol (182 mL). Purification by flash chromatography on silica (dichloromethane) yielded the titled compound as a colourless oil (2.68 g, 91%).

R_f 0.25 (dichloromethane);

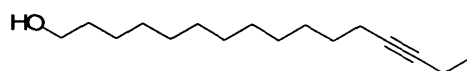
ν_{\max} (neat)/ cm^{-1} 3387 br s, 2931 m, 2212w;

δ_{H} (300 MHz; CDCl_3) 0.89 (3H t, J 6.8 Hz, CH_3CH_2), 1.26-1.60 (20H, m), 2.14 (4H, m, $\text{CH}_2\text{C}\equiv\text{CHCH}_2$), 3.64 (2H, t, J 6.6 Hz, CH_2OH);

δ_{C} (75.4 MHz; CDCl_3) 14.0 (CH_3), 18.8, 22.6, 24.4, 25.7, 28.5, 28.8, 29.1, 29.3, 30.2, 31.4, 32.8, 36.0, 63.1 (CH_2OH), 80.3 and 80.6 ($\text{C}\equiv\text{C}$);

m/z (+ES) 261 ($[\text{M}+\text{Na}]^+$, 100%).

Hexadec-13-yn-1-ol (117)²³⁴



The above procedure was carried out using the following quantities: **116** (2.25 g, 6.98 mmol) and concentrated HCl/water/methanol (98 mL). Purification by flash chromatography on silica (dichloromethane) yielded the titled compound as a pale yellow oil (1.58g, 70%).

R_f 0.25 (dichloromethane);

ν_{max} (neat)/ cm^{-1} 3387 br s, 2931 m, 2243m;

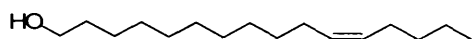
δ_{H} (300 MHz; CDCl_3) 0.89 (3H t, J 7.4 Hz, CH_3CH_2), 1.19-1.56 (20H, m), 2.15 (4H, m, $\text{CH}_2\text{C}\equiv\text{CHCH}_2$), 3.64 (2H, t, J 6.6 Hz, CH_2OH);

δ_{C} (75.4 MHz; CDCl_3) 12.5 (CH_3CH_2), 14.4 (CH_3), 18.7, 25.7, 28.7, 29.1-29.9 (signal overlap), 32.7, 63.1 (CH_2OH), 80.0 and 80.3 ($\text{C}\equiv\text{C}$);

m/z (+ES) 239 (MH^+ , 100%).

General procedure for *cis*-reduction

A solution of alkynyl alcohol (1 eq), quinoline (1.2 eq) and Lindlar catalyst (0.1 eq) in ethanol was vigorously stirred under a hydrogen atmosphere at rt for 18 h. The mixture was filtered through Celite[®] and then concentrated *in vacuo*. The crude residue was dissolved in ethyl acetate (30 mL), washed with aqueous hydrochloric acid solution (1 M, 20 mL) and brine (20 mL), dried over magnesium sulfate, and then concentrated *in vacuo*.

(Z)-Hexadec-11-en-1-ol (98)¹⁵⁶ via Reduction Route

The above procedure was carried out using the following quantities: alkyne **99** (0.40 g, 1.68 mmol), quinoline (0.24 mL, 2.02 mmol), Lindlar catalyst (0.03 g), and ethanol (5 mL). Purification by flash chromatography on silica (dichloromethane) yielded the titled compound as a colourless oil (0.23 g, 56%).

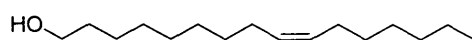
R_f 0.25 (dichloromethane);

ν_{max} (neat)/cm⁻¹ 3332br m, 2925s, 1652 w;

δ_H (300 MHz; CDCl₃) 0.89 (3H, t, *J* 6.9 Hz, CH₃) 1.26-1.57 (20H, m), 2.01 (4H, m, CH₂CH=CHCH₂), 3.62 (2H, t, *J* 6.6 Hz, CH₂OH), 5.34 (2H, t, *J* 4.9 Hz, CH=CH);

δ_C (75.4 MHz; CDCl₃) 14.0 (CH₃), 22.3, 27.0, 27.2, 27.7, 28.9, 29.4, 29.5, 29.6, 29.8, 32.0, 32.8, 32.8, 63.0 (CH₂OH), 129.9 (CH=CH; overlap);

m/z (+ES) 241 (MH⁺, 100%).

(Z)-Hexadec-9-en-1-ol (106)²³⁵

The above procedure was carried out using the following quantities: alkyne **108** (1.20 g, 5.04 mmol), quinoline (0.72 mL, 6.05 mmol), Lindlar catalyst (0.10 g), and ethanol (10 mL). Purification by flash chromatography on silica (dichloromethane) yielded the titled compound as a colourless oil (0.65 g, 53%).

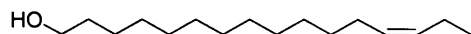
R_f 0.25 (dichloromethane);

ν_{max} (neat)/cm⁻¹ 3332br m, 2925s, 1651w;

δ_H (300 MHz; CDCl₃) 0.90 (3H, t, *J* 6.9 Hz, CH₃) 1.19-1.60 (20H, m), 2.01 (4H, m, CH₂CH=CHCH₂), 3.64 (2H, t, *J* 6.6 Hz, CH₂OH), 5.35 (2H, m, CH=CH);

δ_C (75.4 MHz; CDCl₃) 14.0 (CH₃), 22.7, 26.1, 27.5, 27.6, 28.4, 29.6, 29.8, 29.9, 30.0, 30.1, 32.4, 33.1, 63.4 (CH₂OH), 130.2 (CH=CH; overlap);

m/z (+ES) 241 (MH⁺, 100%).

(Z)-Hexadec-13-en-1-ol (118)²³⁶

The above procedure was carried out using the following quantities: alkyne **117** (0.90 g, 3.78 mmol), quinoline (0.54 mL, 4.54 mmol), Lindlar catalyst (0.08 g), and ethanol (10 mL). Purification by flash chromatography on silica (dichloromethane) yielded the titled compound as a colourless oil (0.75 g, 83%).

R_f 0.25 (dichloromethane);

ν_{\max} (neat)/ cm^{-1} 3332br m, 2926s, 1653w;

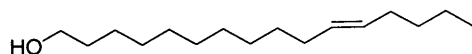
δ_H (300 MHz; CDCl_3) 0.94 (3H, t, 7.5 Hz, CH_3) 1.15-1.37 (18H, m), 1.50 (2H, m, $\text{CH}_2\text{CH}_2\text{OH}$), 2.02 (4H, m, $\text{CH}_2\text{CH}=\text{CHCH}_2$), 3.63 (2H, t, J 6.6 Hz, CH_2OH), 5.31 (2H, m, $\text{CH}=\text{CH}$);

δ_C (75.4 MHz; CDCl_3) 14.4 (CH_3), 25.7, 27.1, 29.3-29.8 (signal overlap), 32.8, 63.1 (CH_2OH), 129.4 ($\text{HC}=\text{CH}$; overlap);

m/z (+ES) 241 (MH^+ , 100%).

General procedure for *trans*-reduction

To a solution of lithium aluminium hydride (LiAlH_4 ; 3.5 eq) in anhydrous diglyme at -10°C was added dropwise alkynyl alcohol (1 eq) in diglyme. The mixture was heated at 140°C for 72 h. Ethyl acetate (20 mL) and water (40 mL) were added, and the product extracted with diethyl ether (3×30 mL). The combined organic extracts were washed with saturated sodium hydrogencarbonate (60 mL), water (60 mL) and brine (60 mL), dried over magnesium sulfate, and then evaporated *in vacuo*.

(E)-Hexadec-11-en-1-ol (100)¹⁶⁰

The above procedure was carried out using the following quantities: LiAlH_4 (0.22 g, 5.88 mmol), diglyme (5 mL), and alkyne **99** (0.40 g, 1.68 mmol) in diglyme (1 mL). Purification by flash chromatography on silica (dichloromethane) yielded the titled compound as a pale yellow oil (0.20 g, 51%).

R_f 0.25 (dichloromethane);

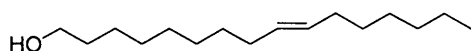
ν_{\max} (neat)/ cm^{-1} 3314br m, 2924s, 1675w;

δ_{H} (300 MHz; CDCl_3) 0.88 (3H, t, J 6.9 Hz, CH_3) 1.18-1.51 (20H, m), 2.03 (4H, m, $\text{CH}_2\text{CH}=\text{CHCH}_2$), 3.64 (2H, t, J 6.6 Hz, CH_2OH), 5.38 (2H, t, J 4.9 Hz, $\text{CH}=\text{CH}$);

δ_{C} (75.4 MHz; CDCl_3) 14.0 (CH_3), 22.7, 26.1, 27.2, 27.5, 28.5, 29.4, 29.8, 29.9, 30.1, 30.2, 32.2, 33.3, 63.4 (CH_2OH), 130.0 ($\text{CH}=\text{CH}$; overlap);

m/z (+ES) 241 (MH^+ , 100%).

(*E*)-Hexadec-9-en-1-ol (107)²³⁷



The above procedure was carried out using the following quantities: LiAlH_4 (0.56 g, 14.7 mmol), diglyme (13 mL), and alkyne **108** (1.00 g, 4.20 mmol) in diglyme (2 mL). Purification by flash chromatography on silica (dichloromethane) yielded the titled compound as a pale yellow oil (0.55 g, 54%).

R_f 0.25 (dichloromethane);

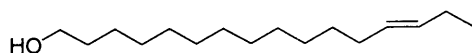
ν_{\max} (neat)/ cm^{-1} 3332br m, 2925s, 1674w;

δ_{H} (300 MHz; CDCl_3) 0.90 (3H, t, J 6.9 Hz, CH_3) 1.19-1.60 (20H, m), 2.02 (4H, m, $\text{CH}_2\text{CH}=\text{CHCH}_2$), 3.64 (2H, t, J 6.6 Hz, CH_2OH), 5.38 (2H, m, $\text{CH}=\text{CH}$);

δ_{C} (75.4 MHz; CDCl_3) 14.1 (CH_3), 22.7, 24.4, 25.7, 27.2, 29.9, 29.2, 29.7, 32.8, 63.0 (CH_2OH), 130.2 ($\text{CH}=\text{CH}$; overlap);

m/z (+ES) 241 (MH^+ , 100%).

(*E*)-Hexadec-13-en-1-ol (119)²³⁸



The above procedure was carried out using the following quantities: LiAlH_4 (0.38 g, 10.0 mmol), diglyme (7 mL), and alkyne **117** (0.68 g, 2.86 mmol) in diglyme (2 mL). Purification by flash chromatography on silica (dichloromethane) yielded the titled compound as a pale yellow oil (0.48 g, 70%).

R_f 0.25 (dichloromethane);

ν_{\max} (neat)/ cm^{-1} 3334br m, 2924s, 1674m;

δ_{H} (300 MHz; CDCl_3) 0.95 (3H, t, J 7.4 Hz, CH_3), 1.19-1.37 (18H, m), 1.54 (2H, m, $\text{CH}_2\text{CH}_2\text{OH}$), 1.96 (4H, m, $\text{CH}_2\text{CH}=\text{CHCH}_2$), 3.56 (2H, t, J 6.6 Hz, CH_2OH), 5.39 (2H, m, $\text{CH}=\text{CH}$);

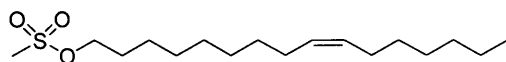
δ_{C} (75.4 MHz; CDCl_3) 14.4 (CH_3), 25.6, 26.0, 29.2-29.7 (signal overlap), 32.6, 63.1 (CH_2OH), 129.4 and 130.0 ($\text{HC}=\text{CH}$; overlap);

m/z (+ES) 241 (MH^+ , 100%).

General procedure for mesylation

A solution of alcohol (1 eq) and methanesulfonyl chloride (1.2 eq) in anhydrous dichloromethane was stirred at rt for 30 min. After cooling to 0 °C, triethylamine (1.5 eq) was added dropwise, and the mixture stirred at rt for 18 h. Dichloromethane (20 mL) was added and the mixture washed with water (30 mL), saturated sodium hydrogencarbonate solution (30 mL) and brine (30 mL), dried over magnesium sulfate, and then concentrated *in vacuo*.

(Z)-Hexadec-9-enyl methanesulfonate (120)²³⁵

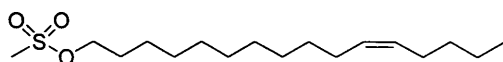


The above procedure was carried out using the following quantities: alcohol **106** (0.77 g, 3.20 mmol), methanesulfonyl chloride (0.30 mL, 3.83 mmol), dichloromethane (15 mL) and triethylamine (0.68 mL, 4.80 mmol). Purification by flash chromatography on silica (50% hexane in dichloromethane) yielded the titled compound as a pale yellow oil (0.72 g, 71%).

R_f 0.73 (dichloromethane);

δ_{H} (300 MHz; CDCl_3) 0.90 (3H, m, CH_3CH_2), 1.38 (18H, m), 1.75 (2H, m, OCH_2CH_2), 2.02 (4H, m, $\text{CH}_2\text{CH}=\text{CHCH}_2$), 2.99 (3H, s, CH_3SO_2), 4.23 (2H, t, J 6.8 Hz, OCH_2), 5.34 (2H, m, $\text{CH}=\text{CH}$);

m/z (+ES) 319 (MH^+ , 100%).

(Z)-Hexadec-11-enyl methanesulfonate (121)²³⁵

The above procedure was carried out using the following quantities: alcohol **98** (0.80 g, 3.30 mmol), methanesulfonyl chloride (0.31 mL, 4.00 mmol), dichloromethane (15 mL) and triethylamine (0.70 mL, 5.00 mmol). Purification by flash chromatography on silica (50% dichloromethane in hexane) yielded the titled compound as a pale yellow oil (0.54 g, 48%).

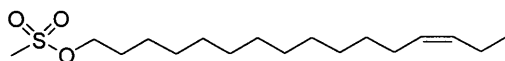
R_f 0.65 (dichloromethane);

ν_{max} (neat)/cm⁻¹ 2927s, 1736w, 1056br w;

δ_H (300 MHz; CDCl₃) 0.90 (3H, t, *J* 6.9 Hz, CH₃CH₂), 1.36 (18H, m), 1.73 (2H, m, OCH₂CH₂), 2.01 (4H, m, CH₂CH=CHCH₂), 3.00 (3H, s, CH₃SO₂), 4.23 (2H, t, *J* 6.7 Hz, OCH₂), 5.35 (2H, m, CH=CH);

δ_C (75.4 MHz; CDCl₃) 14.3 (CH₃CH₂), 22.7, 26.1, 27.3, 27.6, 28.4, 29.2-30.1 (signal overlap), 32.4, 37.8 (CH₃SO₂), 70.5 (CH₂O), 130.3 (CH=CH; overlap);

m/z (+ES) 319 (MH⁺, 100%).

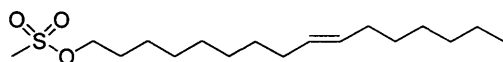
(Z)-Hexadec-13-enyl methanesulfonate (122)

The above procedure was carried out using the following quantities: alcohol **118** (0.65 g, 2.70 mmol), methanesulfonyl chloride (0.25 mL, 3.24 mmol), dichloromethane (10 mL) and triethylamine (0.57 mL, 4.06 mmol). Purification by flash chromatography on silica (50% dichloromethane in hexane) yielded the titled compound as a colourless oil (0.51 g, 60%).

R_f 0.76 (dichloromethane);

δ_H (300 MHz; CDCl₃) 0.89 (3H, t, *J* 7.3 Hz, CH₃CH₂), 1.33 (18H, m), 1.74 (2H, m, OCH₂CH₂), 2.04 (4H, m, CH₂CH=CHCH₂), 3.01 (3H, s, CH₃SO₂), 4.24 (2H, t, *J* 6.7 Hz, OCH₂), 5.34 (2H, m, CH=CH);

m/z (+ES) 319 (MH⁺, 100%).

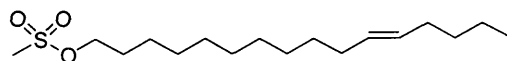
(E)-Hexadec-9-enyl methanesulfonate (123)

The above procedure was carried out using the following quantities: alcohol **107** (0.48 g, 1.99 mmol), methanesulfonyl chloride (0.18 mL, 2.40 mmol), dichloromethane (10 mL) and triethylamine (0.42 mL, 3.00 mmol). Purification by flash chromatography on silica (50% dichloromethane in hexane) yielded *the titled compound* as a colourless oil (0.54 g, 48%).

R_f 0.70 (dichloromethane);

δ_H (300 MHz; $CDCl_3$) 0.89 (3H, m, CH_3CH_2), 1.38 (18H, m), 1.75 (2H, m, OCH_2CH_2), 2.02 (4H, m, $CH_2CH=CHCH_2$), 2.99 (3H, s, CH_3SO_2), 4.23 (2H, t, J 6.8 Hz, OCH_2), 5.38 (2H, m, $HC=CH$);

m/z (+ES) 319 (MH^+ , 100%).

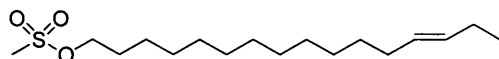
(E)-Hexadec-11-enyl methanesulfonate (124)

The above procedure was carried out using the following quantities: alcohol **100** (0.68 g, 2.82 mmol), methanesulfonyl chloride (0.33 mL, 4.32 mmol), dichloromethane (12 mL) and triethylamine (0.60 mL, 4.32 mmol). Purification by flash chromatography on silica (50% dichloromethane in hexane) yielded *the titled compound* as a colourless oil (0.60 g, 76%).

R_f 0.75 (dichloromethane);

δ_H (300 MHz; $CDCl_3$) 0.90 (3H, m, CH_3CH_2), 1.38 (18H, m), 1.75 (2H, m, OCH_2CH_2), 2.02 (4H, m, $CH_2CH=CHCH_2$), 2.98 (3H, s, CH_3SO_2), 4.23 (2H, t, J 6.8 Hz, OCH_2), 5.38 (2H, m, $CH=CH$);

m/z (+ES) 319 (MH^+ , 100%).

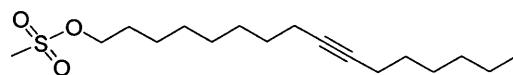
(E)-Hexadec-13-enyl methanesulfonate (125)

The above procedure was carried out using the following quantities: alcohol **119** (0.65 g, 2.70 mmol), methanesulfonyl chloride (0.25 mL, 3.24 mmol), dichloromethane (10 mL) and triethylamine (0.57 mL, 4.06 mmol). Purification by flash chromatography on silica (50% dichloromethane in hexane) yielded *the titled compound* as a colourless oil (0.47 g, 55%).

R_f 0.75 (dichloromethane);

δ_H (300 MHz; $CDCl_3$) 0.90 (3H, m, CH_3CH_2), 1.34 (18H, m), 1.75 (2H, m, OCH_2CH_2), 2.02 (4H, m, $CH_2CH=CHCH_2$), 2.99 (3H, s, CH_3SO_2), 4.23 (2H, t, J 6.8 Hz, OCH_2), 5.37 (2H, m, $CH=CH$);

m/z (+ES) 319 (MH^+ , 100%).

Hexadec-9-ynyl methanesulfonate (126)

The above procedure was carried out using the following quantities: alcohol **108** (0.50 g, 2.10 mmol), methanesulfonyl chloride (0.20 mL, 2.50 mmol), dichloromethane (10 mL) and triethylamine (0.44 mL, 3.20 mmol). Purification by flash chromatography on silica (50% dichloromethane in hexane) yielded *the titled compound* as a colourless oil (0.51 g, 91%).

R_f 0.67 (dichloromethane);

δ_H (300 MHz; $CDCl_3$) 0.90 (3H, m, CH_3CH_2), 1.38 (18H, m), 1.76 (2H, m, OCH_2CH_2), 2.12 (4H, m, $CH_2C\equiv CHCH_2$), 3.01 (3H, s, CH_3SO_2), 4.24 (2H, t, J 6.9 Hz, OCH_2);

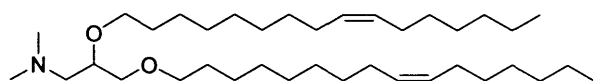
m/z (+ES) 317 (MH^+ , 100%).

General procedure for dietherification

Sodium hydride (60%; 3 eq) was stirred in anhydrous toluene at rt for 15 min. 3-(Dimethylamino)propane-1,2-diol (1 eq) was added and the mixture stirred at 50 °C

for 30 min. After addition of the selected mesylate (**120-126**, 2.5-3 eq), the reaction mixture was heated at reflux for 72 h. Water (15 mL) was added and the product extracted with ethyl acetate (3 × 20 mL), the combined organic extracts washed with saturated sodium hydrogencarbonate (25 mL) and brine (25 mL), dried over magnesium sulfate, and then concentrated *in vacuo*.

2,3-Di-[(*Z*)-hexadec-9-enyloxy]propyl-*N,N*-dimethylamine (**128**)



The above procedure was carried out using the following quantities: sodium hydride (90 mg, 2.26 mmol), toluene (5 mL), diol **37** (0.11 g, 0.91 mmol), and mesylate **120** (0.72 g, 2.26 mmol). Purification by flash chromatography on silica (5% methanol in dichloromethane) yielded *the titled compound* as a pale yellow oil (0.22 g, 44%).

R_f 0.38 (5% methanol in dichloromethane);

ν_{max} (neat)/cm⁻¹ 2926s, 2856s, 1119br m, 1042m;

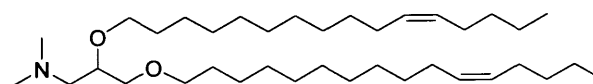
δ_H (300 MHz; CDCl₃) 0.87 (6H, t, *J* 6.9 Hz, 2 × CH₃CH₂) 1.19-1.40 (36H, m), 1.53 (4H, m, 2 × OCH₂CH₂), 2.01 (8H, m, 2 × CH₂CH=CHCH₂), 2.33 (6H, s, N(CH₃)₂), 2.50 (2H, m, NCH₂CH), 3.39-3.62 (7H, m, CH₂OCH₂, CH₂OCH₂), 5.35 (4H, m, 2 × CH=CH);

δ_C (75.4 MHz; CDCl₃) 14.0 (CH₃CH₂), 22.3, 26.1, 26.9, 27.2, 27.3, 29.3–30.2 (signal overlap), 32.0, 46.0 (N(CH₃)₂), 60.9 (NCH₂CH), 70.1 and 71.7 (CHCH₂O, OCH₂CH₂; overlap), 76.8 (CHCH₂O), 129.8 and 129.9 (CH=CH);

m/z (+HRFAB) 564.5723 (MH⁺, C₃₇H₇₄NO₂ requires 564.5714);

m/z (+ES) 565 (MH⁺, 80%).

2,3-Di-[(*Z*)-hexadec-11-enyloxy]propyl-*N,N*-dimethylamine (**129**)¹⁵¹



The above procedure was carried out using the following quantities: sodium hydride (75 mg, 1.88 mmol), toluene (5 mL), diol **37** (75 mg, 0.63 mmol), and mesylate **121**

(0.50 g, 1.57 mmol). Purification by flash chromatography on silica (5% methanol in dichloromethane) yielded *the titled compound* as a pale yellow oil (0.12 g, 34%).

R_f 0.38 (5% methanol in dichloromethane);

ν_{max} (neat)/cm⁻¹ 2924s, 2818s, 1630w, 1118br m, 1042m;

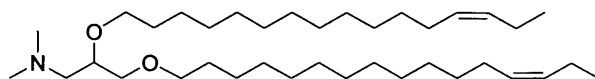
δ_H (300 MHz; CDCl₃) 0.85 (6H, t, *J* 6.9 Hz, 2 × CH₃CH₂) 1.20-1.40 (36H, m), 1.55 (4H, m, 2 × OCH₂CH₂), 2.05 (8H, m, 2 × CH₂CH=CHCH₂), 2.34 (6H, s, N(CH₃)₂), 2.48 (2H, m, NCH₂CH), 3.45-3.67 (7H, m, CHOCH₂, CH₂OCH₂), 5.34 (4H, m, 2 × CH=CH);

δ_C (75.4 MHz; CDCl₃) 14.3 (CH₃CH₂), 22.2, 22.4, 26.2, 26.9, 27.2, 29.3-30.2 (signal overlap), 31.9, 32.0, 46.1 (N(CH₃)₂), 61.0 (NCH₂CH), 70.2 (CHCH₂O), 71.7 and 71.8 (OCH₂CH₂), 77.0 (CHOCH₂), 129.9 (CH=CH; overlap);

***m/z* (+HRFAB)** 564.5718 (MH⁺, C₃₇H₇₄NO₂ requires 564.5720);

***m/z* (+ES)** 565 (MH⁺, 35%), 613 (100%);

2,3-Di-[(*Z*)-hexadec-13-enyloxy]propyl-*N,N*-dimethylamine (130)



The above procedure was carried out using the following quantities: sodium hydride (0.14 g, 3.34 mmol), toluene (7 mL), diol **37** (0.14 g, 1.13 mmol), and mesylate **122** (0.90 g, 2.83 mmol). Purification by flash chromatography on silica (5% methanol in dichloromethane) yielded *the titled compound* as a pale yellow oil (0.07 g, 11%).

R_f 0.38 (5% methanol in dichloromethane);

ν_{max} (neat)/cm⁻¹ 2924s, 2853s, 1654w, 1187br m, 1044m;

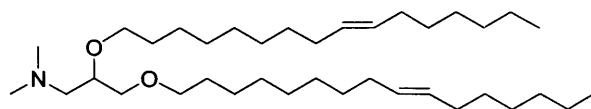
δ_H (300 MHz; CDCl₃) 0.96 (6H, m, 2 × CH₃CH₂) 1.18-1.40 (36H, m), 1.54 (4H, m, 2 × OCH₂CH₂), 2.01 (8H, m, 2 × CH₂CH=CHCH₂), 2.30 (6H, s, N(CH₃)₂), 2.46 (2H, m, NCH₂CH), 3.31-3.65 (7H, m, CHOCH₂, CH₂OCH₂), 5.36 (4H, m, 2 × CH=CH);

δ_C (75.4 MHz; CDCl₃) 14.0 (CH₃CH₂), 22.4, 26.0, 27.4, 28.3, 29.2-30.1 (signal overlap), 31.1, 32.2, 46.1 (N(CH₃)₂), 61.0 (NCH₂CH), 70.2 (CHCH₂O), 71.6 and 71.8 (OCH₂CH₂), 76.8 (CHCH₂O), 130.3 and 130.4 (CH=CH; overlap);

m/z (+HRES) 564.5723 (MH^+ , $C_{37}H_{74}NO_2$ requires 564.5720);

m/z (+ES) 565 (MH^+ , 32%), 613 (100%).

2,3-Di-[(*E*)-hexadec-9-enyloxy]propyl-*N,N*-dimethylamine (131)



The above procedure was carried out using the following quantities: sodium hydride (53 mg, 1.32 mmol), toluene (6 mL), diol **37** (63 mg, 0.53 mmol), and mesylate **123** (0.42 g, 1.32 mmol). Purification by flash chromatography on silica (5% methanol in dichloromethane) yielded *the titled compound* as a pale yellow oil (60 mg, 20%).

R_f 0.40 (5% methanol in dichloromethane);

ν_{\max} (neat)/ cm^{-1} 2925s, 2853s, 1687w, 1121br m, 1042m;

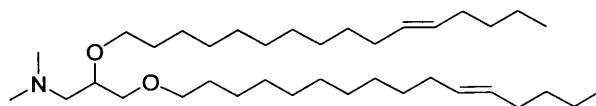
δ_H (300 MHz; $CDCl_3$) 0.87 (6H, t, J 6.6 Hz, $2 \times CH_3CH_2$) 1.27 (36H, m), 1.55 (4H, m, $2 \times OCH_2CH_2$), 1.96 (8H, m, $2 \times CH_2CH=CHCH_2$), 2.29 (6H, s, $N(CH_3)_2$), 2.43 (2H, t, J 5.6 Hz, NCH_2CH), 3.40-3.62 (7H, m, $CHOCH_2$, CH_2OCH_2), 5.38 (4H, m, $2 \times CH=CH$);

δ_C (75.4 MHz; $CDCl_3$) 14.1 (CH_3CH_2), 22.7, 26.2, 28.9, 29.1–30.2 (signal overlap), 31.8, 32.6, 46.2 ($N(CH_3)_2$), 61.0 (NCH_2CH), 70.2 ($CHCH_2O$), 71.6 and 71.9 (OCH_2CH_2), 77.2 ($CHOCH_2$), 130.3 and 130.4 ($CH=CH$);

m/z (+HRFAB) 564.5703 (MH^+ , $C_{37}H_{74}NO_2$ requires 564.5714);

m/z (+ES) 565 (MH^+ , 36%), 613 (100%).

2,3-Di-[(*E*)-hexadec-11-enyloxy]propyl-*N,N*-dimethylamine (132)



The above procedure was carried out using the following quantities: sodium hydride (77 mg, 1.93 mmol), toluene (5 mL), diol **37** (92 mg, 0.77 mmol), and mesylate **132** (0.54 g, 1.70 mmol). Purification by flash chromatography on silica (5% methanol in dichloromethane) yielded *the titled compound* as a pale yellow oil (43 mg, 25%).

R_f 0.38 (5% methanol in dichloromethane);

ν_{\max} (neat)/cm⁻¹ 2926s, 2856s, 1121br m, 1042m;

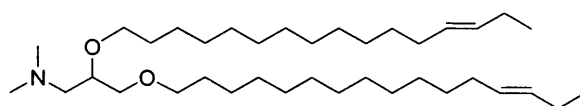
δ_{H} (300 MHz; CDCl₃) 0.89 (6H, m, 2 × CH₃CH₂) 1.20-1.43 (36H, m), 1.55 (4H, m, 2 × OCH₂CH₂), 1.96 (8H, m, 2 × CH₂CH=CHCH₂), 2.28 (6H, s, N(CH₃)₂), 2.42 (2H, m, NCH₂CH), 3.40-3.62 (7H, m, CHOCH₂, CH₂OCH₂), 5.37 (4H, m, 2 × CH=CH);

δ_{C} (75.4 MHz; CDCl₃) 14.1 (CH₃CH₂), 22.7, 26.2, 28.8, 29.2–30.3 (signal overlap), 31.6, 32.6, 46.1 (N(CH₃)₂), 61.1 (NCH₂CH), 70.2 (CHCH₂O), 71.7 and 71.9 (OCH₂CH₂), 77.3 (CHOCH₂), 130.0 and 130.3 (CH=CH);

m/z (+HRFAB) 564.5713 (MH⁺, C₃₇H₇₄NO₂ requires 564.5720);

m/z (+ES) 565 (MH⁺, 100%).

2,3-Di-[(*E*)-hexadec-13-enyloxy]propyl-*N,N*-dimethylamine (133)



The above procedure was carried out using the following quantities: sodium hydride (0.14 g, 3.34 mmol), toluene (10 mL), diol **37** (0.14 g, 1.13 mmol), and mesylate **125** (1.10 g, 3.34 mmol). Purification by flash chromatography on silica (5% methanol in dichloromethane) yielded *the titled compound* as a pale yellow oil (0.12 g, 19%).

R_f 0.35 (5% methanol in ethyl acetate);

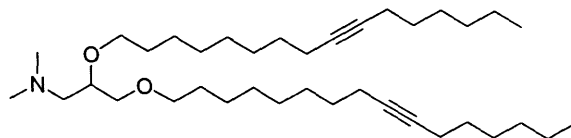
ν_{\max} (neat)/cm⁻¹ 2925s, 2818s, 1685w, 1185br m, 1043m;

δ_{H} (300 MHz; CDCl₃) 0.90 (6H, t, *J* 7.4 Hz, 2 × CH₃CH₂) 1.15-1.38 (36H, m), 1.53 (4H, m, 2 × OCH₂CH₂), 1.95 (8H, m, 2 × CH₂CH=CHCH₂), 2.32 (6H, s, N(CH₃)₂), 2.45 (2H, m, NCH₂CH), 3.39-3.60 (7H, m, CHOCH₂, CH₂OCH₂), 5.38 (4H, m, 2 × CH=CH);

δ_{C} (75.4 MHz; CDCl₃) 14.0 (CH₃CH₂), 25.6, 26.1, 29.2-29.6 (signal overlap), 30.6, 32.6, 46.1 (N(CH₃)₂), 61.0 (NCH₂CH), 70.2 (CHCH₂O), 71.6 and 71.7 (OCH₂CH₂), 76.8 (CHCH₂O), 129.3 and 131.8 (CH=CH; overlap);

m/z (+HRFAB) 564.5718 (MH⁺, C₃₇H₇₄NO₂ requires 564.5720);

m/z (+ES) 565 (MH⁺, 37%), 613 (100%).

2,3-Di-(hexadec-9-ynyloxy)propyl-*N,N*-dimethylamine (134)

The above procedure was carried out using the following quantities: sodium hydride (65 mg, 1.61 mmol), toluene (6 mL), diol **37** (77 mg, 0.65 mmol), and mesylate **133** (0.51 g, 1.61 mmol). Purification by flash chromatography on silica (5% methanol in dichloromethane) yielded *the titled compound* as a pale yellow oil (0.20 g, 56%).

R_f 0.35 (5% methanol in dichloromethane);

ν_{\max} (neat)/ cm^{-1} 2930s, 2856s, 1119br m, 1043m;

δ_H (300 MHz; CDCl_3) 0.89 (6H, t, J 6.8 Hz, CH_3CH_2), 1.26-1.60 (40H, m), 2.13 (8H, t, J 6.8 Hz, $2 \times \text{CH}_2\text{C}\equiv\text{CCH}_2$), 2.31 (6H, s, $\text{N}(\text{CH}_3)_2$), 2.48 (2H, m, NCH_2CH), 3.40-3.60 (7H, m, CHOCH_2 , CH_2OCH_2);

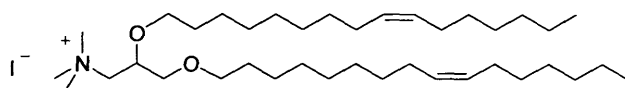
δ_C (75.4 MHz; CDCl_3) 14.1 (CH_3), 18.8 ($\text{CH}_2\text{C}\equiv\text{CCH}_2$), 22.6, 26.1, 28.5-29.6 (signal overlap), 30.1, 31.4, 45.9 ($\text{N}(\text{CH}_3)_2$), 60.8 (NCH_2CH), 70.1 (CHCH_2O), 71.6 (OCH_2CH_2 ; overlap), 76.7 (CHCH_2O), 80.2 and 80.3 ($\text{C}\equiv\text{C}$);

m/z (+HRFAB) 560.5406 (MH^+ , $\text{C}_{37}\text{H}_{70}\text{NO}_2$ requires 560.5406).

m/z (+ES) 561 (MH^+ , 100%).

General procedure for quaternisation with iodomethane

The amine **128-134** (1 eq) and iodomethane were stirred in a sealed tube at rt for 18 h. Excess iodomethane was removed *in vacuo*.

2,3-Di-[(*Z*)-hexadec-9-enyloxy]propyl-*N,N,N*-trimethylammonium iodide (135)

The above procedure was carried out using the following quantities: amine **128** (0.10 g, 0.18 mmol) and iodomethane (2.50 mL). Purification by flash chromatography on silica (5% methanol in dichloromethane) yielded *the titled compound* as a yellow oil (0.11 g, 95%).

R_f 0.35 (5% methanol in dichloromethane);

ν_{\max} (neat)/ cm^{-1} 2924s, 2855s, 1651w, 1123br m;

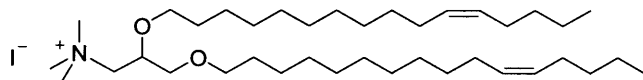
δ_H (300 MHz; CDCl_3) 0.87 (6H, t, J 6.8 Hz, $2 \times \text{CH}_3\text{CH}_2$), 1.20–1.40 (36H, m), 1.55 (4H, m, $2 \times \text{OCH}_2\text{CH}_2$), 2.01 (8H, m, $2 \times \text{CH}_2\text{CH}=\text{CHCH}_2$), 3.41 (4H, m, $2 \times \text{OCH}_2\text{CH}_2$), 3.50 (9H, s, $\text{N}^+(\text{CH}_3)_3$), 3.55–3.73 (3H, m, $\text{CHCH}_2\text{OCH}_2$), 4.04 (2H, m, N^+CH_2), 5.34 (4H, m, $2 \times \text{CH}=\text{CH}$);

δ_C (75.4 MHz; CDCl_3) 14.1 (CH_3CH_2), 22.7, 26.0, 26.3, 27.2, 29.0–30.0 (signal overlap), 55.2 ($\text{N}^+(\text{CH}_3)_3$), 68.1 (N^+CH_2), 69.3 and 72.1 (CHCH_2O , OCH_2CH_2 ; overlap), 73.5 (CHCH_2O), 129.8 and 130.3 ($\text{CH}=\text{CH}$);

m/z (+HRFAB) 578.5851 ($[\text{M}-\text{I}]^+$, $\text{C}_{38}\text{H}_{76}\text{NO}_2$ requires 578.5871);

m/z (+FAB) 578 ($[\text{M}-\text{I}]^+$, 100%).

2,3-Di-[(Z)-hexadec-11-enyloxy]propyl-*N,N,N*-trimethylammonium iodide (136)¹⁵¹



The above procedure was carried out using the following quantities: amine **129** (0.10 g, 0.18 mmol) and iodomethane (2.50 mL). Purification by flash chromatography on silica (5% methanol in dichloromethane) yielded *the titled compound* as a yellow oil (0.11 g, 95%).

ν_{\max} (neat)/ cm^{-1} 2922s, 2853s, 1654w, 1123br m;

R_f 0.35 (5% methanol in dichloromethane);

δ_H (300 MHz; CDCl_3) 0.89 (6H, t, J 6.9 Hz, $2 \times \text{CH}_3\text{CH}_2$), 1.25–1.40 (36H, m), 1.55 (4H, m, $2 \times \text{OCH}_2\text{CH}_2$), 2.05 (8H, m, $2 \times \text{CH}_2\text{CH}=\text{CHCH}_2$), 3.36 (4H, t, J 6.8 Hz, $2 \times \text{OCH}_2\text{CH}_2$), 3.49 (9H, s, $\text{N}^+(\text{CH}_3)_3$), 3.50–3.75 (3H, m, $\text{CHCH}_2\text{OCH}_2$), 4.05 (2H, m, N^+CH_2), 5.35 (4H, m, $2 \times \text{CH}=\text{CH}$);

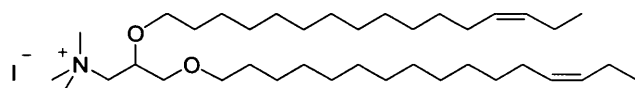
δ_C (75.4 MHz; CDCl_3) 14.0 (CH_3CH_2), 22.2, 22.4, 26.2, 26.6, 26.9–30.4 (signal overlap), 32.6, 55.3 ($\text{N}^+(\text{CH}_3)_3$), 68.1 (N^+CH_2), 69.3 and 72.2 (CHCH_2O , OCH_2CH_2 ; overlap), 73.5 (CHCH_2O), 130.0 and 130.3 ($\text{CH}=\text{CH}$);

m/z (+HRFAB) 578.5874 ($[\text{M}-\text{I}]^+$, $\text{C}_{38}\text{H}_{76}\text{NO}_2$ requires 578.5871);

Anal. (C₃₈H₇₆INO₂) found C, 66.58; H, 11.56; N, 1.92; I, 18.11; requires C, 64.29; H, 11.36; N, 1.92; I, 17.98;

m/z (+ES) 579 ([M-I]⁺, 100%).

2,3-Di-[(Z)-hexadec-13-enyloxy]propyl-N,N,N-trimethylammonium iodide (137)



The above procedure was carried out using the following quantities: amine **137** (0.10 g, 0.18 mmol) and iodomethane (2.50 mL). Purification by flash chromatography on silica (5% methanol in dichloromethane) yielded *the titled compound* as a yellow oil (0.10 g, 93%).

ν_{\max} (neat)/cm⁻¹ 2922s, 2853s, 1653w, 1123br m;

R_f 0.35 (5% methanol in dichloromethane);

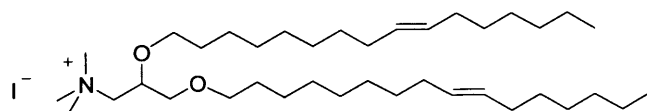
δ_{H} (300 MHz; CDCl₃) 0.96 (6H, m, 2 × CH₃CH₂) 1.16-1.44 (36H, m), 1.54 (4H, m, 2 × OCH₂CH₂), 1.98 (8H, m, 2 × CH₂CH=CHCH₂), 3.34-3.78 (16H, m, N⁺(CH₃)₃, 2 × OCH₂CH₂, CHCH₂OCH₂), 4.00 (2H, m, N⁺CH₂), 5.35 (4H, m, 2 × CH=CH);

δ_{C} (75.4 MHz; CDCl₃) 14.0 (CH₃CH₂), 22.2, 22.3, 26.1, 26.8, 27.3, 29.3–31.6 (signal overlap), 32.4, 55.2 (N⁺(CH₃)₃), 68.2 (N⁺CH₂), 69.4 and 72.2 (CHCH₂O, OCH₂CH₂; overlap), 73.6 (CHCH₂O), 130.3 and 130.4 (CH=CH);

m/z (+HRFAB) 578.5870 ([M-I]⁺, C₃₈H₇₆NO₂ requires 578.5871);

m/z (+FAB) 579 ([M-I]⁺, 100%).

2,3-Di-[(E)-hexadec-9-enyloxy]propyl-N,N,N-trimethylammonium iodide (138)



The above procedure was carried out using the following quantities: amine **131** (50 mg, 0.09 mmol) and iodomethane (2.50 mL). Purification by flash chromatography on silica (5% methanol in dichloromethane) yielded *the titled compound* as a yellow oil (58 mg, 94%).

R_f 0.30 (5% methanol in dichloromethane);

ν_{\max} (neat)/ cm^{-1} 2920s, 2851s, 1124br m;

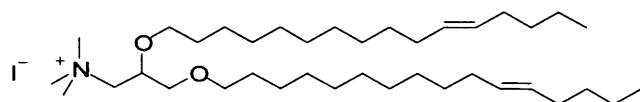
δ_H (300 MHz; CDCl_3) 0.86 (6H, m, $2 \times \text{CH}_3\text{CH}_2$), 1.15–1.48 (36H, m), 1.54 (4H, m, $2 \times \text{OCH}_2\text{CH}_2$), 1.95 (8H, m, $2 \times \text{CH}_2\text{CH}=\text{CHCH}_2$), 3.42–3.80 (16H, m, $\text{N}^+(\text{CH}_3)_3$, $2 \times \text{OCH}_2\text{CH}_2$, $\text{CHCH}_2\text{OCH}_2$), 4.05 (2H, m, N^+CH_2), 5.37 (4H, m, $2 \times \text{CH}=\text{CH}$);

δ_C (75.4 MHz; CDCl_3) 14.0 (CH_3CH_2), 22.2, 26.0, 26.2, 29.2–30.0 (signal overlap), 31.8, 32.3, 32.6, 55.2 ($\text{N}^+(\text{CH}_3)_3$), 68.1 (N^+CH_2), 69.3 and 72.1 (CHCH_2O , OCH_2CH_2 ; overlap), 73.5 (CHCH_2O), 130.3 ($\text{CH}=\text{CH}$; overlap);

m/z (+HRFAB) 578.5878 ($[\text{M}-\text{I}]^+$, $\text{C}_{38}\text{H}_{76}\text{NO}_2$ requires 578.5871);

m/z (+FAB) 579 ($[\text{M}-\text{I}]^+$, 100%).

2,3-Di-[(*E*)-hexadec-11-enyloxy]propyl-*N,N,N*-trimethylammonium iodide (139)



The above procedure was carried out using the following quantities: amine **132** (45 mg, 0.08 mmol) and iodomethane (2.00 mL). Purification by flash chromatography on silica (5% methanol in dichloromethane) yielded *the titled compound* as a yellow oil (53 mg, 95%).

R_f 0.35 (5% methanol in dichloromethane);

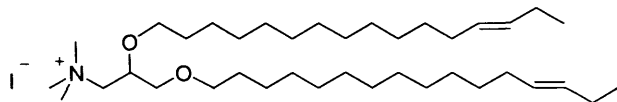
ν_{\max} (neat)/ cm^{-1} 2922s, 2853s, 1124br m;

δ_H (300 MHz; CDCl_3) 0.87 (6H, m, $2 \times \text{CH}_3\text{CH}_2$), 1.20–1.41 (36H, m), 1.55 (4H, m, $2 \times \text{OCH}_2\text{CH}_2$), 2.02 (8H, m, $2 \times \text{CH}_2\text{CH}=\text{CHCH}_2$), 3.43 (4H, t, J 6.8 Hz, $2 \times \text{OCH}_2\text{CH}_2$), 3.49 (9H, s, $\text{N}^+(\text{CH}_3)_3$), 3.50–3.80 (3H, m, $\text{CHCH}_2\text{OCH}_2$), 4.06 (2H, m, N^+CH_2), 5.37 (4H, m, $2 \times \text{CH}=\text{CH}$);

δ_C (75.4 MHz; CDCl_3) 14.0 (CH_3CH_2), 22.2 (overlap), 26.1, 26.2, 29.2–32.6 (signal overlap), 55.3 ($\text{N}^+(\text{CH}_3)_3$), 67.9 (N^+CH_2), 69.3 and 72.1 (CHCH_2O , OCH_2CH_2 ; overlap), 73.5 (CHCH_2O), 130.3 ($\text{CH}=\text{CH}$; overlap);

m/z (+HRFAB) 578.5870 ($[\text{M}-\text{I}]^+$, $\text{C}_{38}\text{H}_{76}\text{O}_2\text{N}$ requires 578.5871);

m/z (+FAB) 579 ($[\text{M}-\text{I}]^+$, 100%).

2,3-Di-[(E)-hexadec-13-enyloxy]propyl-*N,N,N*-trimethylammonium iodide (141)

The above procedure was carried out using the following quantities: amine **133** (0.10 g, 0.16 mmol) and iodomethane (2.50 mL). Purification by flash chromatography on silica (5% methanol in dichloromethane) yielded *the titled compound* as a yellow oil (0.11 g, 90%).

R_f 0.35 (5% methanol in dichloromethane);

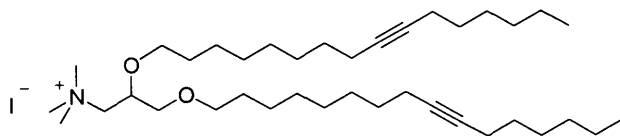
ν_{\max} (neat)/ cm^{-1} 2920s, 2851s, 1123br m;

δ_H (300 MHz; CDCl_3) 0.94 (6H, t, J 7.4 Hz, $2 \times \text{CH}_3\text{CH}_2$), 1.10–1.38 (36H, m), 1.54 (4H, m, $2 \times \text{OCH}_2\text{CH}_2$), 1.96 (8H, m, $2 \times \text{CH}_2\text{CH}=\text{CHCH}_2$), 3.35–3.75 (16H, m, $\text{N}^+(\text{CH}_3)_3$, $2 \times \text{OCH}_2\text{CH}_2$, $\text{CHCH}_2\text{OCH}_2$), 3.98 (2H, m, N^+CH_2), 5.35 (4H, m, $2 \times \text{CH}=\text{CH}$);

δ_C (75.4 MHz; CDCl_3) 14.0 (CH_3CH_2), 22.7–25.6, 26.1, 26.4, 29.2–30.0 (signal overlap), 32.6, 55.0 ($\text{N}^+(\text{CH}_3)_3$), 68.0 (N^+CH_2), 69.3 and 72.1 (CHCH_2O , OCH_2CH_2 ; overlap), 73.6 (CHCH_2O), 129.4 and 131.9 ($\text{CH}=\text{CH}$);

m/z (+HRFAB) 578.5878 ($[\text{M}-\text{I}]^+$, $\text{C}_{38}\text{H}_{76}\text{NO}_2$ requires 578.5871);

m/z (+FAB) 579 ($[\text{M}-\text{I}]^+$, 100%).

2,3-Di-(hexadec-9-ynyloxy)propyl-*N,N,N*-trimethylammonium iodide (141)

The above procedure was carried out using the following quantities: amine **134** (0.10 g, 0.18 mmol) and iodomethane (2.50 mL). Purification by flash chromatography on silica (5% methanol in dichloromethane) yielded *the titled compound* as a yellow oil (0.82 g, 65%).

ν_{\max} (neat)/ cm^{-1} 2930s, 2856s, 1123br m;

R_f 0.35 (5% methanol in dichloromethane);

δ_{H} (300 MHz; CDCl_3) 0.88 (6H, m, $2 \times \text{CH}_3\text{CH}_2$), 1.17–1.80 (40H, m), 2.14 (8H, m, $2 \times \text{CH}_2\text{C}\equiv\text{CCH}_2$), 3.42 (4H, t, J 6.8 Hz, $\text{CH}_2\text{CH}_2\text{O}$), 3.50 (9H, s, $\text{N}^+(\text{CH}_3)_3$), 3.24–3.77 (7H, m, $\text{CHCH}_2\text{OCH}_2$, OCH_2CH_2), 4.06 (2H, m, N^+CH_2);

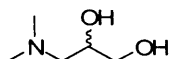
δ_{C} (75.4 MHz; CDCl_3) 14.1 (CH_3CH_2), 18.8 ($\text{CH}_2\text{C}\equiv\text{CCH}_2$), 22.6, 26.0, 26.2, 28.5–30.0 (signal overlap), 31.4, 55.1 ($\text{N}^+(\text{CH}_3)_3$), 67.9 (N^+CH_2), 69.3 and 72.1 (CHCH_2O , OCH_2CH_2 ; overlap), 73.6 (CHCH_2O), 80.1 and 80.3 ($\text{C}\equiv\text{C}$);

m/z (+HRFAB) 574.5554 ($[\text{M}-\text{I}]^+$, $\text{C}_{38}\text{H}_{72}\text{NO}_2$ requires 574.5558);

m/z (+FAB) 574 ($[\text{M}-\text{I}]^+$, 100%).

8.4 Synthesis of Chiral Lipid Analogues

**(*R*)-3-(Dimethylamino)propane-1,2-diol (145a) and
(*S*)-3-(dimethylamino)propane-1,2-diol (145b)**¹⁵¹



The same procedure was used for both enantiomers.

Dimethylamine hydrochloride (3.23 g, 39.6 mmol) and (*S*)-3-chloro-1,2-propanediol **144a** (0.50 mL, 3.43 mmol) were subsequently added to a solution of sodium hydroxide (1.98 g, 49.5 mmol) in water (5 mL) in a sealed tube at 0 °C. After stirring at rt for 18 h, water (5 mL) was added and the product extracted with chloroform (3 × 10 mL). The combined organic extracts were dried over magnesium sulfate and concentrated *in vacuo* to yield *the titled compound* as a pale yellow oil (0.33 g, 91% for *R*-enantiomer).

ν_{\max} (neat)/cm⁻¹ 3356 br s;

δ_{H} (300 MHz; CDCl₃) 2.33 (1H, dd, *J* 4.0, 12.3 Hz, NCHHCH), 2.30 (6H, s, 2 × CH₃), 2.50 (1H, m, NCHHCH), 2.94 (1H, br s, OH), 3.49 (1H, dd, *J* 4.5, 11.3 Hz, CHHOH) 3.69-3.80 (2H, m, CHHOH, CH₂CHCH₂);

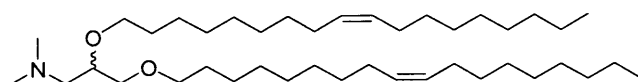
δ_{C} (75.4 MHz; CDCl₃) 45.6 (CH₃), 61.7 (NCH₂), 65.0 (CH₂OH), 67.6 (CH₂CHCH₂);

m/z (ES⁺) 119.95 (MH⁺, 100%);

$[\alpha]_{\text{D}}^{22}$ (**145a**) +17.1° (*c* 0.67, CHCl₃);

$[\alpha]_{\text{D}}^{22}$ (**145b**) -20.1° (*c* 0.67, CHCl₃).

**(*R*)-2,3-Di-[(*Z*)-octadec-9-enyloxy]propyl-*N,N*-dimethylamine (147a) and
(*S*)-2,3-di-[(*Z*)-octadec-9-enyloxy]propyl-*N,N*-dimethylamine (147b)**¹⁵¹



The same procedure was used for both enantiomers.

Sodium hydride (60%; 0.38 g, 10.1 mmol) was stirred in anhydrous toluene (20 mL) at rt for 15 min. The diol **145a** (0.40 g, 3.36 mmol) was added and the mixture stirred at 50 °C for 30 min. After addition of the mesylate **93** (3.20 g, 10.1

mmol), the reaction mixture was heated at reflux for 72 h. Water (30 mL) was added and the product extracted with ethyl acetate (3 × 20 mL), the combined organic extracts washed with saturated sodium hydrogencarbonate (25 mL) and brine (25 mL), dried over magnesium sulfate, and then concentrated *in vacuo*. Purification by flash chromatography on silica (5% methanol in dichloromethane) yielded *the titled compound* as a pale yellow oil (0.98 g, 47% for *R*-enantiomer).

R_f 0.38 (5% methanol in dichloromethane);

ν_{\max} (neat)/ cm^{-1} 2925s, 2854s, 1653w, 1120br m;

δ_H (300 MHz; CDCl_3) 0.81 (6H, t, J 7.3 Hz, CH_3CH_2) 1.15–1.33 (44H, m), 1.48 (4H, m, $2 \times \text{OCH}_2\text{CH}_2$), 1.92 (8H, m, $2 \times \text{CH}_2\text{CH}=\text{CHCH}_2$), 2.27 (6H, s, $\text{N}(\text{CH}_3)_2$), 2.33 (2H, m, NCH_2CH), 3.31–3.67 (7H, m, $\text{CHCH}_2\text{OCH}_2$, OCH_2CH_2), 5.34 (4H, m, $2 \times \text{CH}=\text{CH}$);

δ_C (75.4 MHz; CDCl_3) 14.5 (CH_3CH_2), 23.0, 26.5, 27.6, 29.5–30.2 (signal overlap), 30.6, 32.3, 46.7 ($\text{N}(\text{CH}_3)_2$), 61.5 (NCH_2CH), 70.6 (CHCH_2O), 72.0 and 72.5 (OCH_2CH_2), 77.4 (CHOCH_2), 130.2 and 130.3 ($\text{CH}=\text{CH}$);

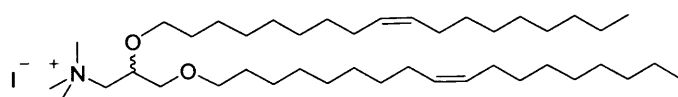
m/z (+HRFAB) 620.6331 (MH^+ , $\text{C}_{41}\text{H}_{82}\text{NO}_2$ requires 620.6346);

m/z (+ES) 621 (MH^+ , 100%);

$[\alpha]_D^{22}$ (147a) +2.7° (c 0.67, CHCl_3) (*R*-enantiomer);

$[\alpha]_D^{22}$ (147b) -2.4° (c 0.67, CHCl_3) (*S*-enantiomer).

(*R*)-2,3-Di-[(*Z*)-octadec-9-enoxy]propyl-*N,N,N*-trimethylammonium iodide (148a) and (*S*)-2,3-di-[(*Z*)-octadec-9-enoxy]propyl-*N,N,N*-trimethylammonium iodide (148b)¹⁵¹



The same procedure was used for both enantiomers.

The amine **147a** (0.10 g, 0.18 mmol) and iodomethane (2.50 mL) were stirred in a sealed tube at rt for 12 h. Excess iodomethane was evaporated *in vacuo*. Purification by flash chromatography on silica (5% methanol in dichloromethane) yielded *the titled compound* as a yellow oil (0.12 g, 97% for *R*-enantiomer).

R_f 0.35 (5% methanol in dichloromethane);

ν_{\max} (neat)/ cm^{-1} 2925s, 2854s, 1191br m;

δ_H (300 MHz; CDCl_3) 0.86 (6H, t, J 6.7 Hz, $2 \times \text{CH}_3\text{CH}_2$) 1.20-1.35 (44H, m), 1.53 (4H, m, $2 \times \text{OCH}_2\text{CH}_2$), 1.96 (8H, m, $2 \times \text{CH}_2\text{CH}=\text{CHCH}_2$), 3.46 (4H, t, J 6.8 Hz, OCH_2CH_2), 3.51 (9H, s, $\text{N}^+(\text{CH}_3)_3$), 3.54-3.72 (3H, m, $\text{CHCH}_2\text{OCH}_2$), 4.07 (2H, m, N^+CH_2), 5.35 (4H, m, $2 \times \text{CH}=\text{CH}$);

δ_C (75.4 MHz; CDCl_3) 13.9 (CH_3CH_2), 22.4, 25.8, 26.0, 27.0, 29.0-30.4 (signal overlap), 31.9, 32.4, 55.1 ($\text{N}^+(\text{CH}_3)_3$), 67.9 (N^+CH_2), 69.1 and 71.9 (CHCH_2O , OCH_2CH_2 ; overlap), 73.3 (CHCH_2O), 129.5 and 129.8 ($\text{CH}=\text{CH}$);

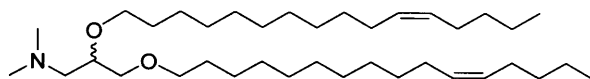
m/z (+ES) 635 ($[\text{M}-\text{I}]^+$, 100%);

m/z (+HRFAB) 634.6479 ($[\text{M}-\text{I}]^+$, $\text{C}_{42}\text{H}_{84}\text{NO}_2$ requires 634.6502);

$[\alpha]_D^{22}$ (148a) +21.6° (c 0.67, CHCl_3) (*R*-enantiomer);

$[\alpha]_D^{22}$ (148b) -22.2° (c 0.67, CHCl_3) (*S*-enantiomer).

(*R*)-2,3-Di-[(*Z*)-hexadec-11-enyloxy]propyl-*N,N*-dimethylamine (149a) and
(*S*)-2,3-di-[(*Z*)-hexadec-11-enyloxy]propyl-*N,N*-dimethylamine (149b)¹⁵¹



The same procedure was used for both enantiomers.

Sodium hydride (60%; 0.12 g, 3.00 mmol) was stirred in anhydrous toluene (5 mL) at rt for 15 min. The diol **145a** (0.12 g, 1.00 mmol) was added and the mixture stirred at 50 °C for 30 min. After addition of the mesylate **93** (0.95 g, 10.1 mmol), the reaction mixture was heated at reflux for 72 h. Water (20 mL) was added and the product extracted with ethyl acetate (3×15 mL), the combined organic extracts washed with saturated sodium hydrogencarbonate (20 mL) and brine (20 mL), dried over magnesium sulfate, and then concentrated *in vacuo*. Purification by flash chromatography on silica (5% methanol in dichloromethane) yielded the titled compound as a pale yellow oil (88 mg, 14% for *R*-enantiomer).

R_f 0.38 (5% methanol in dichloromethane);

ν_{\max} (neat)/ cm^{-1} 2925s, 2855s, 1459m, 1119br m;

δ_{H} (300 MHz; CDCl_3) 0.90 (6H, m, $2 \times \text{CH}_3\text{CH}_2$) 1.20-1.40 (36H, m), 1.57 (4H, m, $2 \times \text{OCH}_2\text{CH}_2$), 2.05 (8H, m, $2 \times \text{CH}_2\text{CH}=\text{CHCH}_2$), 2.29 (6H, s, $\text{N}(\text{CH}_3)_2$), 2.42 (2H, m, NCH_2CH), 3.39-3.65 (7H, m, CHOCH_2 , CH_2OCH_2), 5.37 (4H, m, $2 \times \text{CH}=\text{CH}$);

δ_{C} (75.4 MHz; CDCl_3) 14.0 (CH_3CH_2), 22.3, 26.1, 27.1, 27.3, 29.3-30.1 (signal overlap), 31.8, 46.7 ($\text{N}(\text{CH}_3)_2$), 61.1 (NCH_2CH), 70.2 and 71.6 (CHCH_2O , OCH_2CH_2 ; overlap), 77.2 (CHOCH_2), 129.8 and 129.9 ($\text{CH}=\text{CH}$);

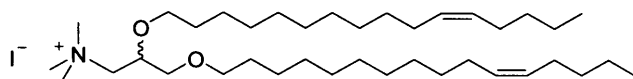
m/z (+ES) 589 ($[\text{M}+\text{Na}]^+$, 80%).

m/z (+HRFAB) 564.5734 (MH^+ , $\text{C}_{37}\text{H}_{74}\text{NO}_2$ requires 564.5720);

$[\alpha]_{\text{D}}^{22}$ (149a) $+4.8^\circ$ (c 0.67, CHCl_3) (*R*-enantiomer);

$[\alpha]_{\text{D}}^{22}$ (149b) -3.9° (c 0.67, CHCl_3) (*S*-enantiomer).

(*R*)-2,3-Di-[(*Z*)-hexadec-11-enyloxy]propyl-*N,N,N*-trimethylammonium iodide (150a) and (*S*)-2,3-di-[(*Z*)-hexadec-11-enyloxy]propyl-*N,N,N*-trimethylammonium iodide (146b)¹⁵¹



The same procedure was used for both enantiomers.

The amine **145a** (80 mg, 0.13 mmol) and iodomethane (2.00 mL) were stirred in a sealed tube at rt for 12 h. Excess iodomethane was evaporated *in vacuo*. Purification by flash chromatography on silica (5% methanol in dichloromethane) yielded the titled compound as a yellow oil (91 mg, 95% for *R*-enantiomer).

R_f 0.30 (5% methanol in dichloromethane);

ν_{max} (neat)/ cm^{-1} 2922s, 2853s, 1654w, 1123br m;

δ_{H} (300 MHz; CDCl_3) 0.87 (6H, m, $2 \times \text{CH}_3\text{CH}_2$), 1.20-1.35 (36H, m), 1.55 (4H, m, $2 \times \text{OCH}_2\text{CH}_2$), 2.01 (8H, m, $2 \times \text{CH}_2\text{CH}=\text{CHCH}_2$), 3.42 (4H, t, J 6.8 Hz, OCH_2CH_2), 3.47 (9H, s, $\text{N}^+(\text{CH}_3)_3$), 3.55-3.72 (3H, m, $\text{CHCH}_2\text{OCH}_2$), 4.03 (2H, m, N^+CH_2), 5.35 (4H, m, $2 \times \text{CH}=\text{CH}$);

δ_{C} (75.4 MHz; CDCl_3) 14.0 (CH_3CH_2), 22.1, 22.3, 26.0, 26.2, 26.9, 27.1, 29.3-30.0 (signal overlap) 31.8, 32.0, 32.3, 32.6, 55.2 ($\text{N}^+(\text{CH}_3)_3$), 68.0 (N^+CH_2), 69.3 and 72.1 (CHCH_2O , OCH_2CH_2 ; overlap), 73.5 (CHCH_2O), 129.9 and 130.3 ($\text{CH}=\text{CH}$);

m/z (+ES) 579 ($[M-I]^+$, 100%).

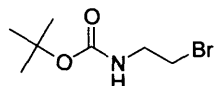
m/z (+HRFAB) 578.5894 ($[M-I]^+$, $C_{38}H_{76}NO_2$ requires 578.5871).

$[\alpha]^{22}_D$ (150a) +17.4 ° (c 0.67, $CHCl_3$) (*R*-enantiomer);

$[\alpha]^{22}_D$ (150b) -17.1 ° (c 0.67, $CHCl_3$) (*S*-enantiomer).

8.5 Fluorescently-Labelled Lipids

2-(*t*-Butyloxycarbonylamino)ethyl bromide (**153**)¹⁷⁵



A solution of 2-bromoethylamine hydrobromide (3.00 g, 14.6 mmol) and di-*tert*-butyl dicarbonate (4.37 g, 20.0 mmol) in THF (25 mL) and sodium hydroxide solution (2.0 M, 25 mL) was stirred at rt for 3 h. The mixture was carefully acidified with aqueous acetic acid (2 M) until pH 4-5, and the product extracted with ethyl acetate (3 × 40 mL). The combined organic extracts were washed with water (50 mL) and brine (50 mL), dried over magnesium sulfate, and then concentrated *in vacuo* to yield the titled compound as a colourless oil (2.19 g, 67%).

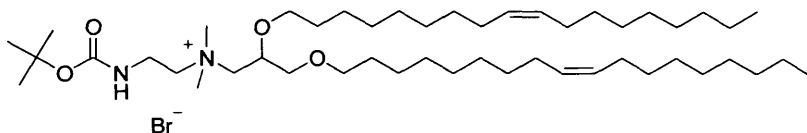
ν_{\max} (neat)/cm⁻¹ 3371 m, 1692 m;

δ_{H} (300 MHz; CDCl₃) 1.40 (9H, s, 3 × CH₃), 3.42-3.54 (4H, m, NHCH₂CH₂Br), 4.93 (1H, s, br, NH);

δ_{C} (75.4 MHz; CDCl₃) 26.4 (C(CH₃)₃), 31.6 (CH₂Br), 41.5 (NHCH₂), 78.7 (C(CH₃)₃), 154.6 (C=O);

m/z (+ES) 226 (MH⁺[⁸¹Br], 89%), 224 (MH⁺[⁷⁹Br], 100%).

2,3-Di-[(*Z*)-octadec-9-enyloxy]propyl-*N*-[2-(*tert*-butoxycarbonylamino)ethyl]-*N*,*N*-dimethylammonium bromide (**154**)



A solution of bromide **153** (0.34 g, 1.50 mmol) and amine **94** (0.62 g, 1.00 mmol) in acetone (3 mL) was heated in a sealed tube at 60 °C for 24 h. The mixture was concentrated *in vacuo*, and the product purified by flash chromatography on silica (gradient; dichloromethane to 10% methanol in dichloromethane) to give the titled compound as an orange oil (0.36 g, 42%).

ν_{\max} (neat)/cm⁻¹ 3371 m, 2928 s, 2847 s, 1697 m;

R_f 0.26 (10% methanol in dichloromethane);

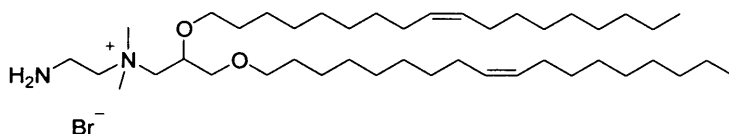
δ_H (300 MHz; $CDCl_3$) 0.88 (6H, t, J 7.0 Hz, $2 \times CH_3CH_2$), 1.35 (44H, m), 1.40 (9H, s, $C(CH_3)_3$), 1.60 (4H, m, $2 \times OCH_2CH_2$), 2.05 (8H, m, $2 \times CH_2CH=CHCH_2$), 3.35 (6H, s, $N^+(CH_3)_2$), 3.40-4.05 (13 H, m, $NCH_2CH_2N^+CH_2CHCH_2$, $2 \times OCH_2CH_2$), 5.40 (4H, m, $CH=CH$), 6.15 (1H, s, br, NH);

δ_C (75.4 MHz; $CDCl_3$) 14.8 (CH_3CH_2), 22.7, 23.1, 26.4-30.4 (signal overlap), 32.3, 33.0, 35.9 ($NHCH_2$), 53.3 (N^+CH_3 ; overlap), 64.9, 67.2, 68.6, 72.5, 73.6 ($CHCH_2O$), 80.6 ($C(CH_3)_3$), 130.1 and 130.4 ($CH=CH$), 156.8 ($C=O$);

m/z (+HRES) 763.7287 ($[M-Br]^+$, $C_{48}H_{95}N_2O_4$ requires 763.7292);

m/z (+ES) 764 ($[M-Br]^+$, 100%).

2,3-Di-[(Z)-octadec-9-enyloxy]propyl-N-(2-aminoethyl)-N,N-dimethylammonium bromide (155)



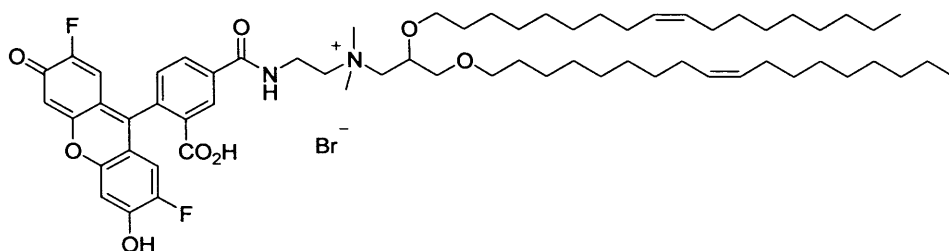
Compound **154** (0.10 g, 0.12 mmol) was stirred in a mixture of trifluoroacetic acid/dichloromethane (1:1, 5 mL) at rt for 18 h. The mixture was quenched by sodium hydrogencarbonate and the mixture filtered, concentrated *in vacuo*, and then purified by flash chromatography on silica (gradient; dichloromethane to 15% methanol in dichloromethane) yielded *the titled compound* as a pale yellow oil (41 mg, 46%).

ν_{max} (neat)/ cm^{-1} 3418 m, 2926 s, 2855 s;

R_f 0.21 (15% methanol in dichloromethane);

δ_H (300 MHz; $CDCl_3$) 0.87 (6H, m, $2 \times CH_3CH_2$), 1.27 (44H, m), 1.54 (4H, m, $2 \times OCH_2CH_2$), 1.99 (8H, m, $2 \times CH_2CH=CHCH_2$), 3.39-4.16 (6H, s), 3.40-4.05 (19 H, m, $N^+(CH_3)_2$, $NCH_2CH_2N^+CH_2CHCH_2$, $2 \times OCH_2CH_2$), 5.34 (4H, m, $CH=CH$);

m/z (+ES) 664 ($[M-Br]^+$, 100%).

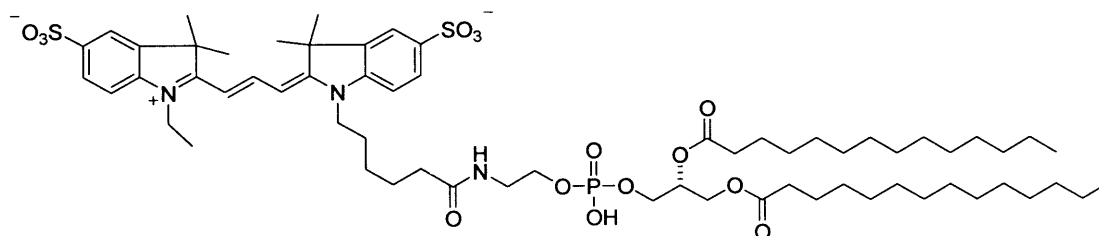
Oregon Green[®] labelled DOTMA (151)

A solution of amine **155** (1.00 mg, 1.22 μmol) and Oregon Green[®] 488 succinimidyl ester (1.00 mg, 1.35 μmol) in DMSO (0.20 mL) and phosphate buffer solution (pH 7.5, 0.2 mL) was stirred in the dark at rt for 48 h. The product was concentrated *in vacuo* and purified by preparative silica TLC (25% methanol in dichloromethane) to yield *the titled compound* as a light-sensitive orange solid (0.50 mg approx., 32%), which was stored in the refrigerator before use.

UV λ_{max} 500.3 nm;

R_f 0.74 (25% methanol in dichloromethane);

m/z (+ES) 1058 ([M-Br]⁺, 3%), 413 (Oregon green acid, 100%).

CyTM3 labelled phospholipid derivative (157)

A solution of 1,2-dimyristoyl-*sn*-glycero-3-phosphoethanolamine (1.00 mg, 1.58 μmol), CyTM3 monofunctional succinimidyl ester (1.00 mg, 1.31 μmol) and triethylamine (5 μL) in DMSO (0.20 mL) and phosphate buffer (pH 7.5, 0.2 mL) was stirred in the dark at rt for 96 h. The product was concentrated *in vacuo* and purified by preparative silica TLC (25% methanol in dichloromethane) to yield *the titled compound* as a light-sensitive pink solid (0.41 mg approx., 25%), which was stored in the refrigerator before use.

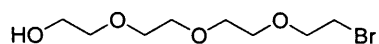
UV λ_{max} 533.5 nm;

R_f 0.71 (25% methanol in dichloromethane);

m/z (+ES) 1249 ([M+2H]⁺, 22%), 653 (CyTM3 acid, 50%).

8.6 PEG-Lipid Conjugates Synthesis

11-Bromo-3,6,9-trioxoundecan-1-ol (163)²³⁹



A solution of tetra(ethylene)glycol (3.00 g, 15.5 mmol) and aqueous hydrobromic acid (48%; 3.10 mL, 18.6 mmol) in toluene (27 mL) was heated at reflux for 72 h. The solution was neutralised by saturated sodium hydrogencarbonate solution, water (30 mL) was added, and the product extracted with dichloromethane (3 × 40 mL). The combined organic extracts were washed with brine (80 mL), dried over sodium sulfate, and then concentrated *in vacuo*. Purification by flash chromatography on reverse phase silica (gradient; water to 50% acetonitrile in water) yielded the titled compound as a pale yellow oil (1.78 g, 45%).

R_f 0.77 (50% acetonitrile in water);

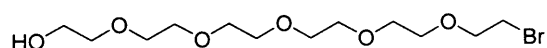
ν_{\max} (neat)/ cm^{-1} 3415br w, 2920br s, 1120br s, 1070s;

δ_H (300 MHz; CDCl_3) 2.31 (1H, s, br, OH) 3.47 (2H, t, J 6.3 Hz, CH_2Br), 3.59-3.74 (12H, m, OCH_2), 3.80 (2H, t, J 6.3 Hz, CH_2OH);

δ_C (75.4 MHz; CDCl_3) 30.2 (CH_2Br), 61.7 (CH_2OH), 70.3-70.7 (signal overlap), 71.2, 72.6;

m/z (+ES) 259 ($\text{MH}^+[^{81}\text{Br}]$, 23%), 257 ($\text{MH}^+[^{79}\text{Br}]$, 25%), 89 (100%).

17-Bromo-3,6,9,12,15-pentaoxoheptadecan-1-ol (164)¹⁸⁵



A solution of hexa(ethylene)glycol (3.00 g, 10.6 mmol) and aqueous hydrobromic acid (48%; 2.13 mL, 17.0 mmol) in toluene (20 mL) was heated at reflux for 72 h. The solution was neutralised by the addition of saturated sodium hydrogencarbonate solution, water (25 mL) was added, and the product extracted with dichloromethane (3 × 30 mL). The combined organic extracts were washed with brine (80 mL), dried over sodium sulfate, and then concentrated *in vacuo*. Purification by flash chromatography on reverse phase silica (gradient; water to 50% acetonitrile in water) yielded the titled compound as a yellow oil (1.42 g, 39%).

R_f 0.75 (50% acetonitrile in water);

ν_{\max} (neat)/ cm^{-1} 3418br w, 2922br s, 1109br s, 1069s;

δ_H (300 MHz; CDCl_3) 2.65 (1H, s, br, OH) 3.44 (2H, t, J 6.3 Hz, CH_2Br), 3.56-3.70 (20H, m, OCH_2), 3.78 (2H, t, J 6.3 Hz, CH_2OH);

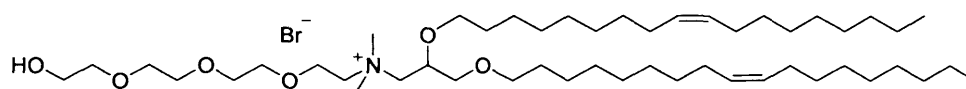
δ_C (75.4 MHz; CDCl_3) 30.3 (CH_2Br), 61.7 (CH_2OH), 70.3-70.6 (signal overlap), 71.2, 72.5;

m/z (+ES) 347 ($\text{MH}^+[^{81}\text{Br}]$, 30%), 345 ($\text{MH}^+[^{79}\text{Br}]$, 35%), 89 (100%).

General procedure for PEG-lipid formation

A solution of amine (1 eq) and PEGylated bromide (1 eq) in anhydrous methanol was heated in a sealed tube at 40 °C for 24 h. The mixture was concentrated *in vacuo*.

2,3-Di-[(Z)-octadec-9-enyloxy]propyl-*N*-(2-{2-[2-(2-hydroxyethoxy)ethoxy]ethoxy}ethyl)-*N,N*-dimethylammonium bromide (165)¹⁸⁶



The above procedure was carried out using the following quantities: amine **94** (0.30 g, 0.48 mmol), bromide **163** (0.14 g, 0.48 mmol) and methanol (2 mL). The crude product was purified by recrystallisation (ethyl acetate) at low temperature (-15 °C) to yield *the titled compound* as a pale yellow oil (0.25 g, 58%).

R_f 0.23 (10% methanol in dichloromethane);

ν_{\max} (neat)/ cm^{-1} 3402br m, 2922s, 2853s, 1634w, 1167m;

δ_H (300 MHz; CDCl_3) 0.85 (6H, t, J 7.0 Hz, $2 \times \text{CH}_3\text{CH}_2$), 1.15-1.42 (44H, m), 1.54 (4H, m, $2 \times \text{OCH}_2\text{CH}_2$), 2.01 (8H, m, $2 \times \text{CH}_2\text{CH}=\text{CHCH}_2$), 2.58 (1H, s, br, OH), 3.43 (6H, s, $\text{N}^+(\text{CH}_3)_2$), 3.48-4.25 (25H, m, N^+CH_2 , CHCH_2O , $2 \times \text{OCH}_2\text{CH}_2$, PEG- $\text{OCH}_2\text{CH}_2\text{O}$), 5.35 (4H, m, $2 \times \text{CH}=\text{CH}$);

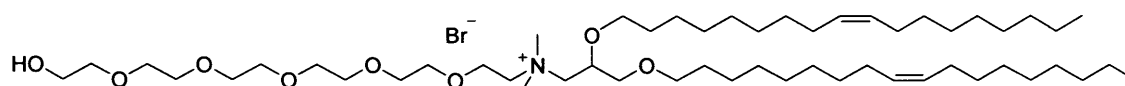
δ_C (75.4 MHz; CDCl_3) 14.4 (CH_3CH_2), 23.0, 26.4, 26.6, 29.7, 29.9, 30.0, 30.1-30.4 (signal overlap), 32.3, 33.0, 53.5 and 54.0 ($\text{N}^+(\text{CH}_3)_2$), 61.7, 66.1, 67.1, 69.1, 69.7, 70.6-72.4 (signal overlap), 73.9, 130.2 and 130.4 ($\text{CH}=\text{CH}$);

m/z (+HRFAB) 796.7399 ($[\text{M}-\text{Br}]^+$, $\text{C}_{49}\text{H}_{98}\text{NO}_6$ requires 796.7394);

Anal. (C₄₉H₉₈BrNO₆·H₂O) found C, 66.26; H, 11.02; N, 1.55; requires C, 65.74; H, 11.26; N, 1.56;

m/z (+FAB) 796 ([M-Br]⁺, 100%).

2,3-Di-[(Z)-octadec-9-enyloxy]propyl-N-{2-[2-(2-{2-(2-hydroxyethoxy)ethoxy}ethoxy)ethoxy]ethyl}-N,N-dimethylammonium bromide (166)¹⁸⁶



The above procedure was carried out using the following quantities: amine **94** (0.10 g, 0.16 mmol), bromide **164** (60 mg, 0.18 mmol) and methanol (1 mL). Purification by flash chromatography on silica (10% methanol in dichloromethane) yielded *the titled compound* as a yellow oil (53 mg, 32%).

R_f 0.24 (10% methanol in dichloromethane);

ν_{max} (neat)/cm⁻¹ 3389br m, 2924s, 2853s, 1634w, 1117br s;

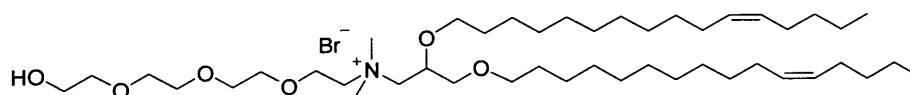
δ_H (300 MHz; CDCl₃) 0.84 (6H, t, *J* 6.6 Hz, 2 × CH₃CH₂) 1.14-1.35 (44H, m), 1.51 (4H, m, 2 × OCH₂CH₂), 1.96 (8H, m, 2 × CH₂CH=CHCH₂), 2.71 (1H, s, br, OH), 3.40 (6H, s, N⁺(CH₃)₂), 3.50-4.10 (33H, m, CHCH₂O, 2 × OCH₂CH₂, PEG-OCH₂CH₂O), 5.30 (4H, m, 2 × CH=CH);

δ_C (75.4 MHz; CDCl₃) 14.1 (CH₃CH₂), 22.7, 26.0, 26.2, 27.2, 29.2, 29.3, 29.5, 29.7, 29.8, 30.0, 31.9, 32.6, 53.1 and 53.3 (N⁺(CH₃)₂), 65.1, 66.7, 68.7, 69.2, 70.0-70.5 (signal overlap), 72.0, 72.8, 73.5, 129.8 and 130.2 (CH=CH);

m/z (+HRES) 884.7975 ([M-Br]⁺, C₅₃H₁₀₆NO₆ requires 884.7913);

m/z (+ES) 885 ([M-Br]⁺, 100%).

2,3-Di-[(Z)-hexadec-11-enyloxy]propyl-N-(2-{2-[2-(2-hydroxyethoxy)ethoxy]ethoxy}ethyl)-N,N-dimethylammonium bromide (167)¹⁸⁶



The above procedure was carried out using the following quantities: amine **129** (0.10 g, 0.17 mmol), bromide **163** (58 mg, 0.20 mmol) and methanol (1 mL). Purification by flash chromatography on silica (10% methanol in dichloromethane) yielded *the titled compound* as a yellow oil (64 mg, 43%).

R_f 0.24 (10% methanol in dichloromethane);

ν_{\max} (neat)/ cm^{-1} 3385br s, 2924s, 2853s, 1634m, 1119br s;

δ_H (300 MHz; CDCl_3) 0.87 (6H, m, $2 \times \text{CH}_3\text{CH}_2$), 1.15-1.42 (36H, m), 1.53 (4H, m, $2 \times \text{OCH}_2\text{CH}_2$), 2.00 (8H, m, $2 \times \text{CH}_2\text{CH}=\text{CHCH}_2$), 2.29 (1H, s, br, OH), 3.43 (6H, s, $\text{N}^+(\text{CH}_3)_2$), 3.48-4.25 (25H, m, CHCH_2O , $2 \times \text{OCH}_2\text{CH}_2$, PEG- $\text{OCH}_2\text{CH}_2\text{O}$), 5.32 (4H, m, $2 \times \text{CH}=\text{CH}$);

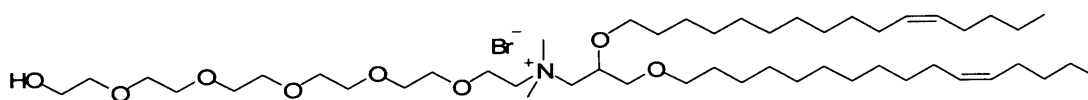
δ_C (75.4 MHz; CDCl_3) 14.0 (CH_3CH_2), 22.3, 26.1, 26.2, 26.9, 27.2, 29.3-30.0 (signal overlap), 32.0, 53.0 and 53.6 ($\text{N}^+(\text{CH}_3)_2$), 61.2, 65.2, 66.6, 68.6, 69.2, 70.1-70.5 (signal overlap), 72.0, 72.6, 73.5, 129.9 and 130.3 ($\text{CH}=\text{CH}$);

m/z (+HRFAB) 740.6775 ($[\text{M}-\text{Br}]^+$, $\text{C}_{45}\text{H}_{90}\text{NO}_6$ requires 740.6768);

Anal. ($\text{C}_{45}\text{H}_{90}\text{BrNO}_6 \cdot 3\text{H}_2\text{O}$) found C, 62.01; H, 11.04; N, 1.53; requires C, 61.76; H, 11.06; N, 1.60;

m/z (+FAB) 741 ($[\text{M}-\text{Br}]^+$, 100%).

2,3-Di-[(Z)-hexadec-11-enyloxy]propyl-N-{2-[2-(2-{2-[2-(2-hydroxyethoxy)ethoxy]ethoxy}ethoxy)ethoxy]ethyl}-N,N-dimethylammonium bromide (168)¹⁸⁶



The above procedure was carried out using the following quantities: amine **129** (0.10 g, 0.16 mmol), bromide **164** (75 mg, 0.20 mmol) and methanol (1 mL). Purification by flash chromatography on silica (10% methanol in dichloromethane) yielded *the titled compound* as a pale yellow oil (73 mg, 44%).

R_f 0.24 (10% methanol in dichloromethane);

ν_{\max} (neat)/ cm^{-1} 3400br s, 2924s, 2853s, 1634w, 1115br s;

δ_{H} (300 MHz; CDCl_3) 0.83 (6H, m, $2 \times \text{CH}_3\text{CH}_2$) 1.15-1.40 (36H, m), 1.49 (4H, m, $2 \times \text{OCH}_2\text{CH}_2$), 1.96 (8H, m, $2 \times \text{CH}_2\text{CH}=\text{CHCH}_2$), 2.87 (1H, s, br, OH), 3.46 (6H, s, $\text{N}^+(\text{CH}_3)_2$), 3.47-4.10 (33H, m, CHCH_2O , $2 \times \text{OCH}_2\text{CH}_2$, PEG- $\text{OCH}_2\text{CH}_2\text{O}$), 5.30 (4H, m, $2 \times \text{CH}=\text{CH}$);

δ_{C} (75.4 MHz; CDCl_3) 14.0 (CH_3CH_2), 22.2, 22.3, 26.0, 26.2, 26.9, 27.2, 29.2-30.0 (signal overlap), 31.9, 32.2, 32.6, 53.2 ($\text{N}^+(\text{CH}_3)_2$), 61.1, 64.8, 65.0, 65.6, 68.7, 69.2, 69.9-70.4 (signal overlap), 71.9, 72.6, 73.4, 129.8 and 130.3 ($\text{CH}=\text{CH}$);

m/z (+HRES) 828.7266 ($[\text{M}-\text{Br}]^+$, $\text{C}_{49}\text{H}_{98}\text{NO}_8$ requires 828.7287);

m/z (+ES) 829 ($[\text{M}-\text{Br}]^+$, 100%).

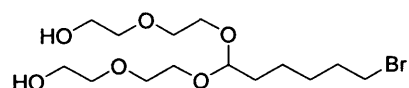
8.7 pH-Sensitive PEG-Lipid Conjugates

General procedure for acetal linker formation

To a solution of the bromo alcohol (1 eq), *N*-methylmorpholine-*N*-oxide (NMO; 1.1 eq) and activated molecular sieves (4Å, powdered; 300 mg per mmol) in anhydrous dichloromethane, was added tetra-*n*-propylammonium perruthenate (TPAP; 0.1 eq). After stirring at rt for 10 min, the suspension was filtered through a small plug of silica gel (~2 cm) and the residue washed with dichloromethane (3 × 20 mL), and the combined organic filtrates concentrated *in vacuo* to yield the corresponding aldehyde, which was subsequently used without further purification.

A solution of the crude aldehyde (1 eq), PEG-alcohol (4 eq), *p*TsOH·H₂O (0.3 eq) and activated powdered molecular sieves (4Å; 400 mg per mmol) in anhydrous dichloromethane was stirred at rt for 48 h. The suspension was filtered through a small plug of silica gel (~2 cm) and the residue washed with dichloromethane (3 × 20 mL), the combined organic filtrates washed with saturated sodium hydrogencarbonate solution (30 mL), water (30 mL) and brine (30 mL), dried over sodium sulfate, and then concentrated *in vacuo*.

7-(5-Bromopentyl)-3,6,8,11-tetraoxatridecane-1,13-diol (182)



The above procedure was carried out using the following quantities: 1-bromohexan-6-ol (**180**) (1.76 g, 10.3 mmol), NMO (1.33 g, 11.3 mmol), molecular sieves (3.0 g), dichloromethane (40 mL), TPAP (0.37 g, 1.03 mmol); diethylene glycol (4.63 mL, 51.5 mmol), *p*TsOH·H₂O (0.59 g, 3.90 mmol), molecular sieves (4.0 g) and dichloromethane (50 mL). Purification by flash chromatography on silica (gradient; dichloromethane to 5% methanol in dichloromethane) yielded *the titled compound* as a pale yellow oil (0.45 g, 12%).

*R*_f 0.38 (5% methanol in dichloromethane);

*ν*_{max} (neat)/cm⁻¹ 3362br s, 2924s, 1124m, 1074br m;

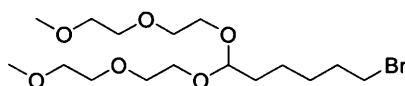
δ_{H} (300 MHz; CDCl_3) 1.35 (4H, m, $\text{CHCH}_2\text{CH}_2\text{CH}_2$), 1.59 (2H, dt, J 5.7, 8.2 Hz, CHCH_2CH_2), 1.79 (2H, tt, J 6.7, 7.1 Hz, $\text{CH}_2\text{CH}_2\text{Br}$), 3.27 (2H, t, J 5.7 Hz, OH), 3.36 (2H, t, J 6.7 Hz, CH_2Br), 3.51-3.82 (16H, m, $\text{PEG-OCH}_2\text{CH}_2$), 4.54 (2H, t, J 5.7 Hz, OCHO);

δ_{C} (75.4 MHz; CDCl_3) 23.8 (CHCH_2CH_2), 27.8 ($\text{CHCH}_2\text{CH}_2\text{CH}_2$), 32.6 (CH_2Br), 32.8 and 33.8 (CHCH_2 , $\text{CH}_2\text{CH}_2\text{Br}$), 61.6 (CH_2OH), 64.3 (CHOCH_2), 70.5 ($\text{CHOCH}_2\text{CH}_2$), 72.7 ($\text{CH}_2\text{CH}_2\text{OH}$), 102.8 (OCHO);

m/z (+ES) 398 ($[\text{M}(^{81}\text{Br})+\text{Na}]^+$, 95%), 396 ($[\text{M}(^{79}\text{Br})+\text{Na}]^+$, 100%);

m/z (+HRES) 395.1039 ($[\text{M}(^{79}\text{Br})+\text{Na}]^+$, $\text{C}_{14}\text{H}_{29}\text{BrO}_6\text{Na}$ requires 395.1040).

9-(5-Bromopentyl)-2,5,8,10,13,16-hexaoxaheptadecane (185)



The above procedure was carried out using the following quantities: bromo alcohol **180** (1.76 g, 10.3 mmol), NMO (1.33 g, 11.3 mmol), molecular sieves (3.0 g), dichloromethane (40 mL), TPAP (0.37 g, 1.03 mmol); diethylene glycol methyl ether (**183**) (3.63 mL, 30.9 mmol), $p\text{TsOH}\cdot\text{H}_2\text{O}$ (0.59 g, 3.90 mmol), molecular sieves (4.0 g) and dichloromethane (50 mL). Purification by chromatography on neutral alumina (gradient; dichloromethane to 2% methanol in dichloromethane) yielded *the titled compound* as a pale yellow oil (1.45 g, 35%).

R_f 0.43 (2% methanol in dichloromethane);

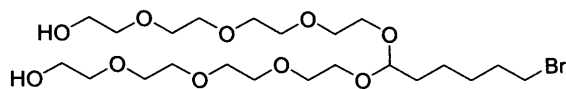
ν_{max} (neat)/ cm^{-1} 2930s, 1113br s, 1078br s, 1028m;

δ_{H} (300 MHz; CDCl_3) 1.38 (4H, m, $\text{CHCH}_2\text{CH}_2\text{CH}_2$), 1.59 (2H, dt, J 5.7, 8.3 Hz, CHCH_2CH_2), 1.81 (2H, tt, J 6.8, 7.0 Hz, $\text{CH}_2\text{CH}_2\text{Br}$), 3.35 (6H, s, CH_3), 3.24-3.49 (4H, m, CH_2Br), 3.51-3.82 (16H, m, $\text{PEG-OCH}_2\text{CH}_2$), 4.56 (2H, t, J 5.7 Hz, OCHO);

δ_{C} (75.4 MHz; CDCl_3) 23.8 (CHCH_2CH_2), 27.9 ($\text{CHCH}_2\text{CH}_2\text{CH}_2$), 32.7 (CH_2Br), 33.0 ($\text{CH}_2\text{CH}_2\text{Br}$), 33.7 (CHCH_2), 59.0 (CH_3), 64.4 (CHOCH_2), 70.5 and 70.6 (CH_2OCH_2), 72.0 (CH_3OCH_2), 103.1 (OCHO);

m/z (+ES) 424 ($[\text{M}(^{81}\text{Br})+\text{Na}]^+$, 94%), 423 ($[\text{M}(^{79}\text{Br})+\text{Na}]^+$, 100%);

m/z (+HRES) 423.1351 ($[\text{M}(^{79}\text{Br})+\text{Na}]^+$, $\text{C}_{13}\text{H}_{33}\text{BrO}_6\text{Na}$ requires 423.1353).

13-(5-Bromopentyl)-3,6,9,12,14,17,20,23-octaoxapentacosane-1,25-diol (186)

The above procedure was carried out using the following quantities: bromo alcohol **180** (1.76 g, 10.3 mmol), NMO (1.33 g, 11.3 mmol), molecular sieves (3.0 g), dichloromethane (40 mL), TPAP (0.37 g, 1.03 mmol); tetra(ethylene)glycol (8.88 mL, 51.5 mmol), *p*TsOH·H₂O (0.59 g, 3.90 mmol), molecular sieves (2.7 g) and dichloromethane (50 mL). Purification by flash chromatography on silica (gradient; dichloromethane to 5% methanol in dichloromethane) yielded *the titled compound* as a pale yellow oil (0.49 g, 9%).

R_f 0.33 (5% methanol in dichloromethane);

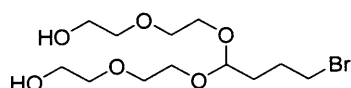
ν_{max} (neat)/cm⁻¹ 3418br m, 2923s, 1185m, 1107m, 1072br m;

δ_H (300 MHz; CDCl₃) 1.33 (4H, m, CHCH₂CH₂CH₂), 1.55 (2H, dt, *J* 5.7, 8.0 Hz, CHCH₂CH₂), 1.79 (2H, tt, *J* 6.8, 7.3 Hz, CH₂CH₂Br), 3.00 (2H, t, *J* 6.3 Hz, OH), 3.36 (2H, t, *J* 6.7 Hz, CH₂Br), 3.50-3.75 (32H, m, PEG-OCH₂CH₂), 4.51 (1H, t, *J* 5.7 Hz, OCHO);

δ_C (75.4 MHz; CDCl₃) 23.8 (CHCH₂CH₂), 27.9 (CHCH₂CH₂CH₂), 32.6 (CH₂Br), 32.9 and 33.8 (CHCH₂, CH₂CH₂Br), 61.6 (CH₂OH), 64.4 (CHOCH₂), 70.3-70.6 (PEG-OCH₂CH₂O; overlap), 72.5 (CH₂CH₂OH), 103.0 (OCHO);

***m/z* (+HRES)** 571.2081 ([M(⁷⁹Br)+Na]⁺, C₂₂H₄₅BrO₁₀Na requires 571.2088);

***m/z* (+ES)** 574 ([M(⁸¹Br)+Na]⁺, 96%), 572 ([M(⁷⁹Br)+Na]⁺, 100%).

7-(3-Bromopropyl)-3,6,8,11-tetraoxatridecane-1,13-diol (187)

The above procedure was carried out using the following quantities: 1-bromobutan-4-ol (1.70 g, 11.1 mmol), NMO (1.47 g, 12.1 mmol), molecular sieves (3.30 g), dichloromethane (45 mL), TPAP (0.39 g, 1.11 mmol); diethylene glycol (3.99 mL, 44.4 mmol), *p*TsOH·H₂O (0.64 g, 3.35 mmol), molecular sieves (4.40 g) and dichloromethane (50 mL). Purification by chromatography on neutral alumina

(gradient; dichloromethane to 2% methanol in dichloromethane) yielded *the titled compound* as a pale yellow oil (0.68 g, 40%).

R_f 0.35 (5% methanol in dichloromethane);

ν_{\max} (neat)/ cm^{-1} 3358br s, 2929s, 1128m, 1063br m;

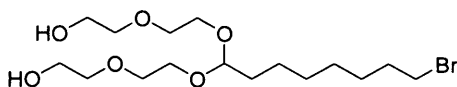
δ_H (300 MHz; CDCl_3) 1.73 (2H, m, CHCH_2), 1.87 (2H, m, $\text{CH}_2\text{CH}_2\text{Br}$), 3.37 (2H, t, J 6.5 Hz, CH_2Br), 3.43 (2H, m, OH), 3.50-3.81 (16H, m, $\text{PEG-OCH}_2\text{CH}_2$), 4.58 (2H, t, J 5.6 Hz, OCHO);

δ_C (75.4 MHz; CDCl_3) 28.0 ($\text{CH}_2\text{CH}_2\text{Br}$), 31.7 (CH_2Br), 33.5 (CHCH_2), 61.8 (CH_2OH), 64.6 (CHOCH_2), 70.6 ($\text{CHOCH}_2\text{CH}_2$), 72.8 ($\text{CH}_2\text{CH}_2\text{OH}$), 102.2 (OCHO);

m/z (+HRES) 367.0723 ($[\text{M}(^{79}\text{Br})+\text{Na}]^+$, $\text{C}_{12}\text{H}_{25}\text{BrO}_6\text{Na}$ requires 367.0727).

m/z (+ES) 369 ($[\text{M}(^{81}\text{Br})+\text{Na}]^+$, 97%), 367 ($[\text{M}(^{79}\text{Br})+\text{Na}]^+$, 100%).

7-(7-Bromoheptyl)-3,6,8,11-tetraoxatridecane-1,13-diol (188)



The above procedure was carried out using the following quantities: 1-bromooctan-8-ol (2 g, 9.57 mmol), NMO (1.12 g, 9.57 mmol), molecular sieves (3.0 g), dichloromethane (40 mL), TPAP (0.34 g, 0.96 mmol); diethylene glycol (5.18 mL, 57.6 mmol), $p\text{TsOH}\cdot\text{H}_2\text{O}$ (0.55 g, 2.91 mmol), molecular sieves (4.0 g) and dichloromethane (40 mL). Purification by flash chromatography on silica (gradient; dichloromethane to 3% methanol in dichloromethane) yielded *the titled compound* as colourless oil (1.50 g, 39%).

R_f 0.35 (5% methanol in dichloromethane);

ν_{\max} (neat)/ cm^{-1} 3434br s, 2930s, 1128br m, 1071br m;

δ_H (300 MHz; CDCl_3) 1.22-1.47 (8H, m, $\text{CHCH}_2\text{CH}_2\text{CH}_2\text{CH}_2\text{CH}_2$), 1.60 (2H, m, CHCH_2CH_2), 1.82 (2H, tt, J 6.8, 7.1 Hz, $\text{CH}_2\text{CH}_2\text{Br}$), 3.22 (2H, t, J 6.2 Hz, OH), 3.37 (2H, t, J 6.8 Hz, CH_2Br), 3.56-3.76 (16H, m, $\text{PEG-OCH}_2\text{CH}_2$), 4.56 (2H, t, J 6.0 Hz, OCHO);

δ_c (75.4 MHz; $CDCl_3$) 24.6 ($CHCH_2CH_2$), 28.0, 28.6 and 29.2 ($CH_2CH_2CH_2CH_2Br$), 32.7 (CH_2Br), 33.0 (CH_2CH_2Br), 34.0 ($CHCH_2$), 61.7 (CH_2OH), 64.3 ($CHOCH_2$), 70.6 ($CHOCH_2CH_2$), 72.7 (CH_2CH_2OH), 102.9 ($OCHO$);

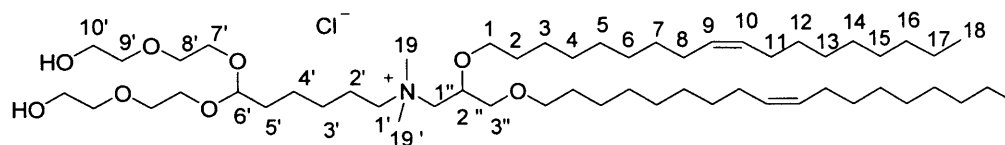
m/z (+HRES) 423.1361 ($[M(^{79}Br)+Na]^+$, $C_{16}H_{33}BrO_6Na$ requires 423.1353);

m/z (+ES) 425 ($[M(^{81}Br)+Na]^+$, 100%), 423 ($[M(^{79}Br)+Na]^+$, 83%).

General procedure for PEG-acetal lipid formation

The acetal bromide (1 eq) and tertiary amine (1.3 eq) were heated in a sealed tube at 40 °C for 48 h. The mixture was dissolved in a 1:1 mixture of chloroform/methanol, passed through an Amberlite® IRA-400 (Cl) ion exchange column eluting with chloroform/methanol (1:1), and then concentrated *in vacuo*.

N-{2,3-Bis[(*Z*)-octadec-9-enyloxy]propyl}-6,6-bis[2-(2-hydroxyethoxy)ethoxy]-*N,N*-dimethylhexan-1-aminium chloride (190)



The above procedure was carried out using the following quantities: amine **94** (0.30 g, 0.48 mmol) and bromide **182** (0.16 g, 0.44 mmol). Purification by flash chromatography on silica (5% methanol in dichloromethane) yielded *the titled compound* as a yellow oil (0.12g, 29%).

R_f 0.34 (5% methanol in dichloromethane);

ν_{max} (neat)/ cm^{-1} 3357br m, 2924s, 1622m, 1124m, 1078br m;

δ_H (300 MHz; $CDCl_3$) 0.86 (6H, t, J 6.7 Hz, H-18), 1.15-1.38 (46H, m), 1.44 (2H, m, H-4'), 1.53 (4H, m, H-2), 1.65 (2H, dt, J 6.0, 6.2 Hz, H-5'), 1.79 (2H, m, H-2'), 1.90-2.06 (8H, m, H-8, 11), 2.46 (2H, s, br, OH), 3.29 (3H, s, H-19), 3.33 (3H, s, H-19'), 3.32-3.50 (8H, m, H-1, 1', 1''), 3.52-3.91 (18H, m, H-3'', 7', 8', 9', 10'), 3.97 (1H, m, H-2''), 4.65 (1H, t, J 5.6 Hz, H-6'), 5.34 (4H, m, H-9, 10);

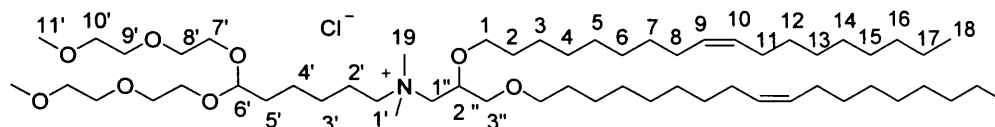
δ_c (75.4 MHz; $CDCl_3$) 14.1 (C-18), 22.6 (C-17), 22.7, 23.9, 25.7, 26.0, 26.2, 27.2, 29.3-30.2 (signal overlap), 31.9, 32.6, 32.8, 51.9 (C-19), 52.3 (C-19'), 61.5 (C-10'),

64.9, 65.2, 68.5, 69.4, 70.5, 72.0, 72.7, 73.3 (C-2''), 103.0 (C-6'), 129.8 and 130.0 (C-9, 10);

m/z (+HRES) 912.8235 ($[M-Cl]^+$, $C_{55}H_{110}NO_8$ requires 912.8236);

m/z (+ES) 914 ($[M-Cl]^+$, 100%).

***N*-{2,3-Bis[(*Z*)-octadec-9-enyloxy]propyl}-6,6-bis[2-(2-methoxyethoxy)ethoxy]-*N,N*-dimethylhexan-1-aminium chloride (191)**



The above procedure was carried out using the following quantities: amine **94** (0.30 g, 0.48 mmol) and bromide **185** (0.18 g, 0.44 mmol). Purification by flash chromatography on silica (2% methanol in dichloromethane) yielded *the titled compound* as a pale yellow oil (0.21 g, 44%).

R_f 0.41 (2% methanol in dichloromethane);

ν_{\max} (neat)/ cm^{-1} 2924s, 1633m, 1123br s, 1086m, 1030w;

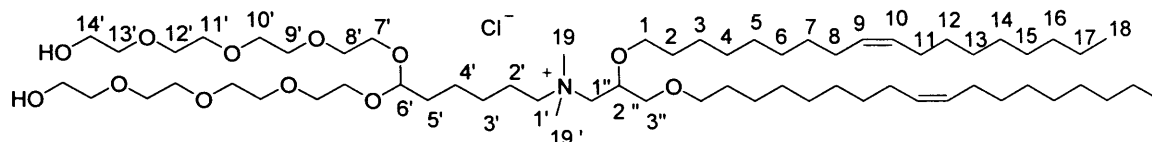
δ_H (300 MHz; CDCl_3) 0.80 (6H, t, J 6.6 Hz, H-18), 1.15-1.41 (50H, m), 1.47 (4H, m, H-2), 1.55 (2H, m, H-5'), 1.67 (2H, m, H-2'), 1.83-2.10 (8H, m, H-8, 11), 3.30 (6H, s, H-19), 3.30-3.43 (14H, m, H-1, 1', 19, 1''), 3.46-3.91 (18H, m, H-3'', 7', 8', 9', 10'), 3.99 (1H, m, H-2''), 4.50 (1H, t, J 5.6 Hz, H-6'), 5.28 (4H, m, H-9, 10);

δ_C (125.8 MHz; CDCl_3) 14.5 (C-18), 23.0, 23.1, 24.6, 26.4, 26.6, 27.6, 29.6-30.4 (signal overlap), 32.7, 33.2, 52.3 and 52.6 (C-19), 59.4 (C-11'), 65.0, 65.3, 66.6, 68.9, 69.7, 70.8, 71.0, 72.3, 73.8 (C-2''), 103.1 (C-6'), 130.1 and 130.4 (C-9, 10);

m/z (+HRFAB) 941.8602 ($[M-Cl]^+$, $C_{57}H_{114}NO_8$ requires 941.8622);

m/z (+FAB) 941 ($[M-Cl]^+$, 100%).

***N*-{2,3-Bis[(*Z*)-octadec-9-enyloxy]propyl}-6,6-bis{2-[2-(2-hydroxyethoxy)ethoxy]}-*N,N*-dimethylhexan-1-aminium chloride (192)**



The above procedure was carried out using the following quantities: amine **94** (0.30 g, 0.48 mmol) and bromide **186** (0.24 g, 0.44 mmol). Purification by flash chromatography on silica (5% methanol in dichloromethane) yielded *the titled compound* as a pale yellow oil (0.18 mg, 33%).

R_f 0.31 (5% methanol in dichloromethane);

ν_{max} (neat)/cm⁻¹ 3362br s, 2924s, 1643w, 1124br m, 1082br m;

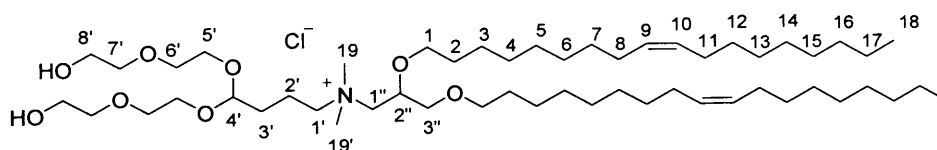
δ_H (300 MHz; CDCl₃) 0.85 (6H, t, *J* 6.5 Hz, H-18), 1.15-1.41 (46H, m), 1.39 (2H, m, H-4'), 1.52 (4H, m, H-2), 1.62 (2H, m, H-5'), 1.74 (2H, m, H-2'), 1.97 (8H, m, H-8, 11), 2.78 (2H, s, br, OH), 3.31 (3H, s, H-19), 3.34 (3H, s, H-19'), 3.35- 3.50 (8H, m, H-1, 1', 1''), 3.51-3.93 (34H, m, H-3'', H-7' to H-14'), 4.03 (1H, m, H-2''), 4.58 (1H, t, *J* 5.4 Hz, H-6'), 5.34 (4H, m, H-9, 10);

δ_C (75.4 MHz; CDCl₃) 14.1 (C-18), 22.5 (C-17), 22.7, 23.9, 25.8, 26.0, 26.2, 27.2, 29.3-30.0 (signal overlap), 31.9, 32.5, 32.6, 52.0 (C-19; overlap), 61.4 (C-14'), 64.1, 65.1, 68.5, 69.3, 70.1, 70.4, 70.5-70.6 (signal overlap), 72.0, 72.8, 73.4 (C-2''), 103.0 (C-6''), 129.8 and 130.0 (C-9, 10);

***m/z* (+HRES)** 1088.9280 ([M-Cl]⁺, C₆₃H₁₂₆NO₁₂ requires 1088.9275);

***m/z* (+ES)** 1090 ([M-Cl]⁺, 100%);

***N*-{2,3-Bis[(*Z*)-octadec-9-enyloxy]propyl}-4,4-bis[2-(2-hydroxyethoxy)ethoxy]-*N,N*-dimethylbutan-1-aminium chloride (193)**



The above procedure was carried out using the following quantities: amine **94** (0.15 g, 0.43 mmol) and bromide **187** (0.35 g, 0.57 mmol). Purification by flash

chromatography on silica (5% methanol in dichloromethane) yielded *the titled compound* as a pale yellow oil (81 mg, 21%).

R_f 0.32 (5% methanol in dichloromethane);

ν_{max} (neat)/cm⁻¹ 3383br s, 2924s, 1634w, 1123br m, 1080m;

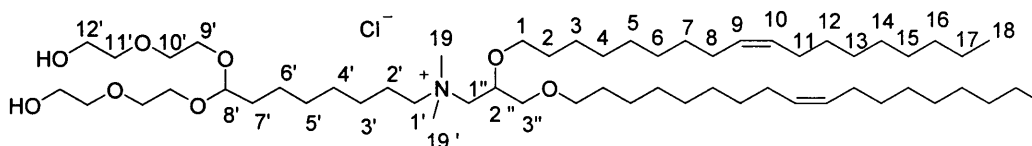
δ_H (300 MHz; CDCl₃) 0.83 (6H, t, *J* 6.6 Hz, H-18), 1.13-1.39 (44H, m), 1.50 (4H, m, H-2), 1.74 (2H, m, H-3'), 1.83-2.05 (10H, m, H-8, 11, 2'), 3.28 (3H, s, H-19), 3.31 (3H, s, H-19'), 3.39 (4H, t, *J* 6.9 Hz, H-1), 3.48-3.94 (22H, m), 4.00 (1H, m, H-2''), 4.79 (1H, m, H-4'), 5.33 (4H, m, H-9, 10).

δ_C (75.4 MHz; CDCl₃) 14.1 (C-18), 17.9 (C-2'), 22.7 (C-17), 26.0, 26.2, 27.2, 29.2-30.2 (signal overlap), 31.9, 32.6, 51.9 (C-19), 52.2 (C-19'), 61.2 (C-8'), 65.1, 65.9, 66.0, 68.8, 69.3, 70.6, 72.0, 72.7, 73.3 (C-2''), 103.0 (C-4''), 129.8 and 129.9 (C-9, 10);

***m/z* (+HRES)** 885.7988 ([M-Cl]⁺, C₅₃H₁₀₇NO₆ requires 885.7991);

***m/z* (+ES)** 885 ([M-Cl]⁺, 100%).

***N*-{2,3-Bis[(*Z*)-octadec-9-enyloxy]propyl}-8,8-bis[2-(2-hydroxyethoxy)ethoxy]-*N,N*-dimethyloctan-1-aminium chloride (**194**)**



The above procedure was carried out using the following quantities: amine **94** (0.27 g, 0.44 mmol) and bromide **188** (0.16 g, 0.4 mmol). Purification by flash chromatography on silica (5% methanol in dichloromethane) yielded *the titled compound* as a pale yellow oil (81 mg, 21%).

R_f 0.32 (5% methanol in dichloromethane);

ν_{max} (neat)/cm⁻¹ 3331br m, 2924s, 1661m, 1126br m 1069m

δ_H (300 MHz; CDCl₃) 0.85 (6H, t, *J* 6.7 Hz, H-16), 1.15-1.45 (52H, m), 1.52 (4H, m, H-17), 1.62 (2H, m, H-7'), 1.73 (2H, m, H-2'), 1.88-2.05 (8H, m, H-8, 11), 3.36 (3H, s, H-19), 3.38 (3H, s, H-19'), 3.31-3.50 (8H, m, H-1, 1', 1''), 3.50-3.80 (18H, m, H-2'',

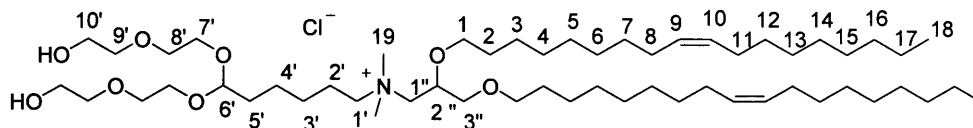
9', 10', 11', 12'), 4.01 (1H, m, H-2''), 4.60 (1H, t, J 5.8 Hz, H-8'), 5.34 (4H, m, H-9, 10);

δ_C (75.4 MHz; $CDCl_3$) 14.1 (C-18), 22.7 (C-27), 22.8, 24.3, 26.0, 26.2, 27.2, 28.9-29.8 (signal overlap), 31.9, 33.0, 52.1 (C-19 and 19'; overlap), 61.6 (C-12'), 64.6, 64.9, 68.4, 69.3, 70.6, 72.0, 72.7, 73.4 (C-2''), 103.0 (C-6'), 129.8 and 130.0 (C-9, 10);

m/z (+HRES) 941.8659 ($[M-Cl]^+$, $C_{57}H_{115}NO_8$ requires 941.8617);

m/z (+ES) 941 ($[M-Cl]^+$, 100%).

***N*-{2,3-Bis[(*Z*)-hexadec-11-enyloxy]propyl}-6,6-bis[2-(2-hydroxyethoxy)ethoxy]-*N,N*-dimethylhexan-1-aminium chloride (195)**



The above procedure was carried out using the following quantities: amine **129** (0.27 g, 0.48 mmol) and bromide **182** (0.16 g, 0.44 mmol). Purification by flash chromatography on silica (5% methanol in dichloromethane) yielded *the titled compound* as a pale yellow oil (0.13g, 34%).

R_f 0.33 (5% methanol in dichloromethane);

ν_{max} (neat)/ cm^{-1} 3358br m, 2924s, 1661m, 1124br m, 1076br m;

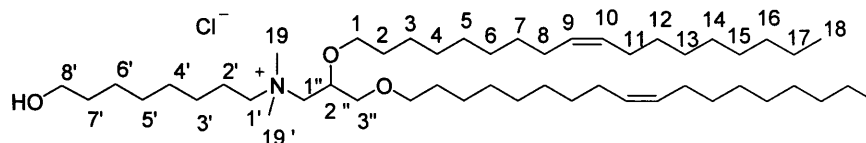
δ_H (300 MHz; $CDCl_3$) 0.86 (6H, t, J 6.9 Hz, H-16), 1.15-1.35 (46H, m), 1.40 (2H, m, H-4'), 1.50 (4H, m, H-2), 1.61 (2H, m, H-5'), 1.79 (2H, m, H-2'), 1.92 (8H, m, H-4, 7), 2.64 (2H, s, br, OH), 3.30-3.46 (14H, m, H-1, 1', 1'', 17), 3.50-3.86 (18H, m, H-3'', 7', 8', 9', 10'), 4.00 (1H, m, H-2''), 4.62 (1H, t, J 5.5 Hz, H-6'), 5.35 (4H, m, H-11, 12);

δ_C (75.4 MHz; $CDCl_3$) 13.9 (C-16), 22.2 (C-17), 22.7, 24.1, 25.8, 26.0, 26.2, 29.2-30.0 (signal overlap), 31.8, 32.2, 32.6, 32.9, 52.1 (C-17), 61.5 (C-10'), 64.9, 66.0 68.5, 69.3, 70.6, 72.0, 72.7, 73.4 (C-2''), 103.0 (C-6'), 130.3 (C-11 and 12; overlap);

m/z (+ES) 857 ($[M-Cl]^+$, 100%);

m/z (+HRES) 857.7660 ($[M-Cl]^+$, $C_{51}H_{102}NO_8$ requires 857.7683).

***N*-{2,3-Bis[(*Z*)-octadec-9-enyloxy]propyl}-8-hydroxy-*N,N*-dimethyloctan-1-aminium chloride (197)**



8-Bromooctan-1-ol (0.15 g, 0.71 mmol) and amine **94** (0.40 g, 0.64 mmol) were heated in a sealed tube at 40 °C for 48 h. The mixture was dissolved in a 1:1 mixture of chloroform/methanol, passed through an Amberlite® IRA-400 (Cl) ion exchange column eluting with chloroform/methanol (1:1), and then concentrated *in vacuo*. Purification by flash chromatography on silica (5% methanol in dichloromethane) yielded *the titled compound* as a colourless oil (0.24 g, 47%).

R_f 0.28 (5% methanol in dichloromethane);

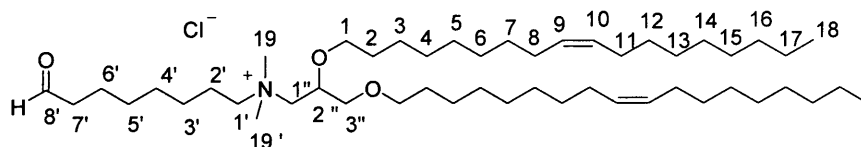
δ_H (300 MHz; $CDCl_3$) 0.85 (6H, t, J 6.4 Hz, H-18), 1.16-1.45 (50H, m), 1.52 (8H, m, H-2, 6', 7'), 1.75 (2H, m, H-2'), 1.90-2.08 (8H, m, H-8, 11), 3.33-3.50 (12H, m, H-1, 8', 19, 19''), 3.52-4.06 (7H, m, H-1', 1'', 2'', 3''), 5.34 (4H, m, H-9, 10);

δ_C (75.4 MHz; $CDCl_3$) 14.1 (C-18), 22.7 (C-17), 25.4, 26.1, 26.3, 27.2, 28.8, 29.3-30.0 (signal overlap), 31.9, 32.4, 32.6, 52.2 and 52.4 (C-19, 19'), 62.5 (C-8'), 64.9, 66.3, 68.4, 69.3 and 72.0 (C-1, 1', 1'', 3''), 73.4 (C-2''), 129.8 and 130.0 (C-9, 10);

m/z (+HRFAB) 749.7592 ($[M-Cl]^+$, $C_{49}H_{99}NO_3$ requires 749.7624);

m/z (+FAB) 749 ($[M-Cl]^+$, 100%);

***N*-{2,3-Bis[(*Z*)-octadec-9-enyloxy]propyl}-*N,N*-dimethyl-8-oxooctan-1-aminium chloride (196)**



To a solution of alcohol **197** (0.23 g, 0.29 mmol), *N*-methylmorpholine-*N*-oxide (41 mg, 0.35 mmol) and activated molecular sieves (4Å, powdered; 100 mg) in anhydrous dichloromethane (5 mL), was added tetra-*n*-propylammonium perruthenate (10 mg, 0.03 mmol). After stirring at rt for 10 min, the suspension was

filtered through a small plug of silica gel (~ 2 cm), and the residue washed with dichloromethane (3 × 10 mL), and then concentrated *in vacuo*. Purification by flash chromatography on silica (3% methanol in dichloromethane) yielded *the titled compound* as a yellow oil (0.12 g, 57%).

R_f 0.30 (3% methanol in dichloromethane);

ν_{max} (neat)/cm⁻¹ 2924s, 1722m, 1634w, 1121br m, 1088m;

δ_H (300 MHz; CDCl₃) 0.87 (6H, t, *J* 6.6 Hz, H-18), 1.17-1.43 (48H, m), 1.54 (8H, m, H-2, 6'), 1.75 (2H, m, H-2'), 1.90-2.07 (8H, m, H-8, 11), 2.44 (2H, dt, *J* 1.4 Hz, 7.2, H-7'), 3.32-3.50 (10H, m, H-1, 19, 19'), 3.52-4.06 (7H, m, H-1', 1'', 2'', 3''), 5.35 (4H, m, H-9, 10), 9.76 (1H, t, *J* 1.5 Hz, H-8');

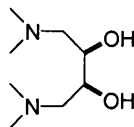
δ_C (125.8 MHz; CDCl₃) 14.5 (C-18), 22.1 (C-17), 23.1, 26.5, 27.6, 29.2, 29.7-30.4 (signal overlap), 32.3, 44.1 (C-7'), 52.5 and 52.8 (C-19, 19'), 68.8, 69.7 and 72.4 (C-1, 1', 1'', 3''; overlap), 73.8 (C-2''), 130.1 (C-9, 10; overlap), 202.9 (C-8');

***m/z* (+HRFAB)** 746.7408 ([M-Cl]⁺, C₄₉H₉₆NO₃ requires 746.7385);

***m/z* (+FAB)** 747 ([M-Cl]⁺, 100%).

8.8 Symmetrical Dicationic Lipids

1,4-Di-(*N,N*-dimethylamino)-2,3-butanediol (**205**)²⁴⁰



Dimethylamine hydrochloride (1.96 g, 24.0 mmol) and *meso*-1,4-dibromo-2,3-butanediol (1.00 g, 4.00 mmol) were subsequently added to a solution of sodium hydroxide (1.28 g, 32.0 mmol) in methanol (7 mL) in a sealed tube at 0 °C. After heated at 80 °C for 24 h, the mixture was concentrated *in vacuo*, and the crude residue dissolved in chloroform (25 mL). The mixture was filtered and the filtrate concentrated *in vacuo* to yield the titled compound as a pale yellow oil (0.69 g, 98%).

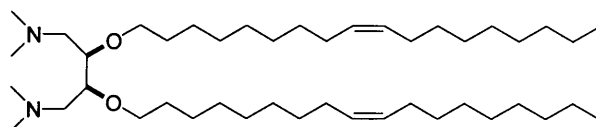
ν_{\max} (neat)/cm⁻¹ 3418br s, 2920s;

δ_{H} (300 MHz; CDCl₃) 2.27 (12H, s, 2 × N(CH₃)₂), 2.35 (2H, dd, *J* 4.9, 12.5 Hz, 2 × NCHH), 2.60 (2H, dd, *J* 8.2, 12.5 Hz, 2 × NCHH), 3.65 (2H, m, 2 × CHOH), 4.45 (2H, br s, 2 × OH);

δ_{C} (75.4 MHz; CDCl₃) 46.2 (N(CH₃)₂), 62.7, (NCH₂) 69.2 (CHOH);

m/z (+ES) 177 ([MH]⁺, 100%).

2,3-Di-[(*Z*)-octadec-9-enyloxy]-1,4-di-(*N,N*-dimethylamino)butane (**206**)



Sodium hydride (60%; 0.40 g, 10.5 mmol) was stirred in anhydrous THF (40 mL) at rt for 15 min. Diol **205** (0.62 g, 3.50 mmol) was added, and the mixture heated at reflux for 4 h. After addition of the mesylate **93** (3.64 g, 10.5 mmol), the mixture was heated at reflux for 48 h. Water (50 mL) was added and the product extracted with ethyl acetate (3 × 50 mL), the combined organic extracts washed with saturated sodium hydrogencarbonate (50 mL) and brine (50 mL), dried over magnesium sulfate, and then concentrated *in vacuo*. Purification by flash chromatography on

silica (gradient; dichloromethane to 10% methanol in dichloromethane) yielded the *titled compound* as dark yellow oil (0.64 g, 27%).

R_f 0.30 (10% methanol in dichloromethane);

ν_{\max} (neat)/ cm^{-1} 2926s, 1655m, 1032w;

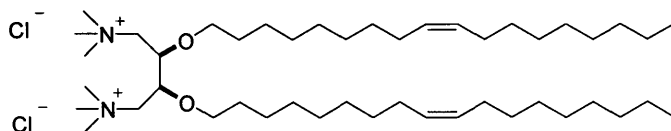
δ_H (300 MHz; CDCl_3) 0.91 (6H, t, J 6.9 Hz, $2 \times \text{CH}_3\text{CH}_2$), 1.15-1.41 (44H, m), 1.55 (4H, m, $2 \times \text{OCH}_2\text{CH}_2$), 2.00 (8H, m, $2 \times \text{CH}_2\text{CH}=\text{CHCH}_2$), 2.24 (14H, m, $2 \times \text{N}(\text{CH}_3)_2$, $2 \times \text{NCHH}$), 2.55 (2H, dd, J 4.2, 12.8 Hz, $2 \times \text{NCHH}$), 3.42-3.75 (6H, m, $2 \times \text{CHO}$, $2 \times \text{OCH}_2\text{CH}_2$), 5.35 (4H, m, $2 \times \text{CH}=\text{CH}$);

δ_C (75.4 MHz; CDCl_3) 14.4 (CH_3CH_2), 23.0, 26.6, 27.6, 29.6-30.1 (signal overlap), 30.6, 32.3, 33.0, 46.6 (NCH_3), 59.5 (NCH_2), 71.2 (OCH_2CH_2), 77.7 (CHO), 130.2 and 130.3 ($\text{CH}=\text{CH}$);

m/z (+HRFAB) 677.6941 (MH^+ , $\text{C}_{44}\text{H}_{89}\text{N}_2\text{O}_2$ requires 677.6924);

m/z (+ES) 678 (MH^+ , 51%), 379 ($\frac{1}{2}\text{M}^+$, 100%).

2,3-Di-[(Z)-octadec-9-enyloxy]-1,4-di-(N,N,N-trimethylammonium)butane dichloride (203)



Diamine **206** (0.31 g, 0.45 mmol) and iodomethane (2.50 mL) were heated in a sealed tube at 90 °C for 24 h. Excess iodomethane was removed *in vacuo*, the crude residue then dissolved in a 1:1 mixture of chloroform/methanol, and passed through an Amberlite® IRA-400 (Cl) ion exchange column eluting with chloroform/methanol (1:1). The filtrate was concentrated *in vacuo* and purified by flash chromatography on silica (10% methanol in dichloromethane) to yield *the titled compound* as a yellow waxy solid (0.37 g, 85%).

R_f 0.22 (10% methanol in dichloromethane);

ν_{\max} (neat)/ cm^{-1} 2917s, 2865s, 1465s;

δ_H (300 MHz; CDCl_3) 0.91 (6H, t, J 6.9 Hz, $2 \times \text{CH}_3\text{CH}_2$), 1.20-1.45 (44H, m), 1.55 (4H, m, $2 \times \text{OCH}_2\text{CH}_2$), 2.00 (8H, m, $2 \times \text{CH}_2\text{CH}=\text{CHCH}_2$), 3.45 (18H, s, $2 \times$

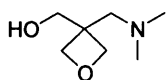
$N^+(CH_3)_3$, 3.75 (2H, m, $2 \times OCHHCH_2$), 4.01 (6H, m, $2 \times OCHHCH_2$, $2 \times N^+CH_2$), 4.50 (2H, m, $2 \times OCH$), 5.35 (4H, m, $2 \times CH=CH$);

δ_C (75.4 MHz; $CDCl_3$) 14.4 (CH_3CH_2), 23.0, 26.7, 27.6, 29.7-30.7, 32.3, 33.0, 55.9 (N^+CH_3), 68.3 (N^+CH_2), 72.5 (OCH_2CH_2), 73.5 (CHO), 130.2 and 130.3 ($CH=CH$);

Anal. ($C_{46}H_{94}N_2O_2 \cdot 2Cl$) found C, 70.82; H, 12.33; N, 3.23; Cl, 10.29; requires C, 71.00, H, 12.18; N, 3.60; Cl, 9.11;

m/z (+ES) 354 ($\frac{1}{2}[M-Cl]^+$, 100%).

3-[(Dimethylamino)methyl]oxetan-3-yl methanol (210)²⁴¹



Dimethylamine hydrochloride (3.74 g, 45.8 mmol) and 2,2-bis(bromomethyl)propane-1,3-diol (1.00 g, 3.82 mmol) were subsequently added to a solution of sodium hydroxide (2.44 g, 61.1 mmol) in water (10 mL) in a sealed tube at 0 °C. After heating at 90 °C for 18 h, the mixture was concentrated *in vacuo* and the crude residue dissolved in chloroform (25 mL), washed with water (30 mL) and brine (30 mL), and then concentrated *in vacuo*. Purification by flash chromatography on silica (dichloromethane) yielded the titled compound as a pale yellow solid (0.40 g, 72%).

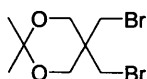
m.p. 60 °C (lit., 62-64 °C);²⁴¹

R_f 0.23 (dichloromethane);

δ_H (300 MHz; $CDCl_3$) 2.25 (6H, s, $2 \times CH_3$), 2.76 (2H, s, CH_2N), 4.06 (2H, s, CH_2OH), 4.38 (2H, d, J 6.2 Hz, $2 \times CCHHO$), 4.48 (2H, d, J 6.2 Hz, $2 \times CCHHO$);

δ_C (75.4 MHz; $CDCl_3$) 42.6 (CH_2CCH_2), 46.6 (NCH_3), 66.8 (CH_2N), 70.0 (CH_2OH), 78.3 (CH_2OCH_2 ; overlap);

m/z (+ES) 146 (MH^+ , 100%).

5,5-Dibromomethyl-2,2-dimethyl-[1,3]-dioxane (211)²⁰⁶

A solution of 2,2-bis(bromomethyl)propane-1,3-diol (5.00 g, 19 mmol) and 2,2-dimethoxypropane (11.6 mL, 95.4 mmol) in glacial acetic acid (40 mL) was heated at reflux for 1 h. The mixture was concentrated *in vacuo*, and the crude residue dissolved in ethyl acetate (40 mL), washed with saturated sodium hydrogencarbonate (40 mL), water (40 mL) and brine (40 mL), dried over magnesium sulphate, and then concentrated *in vacuo*. Purification by flash chromatography on silica (40% dichloromethane in hexane) yielded the titled compound as a colourless oil (3.85 g, 67%).

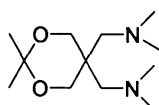
R_f 0.45 (40% dichloromethane in hexane);

ν_{\max} (neat)/ cm^{-1} 2922s, 1107w, 1035br w;

δ_H (300 MHz; CDCl_3) 1.42 (6H, s, $2 \times \text{CH}_3$), 3.58 (4H, s, $2 \times \text{CH}_2\text{Br}$), 3.80 (4H, s, $2 \times \text{OCH}_2$);

δ_C (75.4 MHz; CDCl_3) 23.5 (CH_3), 35.8 (CH_2Br), 37.8 (CH_2CCH_2), 64.9 (OCH_2), 98.9 ($\text{C}(\text{CH}_3)_2$);

m/z (+ES) 325 ($[\text{M}(^{79}\text{Br})+\text{Na}]^+$, 47%), 327 ($[\text{M}(^{81}\text{Br})+\text{Na}]^+$, 100%);

1,1'-(2,2-Dimethyl-1,3-dioxane-5,5-diyl)bis-(*N,N*-dimethylmethanamine) (212)

Dibromide **211** (0.50 g, 1.66 mmol) and aqueous dimethylamine solution (40 wt%; 2 mL) were heated in a sealed tube at 80 °C for 48 h. Water (10 mL) was added, and the product extracted with chloroform (2×15 mL). The combined organic extracts were dried over magnesium sulfate and concentrated *in vacuo* to yield the titled compound as a orange oil, which was used without further purification (0.21 g, 55%).

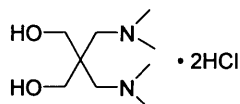
ν_{\max} (neat)/ cm^{-1} 2922s, 1107w, 1035br w;

δ_H (300 MHz; CDCl_3) 1.42 (6H, s, $2 \times \text{CH}_3$), 2.28 (12H, s, $2 \times \text{N}(\text{CH}_3)_2$), 2.34 (4H, s, $2 \times \text{CH}_2\text{N}$), 3.70 (4H, s, $2 \times \text{OCH}_2$);

δ_{C} (75.4 MHz; CDCl_3) 24.0 ($(\text{CH}_3)_2\text{C}$), 39.9 (CH_2CCH_2), 48.7 ($\text{N}(\text{CH}_3)_2$), 61.0 (CH_2N), 64.7 (OCH_2), 97.6 ($\text{C}(\text{CH}_3)_2$);

m/z (+ES) 231 (MH^+ , 100%).

2,2-Di-(dimethylaminomethyl)propane-1,3-diol dihydrochloride (213)²⁴²



Diamine **212** (0.70 g, 0.57 mmol) was stirred in concentrated HCl/water/methanol solution (1:1:5, 49 mL) at rt for 18 h. Water (50 mL) was added and the product extracted with dichloromethane (3×50 mL), the combined organic extracts concentrated *in vacuo* and recrystallised from diethyl ether to yield the titled compound as a pale yellow solid (0.32 g, 55%).

m.p. 204-207 °C (diethyl ether) (lit., 206 °C),²⁴²

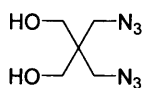
ν_{max} (neat)/ cm^{-1} 3359br m, 2922br s;

δ_{H} (300 MHz; CD_3OD) 3.01 (12H, s, $2 \times \text{HN}^+(\text{CH}_3)_2$), 3.29 (4H, s, $2 \times \text{CH}_2\text{N}^+$), 3.85 (4H, s, $2 \times \text{CH}_2\text{OH}$);

δ_{C} (75.4 MHz; CD_3OD) 29.3 (CH_2CCH_2), 45.9 ($\text{HN}^+(\text{CH}_3)_2$), 57.5 (CH_2N^+), 65.3 (CH_2OH);

m/z (+ES) 191 ($[\text{MH}-2\text{HCl}]^+$, 100%).

2,2Bis(azidomethyl)propane-1,3-diol (218)²⁰⁸



A solution of 2,2-bis(bromomethyl)propane-1,3-diol (1.50 g, 6.05 mmol) and sodium azide (1.97 g, 30.3 mmol) in anhydrous DMF (40 mL) was heated at 100 °C for 48 h. Water (100 mL) was added and the product extracted with diethyl ether (3×50 mL), the combined organic extracts washed with brine (80 mL), dried over magnesium sulfate, and then concentrated *in vacuo*. Purification by flash chromatography on silica (20% acetone in dichloromethane) yielded the titled compound as a colourless oil (1.02 g, 89%).

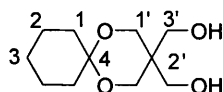
R_f 0.35 (20% acetone in dichloromethane);

δ_H (300 MHz; $CDCl_3$) 2.70 (2H, s, br, $2 \times OH$), 3.40 (4 H, s, $2 \times CH_2OH$), 3.59 (4H, s, $2 \times CH_2N_3$);

δ_C (75.4 MHz; $CDCl_3$) 44.8 (CH_2CCH_2), 51.5 (CH_2N_3), 63.3 (CH_2OH);

m/z (+ES) 187 (MH^+ , 20%), 169 (100%);

3,3-Dihydroxymethyl-1,5-dioxaspiro[5,5]undecane (221)²⁰⁹



A solution of pentaerythritol (3.00g, 22.0 mmol) and $pTsOH \cdot H_2O$ (0.21 g, 0.75 mmol) in anhydrous toluene/DMF solution (2:3, 50 mL) were placed into the lower container of a Soxhlet apparatus. The mixture was heated to 95 °C until complete dissolution of pentaerythritol, and then cyclohexanone (1.52 mL, 15.0 mmol) was added dropwise. The mixture was heated at 130 °C for 48 h, water (50 mL) and saturated sodium hydrogencarbonate (30 mL) were added, and the product extracted with dichloromethane (3×40 mL). The combined organic extracts were washed with brine (50 mL), dried over magnesium sulfate, and then concentrated *in vacuo*. Purification by flash chromatography on silica (30% acetone in hexane) followed by recrystallisation from acetone yielded the titled compound as a white solid (2.85 g, 60%).

m.p. 121-123 °C (acetone) (lit., 123 °C);²⁰⁹

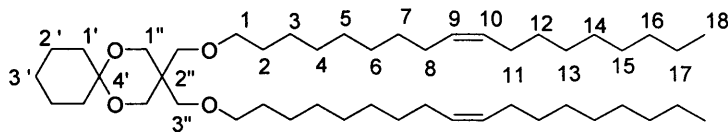
R_f 0.24 (30% acetone in hexane);

ν_{max} (chloroform)/ cm^{-1} 3286br m, 2927s, 1146w, 1107w, 1038m;

δ_H (300 MHz; $CDCl_3$) 1.35-1.59 (6H, m, H-2, 3), 1.75 (4H, m, H-1), 3.74 (4H, s, 3'), 3.77 (4H, s, 1');

δ_C (75.4 MHz; $CDCl_3$) 22.5 (C-2), 25.6 (C-3), 32.5 (C-1), 39.2 (C-2'), 61.9 (C-3'), 65.2 (C-1'), 98.6 (C-4);

m/z (+ES) 239 ($[M+Na]^+$, 100%).

3,3-Di-{[(Z)-octadec-9-enyloxy]methyl}-1,5-dioxaspiro[5,5]undecane (222)

Sodium hydride (95%, 0.35 g, 13.7 mmol) was stirred in anhydrous THF (50 mL) at rt for 15 min. The diol **221** (1.00 g, 4.60 mmol) in anhydrous DMF (5 mL) was added and the mixture heated at 50 °C for 2 h. After addition of the mesylate **93** (4.83 g, 13.9 mmol), the reaction mixture was heated at reflux for 72 h. Water (30 mL) was added and the product extracted with ethyl acetate (3 × 40 mL), the combined organic extracts washed with brine (50 mL), dried over magnesium sulfate, and then concentrated *in vacuo*. Purification by flash chromatography on silica (dichloromethane) yielded *the titled compound* as a pale yellow oil (3.04 g, 90%).

R_f 0.70 (dichloromethane);

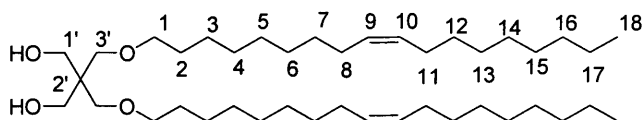
ν_{\max} (neat)/ cm^{-1} 2922s, 1653w, 1105br s, 1042br m;

δ_H (300 MHz; CDCl_3) 0.88 (6H, t, J 6.7 Hz, H-18), 1.16-1.46 (44H, m), 1.55 (10H, m, H-2, 2', 3'), 1.74 (4H, m, H-1'), 2.00 (8H, m, H-8, 11), 3.37 (8H, t, J 6.5 Hz, H-1, 3''), 3.74 (4H, s, H-1''), 5.35 (4H, m, H-9, 10);

δ_C (75.4 MHz; CDCl_3) 14.1 (C-18), 22.6-32.6 (signal overlap), 39.0 (C-2''), 62.0 (C-1''), 70.4 and 71.6 (C-1, 3''), 98.0 (C-4'), 129.8 and 129.9 (C-9, 10);

m/z (+HRES) 717.6740 (MH^+ , $\text{C}_{47}\text{H}_{89}\text{O}_4$ requires 717.6761);

m/z (+ES) 717 (MH^+ , 100%).

2,2-Di-{[(Z)-octadec-9-enyloxy]methyl}propan-1,3-diol (223)

A solution of acetal **222** (3.00 g, 4.18 mmol) in an acetic acid/water (4:1, 30 mL) mixture was stirred at 85 °C for 72 h. Acetic acid was evaporated *in vacuo* and the crude residue dissolved in dichloromethane (40 mL), and then neutralised with saturated sodium hydrogencarbonate. Water (20 mL) was added and the product extracted with dichloromethane (3 × 30 mL), the combined organic extracts washed

with brine (50 mL), dried over magnesium sulfate, and then concentrated *in vacuo*. Purification by flash chromatography on silica (dichloromethane) yielded *the titled compound* as a yellow oil (1.83 g, 69%).

R_f 0.28 (dichloromethane);

ν_{\max} (neat)/ cm^{-1} 3383br m, 2924s, 1109br m, 1043m;

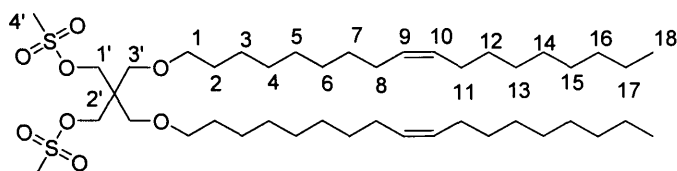
δ_H (300 MHz; CDCl_3) 0.88 (6H, t, J 6.7 Hz, H-18), 1.20-1.43 (44H, m), 1.55 (4H, m, H-2), 2.00 (8H, m, H-8, 11), 3.41 (4H, t, J 6.5 Hz, H-1), 3.50 (4H, s, H-3'), 3.64 (4H, s, H-1'), 5.34 (4H, m, H-9, 10);

δ_C (75.4 MHz; CDCl_3) 14.1 (C-18), 22.7, 26.1, 27.2, 29.3-31.9 (signal overlap), 44.5 (C-2'), 65.5 (C-1'), 72.1 and 73.2 (C-1, 3'), 129.8 and 130.0 (C-9, 10);

m/z (+HRFAB) 637.6100 (MH^+ , $\text{C}_{41}\text{H}_{81}\text{O}_4$ requires 637.6135);

m/z (+FAB) 637 (MH^+ , 100%).

2,2-{Di-[(Z)-octadec-9-enyloxy]methyl}-1,3-{Di-[2-(methanesulfonyloxy)methyl]}propyl ester (224)



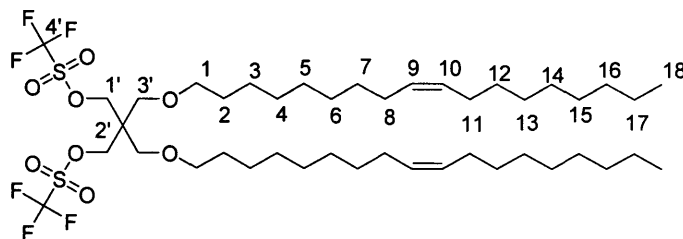
A solution of diol **223** (0.80 g, 1.26 mmol) and methanesulfonyl chloride (0.40 mL, 3.78 mmol) in anhydrous dichloromethane (6 mL) was stirred at rt for 30 min. After cooling to 0 °C, triethylamine (0.44 mL, 3.15 mmol) was added dropwise, and the mixture stirred at for 18 h. Dichloromethane (15 mL) was added and the mixture washed with water (20 mL), saturated sodium hydrogencarbonate solution (20 mL) and brine (20 mL), dried over magnesium sulphate, and then concentrated *in vacuo*. Purification by flash chromatography on silica (50% dichloromethane in hexane) yielded *the titled compound* as a colourless oil (0.92 g, 92%).

R_f 0.35 (50% dichloromethane in hexane);

δ_H (300 MHz; CDCl_3) 0.87 (6H, t, J 6.7 Hz, H-18), 1.20-1.44 (44H, m), 1.52 (4H, m, H-2), 2.01 (8H, m, H-8, 11), 3.01 (6H, s, H-4'), 3.41 (8H, m, H-1, 3'), 4.24 (4H, s, H-1'), 5.35 (4H, m, H-9, 10);

δ_C (75.4 MHz; $CDCl_3$) 14.1 (C-1), 22.7, 26.1, 27.2, 29.3-31.9 (signal overlap), 32.6, 36.9 (C-4'), 44.4 (C-2'), 67.8, 68.4 and 71.8 (C-1, 1', 3'), 129.8 and 130.0 (C-9, 10).

2,2-{Di-[(Z)-octadec-9-enoxy]methyl}-1,3-{Di-[2-(trifluoromethanesulfonyloxy)methyl]}propyl ester (225)



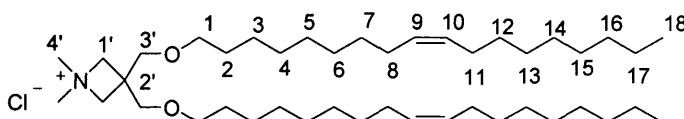
To a solution of trifluoromethanesulfonic anhydride (0.15 mL, 1.10 mmol) and 2,6-di-*tert*-butyl-4-methylpyridine (0.27 mL, 1.18 mmol) in anhydrous dichloromethane (8 mL) was added dropwise diol **223** (0.25 g 0.39 mmol) in anhydrous dichloromethane (4 mL). After stirring at rt for 1 hr, the mixture was concentrated *in vacuo*, the crude residue dissolved in dichloromethane (20 mL), filtered through a short pad (~2 cm) of silica gel, and the filtrate concentrated *in vacuo* to yield the title compound as a yellow oil (0.31 g, 88%), which was used without further purification.

δ_H (300 MHz; $CDCl_3$) 0.88 (6H, t, J 5.9 Hz, H-18), 1.20-1.45 (44H, m), 1.56 (4H, m, H-2), 2.01 (8H, m, H-8, 11), 3.41 (8H, m, H-1, 3'), 4.56 (4H, s, H-1'), 5.35 (4H, m, H-9, 10);

δ_C (75.4 MHz; $CDCl_3$) 14.1 (C-18), 22.7, 26.0, 27.2, 29.3-31.9 (signal overlap), 37.4, 45.0 (C-2'), 67.1 and 71.9 (C-1, 3'), 74.6 (C-1'), 116.2 (C-4'), 129.8 and 130.0 (C-9, 10);

δ_F (282 MHz; $CDCl_3$) 74.7 (CF_3).

3,3-{Di-[(Z)-octadec-9-enoxy]methyl}-*N,N*-dimethylazetidinium chloride (226)



Ditriflate **225** (0.35 g, 0.39 mmol) and dimethylamine solution (2.0 M in THF, 1 mL, 2.00 mmol) were stirred in a sealed tube at rt for 24 h. The mixture was concentrated *in vacuo* and dissolved in a 1:1 mixture of chloroform/methanol, then passed through

an Amberlite® IRA-400 (Cl) ion exchange column eluting with chloroform/methanol (1:1). The solvent was removed *in vacuo* and purified by flash chromatography on silica (10% methanol in dichloromethane) to yield *the titled compound* as a yellow oil (0.11 g, 44%).

R_f 0.33 (10% methanol in dichloromethane);

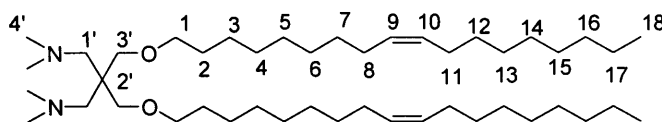
δ_H (300 MHz; $CDCl_3$) 0.87 (6H, t, J 6.6 Hz, H-18), 1.14-1.40 (44H, m), 1.62 (4H, m, H-2), 2.00 (8H, m, H-8, 11), 3.25-3.36 (10H, m, H-1', 4'), 3.53 (4H, t, J 6.8 Hz, H-1), 4.33 (4H, s, H-1'), 5.32 (4H, m, H-9, 10);

δ_C (75.4 MHz; $CDCl_3$) 14.1 (C-18), 22.7, 26.1, 27.2, 29.3-31.9 (signal overlap), 37.2 (C-2'), 52.7 (C-4'), 69.4 and 72.1 (C-1, 1', 3'; overlap), 129.8 and 130.0 (C-9, 10);

m/z (+HRES) 646.6514 ($[M-Cl]^+$, $C_{43}H_{84}NO_2$ requires 646.6497);

m/z (+FAB) 647 ($[M-Cl]^+$, 100%).

2,2-{Di-[(Z)-octadec-9-enyloxy]methyl}-1,3-di-(N,N-dimethyldiamino)propane (214)



Ditriplate **225** (0.35 g, 0.39 mmol) and dimethylamine solution (2.0 M in THF, 4 mL, 8.00 mmol) were stirred in a sealed tube at rt for 24 h. The mixture was concentrated *in vacuo* and purified by flash chromatography on silica (20% methanol in dichloromethane) to yield *the titled compound* as a yellow oil (0.14 g, 52%).

ν_{max} (neat)/ cm^{-1} 2924s, 2855s, 1114br w, 1032w;

R_f 0.25 (20% methanol in dichloromethane);

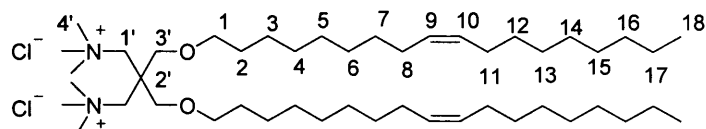
δ_H (300 MHz; $CDCl_3$) 0.87 (6H, t, J 6.7 Hz, H-18), 1.16-1.44 (44H, m), 1.54 (4H, m, H-2), 2.02 (8H, m, H-8, 11), 2.66 (12H, s, H-4'), 2.90 (4H, s, H-1'), 3.37 (8H, m, H-1, 3'), 5.34 (4H, m, H-9, 10);

δ_C (75.4 MHz; $CDCl_3$) 14.1 (C-18), 22.7, 26.2, 27.3, 29.3-31.9 (signal overlap), 47.8 (C-4'), 62.6 (C-1'), 70.3 and 71.6 (C-1, 3'), 129.8 and 130.0 (C-9, 10);

m/z (+ES) 692 (MH^+ , 100%);

m/z (+HRFAB) 691.7062 (MH^+ , $C_{45}H_{91}N_2O_2$ requires 691.7080).

2,2-{Di-[(Z)-octadec-9-enyloxy]methyl}-1,3-di-(N,N,N-trimethylammonium)propane dichloride (227)



Diamine **214** (0.10 g, 0.14 mmol) and iodomethane (2.50 mL) were heated in a sealed tube at 90 °C for 24 h. Excess iodomethane was removed *in vacuo*, and the crude residue dissolved in a 1:1 mixture of chloroform/methanol, and then passed through an Amberlite® IRA-400 (Cl) ion exchange column eluting with chloroform/methanol (1:1). The filtrate was concentrated *in vacuo* and purified by flash chromatography on silica (10% methanol in dichloromethane) to yield *the titled compound* as a pale yellow oil (92 mg, 82%).

R_f 0.20 (20% methanol in dichloromethane);

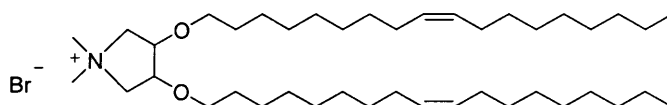
δ_H (300 MHz; $CDCl_3$) 0.88 (6H, m, H-18), 1.15-1.42 (44H, m), 1.56 (4H, m, H-2), 2.00 (8H, m, H-8, 11), 3.38-3.61 (30 H, m, H-1, 1', 3', 4'), 5.34 (4H, m, H-9, 10);

δ_C (75.4 MHz; $CDCl_3$) 14.0 (C-18), 22.6, 26.2, 27.2, 29.2-31.9, 55.7 (C-4'), 68.1, 68.4 and 71.6 (C-1, 1', 3'), 129.7 and 130.0 (C-9, 10);

Anal. ($C_{47}H_{96}Cl_2N_2O_2$) found C, 70.97; H, 11.87; N, 3.43; Cl, 10.14; requires C, 71.26, H, 12.21; N, 3.54; Cl, 8.95;

m/z (+ES) 361 ($\frac{1}{2}[M-Cl]^+$, 100%).

3,4-Di-[(Z)-octadec-9-enyloxy]-N,N-dimethylpyrrolidinium bromide (229a)



A mixture of amine **206** (30 mg, 0.04 mmol) and 2-bromoethanol (30 mg, 0.18 mmol) was stirred in a sealed tube at 40 °C for 24 h. Purification by flash chromatography on silica (5% methanol in dichloromethane) yielded *the titled compound* as a yellow oil (20 mg, 63%).

R_f 0.32 (5% methanol in dichloromethane);

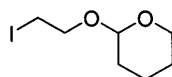
δ_{H} (300 MHz; CDCl_3) 0.87 (6H, t, J 6.7 Hz, $2 \times \text{CH}_3\text{CH}_2$), 1.18-1.43 (44H, m), 1.55 (4H, m, $2 \times \text{OCH}_2\text{CH}_2$), 2.00 (8H, m, $2 \times \text{CH}_2\text{CH}=\text{CHCH}_2$), 3.49 (4H, m, $2 \times \text{OCH}_2\text{CH}_2$), 3.67 (6H, s, $\text{N}^+(\text{CH}_3)_2$), 3.86 (2H, dd, J 2.4, 9.9 Hz, $2 \times \text{CHOCH}_2$), 4.05 (2H, d, J 9.9 Hz, $2 \times \text{N}^+\text{CHH}$), 4.11 (2H, d, J 2.4 Hz, $2 \times \text{N}^+\text{CHH}$), 5.34 (4H, m, $2 \times \text{CH}=\text{CH}$);

δ_{C} (75.4 MHz; CDCl_3) 14.1 (CH_3CH_2), 23.0, 22.7, 26.1, 27.2, 29.3-29.8 (signal overlap), 31.9, 57.7 ($\text{N}^+(\text{CH}_3)_2$), 70.6 (OCH_2), 70.8 (N^+CH_2), 81.4 (CHOCH_2), 129.8 and 130.0 ($\text{CH}=\text{CH}$);

m/z (+HRFAB) 633.6446 ($[\text{M}-\text{Br}]^+$, $\text{C}_{42}\text{H}_{82}\text{NO}$ requires 633.6418);

m/z (+ES), 633 ($[\text{M}-\text{Br}]^+$, 100%).

2-(2-Iodoethoxy)-tetrahydro-2H-pyran (233)²¹¹



1-Iodoethanol (3.50 g, 20.3 mmol) and 3,4-dihydro-2H-pyran (2.44 mL, 24.4 mmol) were stirred in anhydrous dichloromethane (50 mL) at rt. $p\text{TsOH} \cdot \text{H}_2\text{O}$ (0.39 g, 2.03 mmol) was added and the mixture stirred for 2 h, diluted with dichloromethane (30 mL), washed with water (50 mL), saturated sodium hydrogencarbonate solution (50 mL) and brine (50 mL), dried over magnesium sulfate, and then concentrated *in vacuo*. Purification by flash chromatography on silica (5% ethyl acetate in hexane) yielded the titled compound as a colourless oil (4.78 g, 92%).

R_f 0.45 (5% ethyl acetate in hexane);

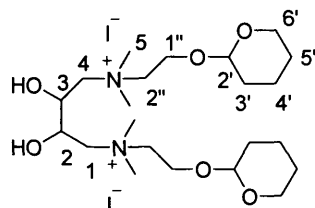
ν_{max} (neat)/ cm^{-1} 2941s, 1121m, 1026m;

δ_{H} (300 MHz; CDCl_3) 1.51-1.86 (6H, m), 3.29 (2H, dt, J 1.3, 6.5 Hz, CH_2I), 3.54 (1H, m, OCHH), 3.72 (1H, m, OCHH), 3.86-4.03 (2H, m, $2 \times \text{OCHH}$), 4.68 (1H, t, J 3.3 Hz, OCHO);

δ_{C} (75.4 MHz; CDCl_3) 3.5 (CH_2I), 19.3, 25.4, 30.5, 62.3 (OCH_2), 68.3 (OCH_2), 98.7 (OCHO);

m/z (+ES) 257 (MH^+ , 100%).

2,3-Dihydroxy-1,4-di-({*N*-[2-(tetrahydro-2*H*-pyran-2-yloxy)]-*N,N*-dimethylammonium}ethyl)butane diiodide (234)



A solution of iodide **233** (0.58 g, 2.27 mmol) and diamine **205** (0.20 g, 1.13 mmol) in anhydrous acetone (4 mL) was stirred in a sealed tube for 7 days. The mixture was concentrated *in vacuo* and dissolved in methanol (25 mL), washed with diethyl ether (3 × 30 mL) and hexane (3 × 30 mL), and then concentrated *in vacuo* to yield the titled compound as a clear yellow gum (0.42 g, 26%).

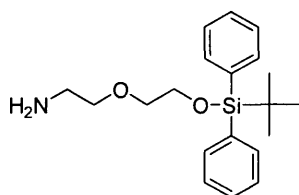
δ_{H} (300 MHz; CDCl_3) 1.55 (8H, m, H-4', 5'), 1.77 (4H, m, H-3'), 3.42-4.29 (28H, m, H-1, 4, 5, 6', 1'', 2''), 4.65 (2H, m, H-2'), 4.71 (2H, d, J 7.9 Hz, H-2, 3);

δ_{C} (75.4 MHz; CDCl_3) 19.4 (C-4'), 25.4 (C-5'), 30.5 (C-3'), 52.4 (C-5), 61.3-69.4 (C-1, 4, 1'', 2'', 6'; overlap), 72.2 (C-2, 3; overlap), 99.9 (C-2');

m/z (+HRES) 434.3331 ($[\text{M}-2\text{I}]^{2+}$, $\text{C}_{22}\text{H}_{46}\text{N}_2\text{O}_6$ requires 434.3345);

m/z (+ES) 561 ($[\text{M}-\text{I}]^+$, 100%), 433 ($[\text{M}-2\text{I}]^{2+}$, 14%).

2-[2-(*tert*-Butyldiphenylsilyloxy)ethoxy]ethylamine (242)²¹²



Imidazole (3.50 g, 51.4 mmol) and *tert*-butyldiphenylsilyl chloride (5.44 mL, 20.9 mmol) were added to 2-(2-aminoethoxy)ethanol (2.00 g, 19.0 mmol). The mixture was stirred at rt for 18 h, dichloromethane (50 mL) and water (50 mL) were added, and the product extracted into dichloromethane (3 × 40 mL). The combined organic extracts were washed with brine (100 mL), dried over magnesium sulfate, and then concentrated *in vacuo*. Purification by flash chromatography on silica (5% methanol in dichloromethane) yielded the titled compound as a colourless oil (4.04 g, 62%)

R_f 0.47 (5% methanol in dichloromethane);

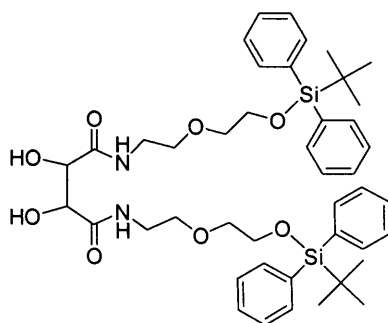
ν_{\max} (neat)/ cm^{-1} 3350br m, 2930s, 1113br s;

δ_{H} (300 MHz; CDCl_3) 1.05 (9H, s, $\text{C}(\text{CH}_3)_3$), 1.63 (2H, s, br, NH_2), 2.84 (2H, t, J 5.2 Hz, CH_2NH_2), 3.48 (2H, t, J 5.2 Hz, $\text{SiOCH}_2\text{CH}_2$), 3.57 (2H, t, J 5.2 Hz, $\text{CH}_2\text{CH}_2\text{N}$), 3.81 (2H, t, J 5.2 Hz, SiOCH_2), 7.49 (6H, m, Ar-H), 7.68 (4H, m, Ar-H);

δ_{C} (75.4 MHz; CDCl_3) 19.2 ($(\text{CH}_3)_3\text{C}$), 26.3 ($(\text{CH}_3)_3\text{C}$), 42.0 (CH_2NH_2), 63.5 (SiOCH_2), 72.2 and 73.4 (CH_2OCH_2), 127.7, 129.6, 133.7 and 135.6 (Ar-C);

m/z (+FAB) 344 (MH^+ , 100%).

***N,N'*-Di-{2-[2-(*tert*-butyldiphenylsilanyloxy)ethoxy]ethyl}-2,3-dihydroxysuccinamide (243)**



To a solution of DL-tartaric acid (0.60 g, 1.05 mmol), *N*-(3-dimethylaminopropyl)-*N'*-ethylcarbodiimide hydrochloride (1.99 g, 10.4 mmol) and 1-hydroxy-1*H*-benzotriazole (1.40 g, 10.4 mmol) in anhydrous DMF (18 mL) was added triethylamine (1.55 mL, 11.0 mmol) and amine **242** (3.57 g, 10.4 mmol). The mixture was stirred for 18 h, water (50 mL) was added, and the product extracted with di-*tert*-butyl ether (3 × 30 mL). The combined organic extracts were washed with brine (50 mL), dried over sodium sulfate, and then concentrated *in vacuo*. The waxy crude residue was dissolved in methanol (40 mL), washed with hexane (3 × 30 mL), and then concentrated *in vacuo* to yield the titled compound as a yellow gum (3.02 g, 94%).

ν_{\max} (neat)/ cm^{-1} 3335br m, 2930s, 1683s, 1113br m;

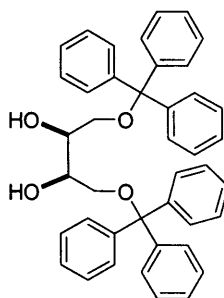
δ_{H} (300 MHz; CDCl_3) 1.05 (18H, s, 2 × $\text{C}(\text{CH}_3)_3$), 3.48 (12 H, m, 2 × $\text{NCH}_2\text{CH}_2\text{OCH}_2$), 3.79 (2H, t, J 5.1 Hz, 2 × CH_2OSi), 4.27 (2H, s, 2 × OCHC=O), 5.14 (2H, br s, 2 × NHCH_2), 7.35-7.43 (12 H, m, Ar-H), 7.65-7.70 (8H, m, Ar-H);

δ_C (75.4 MHz; $CDCl_3$) 19.2 ($((CH_3)_3C)$), 26.8 ($((CH_3)_3C)$), 39.0 ($NHCH_2$), 63.4 (CH_2OSi), 70.6 ($OCHC=O$), 69.5 and 72.4 (CH_2OCH_2), 127.7, 129.7, 133.6 and 135.6 (Ar-C), 173.7 ($C=O$);

m/z (+HRFAB) 801.3990 (MH^+ , $C_{44}H_{61}N_2O_8Si_2$ requires 801.3966);

m/z (+FAB) 801 (MH^+ , 100%).

***meso*-1,4-Di-(triphenylmethyl)-butane-2,3-diol (250)**²¹³



A solution of *meso*-erythritol (3.00 g, 24.6 mmol) and triphenylmethyl chloride (15.0 g, 27.0 mmol) in anhydrous pyridine/dichloromethane mixture (1:1, 60 mL) was stirred at rt for 18 h. Dichloromethane (40 mL) was added, and the mixture washed with hydrochloric acid solution (2M, 50 mL), sodium carbonate solution (2M, 50 mL) and water (50 mL), dried over magnesium sulfate, and then concentrated *in vacuo*. Purification by flash chromatography on silica (10% ethyl acetate in toluene) yielded the titled compound as a white solid (5.46 g, 37%).

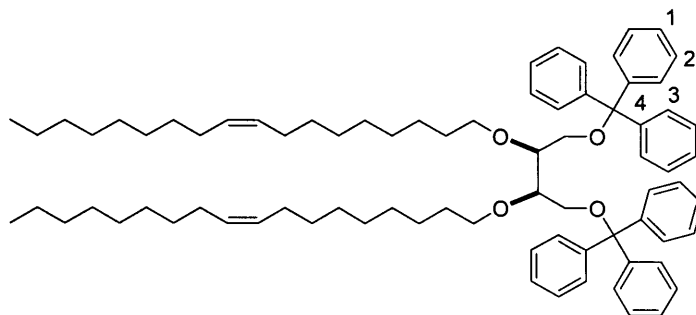
m.p. 186 °C (lit, 182-184 °C);²⁴³

R_f 0.39 (30% acetone in hexane);

δ_H (300 MHz; $CDCl_3$) 2.65 (2H, br s, $2 \times OH$), 3.21 (4H, d, J 4.4 Hz, $2 \times CH_2O$), 3.83 (2H, m, CH_2CHOH), 7.20-7.60 (30H, m, Ar-H);

δ_C (75.4 MHz; $CDCl_3$) 65.0 ($CHCH_2$), 71.8 ($CHCH_2$), 87.4 (CPh_3), 127.5, 128.3, 128.9 and 144.0 (Ar-C);

m/z (+ES) 607 (MH^+ , 26%), 243 (Ph_3C^+ , 100%);

meso-2,3-Di-[(Z)-octadec-9-enyloxy]-1,4-di-(triphenylmethyloxy)butane (251)

Sodium hydride (95%, 0.12 g, 4.60 mmol) was stirred in anhydrous DMF (20 mL) at rt for 15 min. The diol **250** (0.93 g, 1.53 mmol) in anhydrous DMF (5 mL) was added and the mixture heated at 50 °C for 1 h. After addition of the mesylate **93** (1.60 g, 4.60 mmol), the reaction mixture was heated at reflux for 72 h. Water (40 mL) was added and the product extracted with ethyl acetate (3 × 40 mL), the combined organic extracts washed with brine (50 mL), dried over magnesium sulfate, and then concentrated *in vacuo*. Purification by flash chromatography on silica (5% methanol in dichloromethane) yielded *the titled compound* as a pale yellow oil (0.67 g, 38%).

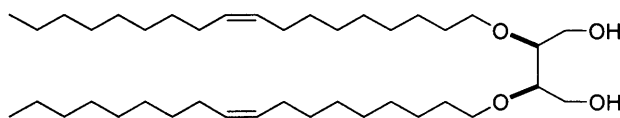
R_f 0.63 (dichloromethane);

δ_H (300 MHz; $CDCl_3$) 0.87 (6H, m, 2 × CH_3), 1.11-1.46 (48H, m), 2.01 (8H, m, 2 × $CH_2CH=CHCH_2$), 3.16 (2H, d, J 9.2 Hz, 2 × $OCHCH_2$), 3.24-3.39 (4H, m, 2 × $OCHHCH_2$, 2 × $OCHCHHO$), 3.52-3.59 (4H, m, 2 × $OCHHCH_2$, 2 × $OCHCHHO$), 5.34 (4H, m, 2 × $CH=CH$), 7.17-7.71 (30H, m, Ar-H);

δ_C (75.4 MHz; $CDCl_3$) 14.1 (CH_3), 22.7, 26.2, 27.3, 29.3-29.8 (signal overlap), 31.9, 62.1 ($CHCH_2O$), 71.3 (OCH_2CH_2), 78.2 ($CHCH_2O$), 86.4 (CPh_3), 126.8, 127.7 and 128.8 (C-1, 2, 3), 129.9 ($CH=CH$), 144.3 (C-4);

m/z (+HRFAB) 1129.7976 ($[M+Na]^+$, $C_{78}H_{106}O_4Na$ requires 1129.7983);

m/z (+FAB) 1131 ($[M+Na]^+$, 21%), 243 (Ph_3C^+ , 100%).

meso-2,3-Di-[(Z)-octadec-9-enyloxy]butane-1,4-diol (248)

To a solution of ditrityl **251** (0.50, 0.45 mmol) in anhydrous dichloromethane (10 mL) was added trifluoroacetic acid (84 μ L, 1.13 mmol) and triethylsilane (0.18 mL, 1.13 mmol). The mixture was stirred at rt for 30 min and then concentrated *in vacuo*. Purification by flash chromatography on silica (dichloromethane) yielded *the titled compound* as a colourless oil (0.16 g, 57%).

R_f 0.24 (dichloromethane);

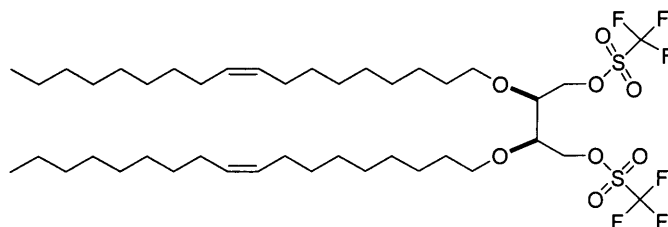
ν_{\max} (neat)/ cm^{-1} 3379br s, 2924s, 1651w, 1096 br m, 1034m;

δ_H (300 MHz; CDCl_3) 0.88 (6H, t, J 6.7 Hz, $2 \times \text{CH}_3$), 1.17-1.40 (44H, m), 1.54 (4H, tt, J 6.6, 6.7 Hz, $2 \times \text{OCH}_2\text{CH}_2$), 2.00 (8H, m, $2 \times \text{CH}_2\text{CH}=\text{CHCH}_2$), 3.42 (2H, m, $2 \times \text{OCHCH}_2$), 3.58 (4H, m, $2 \times \text{OCH}_2\text{CH}_2$), 3.67 (4H, m, $2 \times \text{CHHOH}$), 3.79 (4H, dd, J 3.5, 12.6 Hz, $2 \times \text{CHHOH}$), 5.34 (4H, m, $2 \times \text{CH}=\text{CH}$);

δ_C (75.4 MHz; CDCl_3) 14.1 (CH_3), 22.7, 26.1, 27.2, 29.3-30.1 (signal overlap), 31.9, 61.3 (CH_2OH), 70.8 (OCH_2CH_2), 79.2 (OCHCH_2), 129.8 and 130.0 ($\text{CH}=\text{CH}$);

m/z (+HRES) 645.5779 ($[\text{M}+\text{Na}]^+$, $\text{C}_{40}\text{H}_{78}\text{O}_4\text{Na}$ requires 645.5792);

m/z (+ES) 646 ($[\text{M}+\text{Na}]^+$, 100%);

2,2-{Di-[(Z)-octadec-9-enyloxy]methyl}-1,4-{Di-[2-(trifluoromethanesulfonyloxy)methyl]}butyl ester (252)

To a solution of trifluoromethanesulfonic anhydride (93 μ L, 0.67 mmol) and 2,6-di-*tert*-butyl-4-methylpyridine (0.15 mL, 0.67 mmol) in anhydrous dichloromethane (5 mL) was added dropwise diol **248** (0.14 g 0.22 mmol) in anhydrous dichloromethane (2 mL). After stirring at rt for 1 hr, the mixture was concentrated *in vacuo*. The crude

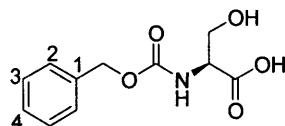
residue was dissolved in dichloromethane (10 mL), filtered through a short pad (~ 2 cm) of silica, and the filtrate concentrated *in vacuo* to yield *the title compound* as a yellow oil (0.15 g, 76%), which was used without further purification.

δ_{H} (300 MHz; CDCl_3) 0.88 (6H, m, $2 \times \text{CH}_3$), 1.17-1.40 (44H, m), 1.55 (4H, m, $2 \times \text{OCH}_2\text{CH}_2$), 2.00 (8H, m, $2 \times \text{CH}_2\text{CH}=\text{CHCH}_2$), 3.55-3.67 (4H, m, $2 \times \text{OCH}_2\text{CH}_2$), 4.05 (4H, m, $2 \times \text{CHCH}_2$), 4.32- 4.45 (4H, m, $2 \times \text{OCHCH}_2$), 5.35 (4H, m, $2 \times \text{CH}=\text{CH}$);

δ_{F} (282 MHz; CDCl_3) 74.7 (CF_3).

8.9 Lipopeptides and Immunoliposomes

(S)-2-Benzylloxycarbonylamino-3-hydroxypropionic acid (**258**)²¹⁵



To a suspension of sodium hydrogencarbonate (10.0 g 119 mmol) in THF (25 mL) and water (50 mL) at rt was carefully added L-serine (5.00 g, 47.7 mmol). After stirring for 10 min, benzyl chloroformate (7.50 mL, 52.5 mmol) was added dropwise over 30 min, and stirring continued for 1 h. The mixture was washed with diethyl ether (2 × 25 mL) and carefully acidified with hydrochloric acid solution (1 M) to pH 3, the product extracted with ethyl acetate (2 × 25 mL), and the combined organic phase washed with hydrochloric acid solution (2 × 25 mL) and brine (40 mL), dried over magnesium sulfate, and then concentrated *in vacuo*. Recrystallisation from chloroform/hexane yielded the titled compound as a white solid (8.23 g, 78%).

m.p. 115–117 °C (chloroform/hexane) (lit., 114–115 °C);²⁴⁴

ν_{\max} (nujol)/cm⁻¹ 3345br s, 3334s, 1745m, 1688m;

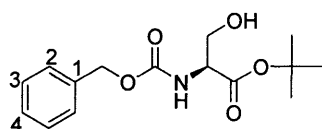
δ_{H} (300 MHz; D₂O) 3.90 (2H, m, CH₂OH), 4.30 (1H, m, NCH), 5.15 (2H, s, PhCH₂), 7.36–7.46 (5H, m, Ar-H);

δ_{C} (75.4 MHz; D₂O) 58.0 (NCH), 63.3 (CH₂OH), 67.1 (PhCH₂), 128.6, 128.7 and 129.2 (C-2, 3, 4), 138.4 (C-1), 157.0 (NC=O), 172.4 (OC=O);

m/z (+ES) 262 ([M+Na]⁺, 100%);

$[\alpha]_{\text{D}}^{13} +2.30^{\circ}$ (*c* 1.41, MeOH) (lit., +2.45 °, *c* 0.42, MeOH).²¹⁷

(S)-2-Benzylloxycarbonylamino-3-hydroxypropionic acid *tert*-buty ester (**259**)²¹⁶



A solution of acid **258** (8.23 g, 36.7 mmol), benzyltriethylammonium chloride (8.40 g, 36.6 mmol) and potassium carbonate (33.0 g, 239 mmol) in anhydrous acetonitrile (66 mL) was stirred vigorously at rt for 5 h. 2-Bromo-2-methyl propane (41.1 mL,

374.3 mmol) was added and the mixture heated at 50 °C for 3 h. Anhydrous acetonitrile (40 mL) was added and stirring was continued at 50 °C for 18 h. The mixture was concentrated *in vacuo*, the crude residue dissolved in water (100 mL), and the product extracted with ethyl acetate (3 × 100 mL). The combined organic extracts were washed with water (150 mL) and brine (150 mL), dried over magnesium sulfate, and then concentrated *in vacuo*. Recrystallisation from ethyl acetate/hexane yielded the titled compound as a white solid (4.53 g, 45%).

m.p. 85-87 °C (ethyl acetate/hexane) (lit., 89-90 °C);²⁴⁵

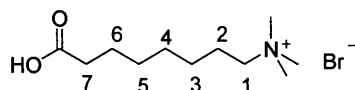
δ_{H} (300 MHz; CDCl₃) 1.46 (9H, s, C(CH₃)₃), 2.47 (1H, s, br, OH), 3.93 (2H, dd, *J* 3.8, 5.9 Hz, CH₂OH), 4.32 (1H, m, NCH), 5.06 (2H, s, PhCH₂), 5.65 (1H, m, NH), 7.32 (5H, m, Ar-H);

δ_{C} (75.4 MHz; CDCl₃) 28.0 (C(CH₃)₃), 56.7 (NHCH), 63.8 (CH₂OH), 67.1 (PhCH₂), 82.8 (C(CH₃)₃), 128.1, 128.2 and 128.5 (C-2, 3, 4), 136.2 (C-1), 156.2 (OC=O), 169.5 (OC=O);

***m/z* (+ES)** 296 (MH⁺, 100%);

$[\alpha]_{\text{D}}^{13}$ -15.5 ° (*c* 1.13, ethanol) (lit., -15.9 °, *c* 1.10, ethanol).²¹⁸

7-Carboxyheptyl-*N,N,N*-trimethylammonium bromide (261)



A solution of 8-bromoocatanoic acid (0.20 g, 0.87 mmol) and aqueous triethylamine solution (45 wt.%, 1.3 mL, 8.7 mmol) in toluene (4 mL) was heated in a sealed tube at 80 °C for 72 h. The mixture was concentrated *in vacuo* and recrystallised from ethanol to yield *the titled compound* as a white solid (0.15 g, 59%).

m.p. 122 °C (ethanol);

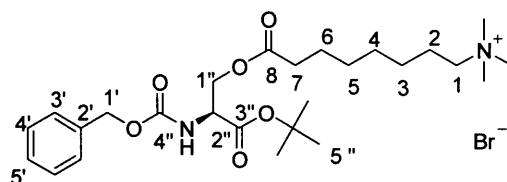
ν_{max} (chloroform)/cm⁻¹ 3018br s, 2945br s, 1720s;

δ_{H} (300 MHz; CD₃OD) 1.28-1.51 (6H, m, H-3, 4, 5), 1.62 (2H, tt, *J* 7.0, 7.3 Hz, H-6), 1.81 (2H, m, H-2), 2.30 (2H, t, *J* 7.3 Hz, H-7), 3.14 (9H, s, N⁺(CH₃)₃), 3.36 (2H, m H-1);

δ_{C} (75.4 MHz; CD_3OD) 23.8, 25.9, 27.1, 29.8, 29.9, 34.8 (C-7), 53.6 (CH_3), 67.8 (C-1), 177.6 (C=O);

m/z (+ES) 202 ($[\text{M}-\text{Br}]^+$, 100%);

(*S*)-[7-(2-Benzoyloxycarbonylamino-2-*tert*-butoxycarbonyl-ethoxycarbonyl)heptyl]-*N,N,N*-trimethylammonium bromide (**262**)



To a solution of alcohol **259** (1.73 g, 5.87 mmol), acid **261** (1.50 g, 5.34 mmol), *N*-(3-dimethylaminopropyl)-*N'*-ethylcarbodiimide hydrochloride (1.38 g, 8.01 mmol) and 1-hydroxy-1*H*-benzotriazole (1.08 g, 8.01 mmol) in anhydrous DMF (40 mL) was added triethylamine (1.20 mL, 8.54 mmol). After stirring for 96 h at rt, the mixture was evaporated *in vacuo*, dissolved in ethyl acetate (50 mL), and then passed through a short pad (~ 5 cm) of Celite[®]. The filtrate was concentrated *in vacuo* and purified by flash chromatography on silica (gradient; dichloromethane to 5% methanol in dichloromethane) to yield *the titled compound* as a pale yellow thick oil (1.08 g, 36%).

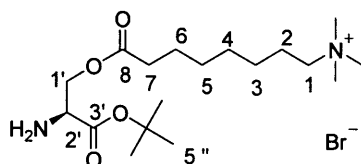
R_f 0.29 (5% methanol in dichloromethane);

δ_{H} (300 MHz; CDCl_3) 1.24 (6H, m, H-3, 4, 5), 1.36 (9H, s, H-5''), 1.48 (2H, tt, J 6.7, 7.3 Hz, H-6), 1.63 (2H, m, H-2), 2.18 (2H, t, J 7.3 Hz, H-7), 3.31 (9H, s, $\text{N}^+(\text{CH}_3)_3$), 3.43 (2H, m, H-1), 4.33 (1H, dd, J 2.4, 11.2 Hz, H-1''), 4.42-4.55 (2H, m, H-1'', 2''), 5.02 (2H, s, H-1'), 5.58 (1H, d, J 7.6 Hz, NH), 7.13-7.32 (5H, m, Ar-H);

δ_{C} (125 MHz; CDCl_3) 22.8 (C-2), 24.4, 25.8, 27.8 (C-5'') 28.6 (overlap), 33.7 (C-7), 53.3 ($\text{N}^+(\text{CH}_3)_3$), 53.9 (C-2''), 64.2, 66.7 and 67.0 (C-1, 1', 1''), 82.9 ($\text{C}(\text{CH}_3)_3$), 128.1, 128.2 and 128.5 (C-3', 4', 5'), 136.1 (C-2'), 155.7 (C-4''), 168.3 and 173.1 (C-8, 3'');

m/z (+ES) 480 ($[\text{M}-\text{Br}]^+$, 100%);

(S)-[7-(2-Amino-2-*tert*-butoxycarbonyl-ethoxycarbonyl)heptyl]-*N,N,N*-trimethylammonium bromide (263)



A solution of compound **262** (0.50 g, 1.04 mmol) and palladium on carbon (50 mg) in ethanol (2 mL) was vigorously stirred under a hydrogen atmosphere at rt for 18 h. The mixture was filtered through a short pad (~2 cm) of Celite[®] and then concentrated *in vacuo* to yield *the titled product* as a colourless oil (0.42 g, 95%).

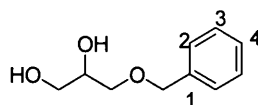
R_f 0.24 (10% methanol in dichloromethane);

δ_H (300 MHz; CDCl₃) 1.25 (6H, m, H-3, 4, 5), 1.36 (9H, s, H-5''), 1.49 (2H, tt, *J* 6.7, 7.3 Hz, H-6), 1.63 (2H, m, H-2), 1.90 (2H, br s, NH₂), 2.17 (2H, t, *J* 7.3 Hz, H-7), 3.35 (9H, s, N⁺(CH₃)₃), 3.43-3.55 (3H, m, H-1, 2'), 4.30-4.53 (2H, m, H-1');

δ_C (125 MHz; CDCl₃) 22.8 (C-2), 24.4, 25.7, 27.6 (C-5') 28.5 (overlap), 33.7 (C-7), 53.0 (C-2'), 53.3 (N⁺(CH₃)₃), 66.7 and 67.0 (C-1, 1'), 82.9 (C(CH₃)₃), 168.5 and 173.1 (C-8, 3');

m/z (+ES) 345 ([M-Br]⁺, 100%).

3-Benzoyloxypropane-1,2-diol (268)²²¹



(±)-Glycidol (2.50 g, 33.7 mmol), cesium fluoride (5.15 g, 33.7 mmol) and benzyl alcohol (4.19 mL, 40.5 mmol) were heated at 120 °C in a sealed tube for 96 h. Purification by flash chromatography on silica (17% hexane in ethyl acetate) yielded the titled compound as a colourless oil (4.37 g, 71%).

R_f 0.30 (17% hexane in ethyl acetate);

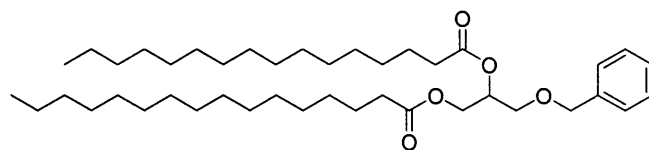
ν_{max} (neat)/cm⁻¹ 3381br s, 2947m, 1078br m;

δ_{H} (300 MHz; CDCl_3) 3.51 (1H, m, CHOH), 3.64 (2H, m, $\text{CH}_2\text{OCH}_2\text{Ph}$), 3.85 (2H, m, CH_2OH), 4.50 (2H, s, CH_2Ph), 7.24-7.35 (5H, m, Ar-H);

δ_{C} (75.4 MHz; CDCl_3) 64.0 (CH_2OH), 70.9 and 71.6 (CH_2OCH_2), 73.5 (CH), 127, 127.8 and 128.5 (C-2, 3, 4), 137.8 (C-1);

m/z (+ES) 205 ($[\text{M}+\text{Na}]^+$, 100%).

3-Benzyl-1,2-di-hexadecanoyl-glycerol (271)²⁴⁶



To a solution of diol **268** (1.50 g, 8.23 mmol), hexadecanoic acid (5.28 g, 20.6 mmol) and 4-dimethylaminopyridine (1.00 g, 8.23 mmol) in anhydrous dichloromethane (10 mL) was added dropwise a solution of *N,N'*-dicyclohexylcarbodiimide (5.10 g, 24.7 mmol) in anhydrous dichloromethane (10 mL). The mixture was stirred at rt for 24 h and then filtration through Celite[®]. The filtrate was concentrated *in vacuo* and purified by flash chromatography on silica (5% ethyl acetate in hexane) to yield the titled compound as a white solid (3.20 g, 59%).

m.p. 38-40 °C (lit., 41-42, ethanol);²⁴⁶

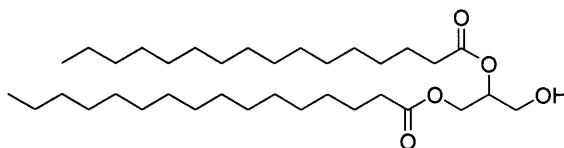
R_f 0.50 (5% ethyl acetate in hexane);

ν_{max} (chloroform)/ cm^{-1} 2924s, 1744s, 1167br m;

δ_{H} (300 MHz; CDCl_3) 0.88 (6H, t, J 6.6 Hz, $2 \times \text{CH}_3$), 1.25 (48H, m), 1.61 (4H, m, $2 \times \text{O}=\text{CCH}_2\text{CH}_2$), 2.27 (4H, m, $2 \times \text{O}=\text{CCH}_2$), 3.58 (2H, d, J 5.2 Hz, BnOCH_2CH), 4.18 (1H, dd, J 6.4, 11.9 Hz, $\text{BnOCH}_2\text{CHCHH}$), 4.34 (1H, dd, J 3.8, 11.9 Hz, $\text{BnOCH}_2\text{CHCHH}$), 4.53 (2H, d, J 3.5 Hz, PhCH_2), 5.24 (1H, m, CH_2CHCH_2), 7.28-7.37 (5H, m, Ar-H);

δ_{C} (75.4 MHz; CDCl_3) 14.1 (CH_3), 22.8, 24.9, 29.1-29.7 (signal overlap), 30.9, 31.9, 34.1 and 34.4 ($2 \times \text{O}=\text{CCH}_2\text{CH}_2$; overlap), 62.8 ($\text{OCH}_2\text{CHCH}_2\text{OBn}$), 68.3 and 71.0 ($\text{PhCH}_2\text{OCH}_2$), 73.3 (CHCH_2), 127.7, 127.8, 128.5 and 137.7 (Ar-C), 173.2 and 173.5 ($2 \times \text{O}=\text{C}$);

m/z (+ES) 660 (MH^+ , 100%).

1,2-Di-hexadecanoyl-glycerol (272)

To a solution of compound **271** (0.88 g, 1.33 mmol) in anhydrous dichloromethane (20 mL) at -78°C was added dropwise boron trichloride solution (1.0 M in dichloromethane, 1.33 mL, 1.33 mmol). After stirring for 10 min at -78°C , the reaction was stirred at rt for 30 min. Water (20 mL) was added dropwise and the mixture extracted with ethyl acetate (3×15 mL), the combined organic extracts washed with brine (30 mL), dried over magnesium sulfate, and then concentrated *in vacuo*. Purification by flash chromatography on silica (30% ethyl acetate in hexane) yielded the titled compound as a white solid (0.52 g, 68%).

m.p. $64\text{--}66^{\circ}\text{C}$ (lit., $67\text{--}68^{\circ}\text{C}$, ethanol);²⁴⁶

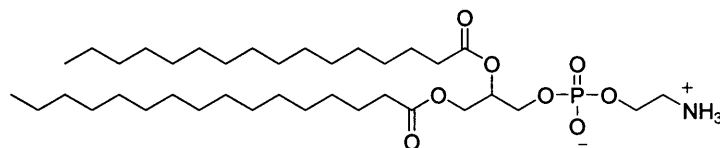
R_f 0.36 (30% ethyl acetate in hexane);

ν_{max} (chloroform)/ cm^{-1} 3422br m, 2924s, 1744s, 1167br m;

δ_{H} (300 MHz; CDCl_3) 0.88 (6H, t, J 6.3 Hz, $2 \times \text{CH}_3$), 1.25 (48H, m), 1.60 (4H, m, $2 \times \text{O}=\text{CCH}_2\text{CH}_2$), 2.32 (2H, t, J 7.3 Hz, $\text{O}=\text{CCH}_2\text{CH}_2$), 2.34 (2H, t, J 7.3 Hz, $\text{O}=\text{CCH}_2\text{CH}_2$), 3.72 (2H, m, OHCH_2), 4.23 (1H, dd, J 5.7, 12.0 Hz, $\text{HOCH}_2\text{CHCHH}$), 4.32 (1H, dd, J 4.5, 11.9 Hz, $\text{HOCH}_2\text{CHCHH}$), 5.08 (1H, m, CH_2CHCH_2);

δ_{C} (75.4 MHz; CDCl_3) 14.1 (CH_3), 22.7, 29.3–29.7 (signal overlap), 34.1 and 34.4 ($2 \times \text{O}=\text{CCH}_2$; overlap), 62.8 ($\text{OCH}_2\text{CHCH}_2\text{OBn}$), 63.3 (CH_2OH), 71.9 (CH_2CHCH_2), 173.4 and 174.1 ($2 \times \text{O}=\text{C}$);

m/z (+ES) 592 ($[\text{M}+\text{Na}]^+$, 100%).

1,2-Di-hexadecanoyl-glycero-3-phosphoethanolamine (265)²²⁶

To a solution of alcohol **272** (0.48 g, 0.84 mmol) and triethylamine (0.24 mL, 1.26 mmol) in anhydrous benzene (15 mL) was added 2-chloro-1,3,2-dioxaphospholane-2-oxide (93 μ L, 1.01 mmol). After stirring for 24 h at rt, the mixture was filtered through Celite[®] and concentrated *in vacuo*, the residue then dissolved in a mixture of anhydrous benzene/acetonitrile (1:1, 60 mL), and a stream of ammonia bubbled through the solution for 6 h. The resulting slurry was concentrated *in vacuo* and purified by flash chromatography on silica (10:4:1, chloroform/methanol/ammonium hydroxide) to yield the titled compound as a white waxy solid (0.12 g, 21%).

m.p. 184-189 °C (lit., 190-191, ethanol);²²⁶

R_f 0.75 (10:4:1, chloroform/methanol/ammonium hydroxide);

δ_{H} (300 MHz; CD₃OD) 0.89 (6H, m, 2 \times CH₃), 1.28 (48H, m), 1.60 (4H, m, 2 \times O=CCH₂CH₂), 2.32 (4H, m, 2 \times O=CCH₂), 3.30 (3H, m, ⁺NH₃), 3.56 (2H, m, CH₂⁺NH₃), 3.85-4.03 (4H, m, CH₂OPOCH₂), 4.17 (1H, m, OCHHCHCH₂OP), 4.44 (1H, m, OCHHCHCH₂OP), 5.22 (1H, m, CH₂CHCH₂);

δ_{P} (121 MHz; CD₃OD) 1.78 (OPO);

***m/z* (-ES)** 691 ([M-H]⁻, 23%).

8.10 Biological Formulation and Methods

Preparation of Lipid Films

Cationic Lipids were either formulated alone or with DOPE (weight ratio, 1:1). Lipid (10 mg/mL; 100 μ L [1 mg of lipid]) in chloroform was placed into a sterile glass vial. The solvents were removed *in vacuo* and further traces of chloroform removed on the high vacuum for 24 h.

Preparation of Liposomes

Sterile water (1 mL) was added to the lipid film, to generate a 1 mg/mL (total lipid) lipid suspension in water. The suspension was allowed to hydrate at 4 °C for 24 h. After warming to 40 °C the mixture was sonicated (bath sonication) for approximately 5 min to generate a clear solution. The resulting liposome formulations were stable for up to 6 months.

Preparation of LID Complexes

The components of the LID vector complex were mixed in lipid/peptide/DNA weight ratios of 0.75:4:1, 2:4:1 or 4:4:1 with DNA at a concentration of 0.25 μ g/mL. The lipid was initially mixed with the peptide and the resulting mixture added to the plasmid DNA.

Transfection methods

In vitro transfections were performed by Dr. Stephanie Grosse (ICH) and carried out as described by Hart *et al.*^{137,140} Samples were analysed 24 h later by luciferase chemiluminescent assays (Promega, Madison, WI, USA) using a Lucy-1 Luminometer (Anthos Ltd., Salzburg, Austria), with activity expressed as relative light units per mg of protein (RLU/mg). Each experiment was performed at least three times.

For *in vivo* transfections, lung tissue was processed and chemiluminescent assays in tissue extracts performed as described by Jenkins *et al.*¹⁸ (performed by Dr. Aris Tagalakis, ICH). Samples were analysed in luciferase assays using a TD-20/20

Luminometer (Turner BioSystems, San Francisco, USA) with activity expressed as RLU/mg. At least seven animals were used per group for luciferase assays.

8.11 Biophysical Methods

Preparation of Calcein-Loaded Liposomes²⁴⁷

Dried lipid film (1 mg of lipid) was hydrated with 1 mL of phosphate buffer (pH 7.5; 136.9 mM NaCl, 2.68 mM KCl, 8.1 mM K₂HPO₄, 1.47 mM KH₂PO₄) containing 80 mM calcein (lipid concentration 1-2 μM), at which concentration its fluorescence was self quenched. After warmed to 40 °C the suspension was sonicated for 5 min to generate a dark purple-orange solution. Non-encapsulated calcein was removed by dialysis at 25 °C (Peribo Sciences UK Ltd, Tattenhall, UK) against several changes in 0.01 M phosphate buffer saline (0.0027 M KCl, 0.137 M NaCl).

Calcein Release Assays

Calcein release assays were performed as described by Sarkar *et al.*^{149,179} Briefly, 8 mL of calcein-loaded liposomes was added to 40 mL of MES-buffered saline (140 mM NaCl, 10 mM MES) at various pH values (pH 5.0-7.4). As the intensity of calcein fluorescence is pH sensitive, the pH of all samples was carefully adjusted to pH 7.4 before determining fluorescence. Calcein fluorescence was measured at $\lambda_{\text{ex}} = 490$ nm and $\lambda_{\text{em}} = 520$ nm, using a Fluoromax-3 fluorimeter (Jobin Yvon Horiba, Middlesex, UK). The percentage leakage of calcein from the lipid was measured using the formula below:

$$\% \text{ leakage} = \left(\frac{I_{\text{pH}} - I_0}{I_{100} - I_0} \right) \times 100$$

where I_0 is the fluorescence at neutral pH, I_{pH} is the fluorescence of the pH range tested (after correction) and I_{100} the totally released calcein from the sample at pH 7.4 after sonication.

TLC Analysis of PEG-Acetal Lipid Degradation

Hydrolysis study of PEG-acetal lipids were performed in duplicate between pH 3.0 and 7.5, at 0.5 pH interval. In each case a liposome formulation (1 mL; 1 mg/mL) containing the PEG-acetal lipid was prepared as describe previously (see Section 8.10). Part of this solution (0.15 mL) was added into HMA buffers (0.55 mL; 10 mM HEPES, 10 mM MES, 10 mM sodium acetate, 100 mM NaCl) at various pH values (pH 3.0-7.5), to achieve final lipid concentrations between 0.19-0.23 mM. After the solutions were incubated at 37 °C for a period of 30 min to 3 h, aliquots (0.30 mL) were removed and immediately neutralised by adding few drops of saturated sodium hydrogencarbonate solution. Few drops of the mixtures were spotted on normal phase silica TLC plates, with few drops of the selected glycol solution (**183**, **184**, **161**; 10 mg/mL in CH₂Cl₂, see Section 4.1.1) spotted as a standard. TLC plates were developed and stained in phosphomolybdic acid (PMA) solution, to show the degradation of the PEG-acetal lipid.

CHAPTER 9

REFERENCES

- (1) Little, P. F. R. *Genome Res.* **2005**, *15*, 1759.
- (2) Schmutz, J.; Wheeler, J.; Grimwood, J.; Dickson, M.; Yang, J.; Caoile, C.; Bajorek, E.; Black, S.; Chan, Y. M.; Denys, M.; Escobar, J.; Flowers, D.; Fotopulos, D.; Garcia, C.; Gomez, M.; Gonzales, E.; Haydu, L.; Lopez, F.; Ramirez, L.; Retterer, J.; Rodriguez, A.; Rogers, S.; Salazar, A.; Tsai, M.; Myers, R. M. *Nature* **2004**, *429*, 365.
- (3) Lotze, M. T. *Gene Ther.* **2005**, *13*, 191.
- (4) Alton, E. W. F. W.; M Stern, M.; Farley, R.; Jaffe, A.; Chadwick, S. L.; Phillips, J.; Davies, J.; Smith, S. N.; Browning, J.; Davies, M. G.; Hodson, M. E.; Durham, S. R.; Li, D.; Jeffery, P. K.; Scallan, M.; Balfour, R.; Eastman, S. J.; Cheng, S. H.; Smith, A. E.; Meeker, D.; Geddes, D. M. *LANCET* **1999**, *353*, 947.
- (5) Griesenbach, U.; Geddes, D. M.; Alton, E. *Gene Ther.* **2004**, *11*, S43.
- (6) Aiuti, A. *Best Prac. Res. Cl. Ha.* **2004**, *17*, 505.
- (7) Strayer, D. S.; Akkina, R.; Bunnell, B. A.; Dropulic, B.; Planelles, V.; Pomerantz, R. J.; Rossi, J. J.; Zaia, J. A. *Mol. Ther.* **2005**, *11*, 823.
- (8) For information see <http://www.wiley.co.uk/wileychi/genmed/clinical/>
- (9) Lecocq, M.; Andrianaivo, F.; Warnier, M. T.; Wattiaux-De Coninck, S.; Wattiaux, R.; Jadot, M. *J. Gene Med.* **2003**, *5*, 142.
- (10) Felnerova, D.; Viret, J. F.; Gluck, R.; Moser, C. *Curr. Opin. Biotechnol.* **2004**, *15*, 518.
- (11) Somia, N.; Verma, I. M. *Nature Rev. Genetics* **2000**, *1*, 91.
- (12) Kohn, D. B.; Sadelain, M.; Glorioso, J. C. *Nature Rev. Cancer* **2003**, *3*, 477.
- (13) Crystal, R. G. *Science* **1995**, *270*, 404.
- (14) Wood, K. J.; Fry, J. *Exp. Rev. Mol. Med.* **1999**, *1*, 1.
- (15) Mulligan, R. C. *Science* **1993**, *260*, 926.
- (16) Gilgenkrantz, H.; Duboc, D.; Juillard, V.; Cuton, D.; Pavirani, A.; Guillet, J. G.; Briand, P.; Kahn, A. *Hum. Gene Ther.* **1995**, *6*, 1265.
- (17) Yang, N. S.; Burkholder, J.; Roberts, B.; Martinell, B.; McCabe, D. *Proc. Natl. Acad. Sci. USA* **1990**, *87*, 267.
- (18) Jenkins, R. G.; Herrick, S. E.; Meng, Q.-H.; Kinnon, C.; Laurent, G. J.; J., M. R.; Hart, S. L. *Gene Ther.* **2000**, *7*, 393.
- (19) Anand, A. 'Gene Delivery' In *Manufacturing of gene therapeutics- methods, processing, regulation, and validation*; Subramani, G., Ed.; Springer-Verlag: New York, 2001, p 245.
- (20) Muruve, D. A. *Hum. Gene Ther.* **2004**, *15*, 1157.
- (21) Marshall, E. *Science* **1999**, *286*, 2244.
- (22) Pack, D. W.; Hoffman, A. S.; Pun, S.; Stayton, P. S. *Nature Rev. Drug Discovery* **2005**, *4*, 581.
- (23) Zhang, S. B.; Xu, Y. M.; Wang, B.; Qiao, W. H.; Liu, D. L.; Li, Z. S. *J. Controlled Release* **2004**, *100*, 165.
- (24) Brown, M. D.; Schatzlein, A. G.; Uchegbu, I. F. *Int. J. Pharm.* **2001**, *229*, 1.

9. References

- (25) Kostiainen, M. A.; Szilvay, G. R.; Smith, D. K.; Linder, M. B.; Ikkala, O. *Angew. Chem. Int. Ed.* **2006**, *45*, 3538.
- (26) Lim, Y.-B.; Han, S.-O.; Kong, H.-U.; Lee, Y.; Park, J.-S.; Jeong, B.; Kim, S. W. *Pharm. Res.* **2000**, *17*, 811.
- (27) Chiou, H. C.; Tangco, M. V.; Levine, S. M.; Robertson, D.; Kormis, K.; Wu, C. H.; Wu, G. Y. *Nucl. Acids Res.* **1994**, *22*, 5439.
- (28) Kabanov, A. V. *PPTS* **1999**, *2*, 365.
- (29) Pouton, C. W.; Lucas, P.; Thomas, B. J.; Uduehi, A. N.; Milroy, D. A.; Moss, S. H. *J. Controlled Release* **1998**, *53*, 289.
- (30) Gruner, S. M.; Cullis, P. R.; Hope, M. J.; Tilcock, C. P. S. *Annu. Rev. Biophys. Biophys. Chem.* **1985**, *14*, 211.
- (31) Walde, P.; Ichikawa, S. *Biomol. Eng.* **2001**, *18*, 143.
- (32) Lasic, D. D. *J. Controlled Release* **1997**, *48*, 203.
- (33) Lian, T.; Ho, R. J. Y. *J. Pharm. Sci.* **2001**, *90*, 667.
- (34) Ulrich, A. S. *Bioscience Rep.* **2002**, *22*, 129.
- (35) Fraley, R.; Subramani, S.; Berg, P.; Papahadjopoulos, D. *J. Biol. Chem.* **1980**, *255*, 10431.
- (36) Wong, Y.; Nicolau, C.; Hans Hofschneider, P. *Gene* **1980**, *10*, 87.
- (37) Felgner, P. L.; Gadek, T. R.; Holm, M.; Roman, R.; Chan, H. W.; Wenz, M.; Northrop, J. P.; Ringold, G. M.; Danielsen, M. *Proc. Natl. Acad. Sci. USA* **1987**, *84*, 7413.
- (38) Miller, A. D. *Angew. Chem. Int. Ed.* **1998**, *37*, 1769.
- (39) For information see <http://www.invitrogen.com/content.cfm?pageid=4011>
- (40) Felgner, J. H.; Kumar, R.; Sridhar, C. N.; Wheeler, C. J.; Tsai, Y. J.; Border, R.; Ramsey, P.; Martin, M.; Felgner, P. L. *J. Biol. Chem.* **1994**, *269*, 2550.
- (41) Zuidam, N. J.; Barenholz, Y. *Biochem. Biophys. Acta* **1998**, *1368*, 115.
- (42) Koltover, I.; Salditt, T.; Radler, J. O.; Sadiyah, C. R. *Science* **1998**, *281*, 78.
- (43) Leventis, R.; Silvius, J. R. *Biochim. Biophys. Acta* **1990**, *1023*, 124.
- (44) Wheeler, C. J.; Felgner, P. L.; Tsai, Y. J.; Marshall, J.; Sukhu, L.; Doh, S. G.; Hartikka, J.; Nietupski, J.; Manthorpe, M.; Nichols, M.; Plewe, M.; Liang, X.; Norman, J.; Smith, A.; Cheng, S. H. *PNAS* **1996**, *93*, 11454.
- (45) Ren, T.; Liu, D. *Bioorg. Med. Chem. Lett.* **1999**, *9*, 1247.
- (46) Ren, T.; Liu, D. *Tetrahedron Lett.* **1999**, *40*, 209.
- (47) Ren, T.; Song, Y. K.; Zhang, G.; Liu, D. *Gene Ther.* **2000**, *7*, 764.
- (48) Behr, J.-P.; Demeneix, B.; Loeffler, J.-P.; Pereaz-Mutul, J. *Proc. Natl. Acad. Sci. USA* **1989**, *86*, 6982.
- (49) Gebeyehu, G.; Jessee, J. A.; Ciccarone, V. C.; Hawley-Nelson, P.; Chytil, A. *US Patent #5,334,761* **1992**.
- (50) For information see <http://www.invitrogen.com/content/sfs/manuals/18324012.pdf>
- (51) Gao, X.; Huang, L. *Biochem. Biophys. Res. Commun.* **1991**, *179*, 280.

9. References

- (52) Caplen, N. J.; Kinrade, E.; Sorgi, F.; Gao, X.; Gruenert, D.; Geddes, D.; Coutelle, C.; Huang, L.; Alton, E. W. F. W.; Williamson, R. *Gene Ther.* **1995**, *2*, 603.
- (53) Oudrhiri, N.; Vigneron, J. P.; Peuchmaur, M.; Leclerc, T.; Lehn, J. M.; Lehn, P. *Proc. Natl. Acad. Sci. USA* **1997**, *94*, 1651.
- (54) Tagawa, T.; Manvell, M.; Brown, N.; Keller, M.; Perouzel, E.; Murray, K. D.; Harbottle, R. P.; Tecle, M.; Booy, F.; Brahimi-Horn, M. C.; Coutelle, C.; Lemoine, N. R.; W., A. E. W. F.; Miller, A. D. *Gene Ther.* **2002**, *9*, 564.
- (55) Spagnou, S.; Miller, A. D.; Keller, M. *Biochemistry* **2004**, *43*, 13348.
- (56) Rose, J. K.; Buonocore, L.; Whitt, M. A. *Biotechniques* **1991**, *10*, 520.
- (57) Meekel, A. A. P.; Wagenaar, A.; Smisterova, J.; Kroeze, J. E.; Haadsma, P.; Bosgraaf, B.; Stuart, M. C. A.; Brisson, A.; Ruiters, M. H. J.; Hoekstra, D.; Engberts, J. *Eur. J. Org. Chem.* **2000**, 665.
- (58) Smisterova, J.; Wagenaar, A.; Stuart, M. C. A.; Polushkin, E.; ten Brinke, G.; Hulst, R.; Engberts, J. B. F. N.; Hoekstra, D. *J. Biol. Chem.* **2001**, *276*, 47615.
- (59) Majeti, B. K.; Singh, R. S.; Yadav, S. K.; Bathula, S. R.; Ramakrishna, S.; Diwan, P. V.; Madhavendra, S. S.; Chaudhuri, A. *Chem. Biol.* **2004**, *11*, 427.
- (60) Ferrari, M. E.; Rusalov, D.; Enas, J.; Wheeler, C. J. *Nucl. Acids Res.* **2002**, *30*, 1808.
- (61) van der Woude, I.; Wagenaar, A.; Meekel, A. A. P.; TerBeest, M. B. A.; Ruiters, M. H. J.; Engberts, J.; Hoekstra, D. *Proc. Natl. Acad. Sci. USA* **1997**, *94*, 1160.
- (62) Obika, S.; Yu, W.; Shimoyama, A.; Uneda, T.; Miyashita, K.; Doi, T.; Imanishi, T. *Bioorg. Med. Chem.* **2001**, *9*, 245.
- (63) Fletcher, S.; Ahmad, A.; Perouzel, E.; Heron, A.; Miller, A. D.; Jorgensen, M. *R. J. Med. Chem.* **2006**, *49*, 349.
- (64) Kirby, A. J.; Camilleri, P.; Engberts, J.; Feiters, M. C.; Nolte, R. J. M.; Soderman, O.; Bergsma, M.; Bell, P. C.; Fielden, M. L.; Rodriguez, C. L. G.; Guedat, P.; Kremer, A.; McGregor, C.; Perrin, C.; Ronsin, G.; van Eijk, M. C. P. *Angew. Chem. Int. Ed.* **2003**, *42*, 1448.
- (65) Rosenzweig, H. S.; Rakhmanova, V. A.; MacDonald, R. C. *Bioconjugate Chem.* **2001**, *12*, 258.
- (66) Aberle, A. M.; Tablin, F.; Zhu, J.; Walker, N. J.; Gruenert, D. C.; Nantz, M. H. *Biochemistry* **1998**, *37*, 6533.
- (67) For information see <http://www.promega.com/faq/tfxtrio.html>
- (68) Schenborn, E.; Oler, J.; Goiffon, W. *Promega Notes* **1996**, *59*, 24.
- (69) Bombelli, C.; Faggioli, F.; Luciani, P.; Mancini, G.; Sacco, M. G. *J. Med. Chem.* **2005**, *48*, 5378.
- (70) Buijnsters, P.; Rodriguez, C. L. G.; Willighagen, E. L.; Sommerdijk, N.; Kremer, A.; Camilleri, P.; Feiters, M. C.; Nolte, R. J. M.; Zwanenburg, B. *Eur. J. Org. Chem.* **2002**, 1397.
- (71) Lasic, D. D.; Needham, D. *Chem. Rev.* **1995**, *95*, 2601.
- (72) Song, Y. K.; Liu, D. *Biochim. Biophys. Acta* **1998**, *1372*, 141.

9. References

- (73) Hong, K. L.; Zheng, W. W.; Baker, A.; Papahadjopoulos, D. *FEBS Lett.* **1997**, *400*, 233.
- (74) Sternberg, B.; Hong, K. L.; Zheng, W. W.; Papahadjopoulos, D. *Biochem. Biophys. Acta* **1998**, *1375*, 23.
- (75) Harvie, P.; Wong, F. M. P.; Bally, M. B. *J. Pharm. Sci.* **2000**, *89*, 652.
- (76) Webb, M. S.; Saxon, D.; Wong, F. M. P.; Lim, H. J.; Wang, Z.; Bally, M. B.; Choi, L. S. L.; Cullis, P. R.; Mayer, L. D. *Biochem. Biophys. Acta* **1998**, *1372*, 272.
- (77) Zhang, Y. P.; Sekirov, L.; Saravolac, E. G.; Wheeler, J. J.; Tardi, P.; Clow, K.; Leng, E.; Sun, R.; Cullis, P. R.; Scherrer, P. *Gene Ther.* **1999**, *6*, 1438.
- (78) Boomer, J. A.; Thompson, D. H. *Chem. Phys. Lipids* **1999**, *99*, 145.
- (79) Boomer, J. A.; Inerowicz, H. D.; Zhang, Z. Y.; Bergstrand, N.; Edwards, K.; Kim, J. M.; Thompson, D. H. *Langmuir* **2003**, *19*, 6408.
- (80) Thompson, D. H.; Shin, J.; Boomer, J.; Kim, J.-M.; Nejat, D. 'Preparation of Plasmenylcholine Lipids and Plasmenyl-Type Liposome Dispersions' In *Methods in Enzymology*; Academic Press: 2004; Vol. Volume 387, p 153.
- (81) Guo, X.; Szoka, F. C. *Bioconjugate Chem.* **2001**, *12*, 291.
- (82) Guo, X.; MacKay, J. A.; Szoka, F. C. *Biophys. J.* **2003**, *84*, 1784.
- (83) Li, W. J.; Huang, Z. H.; MacKay, J. A.; Grube, S.; Szoka, F. C. *J. Gene Med.* **2005**, *7*, 67.
- (84) Gillies, E. R.; Goodwin, A. P.; Frechet, J. M. J. *Bioconjugate Chem.* **2004**, *15*, 1254.
- (85) By, K.; Nantz, M. H. *Angew. Chem. Int. Ed.* **2004**, *43*, 1117.
- (86) Huang, Z.; Guo, X.; Li, W.; MacKay, J. A.; Szoka, F. C. *J. Am. Chem. Soc.* **2006**, *128*, 60.
- (87) Litzinger, D. C.; Huang, L. *Biochim. Biophys. Acta* **1992**, *1113*, 201.
- (88) Hafez, I. M.; Ansell, S.; Cullis, P. R. *Biophys. J.* **2000**, *79*, 1438.
- (89) Edler, K. J. *Philos. Trans. R. Soc. London, Ser. A* **2004**, *362*, 2635.
- (90) Toombes, G. E. S.; Finnefrock, A. C.; Tate, M. W.; Gruner, S. M. *Biophys. J.* **2002**, *82*, 2504.
- (91) Seddon, J. M.; Cevc, G.; Marsh, D. *Biochemistry* **1983**, *22*, 1280.
- (92) Wang, J.; Gao, X.; Xu, Y.; Barron, L.; Szoka, F. C. *J. Med. Chem.* **1998**, *41*, 2207.
- (93) Binder, H.; Gawrisch, K. *J. Phys. Chem. B* **2001**, *105*, 12378.
- (94) Sternberg, B.; Sorgi, L.; Huang, L. *FEBS Lett.* **1994**, *356*, 361.
- (95) Gustafsson, J.; Arvidson, G.; Karlsson, G.; Almgren, M. *Biochim. Biophys. Acta* **1995**, *1235*, 305.
- (96) Radler, J. O.; Koltover, I.; Salditt, T.; Safinya, C. R. *Science* **1997**, *275*, 810.
- (97) May, S.; Harries, D.; Ben-Shaul, A. *Biophys. J.* **2000**, *78*, 1681.
- (98) Templeton, N. S. *Bioscience Reps.* **2002**, *22*, 283.
- (99) Wrobel, I.; Collins, D. *Biochim. Biophys. Acta* **1995**, *1235*, 296.

9. References

- (100) Zabner, J.; Fasbender, A. J.; Moninger, T.; Poellinger, K. A.; Welsh, M. J. *J. Biol. Chem.* **1995**, *270*, 18997.
- (101) Noguchi, A.; Furuno, T.; Kawaura, C.; Nakanishi, M. *FEBS Lett.* **1998**, *433*, 169.
- (102) Stamatatos, L.; Leventis, R.; Zuckermann, M. J.; Silviu, J. R. *Biochemistry* **1988**, *27*, 3917.
- (103) Duzgunes, N.; Goldstein, J. A.; Friend, D. S.; Felgner, P. L. *Biochemistry* **1989**, *28*, 9179.
- (104) Xu, Y.; Szoka, F. C. *Biochemistry* **1996**, *35*, 5616.
- (105) Bhattacharya, S.; Mandal, S. S. *Biochemistry* **1998**, *37*, 7764.
- (106) Capecchi, M. R. *Cell* **1980**, *22*, 479.
- (107) Lechardeur, D.; Sohn, K. J.; Haardt, M.; Joshi, P. B.; Monck, M.; Graham, R. W.; Beatty, B.; Squire, J.; O'Brodovich, H.; Lukacs, G. L. *Gene Ther.* **1999**, *6*, 482.
- (108) Pollard, H.; Toumaniantz, G.; Amos, J. L.; Avet-Loiseau, H.; Guihard, G.; Behr, J. P.; Escande, D. *J. Gene Med.* **2001**, *3*, 153.
- (109) Zanta, M. A.; Belguise-Valladier, P.; Behr, J. P. *Proc. Nat. Acad. Sci. USA* **1999**, *96*, 91.
- (110) Cartier, R.; Reszka, R. *Gene Ther.* **2002**, *9*, 157.
- (111) Oliver, M.; Jorgensen, M. R.; Miller, A. *Tetrahedron Lett.* **2004**, *45*, 3105.
- (112) Kunitake, T.; Okahata, Y. *Bull. Chem. Soc. Jap.* **1978**, *51*, 1877.
- (113) Banerjee, R.; Das, P. K.; Srilakshmi, G. V.; Chaudhuri, A.; Rao, N. M. *J. Med. Chem.* **1999**, *42*, 4292.
- (114) Wolff, J. A. *Nature Biotechnology* **2002**, *20*, 768.
- (115) Hofland, H. E. J.; Masson, C.; Iginla, S.; Osetinsky, I.; Reddy, J. A.; Leamon, C. P.; Scherman, D.; Bessodes, M.; Wils, P. *Mol. Ther.* **2002**, *5*, 739.
- (116) Maruyama, K. *Biosci. Rep.* **2002**, *22*, 251.
- (117) Hart, S. L.; Harbottle, R.; Cooper, R.; Miller, A.; Williamson, R.; Coutelle, C. *Gene Ther.* **1995**, *2*, 552.
- (118) Gregoriadis, G. E.; Neerunjun, D. *Biochem. Biophys. Res. Commun.* **1975**, *65*, 537.
- (119) Martin, F. J.; Hubbell, W. L.; Papahadjopoulos, D. *Biochemistry* **1981**, *20*, 4229.
- (120) Martin, F. J.; Papahadjopoulos, D. *J. Biol. Chem.* **1982**, *257*, 286.
- (121) Maruyama, K.; Takizawa, T.; Yuda, T.; Kennel, S. J.; Huang, L.; Iwatsuru, M. *Biochem. Biophys. Acta* **1995**, *1234*, 74.
- (122) Huang, A.; Kennel, S. J.; Huang, L. *J. Biol. Chem.* **1983**, *258*, 4034.
- (123) Kirpotin, D.; Park, J. W.; Hong, K.; Zalipsky, S.; Li, W. L.; Carter, P.; Benz, C. C.; Papahadjopoulos, D. *Biochemistry* **1997**, *36*, 66.
- (124) Zalipsky, S.; Hansen, C. B.; Lopes de Menezes, D. E.; Allen, T. M. *J. Controlled Release* **1996**, *39*, 153.

9. References

- (125) Maruyama, K.; Takahashi, N.; Tagawa, T.; Nagaike, K.; Iwatsuru, M. *FEBS Lett.* **1997**, *413*, 177.
- (126) Zhang, Y.; Boado, R. J.; Pardridge, W. M. *J. Gene Med.* **2003**, *5*, 157.
- (127) Zhang, Y.; Schlachetzki, F.; Pardridge, W. M. *Mol. Ther.* **2003**, *7*, 11.
- (128) Lee, C. H.; Hsiao, M.; Tseng, Y. L.; Chang, F. H. *J. Biomed. Sci.* **2003**, *10*, 337.
- (129) Pirollo, K. F.; Zon, G.; Rait, A.; Zhou, Q.; Yu, W.; Hogrefe, R.; Chang, E. H. *Hum. Gene Ther.* **2006**, *17*, 117.
- (130) Ruoslahti, E. *Annu. Rev. Cell Dev. Biol.* **1996**, *12*, 697.
- (131) Rankin, S.; Isberg, R. R.; Leong, J. M. *Infect. Immun.* **1992**, *60*, 3909.
- (132) Logan, D.; Abu-Ghazaleh, R.; Blakemore, W.; Curry, S.; Jackson, T.; King, A.; Lea, S.; Lewis, R.; Newman, J.; Parry, N.; Rowlands, D.; Stuart, D.; Fry, E. *Hum. Gene Ther.* **1993**, *362*, 566.
- (133) Wickham, T. J.; Filardo, E. J.; Cheresch, D. A.; Nemerow, G. R. *J. Cell. Biol.* **1994**, *127*, 257.
- (134) Hart, S. L.; Knight, A. M.; Harbottle, R. P.; Mistry, A.; Hunger, H.-D.; Cutler, D. F.; Williamson, R.; Coutelle, C. *J. Biol. Chem.* **1994**, *269*, 12468.
- (135) Isberg, R. P.; Tran Van Nhieu, G. *Trends Cell Biol.* **1995**, *5*, 120.
- (136) Hart, S. L.; Collins, L.; Gustafsson, K.; Fabre, J. W. *Gene Ther.* **1997**, *4*, 1225.
- (137) Harbottle, R. P.; Cooper, R. G.; Hart, S. L.; Ladhoff, A.; McKay, T.; Knight, A. M.; Wagner, E.; Miller, A. D.; Coutelle, C. *Hum. Gene Ther.* **1998**, *9*, 1037.
- (138) Pasqualini, R.; Koivunen, E.; Ruoslahti, E. *Nat. Biotechnol.* **1997**, *15*, 542.
- (139) Cooper, R. G.; Harbottle, R. P.; Schneider, H.; Coutelle, C.; Miller, A. D. *Angew. Chem. Int. Ed.* **1999**, *38*, 1949.
- (140) Hart, S. L.; Arancibia-Carcamo, C. V.; Wolfert, M. A.; Mailhos, C.; O'Reilly, N. J.; Ali, R. R.; Coutelle, C.; George, A. J. T.; Harbottle, R. P.; Knight, A. M.; Larkin, D. F. P.; Levinsky, R. J.; Seymour, L. W.; Thrasher, A. J.; Kinnon, C. *Hum. Gene Ther.* **1998**, *9*, 575.
- (141) Jenkins, R. G.; Meng, Q.-H.; Hodges, R. J.; Lee, L. K.; Bottoms, S. E. W.; Laurent, G. J.; Wills, D.; Ayazi Shamlou, P.; MaAnulty, R.; Hart, S. L. *Gene Ther.* **2003**, *10*, 1026.
- (142) Cunningham, S.; Meng, Q.-H.; Klein, N.; McAnulty, R. J.; Hart, S. L. *J. Gene Med.* **2002**, *4*, 438.
- (143) Compton, S. H.; Mecklenbeck, S.; Mejia, J. E.; Hart, S. L.; Rice, M.; Cervini, R.; Barrandon, Y.; Larin, Z.; Levy, E. R.; Bruckner-Tuderman, L.; Hovnanian, A. *Gene Ther.* **2000**, *7*, 1600.
- (144) Vaysse, L.; Guillaume, C.; Burgelin, I.; Gorry, P.; Ferec, C.; Arveiler, B. *Biochem. Biophys. Res. Commun.* **2002**, *290*, 1489.
- (145) Colin, M.; Maurice, M.; Trugnan, G.; Kornprobst, M.; Harbottle, R. P.; Knight, A.; Cooper, R. G.; Miller, A. D.; Capeau, J.; Coutelle, C.; Barhimi-Horn, M. C. *Gene Ther.* **2000**, *7*, 139.
- (146) Unpublished results by Hailes group.

9. References

- (147) Lee, L. K.; Siapati, E. K.; Jenkins, R. G.; McAnulty, R. J.; Hart, S. L.; Shamlou, P. A. *Med. Sci. Monit.* **2003**, *9*, BR54.
- (148) Colin, M.; Moritz, S.; Fontanges, P.; Kornprobst, M.; Delouis, C.; Keller, M.; Miller, A. D.; Capeau, J.; Coutelle, C.; Barhimi-Horn, M. C. *Gene Ther.* **2001**, *2001*, 1643.
- (149) Writer, M. J.; Hurley, C. A.; Sarkar, S.; Copeman, D. M.; Wong, J. B.; Odlyha, M.; Lawrence, M. J.; Tabor, A. B.; McAnulty, R. J.; Ayazi Shamlou, P.; Hailes, H. C.; Hart, S. L. *J. Liposome Research* **2006**, Accepted.
- (150) Commercially available (100 mg= \$96.85); Order number=T1307, www.tokyokasei.co.jp/
- (151) Hurley, C. A.; Wong, J. B.; Hailes, H. C.; Tabor, A. B. *J. Org. Chem.* **2004**, *69*, 980.
- (152) Pack, D. W.; Chen, G. H.; Maloney, K. M.; Chen, C. T.; Arnold, F. H. *J. Am. Chem. Soc.* **1997**, *119*, 2479.
- (153) Schabub, B.; Blaser, G.; Schlosser, M. *Tetrahedron Lett.* **1985**, *26*, 307.
- (154) Tamura, R.; Saegusa, K.; Kakihana, M.; Oda, D. *J. Org. Chem.* **1988**, *53*, 2723.
- (155) Maryanoff, B. E.; Reitz, A. B.; Mutter, M. S.; Inners, R. R.; Almond, H. R.; Whittle, R. R.; Olfson, R. A. *J. Am. Chem. Soc.* **1986**, *108*, 7664.
- (156) Brown, H. C.; Wang, K. K. *J. Org. Chem.* **1986**, *51*, 4514.
- (157) Brown, H. C.; Lee, H. D.; Kulkarni, S. U. *J. Org. Chem.* **1986**, *51*, 5282.
- (158) Binisti, C.; Assogba, L.; Touboul, E.; Mounier, C.; Huet, J.; Ombetta, J. E.; Dong, C. Z.; Redeuilh, C.; Heymans, F.; Godfroid, J. J. *Eur. J. Med. Chem.* **2001**, *36*, 809.
- (159) Chong, J. M.; Heuft, M. A.; Rabbat, P. *J. Org. Chem.* **2000**, *65*, 5837.
- (160) Sorochinskaya, A. M.; Kovalev, B. G. *J. Org. Chem. USSR (Engl. Transl.)* **1991**, *27*, 621.
- (161) Hanack, M.; Fuchs, K.; Collins, C. J. *J. Am. Chem. Soc.* **1983**, *105*, 4008.
- (162) Nieuwenhuizen, W. F.; Leeuwen, S. v.; Gotz, F.; Egmond, M. R. *Chem. Phys. Lipids* **2002**, *114*, 181.
- (163) Bennett, M. J.; Malone, R. W.; Nantz, M. H. *Tetrahedron Lett.* **1995**, *36*, 2207.
- (164) Bennett, M. J.; Nantz, M. H.; Balasubramaniam, R. P.; Gruenert, D. C.; Malone, R. W. *Biosci. Rep.* **1995**, *15*, 47.
- (165) Nazih, A.; Cordier, Y.; Kolbe, H. V. J.; Heissler, D. *Synlett* **2000**, 635.
- (166) Eppstein, D. A.; Jones, G. H.; Felgner, P. L. *US Patent #689263* **1986**.
- (167) Alquist, F. N.; Slagh, H. R. *US patent #2147226* **1939**.
- (168) Writer, M. J.; Marshall, B.; Pilkington-Miksa, M. A.; Barker, S. E.; Jacobsen, M.; Kritz, A.; Bell, P. C.; Lester, D. H.; Tabor, A. B.; Hailes, H. C.; Klein, N.; Hart, S. H. *J. Drug Targeting* **2004**, *12*, 185.
- (169) Geall, A. J.; S., B. I. *J. Pharm. Biomed. Anal.* **2000**, *22*, 849.
- (170) Kral, T.; Hof, M.; Jurkiewicz, P.; Langner, M. *Cell Mol. Biol. Lett.* **2002**, *7*, 203.

9. References

- (171) Uyechi, L. S.; Gagné, L.; Thurston, G.; Szoka, F. C. *Gene Ther.* **2001**, *8*, 828.
- (172) Zelphati, O.; Szoka, F. C. *Proc. Natl. Acad. Sci. USA* **1996**, *93*, 11493.
- (173) Lin, A. J.; Slack, N. L.; Ahmad, A.; George, C. X.; Samuel, C. E.; Safinya, C. R. *Biophys. J.* **2003**, *84*, 3307.
- (174) Haugland, R. P. *Handbook of Fluorescent Probes and Research Products*; 9th ed.; Molecular Probes, 2002.
- (175) Chen, L.; Sakai, N.; Moshiri, S. T.; Matile, S. *Tetrahedron Lett.* **1998**, *39*, 3627.
- (176) Mujumdar, R. B.; Ernst, L. A.; Mujumdar, S. R.; Lewis, C. J.; Waggoner, A. S. *Bioconjugate Chem.* **1993**, *4*, 105.
- (177) Wiethoff, C. H.; Gill, M. L.; Koe, G. S.; Koel, J. G.; Middaugh, C. R. *J. Bio. Chem.* **2002**, *277*, 44980.
- (178) Keller, M.; Harbottle, R. P.; Perouzel, E.; Colin, M.; Shah, I.; Rahim, A.; Vaysse, L.; Bergau, A.; Moritz, S.; Brahimi-Horn, C.; Coutelle, C.; Miller, A. D. *ChemBioChem* **2003**, *4*, 286.
- (179) Sarkar, S. "Biophysical Characterisation of Plasmid Formulation" *PhD Thesis*, University College London **2005**, p98
- (180) Maurer, N.; Mori, A.; Palmer, L.; Monck, M. A.; Mok, K. W. C.; Mui, B.; Akhong, Q. F.; Cullis, P. R. *Mol. Membr. Biol.* **1999**, *16*, 129.
- (181) Zelphati, O.; Nguyen, C.; Ferrari, M.; Felgner, J.; Tsai, Y.; Felgner, P. L. *Gene Ther.* **1998**, *5*, 1272.
- (182) Hui, S. W.; Kuhl, T. L.; Guo, Y. Q.; Israelachvili, J. *Coll. Surf. B: Biointerfaces* **1999**, *14*, 213.
- (183) Mok, K. W. C.; Lam, A. M. I.; Cullis, P. R. *Biochim. Biophys. Acta* **1999**, *1419*, 137.
- (184) Bianco-Peked, H.; Dori, Y.; Schneider, J.; Sung, L.-P.; Satija, S.; Tirrell, M. *Langmuir* **2001**, *17*, 6931.
- (185) Herve, G.; Hahn, D. U.; Herve, A. C.; Goodworth, K. J.; Hill, A. M.; Hailes, H. C. *Org. Biomol. Chem.* **2003**, *1*, 427.
- (186) Hailes, H. C.; Tabor, A. B.; Wong, J. B.; Pilkington-Miksa, M. A.; Hart, S. L.; Hurley, C. A. *US patent application #2005/0245446* **2005**.
- (187) Drummond, D. C.; Zignani, M.; Leroux, J. C. *Prog. Lipid Res.* **2000**, *39*, 409.
- (188) Guo, X.; Szoka, F. C. *Acc. Chem. Res.* **2003**, *36*, 335.
- (189) Simoes, S.; Moreira, J. N.; Fonseca, C.; Duzgunes, N.; de Lima, M. C. P. *Adv. Drug Deliv. Rev.* **2004**, *56*, 947.
- (190) Fife, T. H.; Jao, L. K. *J. Org. Chem.* **1965**, *30*, 1492.
- (191) Bunce, R. A.; Allison, J. C. *Synth. Commun.* **1999**, *29*, 2175.
- (192) Krohn, K.; Florke, U.; Hofker, U.; Traubel, M. *Eur. J. Org. Chem.* **1999**, *12*, 3495.
- (193) Stowell, J. C.; Keith, D. R. *Synthesis* **1979**, *2*, 132.
- (194) Huang, P. Q.; Arseniyadis, S.; Husson, H. P. *Tetrahedron Lett.* **1987**, *28*, 547.

9. References

- (195) Griffith, W. P.; Ley, S. V.; Whitcombe, G. P.; White, A. D. *J. Chem. Soc., Chem. Commun.* **1987**, 1625.
- (196) Ley, S. V.; Norman, J.; Griffith, W. P.; Marsden, S. P. *Synthesis* **1994**, 639.
- (197) Johnsson, M.; Edwards, K. *Biophys. J.* **2001**, 80, 313.
- (198) Masson, C.; Garinot, M.; Mignet, N.; Wetzter, B.; Mailhe, P.; Scherman, D.; Bessodes, M. *J. Controlled Release* **2004**, 99, 423.
- (199) Menger, F. M.; Keiper, J. S. *Angew. Chem. Int. Ed.* **2000**, 39, 1906.
- (200) Fielden, M. L.; Perrin, C.; Kremer, A.; Bergsma, M.; Stuart, M. C. A.; Camilleri, P.; Engberts, J. B. F. N. *Eur. J. Biochem.* **2001**, 268, 1269.
- (201) Dass, C. R. *J. Mol. Med.* **2004**, 82, 579.
- (202) Scheule, R. K.; StGeorge, J. A.; Bagley, R. G.; Marshall, J.; Kaplan, J. M.; Akita, G. Y.; Wang, K. X.; Lee, E. R.; Harris, D. J.; Jiang, C. W.; Yew, N. S.; Smith, A. E. *Hum. Gene Ther.* **1997**, 8, 689.
- (203) Keogh, M.-C.; Chen, D.; Lupu, F.; Shaper, N.; Schmitt, J. F.; Kakkar, V. V.; Lemoine, N. R. *Gene Ther.* **1997**, 4, 162.
- (204) Papini, A.; Ricci, A.; Taddei, M.; Seconi, G.; P., D. *J. Chem. Soc., Perkin Trans. 1* **1983**, 1894, 2261.
- (205) Carr, S. A.; Weber, W. P. *J. Org. Chem.* **1983**, 50, 2782.
- (206) Bitha, P.; Carvajal, S. G.; Citarella, R. V.; Delossantos, E. F.; Durr, F. E.; Hlavka, J. J.; Lang, S. A.; Lindsay, H. L.; Thomas, J. P.; Wallace, R. E.; Lin, Y. I. *J. Med. Chem.* **1989**, 32, 2063.
- (207) Kolar, C.; Kraemer, H. P.; Dehmel, K. *US patent #4730069* **1985**.
- (208) Bitha, P.; Carvajal, S. G.; Citarella, R. V.; Child, R. G.; Delossantos, E. F.; Dunne, T. S.; Durr, F. E.; Hlavka, J. J.; Lang, S. A.; Lindsay, H. L.; Morton, G. O.; Thomas, J. P.; Wallace, R. E.; Lin, Y. I.; Haltiwanger, R. C.; Pierpont, C. G. *J. Med. Chem.* **1989**, 32, 2015.
- (209) Murgufa, M. C.; Grau, R. J. *Synlett* **2001**, 8, 1229.
- (210) Ambrose, M. G.; Binkley, R. W. *J. Org. Chem.* **1983**, 48, 674.
- (211) Weston, R. J.; Woolhouse, A. D.; Spurr, E. B.; Harris, R. J.; Suckling, D. M. *J. Chem. Ecol.* **1997**, 23, 553.
- (212) Denholm, A. A.; George, M. H.; Hailes, H. C.; Tiffin, P. J.; Widdowson, D. A. *J. Chem. Soc., Perkin Trans. 1* **1995**, 541.
- (213) Paaov, K.; Jorma, V. *#WO8700343* **1987**.
- (214) Pearson, D. A.; Blanchette, M.; Baker, M. L.; Guindon, C. A. *Tetrahedron Lett.* **1989**, 30, 2739.
- (215) Lall, M. S.; Ramtohul, Y. K.; James, M. N. G.; C., V. J. *J. Org. Chem.* **2002**, 67, 1536.
- (216) Anderson, J. T.; Toogood, P. L.; Marsh, E. N. G. *Org. Lett.* **2002**, 4, 4281.
- (217) Hwang, D. R.; Helquist, P.; Shekhani, M. S. *J. Org. Chem.* **1985**, 50, 1264.
- (218) Strazzolini, P.; Scuccato, M.; Giumanini, A. G. *Tetrahedron* **2000**, 56, 3625.
- (219) Davey, T. W.; Hayman, A. R. *Aust. J. Chem.* **1998**, 51, 581.

9. References

- (220) Commercially available (1 g= \$340.00); Order number=850705P, www.avantilipids.com
- (221) Kitaori, K.; Furukawa, Y.; Yoshimoto, H.; Otera, J. *Tetrahedron* **1999**, *55*, 14381.
- (222) Franklin, C. L.; Li, H.; Martin, S. F. *J. Org. Chem.* **2003**, *68*, 7298.
- (223) Martin, S. F.; Josey, J. A. *Tetrahedron Lett.* **1988**, *29*, 3631.
- (224) Xia, J.; Hui, Y. *Tetrahedron Asymm.* **1997**, *8*, 3019.
- (225) Roodsari, F. S.; Wu, D.; Pum, G. S.; Hajdu, J. *J. Org. Chem.* **1999**, *64*, 7727.
- (226) Singh Chadha, J. *Chem. Phys. Lipids* **1968**, *2*, 415.
- (227) Schmitt, L.; Dietrich, C.; Tempé, R. *J. Am. Chem. Soc.* **1994**, *116*, 8485.
- (228) Csuk, R.; Niesen, A.; Tschuch, G.; Moritz, G. *Tetrahedron* **2004**, *60*, 6001.
- (229) Berube, G.; Wheeler, P.; Ford, C. H. J.; Gallant, M.; Tsaltas, Z. *Can. J. Chem.* **1993**, *71*, 1327.
- (230) Baldwin, J. E.; Spring, D. R.; Atkinson, C. E.; Lee, V. *Tetrahedron* **1998**, *54*, 13655.
- (231) Riba, M.; Eizaguirre, M.; Sans, A.; Quero, C.; Guerrero, A. *Pestic. Sci.* **1994**, *41*, 97.
- (232) Odinolov, V. N. D., U. M.; Ishmuratov, G. Yu.; Botsman, L. P.; Vostrikova, O. S.; *Chem. Nat. Compd. (Engl. Transl.)* **1987**, *23*, 286.
- (233) Brauner, A.; Budzikiewicz, H. *Org. Mass Spectrom.* **1983**, *18*, 324.
- (234) He, L.; Byun, H.-S.; Bittman, R. *J. Org. Chem.* **2000**, *65*, 7627.
- (235) Baumann, W. J.; Mangold, H. K. *J. Org. Chem.* **1964**, *29*, 3055.
- (236) Horiike, M.; Yuan, G.; Kim, C.-S.; Hirano, C.; Shibuya, K. *Org. Mass Spectrom.* **1992**, *27*, 944.
- (237) Chattopadhyay, S.; Mamdapur, V. R.; Chadha, M. S. *Indian J. Chem. Sect. B* **1984**, *23*, 236.
- (238) Marques, F. A.; McElfresh, J. S.; Millar, J. G. *J. Braz. Chem. Soc.* **2000**, *11*, 592.
- (239) Bartz, M.; Kuether, J.; Nelles, G.; Weber, N.; Seshadri, R.; Treme, W. J. *Mater. Chem.* **1999**, *9*, 1121.
- (240) Muchow, G.; Vannoorenberghe, Y.; Buono, G. *Tetrahedron Lett.* **1987**, *87*, 6163.
- (241) Chabrier, S.-P. *Bull. Soc. Chim. Fr.* **1961**, 2076.
- (242) Fourneau, M. *Bull. Soc. Chim. Fr.* **1937**, *4*, 1156.
- (243) Valentin, S. *Collect. Czech. Chem. Commun.* **1931**, *3*, 507.
- (244) Scheurer, A.; Mosset, P.; Bauer, W.; Saalfrank, R. W. *Eur. J. Org. Chem.* **2001**, *16*, 3067.
- (245) Schultz, M.; Kunz, H. *Tetrahedron Asymm.* **1993**, *4*, 1205.
- (246) Young, R. C.; Downes, C. P.; Effleston, D. S.; Jones, M.; Macphee, C. H.; Rana, K.; Ward, J. G. *J. Med. Chem.* **1990**, *33*, 641.
- (247) Guo, W.; Gosselin, M. A.; Lee, R. J. *J. Controlled Release* **2002**, *83*, 121.